MAINTAINING A ROBUST AND EFFICIENT METABOLISM: FITNESS CONTRIBUTIONS BY MEMBERS OF THE RID PROTEIN SUPERFAMILY

by

RONNIE LEE FULTON

(Under the Direction of Diana M. Downs)

ABSTRACT

Metabolism is a complex and robust network of biochemical pathways that serve as the foundation for all biological processes of a cell. Therefore, it is imperative that cells modulate their metabolic networks such that they remain efficient in response to dynamic conditions and nutritional needs – either by altering expression or function of enzymes within certain pathways, or by maintaining optimal flux through existing pathways. This dissertation describes fitness contributions by members of the highly conserved Rid superfamily of proteins by moderating the effects of reactive metabolites on the metabolic networks of various organisms. The Rid superfamily is divided into eight subfamilies. The ancestral RidA subfamily is best known for its role in preventing metabolic stress caused by the reactive metabolite 2-aminoacrylate (2AA), while the remaining seven subfamilies (Rid1-7) had no demonstrated physiological role prior to this work. The first study described in this work (Chapter 2) expands the well-established RidA paradigm by identifying a key enzyme damaged by 2AA in *Pseudomonas aeruginosa*. The following three chapters describe physiological functions for two proteins belonging to the Rid2 subfamily, which each moderate flux by deaminating reactive intermediates. Chapter 3

defines the first evidence or a physiological role for a Rid protein beyond the RidA

subfamily by demonstrating that the Rid2 protein, DadY, is required for optimal flux

through the alanine catabolic pathway in P. aeruginosa. Chapter 4 defines metabolic

pathways carried out by the *dbu* operon in *Pseudomonas putida*, along with demonstrating

that the Rid protein, DbuB, is essential for optimal flux through these pathways. This work

also describes that RidA functions beyond metabolite toxicity in Salmonella enterica and

Escherichia coli by demonstrating that RidA proteins also maintain flux through isoleucine

biosynthesis. In total, this work demonstrates that Rid proteins most likely share the

physiological role of moderating flux through their respective metabolic pathway(s) by

deaminating reactive intermediates.

INDEX WORDS:

Rid proteins, reactive intermediates, metabolic network,

deaminate, flux

MAINTAINING A ROBUST AND EFFICIENT METABOLISM: FITNESS CONTRIBUTIONS BY MEMBERS OF THE RID PROTEIN SUPERFAMILY

by

RONNIE L. FULTON

B.S., University of Oklahoma, 2019

A Dissertation Submitted to the Graduate Faculty of The University of Georgia in Partial

Fulfillment of the Requirements for the Degree

DOCTOR OF PHILOSOPHY

ATHENS, GEORGIA

2025

© 2025

Ronnie L. Fulton

All Rights Reserved

MAINTAINING A ROBUST AND EFFICIENT METABOLISM: FITNESS CONTRIBUTIONS BY MEMBERS OF THE RID PROTEIN SUPERFAMILY

by

RONNIE L. FULTON

Major Professor: Diana M. Downs

Committee: Jorge C. Escalante-Semerena

M. Stephen Trent Timothy R. Hoover

Electronic Version Approved:

Ron Walcott Vice Provost for Graduate Education and Dean of the Graduate School The University of Georgia May 2025

DEDICATION

To my sister, Jon'e, for your strength in the face of adversity and your tendency to handle every challenge with poise and tranquility. I am excited to see where your academic journey takes you and I hope I have been a good role model throughout mine. To my mom, for being a constant example of resiliency and for always cheering me on through each of my endeavors. To my dad, for teaching me the value of hard work and for the sacrifices you made to give me opportunities you never had — it brings me so much joy to put "Doctor" in front of our name. Most of all, to my wife and partner, Alexandra Frank, for providing unending love, support and compassion, and for continuously inspiring me to grow intellectually, personally and professionally.

ACKNOWLEDGEMENTS

I would like to first give great thanks to my advisor, Dr. Diana Downs. I truly believe that Diana can make a scientist out of anyone, and I am forever grateful that she elected to take on the challenge of molding this scatterbrained young man, who I am sure did not look like an ideal applicant on paper, into the scientist I am today. I am thankful to Diana for allowing me the freedom to grow as an individual and pursue my own ideas, while also providing guidance and challenging my thinking to ensure that I am growing in the right direction as a scientist. I have also been fortunate enough to receive feedback and guidance from my committee members, Dr. Jorge Escalante-Semerena, Dr. M. Stephen Trent, and Dr. Timothy Hoover. Members of the Downs and Escalante laboratories, both past and current, have also given me scientific guidance and a sense of community over the years. I am particularly thankful to Brandi Buckner and Kailey Ezekiel from the Downs laboratory for providing me with support, along with an occasional escape from the inevitable stresses of scientific research. I would like to thank Regan McCormick and Nicholas Athanasatos for partaking in rigorous debate, both general and scientific, and for always being willing to get lunch or play pool during a hard day. I would also like to thank Dr. Kyle Rosinke for being a consistent friend, from orientation to graduation, and for always taking me on long hikes, despite our apparent differences in preferred pace.

I would like to acknowledge my professors and mentors at the University of Oklahoma, each of whom played a role in fostering my passion for science and in my decision to pursue a PhD at the University of Georgia. I would like to give special thanks

to my research mentor, Dr. Zbigniew Darzynkiewicz, along with the rest of the Zgurskaya laboratory, for fostering my interest and competency in scientific research. I would also like to thank Dr. Ralph Tanner and Dr. Michael McInerney, whose courses first sparked my interest in microbial physiology, and each of whom encouraged me to apply to the University of Georgia for my PhD.

None of us would be where we are today without the efforts of educators. Therefore, I would like to thank each of my teachers from elementary school onward. I would like to express particular gratitude to Dan Thompson, for providing lessons in science, football and life. Your encouragement to apply to the University of Oklahoma was pivotal in my being where, and who, I am today. I express my deepest gratitude to my family and friends back home, along with the communities of Cement and Cyril, Oklahoma for providing support encouragement throughout my life.

To my dog, Barley, for always ensuring I get out of bed early for a long walk and for never forgetting to bring me a gift when I return home. Lastly, to my wife, Alexadra Frank, for your consistent support and encouragement. You are an amazing partner, friend and role model for everyone, especially me. Thank you for always talking through models, helping me practice presentations, and for constantly expanding my vocabulary. I am deeply grateful for everything you do.

TABLE OF CONTENTS

	Pa	age
ACKNO	WLEDGEMENTS	V
СНАРТЕ	ERS	
1	INTRODUCTION AND LITERATURE REVIEW: MODULATORS OF A	L
	ROBUST AND EFFICIENT METABOLISM: PERSPECTIVE AND	
	INSIGHTS FROM THE RID SUPERFAMILY OF PROTEINS	1
	1.1 ABSTRACT	2
	1.2 INTRODUCTION	2
	1.3 MICROBIAL METABOLISM IS A COMPLEX SYSTEM	4
	1.4 CELLULAR METABOLITES INFLUENCE PHYSIOLOGY	6
	1.5 KEY CHALLENGES IN MODELLING METABOLISM	9
	1.6 DEFINITION OF THE RID (YJGF/YER057C/UK114)	
	SUPERFAMILY OF PROTEINS	.12
	1.7 THE RIDA PROTEIN SUBFAMILY: FROM UNKNOWN	
	FUNCTION TO A METABOLIC UNDERSTANDING	.17
	1.8 2-AMINOACRYLATE IS AN ENDOGENOUSLY GENERATED	
	STRESSOR	.24
	1.9 THE 2-AMINOACRYLATE STRESS PARADIGM	.31
	1.10 FUNCTION OF RID PROTEINS EXTENDS BEYOND RIDA AN	۷D
	2-AMINOACRYLATE STRESS	.43

	1.11 GENERAL MODEL FOR THE RID SUPERFAMILY AND
	REMAINING QUESTIONS55
	1.12 INSIGHTS GAINED, AND LESSONS LEARNED FROM
	STUDIES OF THE RID SUPERFAMILY59
	1.13 CONCLUDING REMARKS62
	1.14 REFERENCES62
2	THE CYSTEINE DESULFURASE ISCS IS A SIGNIFICANT TARGET OF
	2-AMINOACRYLATE DAMAGE IN PSEUDOMONAS AERUGINOSA90
	2.1 ABSTRACT91
	2.2 INTRODUCTION91
	2.3 RESULTS94
	2.4 DISCUSSION
	2.5 MATERIALS AND METHODS
	2.6 REFERENCES112
3	DADY (PA5303) IS REQUIRED FOR FITNESS OF <i>PSEUDOMONAS</i>
	AERUGINOSA WHEN GROWTH IS DEPENDENT ON ALANINE
	CATABOLISM
	3.1 ABSTRACT
	3.2 INTRODUCTION
	3.3 RESULTS
	3.4 DISCUSSION143
	3.5 MATERIALS AND METHODS145
	3.6 REFERENCES152

4	FUNCTIONAL CHARACTERIZATION OF THE DBU LOCUS FOR D-
	BRANCHED-CHAIN AMINO ACID CATABOLISM IN PSEUDOMONAS
	PUTIDA
	4.1 ABSTRACT170
	4.2 IMPORTANCE170
	4.3 INTRODUCTION
	4.4 RESULTS173
	4.5 DISCUSSION
	4.6 MATERIALS AND METHODS184
	4.7 REFERENCES190
5	RIDA PROTIENS CONTRIBUTE TO FITNESS OF S. ENTERICA AND E.
	COLI BY REDUCING 2AA STRESS AND MODERATING FLUX TO
	ISOLEUCINE BIOSYNTHESIS
	5.1 ABSTRACT212
	5.2 INTRODUCTION
	5.3 RESULTS216
	5.4 DISCUSSION223
	5.5 MATERIALS AND METHODS226
	5.6 REFERENCES232
6	CONCLUSIONS252

CHAPTER 1

INTRODUCTION AND LITERATURE REVIEW: MODULATORS OF A ROBUST AND EFFICIENT METABOLISM: PERSPECTIVE AND INSIGHTS FROM THE RID SUPERFAMILY OF PROTEINS¹

Reprinted here with permission of the publisher.

¹Fulton, RL and Downs, DM. 2023. *Advances in Microbial Physiology*. 83: 117-179. doi: 10.1016/bs.ampbs.

1.1 ABSTRACT

Metabolism is an integrated network of biochemical pathways that assemble to generate the robust, responsive physiologies of microorganisms. Despite decades of fundamental studies on metabolic processes and pathways, our understanding of the nuance and complexity of metabolism remains incomplete. The ability to predict and model metabolic network structure, and its influence on cellular fitness, is complicated by the persistence of genes of unknown function, even in the best-studied model organisms. This review describes the definition and continuing study of the Rid superfamily of proteins. These studies are presented with a perspective that illustrates how metabolic complexity can complicate the assignment of function to uncharacterized genes. The Rid superfamily of proteins has been divided into eight subfamilies, including the well-studied RidA subfamily. Aside from the RidA proteins, which are present in all domains of life and prevent metabolic stress, most members of the Rid superfamily have no demonstrated physiological role. Recent progress on functional assignment supports the hypothesis that overall, proteins in the Rid superfamily modulate metabolic processes to ensure optimal organismal fitness.

1.2 INTRODUCTION

Microbial metabolism is a complex system of interwoven pathways coordinated by an intricate, multilayered regulatory network. Decades of study have resulted in a solid understanding of the fundamental metabolic processes carried out by microbes. New and emerging tools promise continuing progress in our efforts toward a deeper understanding of this essential feature of all living cells. Studies of microbial metabolism and physiology have evolved from the pre-sequencing era, where biochemical genetic analyses were the primary means to identify and characterize the cellular components of metabolism, to modern times. The advent of sequencing and bioinformatic analyses, and their increasing accessibility, has furthered efforts to describe genome composition and define function based on homologies and established paradigms. Today, the generation of metabolic data is accelerated by the prevalence and availability of rapid global analyses (Cain et al., 2020; Downs et al., 2018; Mallick et al., 2019; Pearcy et al., 2021; Zhou et al., 2022). By incorporating multiple -omics technologies (transcriptomics, proteomics, metabolomics, etc.), one can rapidly generate large data sets that simultaneously describe the levels of transcripts, enzymes, and metabolites in a cell (Abdelhamid et al., 2019; Chen et al., 2021; Downs et al., 2018; Tang, 2011). These technologies, and the data they generate, facilitate hypothesis generation and productively guide direct biochemical and genetic experimentation on the structure and function of metabolic networks (Downs et al., 2018). Despite this remarkable progress and expansion of tools, critical questions in metabolism remain unanswered. Somewhat surprisingly, there are still many genes with no assigned function nor homology with any characterized genes, even in the best studied model organisms – e.g. Escherichia. coli (Merlin et al., 2002; Price et al., 2018), Salmonella. enterica (Blondel et al., 2009; Steffen Porwollik et al., 2014), and Saccharomyces. cerevisiae (Christie et al., 2009; Pena-Castillo & Hughes, 2007).

None-the-less, new functions and conserved paradigms in metabolism are continually discovered and defined. Such discoveries are oftentimes the result of an arduous, winding experimental process, guided by the methodical and open-minded approach that has been trusted to generate new metabolic knowledge for decades. Studies

that defined the YjgF/YER057c/UK114 (Rid) protein superfamily, along with those that identified the biochemical and physiological function of the RidA subfamily, provide an example of such a journey. In this review, we summarize the features of metabolism that contribute to its complexity and describe studies on the Rid superfamily in the context of those elements.

1.3 MICROBIAL METABOLISM IS A COMPLEX SYSTEM

Microbial metabolism is a complex system that consists of individual components and their interactions with one another (Bazurto & Downs, 2011; Enos-Berlage et al., 1998; Dustin C Ernst et al., 2018; Koenigsknecht & Downs, 2010; Voit et al., 2012). By maintaining appropriate levels of gene expression, enzyme concentration, and flux through various pathways, microbes ensure a dynamic and efficient metabolic network that is responsive to both internal and external perturbations. The robustness of microbial metabolic systems can obscure the need for some components, thus posing a challenge in studies to identify new components, biochemical strategies, and regulatory principles.

1.3.1 Components of metabolism.

In a general sense, proteins and metabolites are the basic components of a metabolic system. The proteins present in an organism can be predicted from genome composition based on our understanding of the Central Dogma. Many proteins have a known or predicted enzymatic activity, but filling gaps in our knowledge of protein function remains a challenge. Proteins encoded in the genome fall into one of three general classes: i) known function, ii) predicted function, or iii) unknown function. The latter class is problematic for

investigators, and functional characterization might only be initiated when a lesion in the locus encoding the protein elicits a detectable phenotype. As such, serendipity can play an outsized role in discovering the function of uncharacterized gene products. Metabolites are the second component of a metabolic system. These molecules are not directly encoded in the genome and, therefore, gaining evidence of their existence and role in the cell is not always straightforward. Identification of metabolites is the biggest challenge we face in achieving a complete understanding of the metabolic structure of any organism.

Global approaches (e.g. "-omics") generate data that are helpful to catalog and quantify the components of metabolism. Proteomics approaches define the proteins present and offer general ideas of their relative abundance (Chen et al., 2021; Fortuin & Soares, 2022; Tang, 2011). Metabolomics approaches have the potential to further develop our understanding of the interplay between the enzymatic components of a metabolic system. Each -omics technique comes with caveats that temper the user's ability to make rigorous conclusions. For example, though transcriptomics provides a snapshot of all mRNA present in a cell at a given time, proteomic studies are not yet able to detect all proteins in the cell, or their relative levels. Results of metabolomic analyses are impacted by extraction methods, metabolite quenching and instability of metabolites. Despite these caveats global approaches bring an important perspective and their continuing evolution will expand the toolbox available to probe the composition of the complex system of metabolism (Downs et al., 2018).

1.3.2 Metabolic network structure. Beyond the protein and metabolite components lies the second and third dimensions of a metabolic system. These layers include biochemical

pathways and multiple interactions between pathways and/or individual components, respectively. In total, the interacting components are appropriately visualized as a network. A phenotype represents the overall functional status of the metabolic network in an organism. In response to internal or external perturbations, the structure (i.e. functional capacity) of the metabolic network can be altered to respond appropriately. Responses to a change in network structure are mediated by regulation at the transcriptional, translational, and post-translational levels (Chubukov et al., 2014; Litsios et al., 2018). In a simple scenario, flux through a relevant pathway is moderated by changing enzyme levels or enzymatic activity, in response to an environmental or intracellular signal. Unanticipated phenotypes caused by changes in a single pathway can lead to the definition of new metabolic connections and an increased understanding of metabolic network structure (Bazurto et al., 2017; Dougherty & Downs, 2006; Downs, 2003; Dustin C Ernst et al., 2018; Ernst & Downs, 2016; Koenigsknecht et al., 2012; Lewis et al., 2009; Paxhia & Downs, 2022; Ramos et al., 2008b).

1.4 CELLULAR METABOLITES INFLUENCE PHYSIOLOGY

Like proteins, metabolites serve many roles in the cell. However, unlike proteins, the levels of metabolites cannot be easily determined based on the status of transcription or translation. During steady state growth, when cells are in metabolic equilibrium, each metabolite is maintained at a level that ensures metabolic robustness and optimal fitness of the organism (Sander et al., 2019). Perturbation of this equilibrium can provide insights as to the influence individual metabolites exert on fitness as the cell responds to restore balance. For instance, compromising or eliminating a gene that encodes a biosynthetic

enzyme can disrupt metabolic homeostasis by depleting a product and/or accumulating a substrate of the enzyme. Such a perturbation alters the capacity of the metabolic network and often causes a growth phenotype (Epelbaum et al., 1998; Ernst & Downs, 2016; Fulton et al., 2022; Johnston & Roth, 1979; Lambrecht et al., 2013; Schmitz & Downs, 2004; Trivedi et al., 2018).

Cellular metabolites have multiple regulatory roles in establishing and maintaining metabolic network structure. There is extensive literature describing a role for metabolites as co-effectors in modulating transcriptional regulation, or as signal molecules in regulatory cascades. Importantly, some metabolites modulate the activity of key enzymes via allosteric interactions. The critical role this regulatory strategy plays in maintaining metabolic equilibrium was elegantly shown by a global study in E. coli (Sander et al., 2019). Using a combination of classical genetics, proteomics, metabolomics, and mathematical modeling approaches, the study by Sander et al. queried the effects of allosteric regulation on metabolic robustness. The data showed that the enzymes of seven amino acid biosynthetic pathways are overabundant in wild-type cells. Despite this overprogramming, flux through these pathways was kept at an appropriate level by allosteric inhibition of the relevant enzymes (Sander et al., 2019). This study showed that multi-level regulation of enzyme abundance and allosteric inhibition maximized the efficiency and robustness of amino acid biosynthesis. With additional studies, it is likely that this conclusion will be extrapolated to other nodes of metabolism. Beyond the study by Sander and coworkers, enzymes insensitive to feedback inhibition have contributed to the understanding of metabolic connections and nutritional phenotypes in multiple systems, not the least of which is the RidA system reviewed herein (Bazurto & Downs,

2011; Burns et al., 1979; Csonka et al., 1988; Enos-Berlage et al., 1998; LaRossa & Van Dyk, 1987; Lee et al., 2003; Rajagopal et al., 1998; Schmitz & Downs, 2004; Sheppard, 1964).

Some cellular metabolites can have detrimental effects if they accumulate above desired concentrations due to a mutation or other perturbation of the metabolic system. The potential of metabolites to cause cellular damage is not always predicable a priori. The metabolite and mechanism(s) of damage or stress are typically defined during the process of dissecting metabolic phenotypes. Some metabolites cause direct damage to cellular components and, in turn, provoke global metabolic stress if they are allowed to accumulate or persist in the cell. Such stress can be exacerbated if strategies to cope with the stress have secondary consequences. A familiar example of such collateral damage is the SOS response, which is induced to cope with DNA damage, but often introduces mutations as a consequence (McKenzie et al., 2000). Cysteine can be toxic at high concentrations and in S. enterica, the mechanism of the enzyme charged with detoxifying it (cysteine desulfhydrase) proceeds through a reactive metabolite, which is itself toxic (Ernst et al., 2014). Also, consider molecular species such as glyoxals, generated as intermediates in the oxidative degradation of glucose, peroxidation of lipids, and DNA oxidation. These molecules can irreversibly damage proteins and nucleotides (Lee & Park, 2017; Singh et al., 2001; Thornalley, 1996; Thornalley et al., 1999). When the mechanism used to detoxify reactive electrophilic species, like glyoxals, involves redox active cofactors, the detoxification can generate a redox imbalance that then impairs electron transport (Benov & Fridovich, 2002; Wang et al., 2009). Formaldehyde is a toxic metabolite that nonspecifically reacts with numerous cellular components of all living cells. In some

organisms, including the facultative methylotroph *Methylorubrum extorquens*, formaldehyde is generated during the metabolism of certain substrates. These organisms have developed strategies to rapidly and efficiently detoxify this molecule to prevent direct and indirect metabolic damage (Bazurto et al., 2021). These few examples illustrate the complexity and integration of the metabolic network and the global consequences that local perturbations can have on cellular fitness.

Significantly, a major participant in the RidA paradigm described in this review, is the metabolite 2-aminoacrylate (2AA). 2AA is a reactive enamine/imine species that irreversibly damages enzymes that use a pyridoxal 5'-phosphate (PLP) cofactor. PLP-dependent enzymes are essential in multiple metabolic pathways and reactions of central metabolism (Percudani & Peracchi, 2003). Accumulation of 2AA results in irreversible damage to the PLP cofactor within the active sites of numerous enzymes and thus causes global stress (Borchert, Ernst, et al., 2019). 2AA stress elicits diverse phenotypes that depend on the metabolic network structure around the target enzymes in a particular organism (Irons et al., 2020). RidA proteins moderate the effects of 2AA stress, as described herein.

1.5 KEY CHALLENGES IN MODELLING METABOLISM

With the availability of genomes and the growing ease of annotation, modelling metabolism is becoming increasingly possible in many organisms (Garcia-Jimenez et al., 2021; Karr et al., 2012; Yang et al., 2014; Zimmermann et al., 2021). While metabolic models can generate valuable knowledge, they are generally unable to describe subtleties of regulation and function in metabolism (Bazurto & Downs, 2016; Downs et al., 2018;

Long & Antoniewicz, 2019; McGill et al., 2021; Yung et al., 2019). Features excluded from metabolic models are often those that are difficult to extract from genomic composition yet exert significant influence over metabolic structure and organismal fitness. A number of things impact the ability to extract the structure of a metabolic system from genomic information.

1.5.1 Redundancy complicates interpretation of phenotypes. Cells can encode proteins of similar annotated or actual function that differ in regulation or kinetics – i.e. isozymes. This functional redundancy can complicate characterization, as it is can be difficult to recapitulate the *in vivo* conditions that distinguish the need for the respective isozyme. For instance, aspartate aminotransferase activity can be provided by AspC (EC 2.6.1.1) or TyrB (EC 2.6.1.57) in S. enterica (Gelfand & Steinberg, 1977; Powell & Morrison, 1978) and up to three acetolactate synthases (EC 2.2.1.6) can catalyze the second step of branched chain amino acid biosynthesis (Epelbaum et al., 1998). Pseudomonas putida encodes three putative glyceraldehyde 3-phosphate dehydrogenase (GAPDH) enzymes (Gap-1, Gap-2. PP 3443). These GAPDH isozymes are differentially regulated at the transcriptional level and thus each contribute to growth on a different carbon source (Chavarria et al., 2016). In E. coli, the catabolic (DadX) and anabolic (Alr) alanine racemases are regulated such that each available under the appropriate conditions (Wild et al., 1985). Finally, cold adapted bacteria like *Pseudomonas mandelii* often encode two glucose 6-phosphate dehydrogenase isozymes – Zwf-1 and Zwf-2 (DangThu et al., 2020). When present, isozymes are differentially regulated and/or have unique kinetic properties, such that the metabolic needs of the cell are met by one or both under the appropriate conditions. Some enzymes can

compensate for the loss of one another, such as the case with IIvC (ketol-acid reductoisomerase, EC 1.1.1.86) which, in *E. coli* and *S. enterica*, is an enzyme in branched chain amino acid biosynthesis that also catalyzes the reaction performed by PanE (ketopantoate reductase, EC 1.1.1.169) in pantothenate biosynthesis (Primerano & Burns, 1983). In multiple ways cellular networks use isozymes to support an efficient and robust metabolism. Despite this logical architecture, functional overlap or redundancy can complicate phenotypic analysis aimed at defining the physiological role of a gene or protein. Regulatory and kinetic details of the above examples have been previously characterized, thus in hindsight these strategies are logical. However, in the investigative stages of a project, it is difficult to assign physiological function to two proteins that catalyze the same reaction *in vitro* without a distinguishing phenotype in *in vivo* analysis. Studies of the Rid superfamily are confronted with these complications, as described below.

1.5.2 Lack of data compromises metabolic models. The most pressing issue for comprehensive modelling of metabolism is the need for more information. Numerous enzymes are encoded in microbial genomes, and we still lack critical information that would allow facile, accurate prediction of properties of proteins such as expression levels, kinetic parameters, substrate specificity, etc. Each of these features can significantly impact the function and robustness of a network (Link et al., 2014). The complete set of instructions for configuring a dynamic metabolic network is technically present in the genome. Still, with our current understanding and predictive tools, genomic composition can be mined to suggest metabolic potential but not the three-dimensional configuration of

a metabolic network (Bazurto & Downs, 2016; Bazurto et al., 2016; Borchert & Downs, 2017b). This assessment is supported by studies showing that metabolic network architecture can differ dramatically even between closely related organisms like *S. enterica* and *E. coli* (Bailey et al., 2009; Bazurto et al., 2016; Borchert & Downs, 2017b; Meysman et al., 2013; Winfield & Groisman, 2004).

A classic genetic approach, using rigorous molecular analyses to describe and define underlying causes of a phenotype, can uncover metabolic details and structure not expected *a priori*. These types of analyses are time and labor intensive, but at present they provide the most effective means to generate new knowledge and insights into metabolic network structure (Downs et al., 2018). The unique power of this approach is illustrated in the case studies described in subsequent sections, which identified the function of the large, highly conserved Rid protein superfamily, and provided the foundation for inquiry into uncharted areas of metabolism.

1.6 DESCRIPTION OF THE RID (YJGF/YER057C/UK114) SUPERFAMILY OF PROTEINS

The Rid (**R**eactive **i**ntermediate **d**eaminase) superfamily, originally designated YjgF/YER057c/UK114, is a large family of sequence diverse, small proteins organized into eight subfamilies based on sequence analysis and gene synteny (Niehaus et al., 2015) (Figure 1). The wide-ranging study by Neihaus et al. identified conserved sequence motifs, both within each subfamily and across the Rid superfamily. Key residues for Rid proteins include Tyr17, Ser30, Asn88, Arg 105, and Glu120 (*E. coli* numbering) and variation at these positions was used as evidence to differentiate between the eight subfamilies. The

Glu120 residue is the only residue that is strictly conserved in all Rid proteins. The next most conserved residue is Arg105, which is present in only the RidA and Rid1, 2, and 3 subfamilies and has been shown to be essential for (and predictive of) deaminase activity in these proteins. The residue at the 105 position varies in Rid4, 5 and 6 subfamily proteins but is consistently a tryptophan in the Rid7 proteins. The Asn88 residue is only present in the RidA, Rid1 and Rid2 proteins, and varies considerably in the remaining subfamilies. The Tyr17 residue is conserved in proteins from all subfamilies except for Rid5 proteins, which have a phenylalanine residue at this position, and the Rid2 and Rid3 proteins, which have no specific amino acid at residue 17. Finally, Ser30 is conserved in all subfamilies except Rid2, while some members of Rid6 and Rid7 subfamilies have an alanine at this position. Only the Arg105 residue has been demonstrated to have implications for function in these proteins. Establishing the significance of each of these residues will be beneficial in establishing a consistent model to predict Rid protein function and to rigorously define the properties of each Rid subfamily.

Early reports referencing proteins of the Rid superfamily predate the definition of the family and are now recognized to refer to the archetypal RidA subfamily, which is the only subfamily found in eukaryotes (Irons et al., 2020; Niehaus et al., 2015). The initial reports on members of this protein family date back to the mid-1990s, and continue with numerous reports published prior to functional information that resulted in our understanding of these proteins (Burman et al., 2007; Ceciliani et al., 1996; Deaconescu et al., 2002; Deriu et al., 2003; Knapik et al., 2012; Levy-Favatier et al., 1993; Manjasetty et al., 2004; Mistiniene, 2003; Mistiniene et al., 2005; Parsons et al., 2003; Sinha et al., 1999; Su et al., 2015; Thakur et al., 2009; Volz, 1999; H. M. Zhang et al., 2010).

The first reference to a Rid protein in the literature was an acid-soluble protein isolated from the liver and kidney of rats (Levy-Favatier et al., 1993). In their studies, these authors noticed a novel, 23-kDa protein that co-extracted with the high-mobility group chromatin components that were the focus of the work. When liver or kidney extract from rat were treated with perchloric acid, this small protein was isolated. Alignments using the amino acid sequence, deduced from cDNA, revealed this protein had similarity to the highly conserved heat-shock protein and molecular chaperone, Hsp90. Based on the sequence alignment, the authors suggested a chaperone role for the small acid-soluble protein (Levy-Favatier et al., 1993). This protein was subsequently purified in a later study by another group, who noted that the small protein inhibited translation in cell free extracts. This observation led the authors to describe the protein as a translation initiation inhibitor (Oka et al., 1995). Thus, the first proposed activities for Rid proteins were as a chaperone and a translation inhibitor, designations that persist in the annotations of many genomes today, despite the lack of rigorous confirmation supporting these functional assignments.

The earliest definition of the Rid protein family appears in a study of *E. coli* YjgF (now RidA) as part of a structural genomics initiative (Volz, 1999). Volz identified 24 high-identity homologs of YjgF, that were collectively termed the "YjgF family." This study predated functional characterization or definition of an active site of RidA. Based on topology, location, and sequence conservation among other members of the protein family, Volz suggested three possible active sites. Of note, one of these possible active sites included the Arg105 residue that was later shown to be critical in the active site of RidA proteins (Lambrecht et al., 2012). The Volz study found YjgF to be a homotrimer, an oligomeric configuration that has been validated by dozens of subsequent studies of RidA

proteins from all domains of life and is presumed to be the active form (Irons et al., 2020). The structure of YjgF had significant similarity to the structure of *Bacillus subtilis* chorismate mutase, as the two proteins have the same quaternary structure and the monomers have a single domain folded into a β-sheet that is closely situated with two helices (Volz, 1999) (Figure 1C). Based on the structure of YjgF, Volz suggested that topological similarities between YjgF and chorismate mutase were the result of convergent evolution. This author considered that YjgF (RidA) and chorismate mutase had different functions. Further, Volz suggested the function of YjgF involved amino acids and active site features not used by the chorismate mutase mechanism. Each of these assumptions were partially validated when the function of RidA was defined (Lambrecht et al., 2012).

Prior to the functional characterization of Rid protein family members, comparative analyses of multiple sequences and structures by several groups suggested critical residues for the family (Burman et al., 2007; Ceciliani et al., 1996; Deaconescu et al., 2002; Knapik et al., 2012; Manjasetty et al., 2004; Mistiniene et al., 2003; Mistiniene et al., 2005; Parsons et al., 2003; Pu et al., 2011; Sinha et al., 1999; Thakur et al., 2009; Volz, 1999; H. M. Zhang et al., 2010). As summarized above, alignments of amino acid sequences from RidA homologs across the domains of life identified four invariant residues presumed to be critical for function – Gly31, Asn88, Arg105, and Glu120 (*E. coli* numbering) (Burman et al., 2007; Deaconescu et al., 2002; Deriu et al., 2003; Knapik et al., 2012; Mistiniene et al., 2005; Parsons et al., 2003; Pu et al., 2011; Sinha et al., 1999; Thakur et al., 2009; Volz, 1999; H. M. Zhang et al., 2010). The invariant residues are situated within the predicted active site of the protein. Only these four residues were 100% conserved in RidA proteins.

but other residues comprising the active site had similar characteristics (i.e. hydrophobicity, charge, steric properties) across all homologs (X. Zhang et al., 2010).

Prompted by the lack of biochemical information on RidA proteins, several studies co-crystallized different family members with molecules considered to be potential substrates. The hope was that functional insights could be gained from these studies. The RidA proteins and their co-crystalized metabolites include Hp14.5 from Homo sapiens (cocrystalized with benzoate), TdcF from E. coli (co-crystalized with ethylene glycol, propionate, serine, and 2-ketobutyrate), and PSTPO-PSP from *Pseudomonas syringae* (cocrystalized with glucose) (Burman et al., 2007; Knapik et al., 2012; Mistiniene et al., 2005; X. Zhang et al., 2010). In each of the co-crystallization studies, the relevant metabolite was visibly coordinated by conserved residues that were situated in the presumptive active site. Despite widely documented structural similarity, conserved active site residues, and cocrystal structures, no function nor activity could be assigned to this large protein family in any organism from these structural data. Over time, multiple unrelated roles for RidA proteins were proposed from disparate studies with various organisms, primarily eukaryotes. The listed functions included ribonuclease (Dhawan et al., 2012; Morishita et al., 1999), translation inhibitor (Oka et al., 1995; Schmiedeknecht et al., 1996), heat-shock protein (Volz, 1999), molecular chaperone (Farkas et al., 2004; Volz, 1999), protease activator (Melloni et al., 1998). RidA homologs were also suggested to participate in purine and fatty acid metabolism (Rappu et al., 1999; Sasagawa et al., 1999). In a testament to the utility of a biochemical genetic approach, only after a serendipitous observation of an in vivo activity in S. enterica was the molecular activity of a RidA protein convincingly elucidated (Browne et al., 2006; Enos-Berlage et al., 1998; Schmitz & Downs, 2004). The

studies subsequent to that observation provided rigorous biochemical analysis of the RidA protein in *S. enterica* and benefited from the results of the prior structural studies (Lambrecht et al., 2012; Lambrecht et al., 2013).

1.7 THE RIDA PROTEIN SUBFAMILY: FROM UNKNOWN FUNCTION TO METABOLIC UNDERSTANDING

Although references to RidA (formerly YigF) paralogs date back to the early 1990s, work leading to the functional characterization of this protein family began with an observation in S. enterica in 1998 (Enos-Berlage et al., 1998). Studies over the course of 14 years led to the demonstration that S. enterica RidA is an imine/enamine deaminase with physiologically relevant activity on 2-aminoacrylate (2AA) and 2-aminocrotonate (2AC) (Lambrecht & Downs, 2013; Lambrecht et al., 2012; Lambrecht et al., 2013). When considered in total, investigations into this protein family over 25 years present a case study on metabolic analyses that represents a triumph of in vivo genetics and metabolic detective work. The path taken to generate new metabolic knowledge and highlight key questions about the Rid superfamily has been serendipitous and meandering, as described in the sections below. Similar winding paths through metabolism have been taken, and will continue to be critical, in efforts to define the biochemical function and physiological role of unknown proteins. Without knowledge or functional predictions, the complexities of metabolism challenge our ability to define the activities and understand the roles of proteins of unknown function, some of which are conserved across many or all microorganisms.

1.7.1 Loss of RidA can be beneficial or detrimental. The first reported mutation in the ridA gene of a bacterium was an insertion mutation that restored thiamine synthesis to a purF mutant of S. enterica (Enos-Berlage et al., 1998) (Figure 2A). Thiamine synthesis was used over the years to probe metabolic integration, and numerous mutations that similarly restored thiamine synthesis to a purF mutant had been isolated (Koenigsknecht et al., 2012). Each of the previous mutations acted by diverting metabolic flux from tryptophan, histidine or phosphoribosyl pyrophosphate (PRPP) biosynthetic pathways to allow PurFindependent synthesis of phosphoribosylamine (PRA) (Downs & Roth, 1991; Koenigsknecht et al., 2010; Ramos et al., 2008a, 2008b). The lesions in *ridA* stood out from the other suppressors because they were, i) more frequent and ii) null alleles. When a *ridA* insertion mutation was transduced into a wild-type genetic background, routine nutritional analysis found no growth defect on minimal medium, but a sensitivity to the addition of serine (Enos-Berlage et al., 1998) (Figure 2B). The data showed that loss of RidA had both a positive (i.e. restored thiamine synthesis) and a negative effect (i.e. sensitivity to serine) on the growth of S. enterica. Thus, to be acceptable, any biochemical function proposed for this protein had to explain both effects.

A key finding was that the addition of isoleucine to the medium reversed the two effects of the *ridA* mutation – growth in the presence of serine was restored, and growth of the *purF* mutant in the absence of thiamine was eliminated. Prompted by two reports describing defects in isoleucine synthesis in *S. cerevisiae* strains lacking the RidA homolog Mmf1 (Kim, 2001; Oxelmark et al., 2000), transaminase B (IlvE, EC: 2.6.1.27) activity was assayed in *S. enterica ridA* mutants and found to be impaired (Schmitz & Downs, 2004). Importantly, the specific activity of IlvE was reduced via a post-translational

mechanism in the *ridA* mutant. Exogenous isoleucine restored the activity of IlvE, just as it had ameliorated the other effects of a *ridA* mutation. Genetic analysis using a characterized variant of IlvA (serine/threonine dehydratase, EC: 4.3.1.19) determined that isoleucine exerted its effect in *ridA* mutants via allosteric inhibition of IlvA (Chen et al., 2013; LaRossa & Van Dyk, 1987; Schmitz & Downs, 2004). In total, data from these disparate studies were incorporated into the general model in which an IlvA reaction product, but not the accepted 2-ketobutyrate (2KB), mediated *ridA* phenotypes and the RidA protein neutralized its effect (Schmitz & Downs, 2004). This model proved to be prophetic, despite a lack of understanding of the metabolites involved or mechanism by which the presumed metabolite acted.

The results and working model described above were the foundation for multiple sequential studies, each of which resulted in valid, but incomplete, conclusions about the role of the RidA protein. A study that connected tryptophan biosynthesis and PRA generation gave the first hint of how PRA was being synthesized in a *ridA* mutant (Ramos & Downs, 2003). These studies found that, in the absence of RidA, the tryptophan biosynthetic enzyme complex anthranilate synthase-phosphoribosyl transferase (TrpDE, EC: 4.1.3.27) catalyzed PRA formation (Browne et al., 2006). Subsequent efforts confirmed synthesis of PRA could be achieved by IlvA, TrpD, PRPP and threonine *in vitro*. These experiments recapitulated what occurred *in vivo* in a *ridA* mutant and further, suggested there was an endogenous metabolic difference between *ridA* and wild-type strains. Importantly, when RidA protein was added to the *in vitro* reaction mixture, synthesis of PRA by TrpD was prevented (Lambrecht et al., 2010). These observations were extended by *in vitro* experiments that defined the TrpD/2AC-dependent mechanism

of PRA synthesis and the role RidA played in preventing it (Figure 3). Simply, the 2aminocrotonate product generated by IlvA reacts with PRPP in the active site of TrpD, resulting in a predicted phosphoribosyl-enamine adduct that can be hydrolyzed to PRA (Lambrecht & Downs, 2013). With these data, the molecular mechanism of thiamine synthesis that caused the initial phenotype of a *ridA* mutant was defined. The question arose as to whether the TrpD-dependent pathway for PRA formation was a metabolic artifact in a S. enterica ridA mutant, or if this pathway might be found in another organism as part of its native metabolic structure. Unexpectedly, evidence showed this pathway exists in E. coli and operates in the presence of a functional RidA. Up to 50% of the PRA used for thiamine synthesis in E. coli required the activity of threonine dehydratase (IlvA) and anthranilate synthase component II (TrpD) (Bazurto et al., 2016). This example illustrates differences in metabolic network structure. E. coli and S. enterica share all cellular components required for the TrpD-dependent PRA pathway, yet it functions under different conditions in these two organisms. It remains to be determined what modulates these differences – potentially amino acid pool size variation, subtle differences in enzyme kinetics, etc. The conservation of RidA across the domains of life implied that a role in this non-conserved biosynthetic pathway was not the primary function for which this protein had been maintained.

1.7.2 RidA deaminates reactive enamines/imines. Results from the studies outlined above suggested that RidA acted, by an undefined mechanism, on a product of IlvA before said product: i) was captured by TrpD to generate PRA (Lambrecht & Downs, 2013), ii) contributed to the reduced activity of IlvE (Schmitz, 2006), and iii) prevented growth in

the presence of serine. The decreased IlvE activity was not responsible for the growth defect of a ridA mutant in the presence of serine, consistent with the demonstration that biosynthetic pathways are often overprogrammed – (Sander et al., 2019). A closer look at the mechanism of IlvA shed light on the process occurring in a ridA mutant. In the first step of isoleucine biosynthesis, IlvA catalyzes the dehydration of threonine to the 2aminocrotonate enamine (2AC), which tautomerizes to an imine before being hydrolyzed by solvent water, forming 2KB and free ammonia (Chargaff & Sprinson, 1943; Phillips & Wood, 1965). IlvA similarly dehydrates serine to the respective enamine 2-aminoacrylate (2AA), which likewise tautomerizes to an imine with the final hydrolysis yielding pyruvate and ammonia. Prior in vitro studies showed that enamine/imine species were obligatory intermediates in these reactions, and others catalyzed by some PLP-dependent enzymes (Walsh, 1984). Notably, the *in vitro* studies did not suggest, nor expect, the enamine would leave the active site of the enzyme. The instability of these molecules results in a short halflife in water, leading to the presumed role of free water in the final deamination of enamine/imine species. Lambrecht et al., 2012 made the astute suggestion that RidA acted on enamine/imine metabolites and proposed these molecules could accumulate in vivo in the absence of this protein. This scenario required that the cellular milieu be distinct from the aqueous solutions used for *in vitro* biochemical studies. This clever insight transformed our understanding of the Rid superfamily and emphasized the benefit of integrating results from both in vitro and in vivo experimentation. Data from experiments using a purified system determined that RidA increased the rate of IlvA-mediated 2KB formation from threonine. More specifically, RidA increased the rate of product formation by acting on the enamine/imine intermediate generated by IlvA (Lambrecht et al., 2012). This result

allowed the conclusion that enamine/imine products were released from IlvA and were free in solution. Finally, the data showed that RidA was more efficient than solvent water in deaminating the enamine/imine intermediates to the ketoacid product.

In total, these data established, for the first time, a biochemical activity associated with the RidA protein from *S. enterica* and, as such, laid the foundation for continuing studies on this protein family. An assay was implemented to quantify the rate of deamination IIvA-derived enamine/imine products from threonine and serine – 2AC and 2AA, respectively. PLP-dependent cysteine desulfhydrase, CdsH, can also be used to generate the 2AA metabolite substrate of RidA *in situ* (Ernst et al., 2014). Analysis of RidA variants in these assays showed that the conserved arginine residue (Arg105 in *S. enterica*) is essential for deaminase activity. Consistent with this notion, a RidA^{R105A} variant was unable to complement a *ridA* mutant when provided *in trans* (Lambrecht et al., 2012). Models of the active site and a proposed catalytic mechanism of RidA have been reviewed (Borchert, Ernst, et al., 2019). RidA proteins from across domains had enamine/imine deaminase activity in these assays (Lambrecht et al., 2012), which continue to be used to characterize Rid proteins.

Following the identification of Rid protein deaminase activity, other assays were implemented to facilitate efforts to identify potential Rid substrates. PLP-dependent dehydratases generate a limited number of enamines, but NAD-/FAD-dependent amino acid oxidases generate imine intermediates from a wide array of amino acid substrates, which are then deaminated by water to the corresponding ketoacid (Hafner & Wellner, 1979; Niehaus et al., 2014). Analysis of Rid protein deaminase activity is facilitated by the broad substrate specificity of such oxidases, since it allows commercially available L-

amino acid oxidase (LOX) to be used (Digiovanni et al., 2021; Niehaus et al., 2015) (Figure 4). The addition of semicarbazide to the reaction mixtures is key to the LOX-based deaminase assay. Semicarbazide reacts with imines to generate a semicarbazone compound that can be quantified spectrophotometrically at a wavelength of ~248 nm. In general, these assays do not monitor the ketoacid product of deamination but rather, measure the ability of a Rid protein to compete with semicarbazide for the relevant imine substrate. In this way, activity of a Rid protein is detected as a decrease in the rate of semicarbazide formation. The ability of LOX to generate imines from a wide variety of amino acids has been used in efforts to define the substrate specificity of different Rid proteins (Buckner et al., 2021; Fulton et al., 2022; Hodge-Hanson & Downs, 2017). The LOX assay will be useful in studies to define active site residues that determine said specificity. At present, a limited number of studies have analyzed substrate specificity with Rid proteins. Data from those few studies suggest these in vitro experiments could provide the means to validate and improve the current subfamily classification of Rid proteins moving forward (Fulton et al., 2022; Hodge-Hanson & Downs, 2017)

In one or more of the above assays, RidA paralogs from at least *E. coli*, *B. subtilis*, *Y. pestis*, *P. aeruginosa*, *Campylobacter jejuni*, *Pyrococcus furiosus*, *Saccharomyces cerevisiae*, *Arabidopsis thaliana*, *Zea mays*, *Cucimus sativus*, *Homo sapiens*, *Capra hircus*, *Dermatophagoides farina*, and *Salmo salar* have deaminase activity *in vitro* (Degani et al., 2018; ElRamlawy et al., 2016; Ernst & Downs, 2018; Fulton et al., 2022; Irons et al., 2018; Irons et al., 2019; Lambrecht et al., 2012; Martínez-Chavarría et al., 2020; Whitaker et al., 2021). To our knowledge, every Rid protein that contains the critical arginine residue has enamine/imine deaminase activity on one or more substrates *in vitro*. Based on these data,

genomic annotations would be improved if they included the prediction of deaminase activity for those Rid family members containing the relevant arginine (Arg105). It is equally important that Rid family members lacking the active site arginine ar annotated to indicate they do not have imine/enamine deaminase activity.

1.8 2-AMINOACRYLATE IS AN ENDOGENOUSLY GENERATED METABOLITE STRESSOR

In the physiological context of its discovery, RidA deaminated 2-aminocrotonate (2AC) generated from threonine by IlvA to prevent it from allowing PurF-independent PRA formation (Figure 3) (Enos-Berlage et al., 1998; Lambrecht et al., 2012). The conservation of RidA hinted that deamination of 2AC was not the function of the protein that drove its retention in so many genomes across all domains of life. The sensitivity of a *ridA* mutant of *S. enterica* to exogenous serine led to a proposed role that would be more broadly relevant. Genetic data determined that activity of the PLP-dependent serine/threonine dehydratase, IlvA, was required for the serine-sensitive phenotype. Together these data led to a hypothesis that formation of the serine-derived enamine, 2AA, would be increased by the exogenous serine and that the reactive intermediate would accumulate in a *ridA* mutant. Finally, accumulation of 2AA was suggested to be the root cause of the serine induced lack of growth.

1.8.1 Enzymatic generation and biochemical consequences of 2-aminoacrylate. The suggestion that 2AA accumulation could negatively impact growth was prompted by previous *in vitro* studies. Historically, 2AA was used as a suicide inhibitor to probe the

catalytic mechanism of some PLP-dependent enzymes (Bisswanger, 1981; Kishore, 1984; Tate et al., 1969; Walsh, 1982; Whalen et al., 1985). In these studies, amino acid substrates with a strong electronegative leaving group (e.g. -Cl) bound to the β -carbon were provided to relevant PLP-dependent enzymes in vitro. Many of the queried enzymes had promiscuous β-elimination activity. In this case, 2AA generated during the β-elimination reaction attacks the PLP cofactor, covalently inactivating the enzyme by one of two mechanisms (Eliot & Kirsch, 2004; Likos et al., 1982; Ueno et al., 1982). This type of in vitro study provided precedent for the notion that 2AA could damage PLP-dependent enzymes in the cell and generate the phenotypes characteristic of a ridA mutant. Initially, there seemed to be two obstacles to extrapolating the *in vitro* results to a model for *in vivo* behavior of 2AA. First, the *in vitro* studies mentioned above involved 2AA attacking the same active site in which it was generated. These studies offered no indication that 2AA could leave the active site of one enzyme and enter the active site of another. In contrast, a suitable model for the *in vivo* situation required that 2AA leave the active site of IlvA, where it was generated from serine, and enter the active site of target enzyme(s) elsewhere in the cell. Second, given a reported half-life of 1-3 seconds, it was counterintuitive that the cellular milieu would allow persistence of 2AA to a level that would be detrimental (Burns et al., 1979; Flavin & Slaughter, 1964). Each of these concerns were lessened by data generated with targeted in vitro experiments. Data from these experiments showed that 2AA could leave the active site of one enzyme and attack PLP in the active site of another. These data were critical in the definition of the cellular role of RidA (Lambrecht et al., 2013). In the key experiments, a 2AA generator (IlvA) and a presumed target enzyme (IIvE) were combined with or without serine (the precursor to 2AA) in a reaction mixture.

IlvE is a PLP-dependent transaminase and was considered a potential target for 2AA damage in vivo based on phenotypic results (Lambrecht et al., 2013; Schmitz & Downs, 2004). Transaminase activity of IIvE was assayed after incubation with the 2AA-generating components. Data from these experiments showed that activity of IlvE was decreased following exposure to both serine and IlvA. Furthermore, IlvE was shown to be targeted by 2AA based on mass analysis of the protein before and after incubation with the 2AAgenerating system. Using mass spectrometry, a peak consistent with a modified IlvE protein was found in the samples with serine and IlvA, but not from those without serine added (Lambrecht et al., 2013; Shen et al., 2022). Results from this study successfully recapitulated the *in vivo* mechanism of 2AA stress suggested for a *ridA* mutant. Excitingly, when RidA protein was added to the reaction mixture, the *in situ* generation of 2AA by IlvA and serine did not decrease the activity of IlvE. Together these data painted the picture of metabolic differences between wild type and a ridA mutant, specifically, the persistence of 2AA. The mechanism of 2AA damage is expected to apply to several PLP-dependent enzymes, meaning that multiple enzymes might be impaired when cells experience 2AA stress. In this scenario, 2AA stress would be expected to dampen a variety of metabolic reactions, perturbing the metabolic network and generating the phenotypes observed for a ridA mutant. The correlation between in situ production of 2AA and decreased activity of a target enzyme suggested that enzymatic activity of 2AA targets could be used as a proxy for in vivo 2AA damage.

1.8.2 2-Aminoacrylate damages PLP-dependent enzymes *in vivo*. Biochemical experiments, summarized above, convincingly showed that 2AA could damage PLP-

dependent enzymes *in vitro*. Supported by the genetic analyses of *ridA* mutants, the hypothesis was extended to suggest an outline of 2AA stress *in vivo*. In this scenario 2AA, generated by IIvA acting on serine, would persist in the cell in the absence of the enamine/imine deaminase RidA. The persistence of 2AA would result in damage to specific PLP-dependent enzymes in the cell. 2AA differs from other enamine/imine metabolites that are generated as catalytic intermediates by PLP-dependent enzymes and those generated by NAD/FAD-dependent enzymes. While enamines and imines are characterized by their instability and short half-lives, 2AA appears unique in its ability to covalently modify PLP in enzyme active sites. This unique characteristic is likely due to 2AA being more reactive than other enamines (i.e. 2AC) and its ability to tautomerize between an enamine and imine species. Based on this attribute, 2AA was considered a potential metabolite stressor.

Results from *in vivo* experiments supported an emerging model that was prompted by the biochemical potential unveiled with *in vitro* analyses. Evidence that 2AA persisted in a *ridA* mutant of *S. enterica* was needed to validate this model. Accumulation of 2AA cannot be directly measured in cell extracts due the reactivity and short half-life of the molecule. Two approaches can be used to quantify 2AA persistence *in vivo* in the absence of RidA. In the first instance, enzyme activities of 2AA targets are assayed in crude extracts. A connection between activity and 2AA damage is established by comparing activity of a target enzyme in a wild-type strain and a *ridA* mutant strain, which is presumed to be under 2AA stress. If an enzyme is damaged by 2AA, its activity will be lower in the *ridA* mutant strain. Control experiments assay the same enzyme from the cells grown in a medium with added isoleucine, which allosterically inhibits IlvA – i.e. reduces its activity

and decreases 2AA formation. It follows that activity of a 2AA target enzyme will be restored in the ridA mutant when isoleucine is supplemented in the growth medium. Using this strategy, multiple PLP-dependent enzymes have been shown to be in vivo targets of 2AA damage. These include serine hydroxymethyl transferase (EC: 2.1.2.1) (Flynn & Downs, 2013; Shen et al., 2022), branched-chain amino acid aminotransferase (EC: 2.6.1.42) (Ernst & Downs, 2018; Schmitz & Downs, 2004), aspartate transaminase (EC: 2.6.1.1) (Borchert & Downs, 2017b), aminolevulinic synthase (EC: 2.3.1.37) (Whitaker et al., 2021), and cysteine desulfurase (EC: 2.8.1.7) (Fulton et al., 2022). To confirm that lowered enzyme activity is caused by 2AA-induced damage, the specific activity (not simply total activity) of the enzyme should be determined. While specific activity has not been determined for each enzyme mentioned above, both IIvE and alanine racemase (Alr) had lower specific activity in a *ridA* mutant compared to wild type (Flynn & Downs, 2013; Schmitz & Downs, 2004; Shen et al., 2022). Thus, the data support the notion that 2AA accumulation can be measured by proxy - i.e. comparing activity of a target enzyme with and without the presence of the 2AA stressor. BCAA aminotransferase (IIvE) is the enzyme of choice for these activity assays based on the simplicity of the assay, and the fact that 2AA damage to IlvE has been well established both in vitro and in vivo (Lambrecht et al., 2013; Schmitz & Downs, 2004; Shen et al., 2022). As more PLP-dependent enzymes are identified as targets of 2AA damage, it will be beneficial to establish a streamlined method to catalog all 2AA targets in an organism.

Early biochemical studies showed that after 2AA attack, a 2AA-PLP adduct was covalently bound to the active site of the enzyme (Roise et al., 1984). This adduct provides the means to directly measure, and quantify, enzyme damage caused by 2AA. Treatment

of a 2AA-damaged protein with weak base releases the 2AA-PLP adduct from the enzyme as pyruvate-PLP (Likos et al., 1982). Pyruvate-PLP can be easily distinguished from PLP by high pressure liquid chromatography (HPLC) (Figure 5) (Flynn & Downs, 2013; Shen et al., 2022). Alanine racemase (Alr) was used as a test case, and a protocol was developed to detect and quantify damage caused by 2AA in vivo (Flynn & Downs, 2013). This assay was expanded to determine if other potential target enzymes were damaged in vivo. The relevant enzymes were purified from the wild-type strain and a ridA mutant of S. enterica and treated with base to release cofactors, which were then separated by HPLC (Flynn & Downs, 2013; Schnackerz et al., 1979; Shen et al., 2022). This protocol quantifies the ratio of damaged to undamaged PLP cofactor and can be used with any strain background or growth condition. If an enzyme is damaged by 2AA in vivo, pyruvate-PLP will be present in some percentage of the individual enzymes purified from a ridA mutant. In most cases, the same protein purified from wild-type cells will be occupied only by a PLP cofactor. In contrast, some enzymes (e.g. IlvA) do not release any pyruvate-PLP, even when purified from the ridA mutant, indicating the active site of the protein has not been attacked by 2AA (Shen et al., 2022). In the case of IlvA, this result was particularly interesting since the catalytic mechanism of serine dehydratase generates 2AA. The reason the IlvA active site is not damaged by the 2AA it generates is not understood but is of continuing interest in the context of modelling 2AA stress in vivo.

Several PLP-dependent enzymes are attacked by 2AA *in vivo*. At present, this list includes at least isoleucine aminotransferase (IlvE), alanine racemase (Alr), serine hydroxymethyltransferase (GlyA), aspartate aminotransferase (AspC), phosphoserine aminotransferase (SerC) (Flynn & Downs, 2013; Shen et al., 2022) from *S. enterica*. This

Using this approach, the PLP-dependent enzymes aminolevulinic synthase (Hem1) from *S. cerevisiae* (Whitaker et al., 2021) and cysteine desulfurase (IscS) from *P. aeruginosa* (Fulton et al., 2022) were confirmed as targets of 2AA damage. This method to detect 2AA damage *in vivo* has the potential to facilitate the identification of active site residues that determine 2AA sensitivity, and to explore the properties of an active site that is resistant to attack. The latter features are especially intriguing when an enzyme generates 2AA in its active site, like IlvA. A variant of cysteine desulfurase (IscS) that is less sensitive to 2AA attack than the wild-type enzyme was isolated in *P. aeruginosa* as a suppressor of a 2AA-induced growth defect (Fulton et al., 2022). The IscSQ183P variant had significantly reduced enzymatic activity, highlighting the balance that exists between maintaining (or evolving) a catalytically efficient PLP-dependent active site and protecting said active site from attack by 2AA. More analysis is required to understand the parameters that constrain the evolution of active sites that are resistant to 2AA attack.

Much like the activity-based assays for single enzymes described above, analysis of protein cofactor content is currently a one-at-a-time approach that is laborious and time consuming. To improve our understanding of 2AA damage on a global scale will require creative approaches. An attractive basis for future global analysis is the strategy used by Sieber and colleagues to define the PLP-dependent proteome in different organisms (Hoegl et al., 2018). These investigators developed a workflow with functionalized cofactor probes and a strategy to label PLP-containing enzymes *in vivo*. Derivatization of the probe allowed the proteome to be selectively mined for PLP-associated proteins (Hoegl et al., 2018; Pfanzelt et al., 2022; Wilkinson et al., 2022). It is plausible that this workflow could be

modified to specifically detect enzymes with a covalently modified PLP active site (i.e. damaged by 2AA), and in this way begin to define the proteome of 2AA-damaged PLPdependent enzymes. It is exciting to consider that this method, and/or others, could lead to the definition of a 2AA "adduct-ome" of different organisms. Such a tool would generate insights into the response(s) of different metabolic network structures to the presence of the reactive 2AA metabolite stressor. Additionally, data from such experiments would facilitate the definition of an organism-specific "fingerprint" that would facilitate efforts to define cellular components involved in the generation of, and response to, 2AA stress. Like other global approaches, this process could define underlying consequences of 2AA stress that do not rise to the level of disruption needed to elicit a phenotype and therefore can go undetected. Ultimately, a proteomic approach could be used to define the sensitivity of different enzymes to 2AA, since not every enzyme is damaged to the same extent and not every damaged enzyme results in a detectable phenotypic consequence. Most significantly, a proteomic signature would make it practical to study 2AA stress beyond the model organisms that are easily manipulated in the laboratory.

1.9 THE 2-AMINOACRYLATE STRESS PARADIGM

The activity and physiological role of RidA has been defined with rigorous biochemical and phenotypic analyses, primarily in *S. enterica*, as outlined in the above sections. Data from these studies strongly indicate that RidA is an enamine/imine deaminase, with the physiologically relevant substrate being the reactive metabolite 2AA. Results from these studies defined a paradigm of 2AA stress that is schematically shown in Figure 6. The framework of this stress paradigm is that: i) PLP-dependent removal of β-

functional groups from α-amines generates the enamine/imine pair, 2AA/2-iminopropionate (2IP), ii) the deamination of 2AA/2IP can occur spontaneously by solvent water or by RidA, iii) the rate of spontaneous hydrolysis *in vivo* is insufficient to prevent 2AA accumulation in the absence of RidA, and iv) persisting 2AA results in covalent damage to some portion of sensitive PLP-enzymes. This damage results in decreased activity of the respective enzyme pool(s), eliciting metabolic stress that causes diverse phenotypes and metabolic deficiencies. In bacteria, 2AA is generated by several PLP-dependent enzymes including serine/threonine dehydratases (EC 4.3.1.19), cysteine desulfhydrases (EC 2.5.1.47) and diaminopropionate ammonia-lyases (EC 4.3.1.15). Reactions catalyzed by each of these enzymes have been associated with metabolic stress when RidA is not present, consistent with the role of 2AA as a stressor that is quenched by RidA (Ernst & Downs, 2016; Ernst et al., 2014; Schmitz & Downs, 2004).

The model in Figure 6 is consistent with several relevant observations. In a wild-type cell, 2AA is continually being generated and deaminated to pyruvate without any phenotypic or biochemical evidence that it persists at a level capable of causing damage. The observation that the loss of RidA does not always impair growth is consistent with the fact that deamination of 2AA can occur non-enzymatically by solvent water. This observation indicates that RidA activity is not "essential" to remove 2AA generated under many growth conditions (Borchert, Ernst, et al., 2019; Irons et al., 2020). However, even in the absence of a detectable growth defect, there is biochemical evidence of 2AA damage to PLP-enzymes in a *ridA* mutant of *S. enterica*. This finding indicates that 2AA persists in this background, though not always to a level that perturbs the metabolic network to affect growth. Tellingly, phenotypic defects can be induced in a *ridA* mutant with the

exogenous addition of precursors to 2AA, which increases production of the reactive molecule by various 2AA-generators (Ernst et al., 2016; Ernst et al., 2014; Irons et al., 2019; Lambrecht et al., 2013). These additions lead to a level of 2AA that exceeds the capacity of water-mediated deamination to maintain the activity of target enzymes required for normal growth. Importantly, when a wild-type strain is provided with a similar excess of a 2AA precursor metabolite, there is no apparent physiological defect, confirming that RidA can efficiently quench the elevated levels of 2AA.

2AA stress elicits multiple phenotypes that can be traced to damage of a single PLP-dependent enzyme (i.e. the "critical target" of 2AA). The specific critical target depends on the growth conditions and the metabolic architecture of the organism. Detectable consequences of 2AA damage identified so far include defects in alanine catabolism, Fe-S biosynthesis, heme biosynthesis, and one-carbon metabolism (Borchert & Downs, 2017b; Ernst & Downs, 2018; Flynn & Downs, 2013; Fulton et al., 2022; Shen et al., 2022; Whitaker et al., 2021). A phenotype for which no critical target has been identified is the compromised motility detected in ridA mutants of several organisms (Borchert & Downs, 2017a; Irons et al., 2018; Irons et al., 2019) (Collier, unpublished data). Despite the impaired motility caused by the persistence of 2AA, no PLP-dependent enzyme is known to be directly involved in motility in the relevant organisms. Campylobacter jejuni is an exception and provides an interesting scenario to study this phenomenon. In C. jejuni, PLP-dependent enzymes are indirectly involved in motility. In this organism, the flagellins must be O-glycosylated for their export across the cell membrane and subsequent assembly into the flagellar filament. Synthesis of a relevant glycan for this process, pseudaminic acid (Pse), requires the PLP-dependent transaminase

PseC (EC 2.6.1.92) (Ewing et al., 2009; Schoenhofen et al., 2006). Extrapolation of the 2AA stress paradigm defined in *S. enterica* suggests that 2AA would target the PseC transaminase in *C. jejuni*, decreasing its activity and resulting in decreased motility caused by a decreased synthesis of Pse. However, even if true in *C. jejuni*, damaged PseC would not explain the motility defects in *ridA* mutants of other bacteria. The data gathered so far suggest there may be multiple mechanisms by which 2AA affects motility in bacteria.

One molecule of 2AA is generated with every catalytic turnover of IlvA, or any other PLP-dependent enzyme that generates this reactive stressor metabolite. The RidA enzyme that removes 2AA appears to be constitutively expressed, which distinguishes this paradigm from a canonical stress response system that is regulated in response to a stressor. This feature raises questions that have yet to be addressed. Is RidA a housekeeping enzyme that is needed to maintain metabolic stability? Is it appropriate to designate it a stress-response protein rather than simply a modulator of metabolic homeostasis? Considering these questions is particularly appropriate given our emerging understanding of the function(s) of members of non-RidA subfamilies and their role(s) in the metabolic networks of various organisms, as discussed below.

A conspicuous characteristic of the 2AA system is that PLP- dependent enzymes comprise both the generators of 2AA and known enzyme targets of 2AA. At present, there are no structural characteristics of a PLP-dependent enzyme that can be used to predict if, or how efficiently, a protein will be targeted by 2AA. Enzymes with diverse mechanisms and of distinct fold-types have been shown to be targets of 2AA damage (Fulton et al., 2022; Shen et al., 2022). It will take the analysis of many more enzymes by methods discussed above to generate data necessary to define a consensus active site structure of a

targetable enzyme. Further studies on enzyme structure and mechanism will improve our understanding of how organisms have evolved to ensure a productive, efficient, and robust metabolic network, despite the presence of continuous challenges from reactive metabolites.

1.9.1 2-Aminoacrylate stress perturbs metabolic network function. The model for the RidA paradigm of 2AA stress was derived from data obtained in S. enterica. Since the major components of the system, PLP-enzymes and RidA, are highly conserved across microbes, the initial assumption was that the described paradigm could be extrapolated to other organisms. However, this assumption proved to be only partially correct. The mechanics of 2AA stress are indeed conserved in that PLP-dependent enzymes from any organism are targets of attack (Fulton et al., 2022; Shen et al., 2022; Whitaker et al., 2021), RidA homologs deaminate 2AA (Irons et al., 2019), and serine/threonine dehydratase is a highly conserved enzyme (Percudani & Peracchi, 2003). Thus, most microbes have the components to support a conserved 2AA stress response. As mentioned in the introductory sections, metabolic components do not always predict the structure of the system, and this is true in the case of the RidA paradigm. Despite the conserved ability of organisms to generate 2AA stress, the metabolic consequences (i.e. phenotypic output) of this stress vary, sometimes dramatically, between even closely related organisms. Varied phenotypic outputs reflect differences in metabolic network architecture between organisms. The RidA model presumes that 2AA stress dampens multiple metabolic enzymes (i.e. the PLPdependent enzyme targets). This overall dampening may not result in a growth defect under most conditions, since metabolic networks often possess more enzymatic capacity than needed and are thus able to absorb perturbations (Koenigsknecht et al., 2012; Ramos et al., 2008b; Sander et al., 2019). Context-dependent nutritional requirements, or other phenotypic consequences induced by 2AA stress, can be used to identify the PLP-dependent enzyme(s) critical for stability and/or function of the metabolic network under a given condition. This knowledge is valuable for defining metabolic connections and contributes to the overall understanding of the metabolic network of the relevant organism.

The response of an organism to 2AA stress cannot be predicted a priori and has been queried in the context of physiology in relatively few organisms. In S. enterica, increased 2AA stress caused by exogenous serine, cysteine, or 2,3-diaminopropionate generates a nutritional requirement that is satisfied by glycine. A series of biochemical and genetic analyses showed that inhibition of serine hydroxymethyltransferase (GlyA) by 2AA is the cause of the glycine requirement, making this enzyme the critical target when S. enterica is experiencing 2AA stress (Ernst & Downs, 2016; Flynn & Downs, 2013). Serine hydroxymethyltransferase is one of only two PLP-dependent enzymes that is encoded in the genomes of all free-living organisms, the other being aspartate transaminase (AspC) – another known target of 2AA damage (Percudani & Peracchi, 2003). The broad conservation of GlyA suggested that it might be the conserved critical target in other organisms. Analyses of *ridA* mutants in several organisms showed this was not the case. Even closely related species such as E. coli and S. enterica have significant differences in their response to 2AA stress, despite sharing an overwhelming majority of components in their metabolic networks (Borchert & Downs, 2017b). E. coli has two RidA homologs (RidA and TdcF) and elimination of both of these proteins does not generate an observable metabolic defect nor nutritional requirement. However, a ridA tdcF double mutant does

display a 2AA-dependent motility defect and the transcriptome differs from wild type, confirming the cell is being affected by 2AA (Collier, unpublished data; Borchert, unpublished data). Significantly, a growth defect is generated when 2AA production is artificially increased in an E. coli strain lacking the RidA homologs. This growth defect is not satisfied with glycine supplementation, indicating GlyA is not the critical target when E. coli is under 2AA stress (Borchert & Downs, 2017b). Rather, in an E. coli ridA tdcF mutant, aspartate restores growth under 2AA stress conditions, suggesting the critical target enzyme in E. coli could be aspartate transaminase. A variety of explanations for the differences in metabolic structure that would cause the phenotypic differences between S. enterica and E. coli under 2AA stress can be proposed. Differences in kinetics or substate specificity of key enzymes (i.e. IlvA), differing properties of the cellular milieu such as amino acid concentration, internal pH, local microenvironments, etc. are all considerations that could alter the 2AA stress system in one organism compared to another. In total, the differences in response to 2AA stress highlight our limited ability to define metabolic network structure based on genome composition and enzyme conservation.

In contrast to *E. coli*, *P. aeruginosa ridA* mutants appear ten-fold more sensitive to 2AA than *S. enterica* and exhibit a growth defect in minimal medium, even without serine added to increase 2AA stress (Fulton et al., 2022; Irons et al., 2018). Thiamine restored growth to a *P. aeruginosa ridA* mutant, while glycine supplementation had little to no effect. This nutritional requirement, and subsequent suppressor analysis, led to the conclusion that the cysteine desulfurase required for Fe-S cluster synthesis (IscS) is the critical target of 2AA in *P. aeruginosa* (Fulton et al., 2022). While IscS is not directly tied to thiamine synthesis, past work in *S. enterica* was leveraged to conclude that compromised

Fe-S synthesis indirectly affected thiamine biosynthesis. Although decreased Fe-S cluster synthesis impacts multiple enzymes in the cell, enzymes in thiamine biosynthesis, ThiC and ThiH are most sensitive to this effect (Skovran & Downs, 2000).

The physiological role of RidA has been addressed to different extents in two eukaryotic systems, Arabidopsis thaliana and S. cerevisiase. Niehaus et al., 2014 determined that A. thaliana strains lacking RidA were defective in root development, which was exacerbated by serine and eliminated by isoleucine (Niehaus et al., 2014). These characteristics confirmed the presence of a 2AA stress system with features resembling the RidA paradigm in S. enterica. Presumably, the defect in root development is the consequence of damage to one or more PLP-dependent enzymes which have not been identified. In S. cerevisiae the RidA homolog is Mmf1, named as mitochondrial matrix factor based on the finding that strains lacking this protein lose mitochondrial DNA (Oxelmark et al., 2000) and are defective in isoleucine biosynthesis (Kim, 2001). These two studies were carried out before the biochemical function RidA proteins were known. Subsequent studies defined the role of Mmf1 in the context of the emerging paradigm of 2AA stress in bacteria and found many similarities with the S. enterica paradigm. In the absence of Mmfl, accumulation of 2AA causes transient metabolic stress and irreversible loss of mtDNA (Ernst & Downs, 2018). The relevant 2AA is generated from serine by one of two serine/threonine dehydratases (Cha1p, Ilv1p), which are differentially regulated by transcription and allosteric inhibition, respectively (Ahmed et al., 1976; Bornaes et al., 1993). The PLP-enzyme targets of 2AA that cause the pleotropic effects of 2AA accumulation in S. cerevisiae are presumed to be mitochondrially located but remain unknown. Hem1 (aminolevulinic acid synthase, EC: 2.3.1.37) and Bat1 (branched chain

amino acid transferase) are mitochondrially located and damaged by 2AA (Ernst & Downs, 2018; Whitaker et al., 2021), but neither adequately explains all phenotypes caused by 2AA stress in *S. cerevisiae*. It is interesting to note that in both eukaryotic systems tested to date, RidA is present in a cellular compartment with several key PLP-dependent enzymes, such as those involved in the synthesis of branched chain amino acids, heme, and Fe-S clusters. Continued studies in these systems will provide a better understanding of the significance of this correlation and the critical enzymes in yeast that are affected by 2AA stress.

C. jejuni stands out among the organisms in which 2AA stress has been investigated. C. jejuni lacking the RidA homolog exhibits a motility defect, aberrant flagellar structure, and a defect in autoagglutination (Irons et al., 2019). Striking among these findings was that all phenotypes manifested on nutrient medium. In other organisms, nutrients (i.e. isoleucine) present in rich medium prevent 2AA stress. The IlvA homolog in C. jejuni lacks a regulatory domain and deletion of the gene did not rescue the observed phenotypes (Irons et al., 2019). Thus, in C. jejuni, the source of 2AA and potential target enzymes are not clearly defined, and it remains possible that the role of RidA in this organism differs from other bacteria.

Physiological and biochemical genetic studies of RidA paralogs from various organisms have strengthened the RidA paradigm and expanded our understanding of the effects of reactive intermediates in metabolism. The serendipitous discovery and subsequent characterization of RidA function in *S. enterica* and other organisms, prompted a growing interest in studying other members of the Rid superfamily and their contributions to cellular physiology. Together these studies suggest 2AA stress could be a useful tool in probing nuances that exist in metabolic networks. The diverse manifestations of 2AA

stress across organisms emphasizes the different structures metabolic networks can have even when they contain the same component parts (Downs et al., 2018).

1.9.2 Physiological consequences of 2-aminoacrylate stress. The phenotypes caused by the loss of a RidA protein indicate that 2AA stress impacts the overall physiology of an organism. To fully describe the effects of 2AA stress on a metabolic system, two parameters must be defined: i) the targets of 2AA stress and ii) how they impact the overall function of the metabolic network. At this point, all known targets of 2AA stress are PLP-dependent enzymes, and intriguing questions linger on the global level. What distinguishes the proteins targeted by 2AA from the resistant ones? What are the criteria that determine the hierarchy of damage among different target enzymes? What is the ratio of each protein pool that is inactivated by 2AA? These questions are difficult to address with our current technology and approaches, but with the development of productive global approaches in the future these questions will be approachable. An attractive reductionist approach would be to initiate *in vitro* "competition" between target enzymes. Such an approach would involve providing a population of different target enzymes and exposing them to 2AA generated *in situ*, before monitoring the activity of each enzyme.

Many consequences of 2AA stress are likely to be absorbed by the robustness of the metabolic system and will therefore fail to generate a detectable phenotype. In considering this possibility, global approaches provide the opportunity to identify metabolic changes caused by 2AA stress and better understand the structure of the relevant metabolic network and its response to perturbation. Three studies have taken a global approach to address the indirect consequences of 2AA stress in *S. enterica* not detected by

phenotypic analysis (A. Borchert et al., 2020; Borchert & Downs, 2017a; Borchert, Walejko, et al., 2019). In the first case, the transcriptome of a ridA mutant was compared to that of wild type when the strains were grown in minimal medium – i.e. when no growth phenotype is visible for the *ridA* mutant. The premise of this study was that transcriptional changes would reflect the internal cellular environment and thus identify unknown areas of metabolism that were perturbed by 2AA. It was somewhat surprising that genes involved in metabolic pathways altered by increased 2AA levels (i.e. branched chain amino acids, one carbon metabolism) were not represented by changes in the transcriptional profile of ridA mutants. These results suggested that metabolic perturbations and allosteric regulation are primarily responsible for modulating the response to 2AA stress. It was thus of interest that expression level of multiple genes encoding flagellar assembly components in the ridA mutant were decreased in the ridA mutant. Pursuit of this observation was key in identifying the 2AA-induced motility defect in S. enterica (Borchert & Downs, 2017a). Compromised motility was subsequently identified as a result of the loss of RidA activity in multiple organisms, though the causative mechanism remains unclear. Data from two metabolomic studies of ridA mutants supported the model of 2AA stress that was derived from genetic analyses and consistently, identified differences in metabolite profiles between ridA mutant and wild-type cells. Significantly, these studies showed that the disruption of the metabolic profile caused by a *ridA* mutation was stabilized when the cells were grown with the addition of isoleucine, consistent with the role of isoleucine prevent 2AA synthesis (A. J. Borchert et al., 2020; Borchert, Walejko, et al., 2019). Future studies are needed to expand on these findings, and further expansion of global analyses of ridA mutants in other organisms will increase our understanding of 2AA stress.

Progress in our physiological understanding of 2AA stress is also facilitated by isolating and analyzing suppressing mutations of ridA mutant phenotypes. There are at least two mechanisms to eliminate 2AA-dependent growth defects by altering the structure of the metabolic network: i) mutations that reduce or eliminate 2AA stress, and ii) mutations that allow growth in the presence of 2AA stress, possibly by bypassing a critical enzyme under the relevant condition. A few of these studies have been performed in S. enterica and contributed to the details of the 2AA stress paradigm represented in Figure 6. Suppressor mutations that restore growth of a ridA mutant in the presence of excess 2AA stress most often reduce or eliminate the generation of 2AA. Mechanisms that reduced 2AA production most commonly altered the catalytic capacity of IlvA (Christopherson et al., 2012) or increased the synthesis of threonine/isoleucine (Borchert & Downs, 2018; Christopherson et al., 2012; Fulton et al., 2022). Some studies identified genes that could reduce 2AA stress when provided in trans on a multi-copy plasmid. Specifically, expression of cystathionine β -lyase (MetC, EC4.4.1.8) from S. enterica or the aspartate/glutamate racemase from multiple organisms restored growth of a ridA mutant in the presence of serine (D. C. Ernst et al., 2018; Hodge-Hanson et al., 2018). In each case, the accumulation of 2AA was reduced, as judged from the restored activity of the target protein IlvE, which was used as a proxy for 2AA damage (Fulton et al., 2022; Shen et al., 2022). Biochemical models and in vitro experiments suggested the decrease in 2AA was mediated by a catalytic intermediate produced by the respective enzymes. These metabolites were suspected of reacting with 2AA to generate a stable adduct, which prevented damage to cellular targets. These data show there are multiple means by which a cell can quench 2AA and suggest that, in some organisms, 2AA stress could be managed

without RidA. From another perspective, perhaps RidA is conserved because it forms a functional product from 2AA that is used in a metabolic pathway. In contrast, quenching 2AA with a metabolite would remove the reactive enamine but generate a non-productive adduct product, likely an inefficient metabolic strategy.

In a second scenario, mutations that altered critical targets, or bypassed the need for them, should arise as suppressors. Experiments in *P. aeruginosa* yielded a mutation that altered a target enzyme, IscS, and restored growth to a *ridA* mutant. The resulting IscS variant had two defining features: i) it retained cysteine desulfurase activity, although it was reduced, and ii) the IscS variant was less sensitive to damage by 2AA than the wild-type protein (Fulton et al., 2022). The decreased desulfurase activity of the variant IscS restored growth, but not to the level of wild-type cells. Other suppressor screens have failed to identify variants of additional target enzymes that had increased resistance to 2AA. The difficulty in isolating these mutations may reflect how difficult it is to retain catalytic activity while simultaneously altering sensitivity to 2AA attack. Perhaps this observation is not surprising, as the same active site is responsible for both properties.

1.10 RID FAMILY FUNCTION BEYOND RIDA AND 2-AMINOACRYLATE STRESS

In *S. enterica* RidA modulates pathway flux, blocks a moonlighting activity, and rapidly deaminates the reactive 2AA generated by multiple enzymes (i.e. IlvA, CdsH, DapL) (Browne et al., 2006; Ernst et al., 2016; Ernst et al., 2014; Lambrecht et al., 2013). Significantly, each of these roles was a result of the enamine/imine deaminase activity that unifies members of the RidA subfamily. Once it was defined, the RidA paradigm of 2AA

stress provided a framework to consider the Rid protein superfamily as a whole (Hodge-Hanson & Downs, 2017; Irons et al., 2020; Niehaus et al., 2015). Unlike members of other Rid subfamilies, RidA proteins are found in all domains, leading to the conclusion that the RidA was the ancestral protein from which the remaining seven subfamilies descended (Figure 1A) (Niehaus et al., 2015). Rid1, 2, 3, 4, 5, 6 and 7 proteins are found only in prokaryotic genomes, primarily bacteria, and are particularly abundant in the Pseudomonadota (i.e. Proteobacteria). The NCBI conserved domain database uses a position-specific scoring matrix (Marchler-Bauer et al., 2013) to define the various Rid subfamilies, but it remains difficult to classify Rid proteins by sequence alone. In contrast to the somewhat imprecise definition of the eight subfamilies by sequence characteristics, members of the Rid superfamily are easily separated into two groups based on a critical arginine residue. The relevant arginine (Arg105 in S. enterica) is essential for imine/enamine deaminase activity in all cases where it has been queried experimentally (Buckner et al., 2021; Lambrecht et al., 2012; Niehaus et al., 2015). Based on these data, and the conservation of sequence and structure within the Rid superfamily, proteins with the Arg105 residue (members of the RidA and Rid1, 2 and 3 subfamilies) are considered deaminases. Similarly, those lacking the residue (members of the Rid 4, 5, 6 and 7 subfamilies) are assumed to lack deaminase activity. No member of the latter subfamilies has been reported to have deaminase activity, making it likely these proteins have a distinct, non-deaminase function(s) that may be conserved. Thus far, no exceptions to this designation have been reported.

In the absence of a putative, physiologically relevant imine/enamine substrate, Rid family members are assayed using a generic imine generator. In the commonly used assay,

commercially available FAD-dependent L-amino acid oxidase (LOX) generates imine intermediates *in situ* from a spectrum of amino acids (Buckner et al., 2021; Digiovanni et al., 2021; Fulton & Downs, 2022; Hodge-Hanson & Downs, 2017; Irons et al., 2018; Niehaus et al., 2015) (Figure 4). While convenient, this assay does not give information about the physiological relevance of deaminase activity, or potential substrates. Rather, the LOX assay provides a panel of imine substrates with which various Rid proteins can be tested and compared.

Data from LOX-deaminase assays, combined with *in vivo* complementation experiments, support some distinction between the Rid subfamilies. For instance, among the subfamilies carrying the Arg105 residue – Rid1 proteins consistently complement growth defects of a *ridA* mutant of *S. enterica* when expressed *in trans*, albeit less effectively than RidA proteins. In contrast, Rid2 and Rid3 proteins must be highly expressed to restore growth to a *ridA* mutant under conditions of 2AA stress, and some of these proteins may not complement a *ridA* mutant at all (Hodge-Hanson & Downs, 2017). In general, Rid2 and Rid3 proteins deaminate substrates that RidA and Rid1 proteins have little to no activity with *in vitro*, specifically iminohistidine, iminophenylalanine and iminoarginine (Fulton et al., 2022; Hodge-Hanson & Downs, 2017). While trends seem to be emerging, the correlations between substrate specificity and Rid subfamily are currently based on relatively few data points. Expansion of this type of biochemical analysis will improve our understanding of structure/function relationships in the Rid superfamily and allow a better delineation of the subfamilies.

The study of Rid proteins is emerging as a field with the potential to provide exciting insights into biochemistry, bacterial physiology, and metabolism. Despite the

rigorous characterization of numerous RidA paralogs, little is known about the physiological role(s) of members of other Rid subfamilies. Recent work has demonstrated a physiological role for DadY (Rid2 subfamily) in *P. aeruginosa* and Rid7C (Rid7 subfamily) in *Nonomuraea garenzanensis* (Damiano et al., 2022; Fulton & Downs, 2022) and presented strong biochemical evidence for the function of RutC (Rid1 subfamily) in *E. coli* (Buckner et al., 2021).

1.10.1 Genomic context suggests Rid protein function. Gene clustering in Prokaryotes can imply function, particularly if genes group together with varying configurations across multiple organisms. However, the physiological role of a gene product can rarely be defined by this consideration alone. Analysis of the genomic context of genes encoding Rid proteins in 981 representative genomes found they clustered with genes involved in a variety of metabolic processes (Niehaus et al., 2015). Rid proteins of the subfamilies expected to catalyze deamination tend to cluster with genes encoding PLP-, FAD-, or NAD-dependent enzymes. Enzymes in each of these classes have the ability to generate imine/enamine intermediates in their catalytic mechanisms (Fulton & Downs, 2022; Hafner & Wellner, 1979; He et al., 2011; Irons et al., 2020; Niehaus et al., 2015; Porter & Bright, 1972). For example, proteins DadY (PA5303) and DguB (PA5083) belong to the Rid2 subfamily and are encoded in the genomes of many *Pseudomonas*, as well as some Acinetobacter, species (PubSeed Database, Pseudomonas Genome Database). These genes are in loci with FAD-dependent D-amino acid dehydrogenases, which have been shown to proceed through imine intermediates in their catalytic mechanism (Fulton & Downs, 2022; Hafner & Wellner, 1979; He et al., 2011; He et al., 2014; Porter & Bright, 1972).

Other members of the Rid1, 2, and 3 subfamilies cluster with genes that encode FAD-, NAD-, or PLP-dependent enzymes that are predicted to use diverse substrates such as alcohols, amines, and aromatic compounds (Boulette et al., 2009; Chirino et al., 2013; Chou et al., 2008; Davis et al., 1999; He et al., 2011; He et al., 2014; He & Spain, 1998; Irons et al., 2020; Muraki et al., 2003; Orii et al., 2004; Park & Kim, 2001; Takenaka et al., 2000; Zhou et al., 2013). Based largely on this genomic context, Rid proteins are implicated in the degradation of aromatic compounds in various *Pseudomonas*, *Burkholderia*, *Paraburkholderia*, and *Bordatella* species (Davis et al., 1999; He & Spain, 1998; Irons et al., 2020; Muraki et al., 2003; Niehaus et al., 2015; Orii et al., 2004; Park & Kim, 2001). Definitive classification of the Rid subfamilies, and their functions, awaits definition of clear biochemical properties that distinguish them from one another.

1.10.2 New functions defined for Rid family members. Considerable strides have been made in recent years to enhance our understanding of Rid proteins and their contributions to a robust metabolism. As was the case with RidA, the study of other Rid subfamilies has benefited considerably from investigation in numerous organisms with varying metabolic architectures. These initial studies, summarized below, support the importance of biochemical analysis and creative experimental design in the study of this ubiquitous family of proteins.

1.10.2.a RutC is a 3-aminoacrylate deaminase. The first Rid protein beyond RidA to have a rigorously defined, physiologically relevant biochemical activity is RutC from E. coli. RutC is situated in the rut operon (rutABCDEFG) for pyrimidine utilization. The Rut

pathway was reconstituted in vitro without RutC, RutD or RutE, which led investigators to propose multiple non-enzymatic reactions in the pathway (Kim et al., 2010). This initial work was carried out before deaminase activity had been associated with the Rid family. Based on knowledge of the deaminase activity of those members of the Rid family that contain the critical arginine, further characterization of RutC was pursued (Buckner et al., 2021). In a pure system, RutC had 2AA deaminase activity comparable to that of RidA, yet the protein only partially complemented growth defects of a ridA mutant when provided in trans. With the semicarbazide-based LOX assay RutC deaminated multiple imines. Significantly, RutC was more active on imines derived from histidine, arginine, and phenylalanine than RidA. Thus, RutC had a similar substrate profile as Rid2 and Rid3 proteins (Hodge-Hanson & Downs, 2017). Critically, RutC has in vitro deaminase activity on the substrate implicated in the uracil utilization pathway (Buckner et al., 2021) (Figure 7). In an assay for RutC activity, purified RutB (peroxyureidoacrylate amidohydrolase) generated the 3-aminoacrylate (3AA) enamine species in situ from chemically synthesized ureidoacrylate. Consistent with the biochemistry of the proposed pathway for uracil utilization, RutC increased the rate of 3AA deamination over that achieved by solvent water, when quantified with a coupled assay (Buckner et al., 2021). These data suggested that RutC increases flux through the Rut pathway in vivo by removing a reactive 3AA metabolite released by RutB. Based on the genomic location and defined in vitro substrate for deamination, it was rational to predict a rutC mutation should compromise the utilization of uridine via the Rut pathway. Lesions in the other genes in the operon (i.e. rutB, rutE) had this expected phenotype (Kim et al., 2010), but loss of RutC activity did not result in a detectable defect in uridine catabolism. Despite the lack of an obvious

phenotype, this work described the first activity for a non-RidA subfamily member that could be placed in a physiological context. The study on RutC provided a blueprint for using gene context and the predicted biochemistry of nearby gene products to predict a Rid protein function and furthermore, suggested the need to more closely examine metabolic phenotypes.

1.10.2.b DadY is an iminoalanine deaminase. In many Pseudomonas species, the dad locus encodes genes that comprise a defined catabolic pathway for alanine – an AsnC-type regulator (DadR), FAD-dependent D-amino acid dehydrogenase (DadA) and a PLPdependent alanine racemase (DadX). Some dad loci also encode a member of the Rid2 subfamily (locus tag PA5303) (Fulton et al., 2022; He et al., 2011). No functional role in the catabolism of alanine was attributed to the Rid2 protein in initial studies of the pathway (Boulette et al., 2009; He et al., 2011). Recent work in *P. aeruginosa* led to the designation of the Rid2 protein as DadY and determined its physiological role was to deaminate iminoalanine to pyruvate in the alanine catabolic pathway (Figure 8A). Like many Rid proteins, DadY has 2AA deaminase activity in vitro, but does not complement a ridA mutant in vivo (Buckner et al., 2021; Fulton & Downs, 2022; Hodge-Hanson & Downs, 2017). Even if expression of the plasmid-borne dadY gene is induced, growth is not restored to the *ridA* mutant (Fulton & Downs, 2022). This apparent inconsistency between in vivo and in vitro assays that are presumed to measure the same activity (i.e. 2AA deamination) has arisen with multiple Rid proteins and represents an opportunity to refine the *in vitro* assay. Beyond activity on 2AA, DadY had significant deaminase activity with several imine substrates in the LOX-based assay. The substrate specificity of DadY

distinguished it from RidA despite an overlap in 2AA deaminase activity *in vitro*, a feature also noted for other non-RidA proteins. A model that would incorporate the activity of DadY in alanine catabolism required that the D-amino acid dehydrogenase (DadA) released an imine product into the cellular milieu. Biochemical analyses confirmed that DadA releases an imine into solution where it could form a semicarbazone compound. The addition of DadY to the DadA reaction mixture decreased the rate of semicarbazone formation, demonstrating that DadY was competing with semicarbazide for free imine in aqueous solution (Figure 8B) (Fulton et al., 2022). These data confirmed the biochemical potential for a catabolic pathway involving a deaminase, though a strain lacking *dadY* had no detectable growth defect. This work provided an opportunity to test a key hypothesis about the general contribution of Rid deaminases to a robust metabolic network, discussed below.

1.10.2.c Rid7C is an endoribonuclease. All Rid proteins of the "deaminase class" (i.e. those with the critical arginine residue) queried thus far have some manner of enamine/imine deaminase activity. The challenge to identify the relevant substrate(s) and physiological role of each Rid deaminase remains. However, members of four Rid subfamilies (Rid4, 5, 6, and 7) do not have deaminase activity. It remains to be seen if there is single activity that unifies these remaining proteins, or if multiple activities are represented in these subfamilies. Excitingly, a study in N. garenzanensis led to the definition of the first biochemical activity of a Rid family member lacking the critical arginine residue. In a situation reminiscent of the initial RidA observations, a role for a Rid7 protein was uncovered serendipitously. While investigating potential redundancy between two

paralogs of the beta subunit of RNA polymerase (RpoB) in N. garenzanensis, Damiano and colleagues determined that a Rid7 protein (Rid7C) had endoribonuclease activity (Damiano et al., 2022). Relevant to this study is the fact that this organism encodes two types of RNA polymerase, the result of two distinct beta subunits, RpoB(R) and RpoB(S) (Vigliotta et al., 2005). Significantly, the polymerase containing RpoB(R) controls expression of genes involved in generating secondary metabolites such as the antimicrobial A40926. Based on this involvement, the regulation and physiological function of RpoB(R) was of interest. Two mRNA transcripts encoding for RpoB(R) were found, presumed to be the result of two transcription start sites, and termed TSS1 and TSS2 (Tanaka et al., 2009). The TSS1mRNA formed a secondary structure including a hairpin that occluded the Shine-Dalgarno sequence and therefore suppressed translation of the rpoB(R) gene. In contrast, the TSS2 mRNA lacked the hairpin structure. The second transcript (TSS2) was derived from TSS1 by RNA processing mediated with the endoribonuclease activity of Rid7C (Damiano et al., 2022). Thus, Rid7C indirectly modulated the translation of RpoB(R). Importantly, overexpressing rid7C increased A40926 antibiotic production, a phenotype consistent with identified endoribonuclease activity (Damiano et al., 2022). While details of the endonuclease activity across organisms remain to be explored, the biochemical characterization of a Rid protein lacking the Arg105 residue provides a starting point for efforts to understand the Rid4, 5, 6 and 7 subfamilies. Although Arg105 is the only residue definitive of an activity thus far, variations in other conserved residues could hold the key to the divergent functions of proteins belonging to different subfamilies. The initial characterization of a Rid7 protein from N. garenzanensis extends the understanding of Rid family members that function outside of the RidA paradigm and raise new questions about Rid family members and their role in modulating the metabolic network in diverse microbes (Downs, 2022).

1.10.3 Competitive fitness is an informative phenotype. The general process to define the role of an uncharacterized gene involves both in vitro and in vivo components. When a function for the gene product is demonstrated biochemically and a metabolic role can be hypothesized based on the genomic context of the gene, the definitive result is a phenotype generated by lesions in the relevant gene, the simplest of which are null mutations. Phenotypes that can be easily screened in this process include nutritional requirements, sensitivity to various supplements or antimicrobials, excretion of metabolites, changes in motility and/or biofilm formation, etc. In situations where the predicted phenotype cannot be detected, it is worth considering whether the proposed gene function is incorrect, or whether the condition queried prevents visualization of the phenotype. In some cases, contribution of a gene product to the metabolic network is subtle or context-dependent, such that it complicates or even prevents the detection of a phenotype associated with a lesion in the relevant gene (Borchert & Downs, 2017b; Buckner et al., 2021; Damiano et al., 2022; Fulton & Downs, 2022; He et al., 2014; Irons et al., 2020; Lambrecht et al., 2013; Schmitz & Downs, 2004).

When an anticipated phenotype is not detected for a genetic lesion, two general explanations can be suggested. First, if a redundant activity is encoded in the genome, the absence of the subject gene may not produce a phenotype. Considered in isolation, such a result might prompt the incorrect conclusion that the relevant gene has little or no role in the metabolic network. This caveat is particularly applicable in the cases considered herein,

since genomes often encode multiple Rid family members with similar or indistinguishable activities in vitro. Second, the environment (i.e. temperature, medium, etc.) used for the phenotypic screening may be one in which the relevant gene product is not required and/or not present. This caveat is particularly problematic, as there are countless conditions in which phenotypes can be monitored. This point prompts the question of how one should interpret negative phenotypic results -i.e. does the lack of a phenotype indicate a lack of functional requirement? One way to increase the probability that a phenotype is detected is to sensitize the system of interest. This can be done by further perturbing the metabolic network, by an external stress or genetic modification, such that the system is more sensitive to a slightly compromised function. While it is difficult to design the right combination(s) of stressors in an absence of foundational knowledge of the system, careful selection of experimental conditions and genetic background, along with some amount of creativity and persistence, has proven successful in generating insights into physiological function. Probing varying environmental conditions and/or genetic backgrounds has led to the characterization of multiple genes of unknown function, not the least of which is RidA (Enos-Berlage et al., 1998). Phenotypic analysis has primarily been conducted in a laboratory setting with the relevant strains in pure culture. The contribution(s) of a gene product to the metabolic system might be too subtle to generate a detectable phenotype under standard laboratory conditions. However, if conservation is taken as an indication of significance, one would expect broadly conserved genes to contribute to the fitness of the organism under some condition.

Thus far, Rid proteins with the critical arginine residue catalyze reactions that can also occur non-enzymatically. Thus, it may not be surprising that these proteins are not

essential for function of their respective pathways in all situations. In the case of S. enterica, RidA is not required for steady state growth under most conditions. However, an increase in 2AA levels, caused by serine supplementation, overburdens the rate of non-enzymatic deamination, resulting in a detectable need for RidA. Recall that this perturbation was key in the functional characterization of RidA. The need to monitor the fitness cost(s) associated with loss of a Rid protein with an unknown functional role was first brought to light by the studies on RutC. As noted above, strains lacking RutC activity showed no detectable impairment in their ability utilize uridine as a source of nitrogen (Buckner et al., 2021). The proposed fitness cost of losing RutC activity is yet to be experimentally validated. A similar situation arose with DadY (PA5303) in *P. aeruginosa*, where both the genomic location and biochemical analyses implicated its deaminase activity in the catabolism of alanine (Fulton et al., 2022; Irons et al., 2020). Deletion of the dadY gene had no measurable effect on the ability of P. aeruginosa to use alanine as a carbon or nitrogen source in pure culture under standard laboratory conditions (Fulton et al., 2022). Importantly, strains lacking genes encoding other enzymes in the dad locus (dadA, and dadX) were required for alanine catabolism (Fulton et al., 2022; He et al., 2011). When grown with wild-type P. aeruginosa under conditions requiring the catabolism of alanine, a dadY mutant had a clear defect in competitive fitness (Fulton et al., 2022). These data, coupled with biochemical evidence discussed above, showed the imine deaminase activity of DadY was physiologically significant in a natural, competitive environment (Figure 8). This fitness defect described a critical metabolic role for DadY, despite the protein being considered "non-essential" based on a lack of detected phenotypes in the laboratory. The DadY study highlights the use of competition to probe the role of proteins that may have

subtle contributions to fitness. Like the other ideas discussed throughout, productive use of this approach is likely to require some idea of a metabolic context for the protein of interest. The characterization of DadY represented a milestone in our understanding of Rid proteins and provided the first clear support for the emerging model that members of the Rid superfamily modulate metabolism.

1.11 GENERAL MODEL FOR THE RID SUPERFAMILY AND REMAINING QUESTIONS

Analysis of RidA led to the identification of a biochemical activity (i.e. enamine/imine deamination) that was consistent with the phenotypes generated by its absence in *S. enterica*. The most impactful observation from these studies was that a protein could be required *in vivo* despite the relevant reaction occurring spontaneously. The characterization of 2AA damage, and the subsequent construction of a stress response model, has led all consequences of a *ridA* mutation to be viewed through this lens. For the most part, this view has been supported by the data obtained. However, RidA may also contribute to modulating metabolic flux. For instance, by deaminating 2AC to the pathway intermediate 2KB, RidA potentially maximizes the efficiency of branched chain amino acid biosynthesis. In this scenario, *ridA* mutants would have a fitness defect when grown on minimal medium, despite lack of growth defect in laboratory conditions. Competition experiments, like those implemented to characterize DadY in *P. aeruginosa* are needed to expand our understanding of these possibilities (Fulton et al., 2022).

ridA mutants in bacteria tested thus far have a pronounced motility defect, and/or problems with the generation or assembly of flagella (Borchert & Downs, 2017a; Fulton et

al., 2022; Irons et al., 2018; Irons et al., 2019). Studies in these bacteria (except for *C. jejuni*) found the motility defects were caused by 2AA accumulation by an unknown mechanism (Borchert & Downs, 2017a; Fulton et al., 2022) (A. Collier, unpublished data). The only characterized targets of 2AA damage are PLP-dependent enzymes, none of which are known to be directly involved in motility (Borchert & Downs, 2017a; Macnab, 1992). Compromised motility may be an indirect result of a damaged PLP-dependent enzyme or may indicate a novel mechanism of damage by the reactive species. In either case, the connection between motility and 2AA accumulation provides an opportunity to generate new physiological insights related to the 2AA stress paradigm.

An extended, or additional, role for RidA proteins is supported by the finding that some organisms encode multiple RidA paralogs. The significance of this apparent redundancy is unclear, as only a few systems have been rigorously investigated. *P. aeruginosa* encodes two RidA homologs, one of which (PA5339) was designated the housekeeping RidA, based on phenotypes paralleling the *ridA* mutant in *S. enterica* (Irons et al., 2018). The other RidA homolog (PA3123) had no role in ameliorating 2AA stress *in vivo*, despite biochemical and complementation studies supporting its classification as a *bona fide* RidA protein (Irons et al., 2018; Niehaus et al., 2015). The model eukaryote, *S. cerevisiae* encodes two RidA paralogs, Mmf1 and Hmf1, located in the mitochondria and cytoplasm, respectively (Kim, 2001; Oxelmark et al., 2000). Strains lacking the mitochondrial RidA (Mmf1) have phenotypes reminiscent of a bacterial *ridA* mutant, consistent with mitochondrial location of relevant 2AA-generating and target PLP-enzymes (Ernst & Downs, 2018; Whitaker et al., 2021). Somewhat surprisingly, the loss of the cytoplasmic RidA (Hmf1) elicits no detectable phenotype, even in the absence of

Mmf1. The conservation of RidA homologs in eukaryotes strongly suggests they have an important physiological role.

While the RidA paradigm has been well-established and allows for facile modeling of the role(s) of RidA proteins in various organisms, identifying the role(s) of the non-RidA subfamilies remains challenging. The non-RidA subfamilies can be grouped based on the presence or absence of the arginine critical for deaminase activity (Arg105). The current model suggests that proteins containing the Arg105 residue catalyze deamination reactions that can occur non-enzymatically. The implication of this model is that the relevant Rid proteins are only required for fitness under conditions where the rate of the relevant reaction becomes limiting for growth or fitness. Defining the two Rid protein functions that support this model relied on their genetic context to identify the relevant imine substrate (Buckner et al., 2021; Fulton & Downs, 2022). Many Rid proteins across genomes are in loci that contain genes of unknown function, or that are only annotated with general catalytic functions with no defined substrate (Christie et al., 2009; Merlin et al., 2002; Pena-Castillo & Hughes, 2007; S. Porwollik et al., 2014; Porwollik et al., 2002; Price et al., 2018). Therefore, there is a need to characterize genes surrounding the Rid-encoding gene before a hypothesis can be made for the role of the relevant Rid protein. The general idea that Rid proteins increase fitness by facilitating reactions that are otherwise spontaneous has the potential to define roles for them in diverse metabolic processes. This notion raises an interesting question. Might there be additional reactions in cellular metabolism that have been attributed to spontaneous chemistry that can uncover the role of additional Rid proteins? This exciting possibility should be considered as metabolic studies continue to focus on this large protein superfamily. Moving forward, creative

approaches will be needed to make significant progress in understanding the diverse reactions these proteins are likely to facilitate in supporting fitness of the organism.

One of the most significant recent advances in the understanding the Rid superfamily was the identification of an endonuclease activity for a Rid protein (Rid7C) that lacked the arginine critical for deaminase activity (Damiano et al., 2022). The knowledge that Rid proteins have a physiologically relevant activity not tied to imine/enamine deaminase activity raises exciting questions for future investigation. Will this broad class of Rid proteins (i.e. the Rid4, 5, 6 and 7 subfamilies) be distinguished by substrate specificity, or are there additional biochemical activities yet to be uncovered in these protein subfamilies? What is the connection between the deaminase and endonuclease activities? Does the ancestral RidA subfamily have both activities? Is it possible that some Rid proteins simultaneously lost deaminase activity while gaining a new function, or that they simply lost deaminase activity while retaining another, conserved activity? Future efforts are needed to determine if there is a general activity that ties the "non-deaminase" proteins, or the whole superfamily, together. The conservation of several key residues between deaminase and non-deaminase subfamilies suggests shared activities even between the more distantly related RidA and Rid7 subfamilies (Burman et al., 2007; Niehaus et al., 2015). Excitement about the demonstrated endonuclease activity aside, it is worth remembering that broad assumptions about the Rid family as whole may not be possible based on the activity of a single member. Although precedent set by the RidA paradigm in S. enterica appears to hold true thus far, questions raised above about the role of RidA proteins in modulating metabolic flux have not been addressed. Rigorous experimentation into the potential of all Rid proteins to perform additional, regulatory

functions within their respective pathways could bring our study of this diverse family of proteins closer to establishing a unified model that allows reliable predictions of the functions of various Rid proteins.

Whether accelerating non-enzymatic reactions or regulating gene expression with endonuclease activity, the apparent lack of dramatic phenotypes supports a unifying role of these proteins as modulators of the metabolic network. While the significance of these proteins might be overlooked based on results from classical laboratory experimentation, their broad conservation indicates strong selection for their maintenance and is likely due to evolutionarily significant contributions to fitness in the natural environments of each organism.

1.12 INSIGHTS GAINED AND LESSONS LEARNED FROM STUDIES OF THE RID SUPERFAMILY

The RidA paradigm of 2AA stress, defined in *S. enterica*, provides a context to interpret results in other organisms. While acknowledging there is much to be learned about RidA and the larger Rid protein superfamily, it is worth considering the insights generated by the foundational studies with respect to metabolic network structure. Unraveling the perturbations caused by 2AA stress revealed new insights about metabolic connectivity (Bazurto et al., 2016; Borchert & Downs, 2017b; Browne et al., 2006; Christopherson et al., 2008; Dustin C Ernst et al., 2018; Flynn et al., 2013; Fulton et al., 2022). These results suggest that 2AA stress can be used as a tool to study differences in metabolic network structure, much like the thiamine metabolic node has been (Koenigsknecht & Downs, 2010). Identifying mechanistic details of 2AA-induced phenotypes, defining critical target

enzymes and the resulting perturbations of the networks in various organisms, will provide fundamental new knowledge.

The recruitment of 2AC for the synthesis of the thiamine precursor, phosphoribosylamine (PRA) in a TrpD-dependent pathway was defined in the absence of RidA in *S. enterica* (Figures 2 and 3) (Browne et al., 2006; Lambrecht et al., 2010). Knowledge of this recruited pathway proved to be critical in showing that *E. coli* not only has this pathway, but it functions in the presence of RidA and generates ~50% of the PRA for thiamine synthesis (Bazurto et al., 2016). These results provide precedent for the possibility that other moonlighting activities or recruited pathways that depend on RidA, or other Rid proteins exist.

Characterization of RidA deaminase activity transformed the way we think about non-enzymatic reactions in the cell. Phenotypes resulting from the lack of RidA challenged the often-held notion that significant water was available in the cellular milieu. Despite the short half-life of 2AA in the presence of water, the genetic analysis convincingly led to the conclusion that this enamine could persist in the cellular milieu in the absence of RidA. This conclusion was substantiated by identifying the scars of 2AA damage *in vivo*.

Among Rid family members, those that are deaminases (i.e. have the critical arginine) showed some level of 2AA deaminase activity when tested *in vitro*. However, these non-RidA proteins do not complement a *ridA* mutant to the same degree as *ridA* when expressed *in trans*. This apparent inconsistency raises a concern about *in vitro* assays of Rid proteins and indicates nuances in cellular milieu that are not accounted for with *in vitro* conditions. As it stands, when genome annotation indicates there are multiple RidA proteins, the designation of the relevant housekeeping RidA has been based on phenotypic

analysis (Irons et al., 2018; Irons et al., 2019). Perhaps this approach is not optimal, considering that the loss of Rid proteins often fails to result in a detectable phenotype. The inconsistencies that arise as Rid proteins are analyzed in more organisms emphasize the need to better understand the role(s) of Rid proteins, and the differences between metabolic networks of these organisms. Perhaps more consistent and extensive correlations will emerge as knowledge accumulates from studies of individual Rid proteins across the domains of life. It is worth reiterating that biochemical activity *in vitro* provides information about the potential of an enzyme within a given metabolic network but does not define its function within the network. A more rigorous correlation between activity *in vitro* and *in vivo* for members of this protein superfamily will be critical to piece together the contribution of each Rid protein to the metabolic network it inhabits.

Analysis of the Rid superfamily has emphasized that competitive fitness can be a valuable tool to address the role(s) of genes of unknown function. Characterization of phenotypes displayed in pure culture can be expanded by considering the contribution of a gene product to fitness in the natural niche of an organism. Fitness can be difficult to monitor in pure culture, but it is a critical consideration from an evolutionary perspective. As we continue to refine our understanding of genomes and gene function, it is possible that many of the remaining genes of unknown function will play a modulatory, rather than mandatory, role in maintaining optimal function of the metabolic network. Studies of the RidA subfamily, emphasized how minimal dampening of multiple enzymes (by 2AA) can perturb the metabolic network and how the consequences vary across organisms (i.e., metabolic network architecture). Further, results discussed herein emphasize the many aspects of metabolism that cannot be predicted a priori even with well annotated genomes.

These conclusions illustrate the current inability to extract sufficient knowledge from a genome to model metabolic details and define network structure.

1.13 CONCLUDING REMARKS

Our current understanding of the RidA paradigm of 2AA stress, and the limited knowledge we have on members of other Rid subfamilies, represents only the tip of the iceberg in terms of the role of proteins in this superfamily. Though RidA has been studied in several bacterial systems, we lack an *in vivo* context for RidA activity in higher-order eukaryotes, most eukaryotic microbes, and archaea. Study of the RidA paradigm in the limited number of organisms tested so far has highlighted details and differences in both the paradigm itself, and the architectures of each metabolic network queried. Continuing studies on this intriguing protein superfamily across all domains of life will generate new and exciting insights into the metabolism and physiology of all living cells.

ACKNOWLEDGEMENTS

This work was supported by an award from the competitive grants program at the NIH (GM095837) to D.M.D and a predoctoral traineeship (T32GM007103) to R.L.F.

1.14 REFERENCES

Abdelhamid, Y., Brear, P., Greenhalgh, J., Chee, X., Rahman, T., & Welch, M. (2019). Evolutionary plasticity in the allosteric regulator-binding site of pyruvate kinase isoform PykA from *Pseudomonas aeruginosa*. *J Biol Chem*, 294(42), 15505-15516. https://doi.org/10.1074/jbc.RA119.009156

Ahmed, S. I., Bollon, A. P., Rogers, S. J., & Magee, P. T. (1976). Purification and properties of threonine deaminase from *Saccharomyces cerevisiae*. *Biochimie*, *58*(1-2), 225-232. https://doi.org/10.1016/s0300-9084(76)80374-4

- Bailey, A. M., Constantinidou, C., Ivens, A., Garvey, M. I., Webber, M. A., Coldham, N., Hobman, J. L., Wain, J., Woodward, M. J., & Piddock, L. J. (2009). Exposure of *Escherichia coli* and *Salmonella enterica* serovar Typhimurium to triclosan induces a species-specific response, including drug detoxification. *J Antimicrob Chemother*, 64(5), 973-985. https://doi.org/10.1093/jac/dkp320
- Bazurto, J. V., Bruger, E. L., Lee, J. A., Lambert, L. B., & Marx, C. J. (2021). Formaldehyde-responsive proteins, TtmR and EfgA, reveal a tradeoff between formaldehyde resistance and efficient transition to methylotrophy in *Methylorubrum extorquens*. *J Bacteriol*, 203(9). https://doi.org/10.1128/JB.00589-20
- Bazurto, J. V., Dearth, S. P., Tague, E. D., Campagna, S. R., & Downs, D. M. (2017). Untargeted metabolomics confirms and extends the understanding of the impact of aminoimidazole carboxamide ribotide (AICAR) in the metabolic network of *Salmonella enterica*. *Microb Cell*, 5(2), 74-87. https://doi.org/10.15698/mic2018.02.613
- Bazurto, J. V., & Downs, D. M. (2011). Plasticity in the purine-thiamine metabolic network of *Salmonella* [Research Support, N.I.H., Extramural
- Research Support, Non-U.S. Gov't]. *Genetics*, 187(2), 623-631. https://doi.org/10.1534/genetics.110.124362
- Bazurto, J. V., & Downs, D. M. (2016). Metabolic network structure and function in bacteria goes beyond conserved enzyme components. *Microb Cell*, *3*(6), 260-262. https://doi.org/10.15698/mic2016.06.509
- Bazurto, J. V., Farley, K. R., & Downs, D. M. (2016). An unexpected route to an essential cofactor: *Escherichia coli* relies on threonine for thiamine biosynthesis. *MBio*, 7(1), e01840-01815. https://doi.org/10.1128/mBio.01840-15
- Benov, L., & Fridovich, I. (2002). Induction of the soxRS regulon of *Escherichia coli* by glycolaldehyde. *Arch Biochem Biophys*, 407(1), 45-48. https://doi.org/10.1016/s0003-9861(02)00498-8
- Bisswanger, H. (1981). Substrate specificity of the pyruvate dehydrogenase complex from *Escherichia coli*. *J Biol Chem*, 256(2), 815-822. http://www.ncbi.nlm.nih.gov/entrez/query.fcgi?cmd=Retrieve&db=PubMed&dopt=Citati on&list_uids=7005225
- Blondel, C. J., Jimenez, J. C., Contreras, I., & Santiviago, C. A. (2009). Comparative genomic analysis uncovers 3 novel loci encoding type six secretion systems differentially distributed in *Salmonella* serotypes. *BMC Genomics*, *10*, 354. https://doi.org/1471-2164-10-354 [pii] 10.1186/1471-2164-10-354
- Borchert, A., Gouveia, G., Edison, A., & Downs, D. (2020). ¹H NMR metabolomics confirms serine hydroxymethyltransferase is the primary target of 2-aminoacrylate in a *ridA* mutant of *Salmonella enterica*. *mSys*, *In Revision*.

- Borchert, A. J., & Downs, D. M. (2017a). Endogenously generated 2-aminoacrylate inhibits motility in *Salmonella enterica*. *Sci Rep*, 7(1), 12971. https://doi.org/10.1038/s41598-017-13030-x
- Borchert, A. J., & Downs, D. M. (2017b). The response to 2-aminoacrylate differs in *Escherichia coli* and *Salmonella enterica*, despite shared metabolic components. *J Bacteriol*, 199(14). https://doi.org/10.1128/jb.00140-17
- Borchert, A. J., & Downs, D. M. (2018). Analyses of variants of the Ser/Thr dehydratase IlvA provide insight into 2-aminoacrylate metabolism in *Salmonella enterica*. *J Biol Chem*, 293(50), 19240-19249. https://doi.org/10.1074/jbc.RA118.005626
- Borchert, A. J., Ernst, D. C., & Downs, D. M. (2019). Reactive enamines and imines in vivo: Lessons from the RidA paradigm. *Trends Biochem Sci*, 44(10), 849-860. https://doi.org/10.1016/j.tibs.2019.04.011
- Borchert, A. J., Gouveia, G. J., Edison, A. S., & Downs, D. M. (2020). Proton nuclear magnetic resonance metabolomics corroborates serine hydroxymethyltransferase as the primary target of 2-aminoacrylate in a *ridA* mutant of *Salmonella enterica*. *mSystems*, 5(2). https://doi.org/10.1128/mSystems.00843-19
- Borchert, A. J., Walejko, J. M., Guennec, A. L., Ernst, D. C., Edison, A. S., & Downs, D. M. (2019). Integrated metabolomics and transcriptomics suggest the global metabolic response to 2-aminoacrylate stress in *Salmonella enterica*. *Metabolites*, *10*(1). https://doi.org/10.3390/metabo10010012
- Bornaes, C., Ignjatovic, M. W., Schjerling, P., Kielland-Brandt, M. C., & Holmberg, S. (1993). A regulatory element in the CHA1 promoter which confers inducibility by serine and threonine on *Saccharomyces cerevisiae* genes. *Mol Cell Biol*, *13*(12), 7604-7611. https://doi.org/10.1128/mcb.13.12.7604
- Boulette, M. L., Baynham, P. J., Jorth, P. A., Kukavica-Ibrulj, I., Longoria, A., Barrera, K., Levesque, R. C., & Whiteley, M. (2009). Characterization of alanine catabolism in *Pseudomonas aeruginosa* and its importance for proliferation in vivo. *J Bacteriol*, 191(20), 6329-6334. https://doi.org/10.1128/jb.00817-09
- Browne, B. A., Ramos, A. I., & Downs, D. M. (2006). PurF-independent phosphoribosyl amine formation in *yjgF* mutants of *Salmonella enterica* utilizes the tryptophan biosynthetic enzyme complex anthranilate synthase-phosphoribosyltransferase. *J Bacteriol*, *188*(19), 6786-6792.
- http://www.ncbi.nlm.nih.gov/entrez/query.fcgi?cmd=Retrieve&db=PubMed&dopt=Citation&list_uids=16980480_
- Buckner, B. A., Lato, A. M., Campagna, S. R., & Downs, D. M. (2021). The Rid family member RutC of *Escherichia coli* is a 3-aminoacrylate deaminase. *J Biol Chem*, 100651. https://doi.org/10.1016/j.jbc.2021.100651

- Burman, J. D., Stevenson, C. E., Sawers, R. G., & Lawson, D. M. (2007). The crystal structure of *Escherichia coli* TdcF, a member of the highly conserved YjgF/YER057c/UK114 family. *BMC Struct Biol*, 7, 30. https://doi.org/10.1186/1472-6807-7-30
- Burns, R. O., Hofler, J. G., & Luginbuhl, G. H. (1979). Threonine deaminase from *Salmonella typhimurium*. Substrate-specific patterns of inhibition in an activator site-deficient form of the enzyme. *J Biol Chem*, 254(4), 1074-1079. http://www.ncbi.nlm.nih.gov/entrez/query.fcgi?cmd=Retrieve&db=PubMed&dopt=Citati on&list_uids=368068
- Cain, A. K., Barquist, L., Goodman, A. L., Paulsen, I. T., Parkhill, J., & van Opijnen, T. (2020). A decade of advances in transposon-insertion sequencing. *Nat Rev Genet*, 21(9), 526-540. https://doi.org/10.1038/s41576-020-0244-x
- Ceciliani, F., Faotto, L., Negri, A., Colombo, I., Berra, B., Bartorelli, A., & Ronchi, S. (1996). The primary structure of UK114 tumor antigen. *FEBS Letters*, *393*, 147-150. http://www.ncbi.nlm.nih.gov/pubmed?term=The%20primary%20structure%20of%20UK114%20tumor%20antigen
- Chargaff, E., & Sprinson, D. B. (1943). Studies on the mechanism of deamination of serine and threonine in biological systems. *J Biol Chem*, 151, 273-280.
- Chavarria, M., Goni-Moreno, A., de Lorenzo, V., & Nikel, P. I. (2016). A metabolic widget adjusts the phosphoenolpyruvate-dependent fructose influx in *Pseudomonas putida*. mSystems, 1(6). https://doi.org/10.1128/mSystems.00154-16
- Chen, L., Lu, W., Wang, L., Xing, X., Chen, Z., Teng, X., Zeng, X., Muscarella, A. D., Shen, Y., Cowan, A., McReynolds, M. R., Kennedy, B. J., Lato, A. M., Campagna, S. R., Singh, M., & Rabinowitz, J. D. (2021). Metabolite discovery through global annotation of untargeted metabolomics data. *Nat Methods*, *18*(11), 1377-1385. https://doi.org/10.1038/s41592-021-01303-3
- Chen, P. W., Fonseca, L. L., Hannun, Y. A., & Voit, E. O. (2013). Coordination of rapid sphingolipid responses to heat stress in yeast. *PLoS Comput Biol*, *9*(5), e1003078. https://doi.org/10.1371/journal.pcbi.1003078
- Chirino, B., Strahsburger, E., Agullo, L., Gonzalez, M., & Seeger, M. (2013). Genomic and functional analyses of the 2-aminophenol catabolic pathway and partial conversion of its substrate into picolinic acid in *Burkholderia xenovorans* LB400. *PLoS ONE*, 8(10), e75746. https://doi.org/10.1371/journal.pone.0075746
- Chou, H. T., Kwon, D. H., Hegazy, M., & Lu, C. D. (2008). Transcriptome analysis of agmatine and putrescine catabolism in *Pseudomonas aeruginosa* PAO1. *J Bacteriol*, 190(6), 1966-1975. https://doi.org/10.1128/JB.01804-07

- Christie, K. R., Hong, E. L., & Cherry, J. M. (2009). Functional annotations for the *Saccharomyces cerevisiae* genome: the known and the known unknowns. *Trends Microbiol*, 17(7), 286-294. https://doi.org/10.1016/j.tim.2009.04.005
- Christopherson, M. R., Lambrecht, J. A., Downs, D., & Downs, D. M. (2012). Suppressor analyses identify threonine as a modulator of *ridA* mutant phenotypes in *Salmonella enterica* [Research Support, N.I.H., Extramural Research Support, Non-U.S. Gov't. Research Support, U.S. Gov't, Non-P.H.S.]. *PLoS ONE*, 7(8), e43082. https://doi.org/10.1371/journal.pone.0043082
- Christopherson, M. R., Schmitz, G. E., & Downs, D. M. (2008). YjgF is required for isoleucine biosynthesis when *Salmonella enterica* is grown on pyruvate medium. *J Bacteriol*, 190(8), 3057-3062. https://doi.org/10.1128/JB.01700-07
- Chubukov, V., Gerosa, L., Kochanowski, K., & Sauer, U. (2014). Coordination of microbial metabolism. *Nat Rev Microbiol*, *12*(5), 327-340. https://doi.org/10.1038/nrmicro3238
- Csonka, L. N., Gelvin, S. B., Goodner, B. W., Orser, C. S., Siemieniak, D., & Slightom, J. L. (1988). Nucleotide sequence of a mutation in the *proB* gene of *Escherichia coli* that confers proline overproduction and enhanced tolerance to osmotic stress. *Gene*, 64(2), 199-205. https://doi.org/10.1016/0378-1119(88)90335-6
- Damiano, F., Calcagnile, M., Pasanisi, D., Tala, A., Tredici, S. M., Giannotti, L., Siculella, L., & Alifano, P. (2022). Rid7C, a member of the YjgF/YER057c/UK114 (Rid) protein family, is a novel endoribonuclease that regulates the expression of a specialist rna polymerase involved in differentiation in *Nonomuraea gerenzanensis*. *J Bacteriol*, 204(2), e0046221. https://doi.org/10.1128/JB.00462-21
- DangThu, Q., Jang, S. H., & Lee, C. (2020). Biochemical comparison of two glucose 6-phosphate dehydrogenase isozymes from a cold-adapted *Pseudomonas mandelii*. *Extremophiles*, 24(4), 501-509. https://doi.org/10.1007/s00792-020-01171-3
- Davis, J. K., He, Z., Somerville, C. C., & Spain, J. C. (1999). Genetic and biochemical comparison of 2-aminophenol 1,6-dioxygenase of *Pseudomonas pseudoalcaligenes* JS45 to meta-cleavage dioxygenases: divergent evolution of 2-aminophenol meta-cleavage pathway. *Arch Microbiol*, 172(5), 330-339. https://doi.org/10.1007/s002030050787
- Deaconescu, A. M., Roll-Mecak, A., Bonanno, J. B., Gerchman, S. E., Kycia, H., Studier, F. W., & Burley, S. K. (2002). X-ray structure of *Saccharomyces cerevisiae* homologous mitochondrial matrix factor 1 (Hmf1). *Proteins*, 48(2), 431-436. http://www.ncbi.nlm.nih.gov/entrez/query.fcgi?cmd=Retrieve&db=PubMed&dopt=Citati on&list_uids=12112709
- Degani, G., Barbiroli, A., Regazzoni, L., Popolo, L., & Vanoni, M. A. (2018). Imine deaminase activity and conformational stability of UK114, the mammalian member of the Rid protein family active in amino acid metabolism. *Int J Mol Sci*, 19(4). https://doi.org/10.3390/ijms19040945

Deriu, D., Briand, C., Mistiniene, E., Naktinis, V., & Grutter, M. G. (2003). Structure and oligomeric state of the mammalian tumour-associated antigen UK114. *Acta Crystallogr D Biol Crystallogr*, 59(Pt 9), 1676-1678.

http://www.ncbi.nlm.nih.gov/entrez/query.fcgi?cmd=Retrieve&db=PubMed&dopt=Citation&list_uids=12925811

Dhawan, L., Liu, B., Pytlak, A., Kulshrestha, S., Blaxall, B. C., & Taubman, M. B. (2012). Y-box binding protein 1 and RNase UK114 mediate monocyte chemoattractant protein 1 mRNA stability in vascular smooth muscle cells. *Mol Cell Biol*, *32*(18), 3768-3775. https://doi.org/10.1128/MCB.00846-12

Digiovanni, S., Degani, G., Popolo, L., & Vanoni, M. A. (2021). Using D- and L-amino acid oxidases to generate the imino acid substrate to measure the activity of the novel Rid (enamine/imine deaminase) class of enzymes. *Methods Mol Biol*, *2280*, 199-218. https://doi.org/10.1007/978-1-0716-1286-6 13

Dougherty, M. J., & Downs, D. M. (2006). A connection between iron-sulfur cluster metabolism and the biosynthesis of 4-amino-5-hydroxymethyl-2-methylpyrimidine pyrophosphate in *Salmonella enterica*. *Microbiol.*, *152*(Pt 8), 2345-2353. http://www.ncbi.nlm.nih.gov/entrez/query.fcgi?cmd=Retrieve&db=PubMed&dopt=Citati on&list_uids=16849799_

Downs, D. (2022). Serendipity reveals the function and physiological role of a large family of proteins. *J Bacteriol*, 204(2), e0055621. https://doi.org/10.1128/JB.00556-21

Downs, D. M. (2003). Genomics and bacterial metabolism. *Current Issues in Molecular Biology*, 5(1), 17-25.

http://www.ncbi.nlm.nih.gov/entrez/query.fcgi?cmd=Retrieve&db=PubMed&dopt=Citation&list_uids=12638661

Downs, D. M., Bazurto, J. V., Gupta, A., Fonseca, L. L., & Voit, E. O. (2018). The three-legged stool of understanding metabolism: integrating metabolomics with biochemical genetics and computational modeling. *AIMS Microbiol*, *4*(2), 289-303. https://doi.org/10.3934/microbiol.2018.2.289

Downs, D. M., & Roth, J. R. (1991). Synthesis of thiamine in *Salmonella typhimurium* independent of the purF function. *J Bacteriol*, 173(20), 6597-6604. http://www.ncbi.nlm.nih.gov/entrez/query.fcgi?cmd=Retrieve&db=PubMed&dopt=Citati on&list_uids=1917881

Eliot, A. C., & Kirsch, J. F. (2004). Pyridoxal phosphate enzymes: mechanistic, structural, and evolutionary considerations. *Annu Rev Biochem*, *73*, 383-415. https://doi.org/10.1146/annurev.biochem.73.011303.074021

- ElRamlawy, K. G., Fujimura, T., Baba, K., Kim, J. W., Kawamoto, C., Isobe, T., Abe, T., Hodge-Hanson, K., Downs, D. M., Refaat, I. H., Beshr Al-Azhary, D., Aki, T., Asaoku, Y., Hayashi, T., Katsutani, T., Tsuboi, S., Ono, K., & Kawamoto, S. (2016). Der f 34, a Novel Major House Dust Mite Allergen Belonging to a Highly Conserved Rid/YjgF/YER057c/UK114 Family of Imine Deaminases. *J Biol Chem*, *291*(41), 21607-21615. https://doi.org/10.1074/jbc.M116.728006
- Enos-Berlage, J. L., Langendorf, M. J., & Downs, D. M. (1998). Complex metabolic phenotypes caused by a mutation in *yjgF*, encoding a member of the highly conserved YER057c/YjgF family of proteins. *J Bacteriol*, *180*(24), 6519-6528. http://www.ncbi.nlm.nih.gov/pubmed?term=Complex%20metabolic%20phenotypes%20 caused%20by%20a%20mutation%20in%20yjgF%2C%20encoding%20a%20member%2 0of%20the%20highly%20conserved%20YER057c%2FYjgF%20family%20of%20proteins
- Epelbaum, S., LaRossa, R. A., VanDyk, T. K., Elkayam, T., Chipman, D. M., & Barak, Z. (1998). Branched-chain amino acid biosynthesis in *Salmonella typhimurium*: a quantitative analysis. *Journal of Bacteriology*, *180*(16), 4056-4067. http://www.ncbi.nlm.nih.gov/entrez/query.fcgi?cmd=Retrieve&db=PubMed&dopt=Citati on&list_uids=9696751
- Ernst, D. C., Anderson, M. E., & Downs, D. M. (2016). L-2,3-diaminopropionate generates diverse metabolic stresses in *Salmonella enterica*. *Mol Microbiol*, *101*(2), 210-223. https://doi.org/10.1111/mmi.13384
- Ernst, D. C., Borchert, A. J., & Downs, D. M. (2018). Perturbation of the metabolic network in *Salmonella enterica* reveals cross-talk between coenzyme A and thiamine pathways. *PLoS ONE*, *13*(5), e0197703.
- Ernst, D. C., Christopherson, M. R., & Downs, D. M. (2018). Increased activity of cystathionine beta-lyase suppresses 2-aminoacrylate stress in *Salmonella enterica*. *J Bacteriol*. https://doi.org/10.1128/JB.00040-18
- Ernst, D. C., & Downs, D. M. (2016). 2-aminoacrylate stress induces a context-dependent glycine requirement in *ridA* strains of *Salmonella enterica*. *Journal of Bacteriology*, 198(3), 536-543. https://doi.org/10.1128/jb.00804-15
- Ernst, D. C., & Downs, D. M. (2018). Mmf1p Couples amino acid metabolism to mitochondrial DNA maintenance in *Saccharomyces cerevisiae*. *MBio*, 9(1). https://doi.org/10.1128/mBio.00084-18
- Ernst, D. C., Lambrecht, J. A., Schomer, R. A., & Downs, D. M. (2014). Endogenous synthesis of 2-aminoacrylate contributes to cysteine sensitivity in *Salmonella enterica*. *Journal of Bacteriology*, *196*(18), 3335-3342. https://doi.org/10.1128/jb.01960-14
- Ewing, C. P., Andreishcheva, E., & Guerry, P. (2009). Functional characterization of flagellin glycosylation in *Campylobacter jejuni* 81-176. *J Bacteriol*, *191*(22), 7086-7093. https://doi.org/10.1128/JB.00378-09

- Farkas, A., Nardai, G., Csermely, P., Tompa, P., & Friedrich, P. (2004). DUK114, the *Drosophila* orthologue of bovine brain calpain activator protein, is a molecular chaperone. *Biochem J*, 383(Pt 1), 165-170.
- http://www.ncbi.nlm.nih.gov/entrez/query.fcgi?cmd=Retrieve&db=PubMed&dopt=Citation&list_uids=15250825_
- Flavin, M., & Slaughter, C. (1964). An intermediate trapped by maleimides in a pyridoxal-phosphate potentiated enzymatic elimination reaction. *Biochemistry*, *3*, 885-893.
- http://www.ncbi.nlm.nih.gov/entrez/query.fcgi?cmd=Retrieve&db=PubMed&dopt=Citati on&list_uids=14214072
- Flynn, J. M., Christopherson, M. R., & Downs, D. M. (2013). Decreased coenzyme A levels in ridA mutant strains of *Salmonella enterica* result from inactivated serine hydroxymethyltransferase. *Mol Microbiol*, 89(4), 751-759. https://doi.org/10.1111/mmi.12313
- Flynn, J. M., & Downs, D. M. (2013). In the absence of RidA, endogenous 2-aminoacrylate inactivates alanine racemases by modifying the pyridoxal 5'-phosphate cofactor. *J Bacteriol*, 195(16), 3603-3609. https://doi.org/10.1128/jb.00463-13
- Fortuin, S., & Soares, N. C. (2022). The Integration of proteomics and metabolomics data paving the way for a better understanding of the mechanisms underlying microbial acquired drug resistance. *Front Med (Lausanne)*, *9*, 849838. https://doi.org/10.3389/fmed.2022.849838
- Fulton, R. L., & Downs, D. M. (2022). DadY (PA5303) is required for fitness of *Pseudomonas aeruginosa* when growth is dependent on alanine catabolism. *Microb Cell*, 9(12), 190-201. https://doi.org/10.15698/mic2022.12.788
- Fulton, R. L., Irons, J., & Downs, D. M. (2022). The cysteine desulfurase IscS is a significant target of 2-aminoacrylate damage in *Pseudomonas aeruginosa*. *MBio*, *13*(3), e0107122. https://doi.org/10.1128/mbio.01071-22
- Garcia-Jimenez, B., Torres-Bacete, J., & Nogales, J. (2021). Metabolic modelling approaches for describing and engineering microbial communities. *Comput Struct Biotechnol J*, 19, 226-246. https://doi.org/10.1016/j.csbj.2020.12.003
- Gelfand, D. H., & Steinberg, R. A. (1977). *Escherichia coli* mutants deficient in the aspartate and aromatic amino acid aminotransferases. *Journal of Bacteriology*, 130(1), 429-440.
- http://www.ncbi.nlm.nih.gov/entrez/query.fcgi?cmd=Retrieve&db=PubMed&dopt=Citation&list_uids=15983
- Hafner, E. W., & Wellner, D. (1979). Reactivity of the imino acids formed in the amino acid oxidase reaction. *Biochemistry*, 18(3), 411-417. http://www.ncbi.nlm.nih.gov/pubmed/33698

- He, W., Li, C., & Lu, C. D. (2011). Regulation and characterization of the dadRAX locus for D-amino acid catabolism in *Pseudomonas aeruginosa* PAO1. *J Bacteriol*, 193(9), 2107-2115. https://doi.org/10.1128/JB.00036-11
- He, W., Li, G., Yang, C. K., & Lu, C. D. (2014). Functional characterization of the dguRABC locus for D-Glu and d-Gln utilization in *Pseudomonas aeruginosa* PAO1. *Microbiology*, *160*(Pt 10), 2331-2340. https://doi.org/10.1099/mic.0.081141-0
- He, Z., & Spain, J. C. (1998). A novel 2-aminomuconate deaminase in the nitrobenzene degradation pathway of *Pseudomonas pseudoalcaligenes* JS45. *Journal of Bacteriology*, 180(9), 2502-2506. http://www.ncbi.nlm.nih.gov/pubmed/9573204
- Hodge-Hanson, K. M., & Downs, D. M. (2017). Members of the Rid protein family have broad imine deaminase activity and can accelerate the *Pseudomonas aeruginosa* Darginine dehydrogenase (DauA) reaction in vitro. *PLoS ONE*, *12*(9), e0185544. https://doi.org/10.1371/journal.pone.0185544
- Hodge-Hanson, K. M., Zoino, A., & Downs, D. M. (2018). Expression of PLP-independent racemases can reduce 2-aminoacrylate stress in *Salmonella enterica*. *J Bacteriol*. https://doi.org/10.1128/JB.00751-17
- Hoegl, A., Nodwell, M. B., Kirsch, V. C., Bach, N. C., Pfanzelt, M., Stahl, M., Schneider, S., & Sieber, S. A. (2018). Mining the cellular inventory of pyridoxal phosphate-dependent enzymes with functionalized cofactor mimics. *Nat Chem*, *10*(12), 1234-1245. https://doi.org/10.1038/s41557-018-0144-2
- Irons, J., Hodge-Hanson, K. M., & Downs, D. M. (2018). PA5339, a RidA homolog, is required for full growth in *Pseudomonas aeruginosa*. *J Bacteriol*, 200(22). https://doi.org/10.1128/jb.00434-18
- Irons, J., Sacher, J. C., Szymanski, C. M., & Downs, D. M. (2019). Cj1388 is a RidA homolog and is required for flagella biosynthesis and/or function in *Campylobacter jejuni*. Front Microbiol, 10, 2058. https://doi.org/10.3389/fmicb.2019.02058
- Irons, J. L., Hodge-Hanson, K., & Downs, D. M. (2020). RidA proteins protect against metabolic damage by reactive intermediates. *Microbiol Mol Biol Rev*, 84(3). https://doi.org/10.1128/mmbr.00024-20
- Johnston, H. M., & Roth, J. R. (1979). Histidine mutants requiring adenine: selection of mutants with reduced *hisG* expression in *Salmonella typhimurium*. *Genetics*, 92, 1-15. http://www.ncbi.nlm.nih.gov/pubmed?term=Histidine%20mutants%20requiring%20aden ine%3A%20%20selection%20of%20mutants%20with%20reduced%20hisG%20expression%20in%20Salmonella%20typhimurium
- Karr, J. R., Sanghvi, J. C., Macklin, D. N., Gutschow, M. V., Jacobs, J. M., Bolival, B., Jr., Assad-Garcia, N., Glass, J. I., & Covert, M. W. (2012). A whole-cell computational model predicts phenotype from genotype. *Cell*, *150*(2), 389-401. https://doi.org/10.1016/j.cell.2012.05.044

- Kim, J.-M. Y., Hiroshi; Shirahige, Katsuhiko. (2001). A member of the YER057c/yjgf/Uk114 family links isoleucine biosynthesis to intact mitochondria maintenance in *Saccharomyces cerevisiae*. *Genes to Cells*, 6, 507-517.
- Kim, K. S., Pelton, J. G., Inwood, W. B., Andersen, U., Kustu, S., & Wemmer, D. E. (2010). The Rut pathway for pyrimidine degradation: novel chemistry and toxicity problems. *J Bacteriol*, *192*(16), 4089-4102. https://doi.org/JB.00201-10 [pii]10.1128/JB.00201-10
- Kishore, G. M. (1984). Mechanism-based inactivation of bacterial kynureninase by beta-substituted amino acids. *J Biol Chem*, *259*(17), 10669-10674. http://www.ncbi.nlm.nih.gov/pubmed/6432787
- Knapik, A. A., Petkowski, J. J., Otwinowski, Z., Cymborowski, M. T., Cooper, D. R., Chruszcz, M., Krajewska, W. M., & Minor, W. (2012). Structure of *Escherichia coli* RutC, a member of the YjgF family and putative aminoacrylate peracid reductase of the rut operon. *Acta Crystallogr Sect F Struct Biol Cryst Commun*, 68(Pt 11), 1294-1299. https://doi.org/10.1107/S1744309112041796
- Koenigsknecht, M. J., & Downs, D. M. (2010). Thiamine biosynthesis can be used to dissect metabolic integration [Research Support, N.I.H., Extramural]. *Trends Microbiol*, 18(6), 240-247. https://doi.org/S0966-842X(10)00041-7 [pii]10.1016/j.tim.2010.03.003
- Koenigsknecht, M. J., Fenlon, L. A., & Downs, D. M. (2010). Phosphoribosylpyrophosphate synthetase (PrsA) variants alter cellular pools of ribose 5-phosphate and influence thiamine synthesis in *Salmonella enterica*. *Microbiology*, *156*(Pt 3), 950-959. https://doi.org/10.1099/mic.0.033050-0
- Koenigsknecht, M. J., Lambrecht, J. A., Fenlon, L. A., & Downs, D. M. (2012). Perturbations in histidine biosynthesis uncover robustness in the metabolic network of *Salmonella enterica*. *PLoS ONE*, 7(10), e48207. https://doi.org/10.1371/journal.pone.0048207
- Lambrecht, J. A., Browne, B. A., & Downs, D. M. (2010). Members of the YjgF/YER057c/UK114 family of proteins inhibit phosphoribosylamine synthesis in vitro. *J Biol Chem*, 285(45), 34401-34407. https://doi.org/10.1074/jbc.M110.160515
- Lambrecht, J. A., & Downs, D. M. (2013). Anthranilate phosphoribosyl transferase (TrpD) generates phosphoribosylamine for thiamine synthesis from enamines and phosphoribosyl pyrophosphate. *ACS Chem Biol*, 8(1), 242-248. https://doi.org/10.1021/cb300364k
- Lambrecht, J. A., Flynn, J. M., & Downs, D. M. (2012). Conserved YjgF protein family deaminates reactive enamine/imine intermediates of pyridoxal 5'-phosphate (PLP)-dependent enzyme reactions. *J Biol Chem*, 287(5), 3454-3461. https://doi.org/10.1074/jbc.M111.304477

- Lambrecht, J. A., Schmitz, G. E., & Downs, D. M. (2013). RidA proteins prevent metabolic damage inflicted by PLP-dependent dehydratases in all domains of life. *MBio*, 4(1), e00033-00013. https://doi.org/10.1128/mBio.00033-13
- LaRossa, R. A., & Van Dyk, T. K. (1987). Metabolic mayhem caused by 2-ketoacid imbalances. *Bioessays*, 7, 125-130.
- Lee, C., & Park, C. (2017). Bacterial responses to glyoxal and methylglyoxal: Reactive electrophilic species. *Int J Mol Sci*, 18(1). https://doi.org/10.3390/ijms18010169
- Lee, J. H., Lee, D. E., Lee, B. U., & Kim, H. S. (2003). Global analyses of transcriptomes and proteomes of a parent strain and an L-threonine-overproducing mutant strain. *J Bacteriol*, 185(18), 5442-5451. https://doi.org/10.1128/JB.185.18.5442-5451.2003
- Levy-Favatier, F., Cuisset, L., Nedelec, B., Tichonicky, L., Kruh, J., & Delpech, M. (1993). Characterization, purification, and cDNA cloning of a rat perchloric-acid-soluble 23-kDa protein present only in liver and kidney. *European Journal of Biochemistry*, 212, 665-673.
- Lewis, N. E., Cho, B. K., Knight, E. M., & Palsson, B. O. (2009). Gene expression profiling and the use of genome-scale in silico models of *Escherichia coli* for analysis: providing context for content. *J Bacteriol*, 191(11), 3437-3444. https://doi.org/10.1128/JB.00034-09
- Likos, J. J., Ueno, H., Feldhaus, R. W., & Metzler, D. E. (1982). A novel reaction of the coenzyme of glutamate decarboxylase with L-serine O-sulfate. *Biochemistry*, *21*(18), 4377-4386. http://www.ncbi.nlm.nih.gov/pubmed/6812624
- Link, H., Christodoulou, D., & Sauer, U. (2014). Advancing metabolic models with kinetic information. *Curr Opin Biotechnol*, *29*, 8-14. https://doi.org/10.1016/j.copbio.2014.01.015
- Litsios, A., Ortega, A. D., Wit, E. C., & Heinemann, M. (2018). Metabolic-flux dependent regulation of microbial physiology. *Curr Opin Microbiol*, 42, 71-78. https://doi.org/10.1016/j.mib.2017.10.029
- Long, C. P., & Antoniewicz, M. R. (2019). Metabolic flux responses to deletion of 20 core enzymes reveal flexibility and limits of *E. coli* metabolism. *Metab Eng*, 55, 249-257. https://doi.org/10.1016/j.ymben.2019.08.003
- Macnab, R. M. (1992). Genetics and biogenesis of bacterial flagella. *Annu Rev Genet*, 26, 131-158. https://doi.org/10.1146/annurev.ge.26.120192.001023
- Mallick, H., Franzosa, E. A., McLver, L. J., Banerjee, S., Sirota-Madi, A., Kostic, A. D., Clish, C. B., Vlamakis, H., Xavier, R. J., & Huttenhower, C. (2019). Predictive metabolomic profiling of microbial communities using amplicon or metagenomic sequences. *Nat Commun*, *10*(1), 3136. https://doi.org/10.1038/s41467-019-10927-1

Manjasetty, B. A., Delbruck, H., Pham, D., Mueller, U., Fieber-Erdmann, M., Scheich, C., Sievert, V., Bussow, K., Neisen, F. H., Weihofen, W., Loll, B., Saenger, W., & Heinemann, U. (2004). Crystal structure of *Homo sapiens* protein hp14.5. *Proteins: Stuct Funct Bioinform*, 54, 797-800.

http://www.ncbi.nlm.nih.gov/pubmed?term=Crystal%20structure%20of%20Homo%20sapiens%20protein%20hp14.5

Marchler-Bauer, A., Zheng, C., Chitsaz, F., Derbyshire, M. K., Geer, L. Y., Geer, R. C., Gonzales, N. R., Gwadz, M., Hurwitz, D. I., Lanczycki, C. J., Lu, F., Lu, S., Marchler, G. H., Song, J. S., Thanki, N., Yamashita, R. A., Zhang, D., & Bryant, S. H. (2013). CDD: conserved domains and protein three-dimensional structure. *Nucleic Acids Res*, 41(Database issue), D348-352. https://doi.org/10.1093/nar/gks1243

Martínez-Chavarría, L. C., Sagawa, J., Irons, J., Hinz, A. K., Lemon, A., Graça, T., Downs, D. M., & Vadyvaloo, V. (2020). Putative horizontally acquired genes, highly transcribed during *yersinia pestis* flea infection, are induced by hyperosmotic stress and function in aromatic amino acid metabolism. *J Bacteriol*, 202(11). https://doi.org/10.1128/jb.00733-19

McGill, S. L., Yung, Y., Hunt, K. A., Henson, M. A., Hanley, L., & Carlson, R. P. (2021). *Pseudomonas aeruginosa* reverse diauxie is a multidimensional, optimized, resource utilization strategy. *Sci Rep*, *11*(1), 1457. https://doi.org/10.1038/s41598-020-80522-8

McKenzie, G. J., Harris, R. S., Lee, P. L., & Rosenberg, S. M. (2000). The SOS response regulates adaptive mutation. *Proc Natl Acad Sci U S A*, 97(12), 6646-6651. https://doi.org/10.1073/pnas.120161797

Melloni, E., Michetti, M., Salamino, F., & Pontremoli, S. (1998). Molecular and functional properties of a calpain activator protein specific for *mu*-isoforms. *J Biol Chem*, 273(21), 12827-12831.

http://www.ncbi.nlm.nih.gov/entrez/query.fcgi?cmd=Retrieve&db=PubMed&dopt=Citation&list_uids=9582310

Merlin, C., McAteer, S., & Masters, M. (2002). Tools for characterization of *Escherichia coli* genes of unknown function. *J Bacteriol*, *184*(16), 4573-4581. https://doi.org/10.1128/JB.184.16.4573-4581.2002

Meysman, P., Sanchez-Rodriguez, A., Fu, Q., Marchal, K., & Engelen, K. (2013). Expression divergence between *Escherichia coli* and *Salmonella enterica* serovar Typhimurium reflects their lifestyles. *Mol Biol Evol*, *30*(6), 1302-1314. https://doi.org/10.1093/molbev/mst029

Mistiniene, E. (2003). Oligomeric assembly and ligan binding of the members of the protein family YER057C/YIL051c/YJGF. *Bioconjugate Chemistry*, 14, 1243-1252.

- Mistiniene, E., Luksa, V., Sereikaite, J., & Naktinis, V. (2003). Oligomeric assembly and ligand binding of the members of protein family YER057c/YIL051c/YJGF. *Bioconjug Chem*, 14(6), 1243-1252. https://doi.org/10.1021/bc0341066
- Mistiniene, E., Pozdniakovaite, N., Popendikyte, V., & Naktinis, V. (2005). Structure-based ligand binding sites of protein p14.5, a member of protein family YER057c/YIL051c/YjgF. *Int J Biol Macromol*, *37*(1-2), 61-68. http://www.ncbi.nlm.nih.gov/entrez/query.fcgi?cmd=Retrieve&db=PubMed&dopt=Citati on&list_uids=16198412
- Morishita, R., Kawagoshi, A., Sawasaki, T., Madin, K., Ogasawara, T., Oka, T., & Endo, Y. (1999). Ribonuclease activity of rat liver perchloric acid-soluble protein, a potent inhibitor of protein synthesis. *J Biol Chem*, *274*(29), 20688-20692. http://www.ncbi.nlm.nih.gov/entrez/query.fcgi?cmd=Retrieve&db=PubMed&dopt=Citati on&list_uids=10400702_
- Muraki, T., Taki, M., Hasegawa, Y., Iwaki, H., & Lau, P. C. (2003). Prokaryotic homologs of the eukaryotic 3-hydroxyanthranilate 3,4-dioxygenase and 2-amino-3-carboxymuconate-6-semialdehyde decarboxylase in the 2-nitrobenzoate degradation pathway of *Pseudomonas fluorescens* strain KU-7. *Appl Environ Microbiol*, 69(3), 1564-1572. https://doi.org/10.1128/AEM.69.3.1564-1572.2003
- Niehaus, T. D., Gerdes, S., Hodge-Hanson, K., Zhukov, A., Cooper, A. J., ElBadawi-Sidhu, M., Fiehn, O., Downs, D. M., & Hanson, A. D. (2015). Genomic and experimental evidence for multiple metabolic functions in the RidA/YjgF/YER057c/UK114 (Rid) protein family. *BMC Genomics*, *16*, 382. https://doi.org/10.1186/s12864-015-1584-3
- Niehaus, T. D., Nguyen, T. N., Gidda, S. K., ElBadawi-Sidhu, M., Lambrecht, J. A., McCarty, D. R., Downs, D. M., Cooper, A. J., Fiehn, O., Mullen, R. T., & Hanson, A. D. (2014). *Arabidopsis* and maize RidA proteins preempt reactive enamine/imine damage to branched-chain amino acid biosynthesis in plastids. *Plant Cell*, 26(7), 3010-3022. https://doi.org/10.1105/tpc.114.126854
- Oka, T., Tsuji, H., Noda, C., Sakai, K., Hong, Y. M., Suzuki, I., Munoz, S., & Natori, Y. (1995). Isolation and characterization of a novel perchloric acid-soluble protein inhibiting cell-free protein synthesis. *J Biol Chem*, *270*(50), 30060-30067. http://www.ncbi.nlm.nih.gov/entrez/query.fcgi?cmd=Retrieve&db=PubMed&dopt=Citati on&list_uids=8530410
- Orii, C., Takenaka, S., Murakami, S., & Aoki, K. (2004). A novel coupled enzyme assay reveals an enzyme responsible for the deamination of a chemically unstable intermediate in the metabolic pathway of 4-amino-3-hydroxybenzoic acid in *Bordetella sp.* strain 10d. *Eur J Biochem*, *271*(15), 3248-3254. https://doi.org/10.1111/j.1432-1033.2004.04258.xEJB4258 [pii]

- Oxelmark, E., Marchini, A., Malanchi, I., Magherini, F., Jaquet, L., Hajibagheri, M. A., Blight, K. J., Jauniaux, J. C., & Tommasino, M. (2000). Mmflp, a novel yeast mitochondrial protein conserved throughout evolution and involved in maintenance of the mitochondrial genome. *Mol Cell Biol*, 20(20), 7784-7797. http://www.ncbi.nlm.nih.gov/entrez/query.fcgi?cmd=Retrieve&db=PubMed&dopt=Citati on&list_uids=11003673
- Park, H. S., & Kim, H. S. (2001). Genetic and structural organization of the aminophenol catabolic operon and its implication for evolutionary process. *J Bacteriol*, 183(17), 5074-5081. https://doi.org/10.1128/JB.183.17.5074-5081.2001
- Parsons, L., Bonander, N., Eisenstein, E., Gilson, M., Kairys, V., & Orban, J. (2003). Solution structure and functional ligand screening of HI0719, a highly conserved protein from bacteria to humans in the YjgF/YER057c/UK114 family. *Biochemistry*, 42(1), 80-89.
- http://www.ncbi.nlm.nih.gov/entrez/query.fcgi?cmd=Retrieve&db=PubMed&dopt=Citation&list_uids=12515541
- Paxhia, M. D., & Downs, D. M. (2022). Pyridoxal and alpha-ketoglutarate independently improve function of *Saccharomyces cerevisiae* Thi5 in the metabolic network of *Salmonella enterica*. *J Bacteriol*, 204(1), e0045021. https://doi.org/10.1128/JB.00450-21
- Pearcy, N., Hu, Y., Baker, M., Maciel-Guerra, A., Xue, N., Wang, W., Kaler, J., Peng, Z., Li, F., & Dottorini, T. (2021). Genome-Scale metabolic models and machine learning reveal genetic determinants of antibiotic resistance in *Escherichia coli* and unravel the underlying metabolic adaptation mechanisms. *mSystems*, 6(4), e0091320. https://doi.org/10.1128/mSystems.00913-20
- Pena-Castillo, L., & Hughes, T. R. (2007). Why are there still over 1000 uncharacterized yeast genes? *Genetics*, 176(1), 7-14. https://doi.org/10.1534/genetics.107.074468
- Percudani, R., & Peracchi, A. (2003). A genomic overview of pyridoxal-phosphate-dependent enzymes. *EMBO Rep*, 4(9), 850-854. https://doi.org/10.1038/sj.embor.embor914
- Pfanzelt, M., Maher, T. E., Absmeier, R. M., Schwarz, M., & Sieber, S. A. (2022). Tailored pyridoxal probes unravel novel cofactor-dependent targets and antibiotic hits in critical bacterial pathogens. *Angew Chem Int Ed Engl*, *61*(24), e202117724. https://doi.org/10.1002/anie.202117724
- Phillips, A. T., & Wood, W. A. (1965). The mechanism of action of 5'-adenylic acidactivated threonine dehydratase. *Journal of Biological Chemistry*, 240(12), 4703-4709. http://www.ncbi.nlm.nih.gov/pubmed/5321308
- Porter, D. J., & Bright, H. J. (1972). The kinetics of imino acid accumulation in the Damino acid oxidase reaction. *Biochem Biophys Res Commun*, 46(2), 571-577. https://doi.org/10.1016/s0006-291x(72)80177-3

- Porwollik, S., Santiviago, C. A., Cheng, P., Long, F., Desai, P., Fredlund, J., Srikumar, S., Silva, C. A., Chu, W., Chen, X., Canals, R., Reynolds, M. M., Bogomolnaya, L., Shields, C., Cui, P., Guo, J., Zheng, Y., Endicott-Yazdani, T., Yang, H. J., . . . McClelland, M. (2014). Defined single-gene and multi-gene deletion mutant collections in *Salmonella enterica* sv Typhimurium. *PLoS ONE*, *9*(7), e99820. https://doi.org/10.1371/journal.pone.0099820
- Porwollik, S., Wong, R. M., & McClelland, M. (2002). Evolutionary genomics of *Salmonella*: gene acquisitions revealed by microarray analysis. *Proc Natl Acad Sci U S A*, 99(13), 8956-8961. https://doi.org/10.1073/pnas.122153699
- Powell, J. T., & Morrison, J. F. (1978). Role of the *Escherichia coli* aromatic amino acid aminotransferase in leucine biosynthesis. *Journal of Bacteriology*, *136*(1), 1-4. http://www.ncbi.nlm.nih.gov/entrez/query.fcgi?cmd=Retrieve&db=PubMed&dopt=Citati on&list_uids=361681
- Price, M. N., Wetmore, K. M., Waters, R. J., Callaghan, M., Ray, J., Liu, H., Kuehl, J. V., Melnyk, R. A., Lamson, J. S., Suh, Y., Carlson, H. K., Esquivel, Z., Sadeeshkumar, H., Chakraborty, R., Zane, G. M., Rubin, B. E., Wall, J. D., Visel, A., Bristow, J., . . . Deutschbauer, A. M. (2018). Mutant phenotypes for thousands of bacterial genes of unknown function. *Nature*, 557(7706), 503-509. https://doi.org/10.1038/s41586-018-0124-0
- Primerano, D. A., & Burns, R. O. (1983). Role of acetohydroxyacid isomeroreductase in biosynthesis of pantothenic acid in *Salmonella typhimurium*. *Journal of Bacteriology*, 153(259-269).
- Pu, Y. G., Jiang, Y. L., Ye, X. D., Ma, X. X., Guo, P. C., Lian, F. M., Teng, Y. B., Chen, Y., & Zhou, C. Z. (2011). Crystal structures and putative interface of *Saccharomyces cerevisiae* mitochondrial matrix proteins Mmf1 and Mam33. *J Struct Biol*, 175(3), 469-474. https://doi.org/S1047-8477(11)00137-7 [pii]10.1016/j.jsb.2011.05.005
- Rajagopal, B. S., DePonte, J., 3rd, Tuchman, M., & Malamy, M. H. (1998). Use of inducible feedback-resistant N-acetylglutamate synthetase (argA) genes for enhanced arginine biosynthesis by genetically engineered *Escherichia coli* K-12 strains. *Appl Environ Microbiol*, *64*(5), 1805-1811. https://doi.org/10.1128/AEM.64.5.1805-1811.1998
- Ramos, I., & Downs, D. M. (2003). Anthranilate synthase can generate sufficient phosphoribosyl amine for thiamine synthesis in *Salmonella enterica*. *Journal of Bacteriology*, 185(17), 5125-5132.
- http://www.ncbi.nlm.nih.gov/entrez/query.fcgi?cmd=Retrieve&db=PubMed&dopt=Citati on&list_uids=12923085
- Ramos, I., Vivas, E. I., & Downs, D. M. (2008b). Mutations in the tryptophan operon allow PurF-independent thiamine synthesis by altering flux *in vivo*. *J. Bact.*, 190(3), 815-822.http://www.ncbi.nlm.nih.gov/entrez/query.fcgi?cmd=Retrieve&db=PubMed&dopt=Citation&list_uids=17557816_

- Rappu, P., Shin, B. S., Zalkin, H., & Mantsala, P. (1999). A role for a highly conserved protein of unknown function in regulation of *Bacillus subtilis purA* by the purine repressor. *J Bacteriol*, 181(12), 3810-3815.
- http://www.ncbi.nlm.nih.gov/pubmed?term=A%20role%20for%20a%20highly%20conse rved%20protein%20of%20unknown%20function%20in%20regulation%20of%20Bacillu s%20subtilis%20purA%20by%20the%20purine%20repressor
- Roise, D., Soda, K., Yagi, T., & Walsh, C. T. (1984). Inactivation of the *Pseudomonas striata* broad specificity amino acid racemase by D and L isomers of beta-substituted alanines: kinetics, stoichiometry, active site peptide, and mechanistic studies [Research Support, U.S. Gov't, P.H.S.]. *Biochemistry*, 23(22), 5195-5201. http://www.ncbi.nlm.nih.gov/pubmed/6439237
- Sander, T., Farke, N., Diehl, C., Kuntz, M., Glatter, T., & Link, H. (2019). Allosteric feedback inhibition enables robust amino acid biosynthesis in *E. coli* by enforcing enzyme overabundance. *Cell Syst*, 8(1), 66-75 e68. https://doi.org/10.1016/j.cels.2018.12.005
- Sasagawa, T., Oka, T., Tokumura, A., Nishimoto, Y., Muñoz, S., Kuwahata, M., Okita, M., Tsuji, H., & Natori, Y. (1999). Analysis of the fatty acid components in a perchloric acid-soluble protein. *Biochim Biophys Acta*, *1437*(3), 317-324. https://doi.org/10.1016/s1388-1981(99)00025-6
- Schmiedeknecht, G., Kerkhoff, C., Orso, E., Stohr, J., Aslanidis, C., Nagy, G. M., Knuechel, R., & Schmitz, G. (1996). Isolation and characterization of a 14.5-kDa trichloroacetic-acid-soluble translational inhibitor protein from human monocytes that is upregulated upon cellular differentiation. *Eur J Biochem*, *242*(2), 339-351. http://www.ncbi.nlm.nih.gov/entrez/query.fcgi?cmd=Retrieve&db=PubMed&dopt=Citati on&list_uids=8973653
- Schmitz, G. (2006). A link between yjgF and isoleucine biosynthesis in Salmonella enterica serovar Typhimurium [PhD, University of Wisconsin-Madison]. Madison, Wisconsin.
- Schmitz, G., & Downs, D. M. (2004). Reduced transaminase B (IIvE) activity caused by the lack of *yjgF* is dependent on the status of threonine deaminase (IIvA) in *Salmonella enterica* serovar Typhimurium. *Journal of Bacteriology*, *186*(3), 803-810. https://doi.org/10.1128/jb.186.3.803-810.2004
- Schnackerz, K. D., Ehrlich, J. H., Giesemann, W., & Reed, T. A. (1979). Mechanism of action of D-serine dehydratase. Identification of a transient intermediate. *Biochemistry*, 18(16), 3557-3563. http://www.ncbi.nlm.nih.gov/pubmed/383145

- Schoenhofen, I. C., Lunin, V. V., Julien, J. P., Li, Y., Ajamian, E., Matte, A., Cygler, M., Brisson, J. R., Aubry, A., Logan, S. M., Bhatia, S., Wakarchuk, W. W., & Young, N. M. (2006). Structural and functional characterization of PseC, an aminotransferase involved in the biosynthesis of pseudaminic acid, an essential flagellar modification in *Helicobacter pylori*. *J Biol Chem*, 281(13), 8907-8916. https://doi.org/10.1074/jbc.M512987200
- Shen, W., Borchert, A. J., & Downs, D. M. (2022). 2-Aminoacrylate stress damages diverse PLP-dependent enzymes in vivo. *J Biol Chem*, 298(6), 101970. https://doi.org/10.1016/j.jbc.2022.101970
- Sheppard, D. E. (1964). Mutants of *Salmonella typhimurium* resistant to feedback inhibition by L-histidine. *Genetics*, *50*, 611-623.
- Singh, R., Barden, A., Mori, T., & Beilin, L. (2001). Advanced glycation end-products: a review. *Diabetologia*, 44(2), 129-146. https://doi.org/10.1007/s001250051591
- Sinha, S., Rappu, P., Lange, S. C., Mantsala, P., Zalkin, H., & Smith, J. L. (1999). Crystal structure of *Bacillus subtilis* YabJ, a purine regulatory protein and member of the highly conserved YjgF family. *Proc Natl Acad Sci U S A*, 96(23), 13074-13079. http://www.ncbi.nlm.nih.gov/cgi-
- bin/Entrez/referer?http://www.pnas.org/cgi/content/full/96/23/13074
- Skovran, E., & Downs, D. M. (2000). Metabolic defects caused by mutations in the *isc* gene cluster in *Salmonella enterica* serovar typhimurium: implications for thiamine synthesis. *J. Bacteriol.*, 182(14), 3896-3903.
- http://www.ncbi.nlm.nih.gov/pubmed?term=Metabolic%20defects%20caused%20by%20mutations%20in%20the%20isc%20gene%20cluster%20in%20Salmonella%20enterica%20serovar%20typhimurium%3A%20implications%20for%20thiamine%20synthesis
- Su, P., Feng, T., Zhou, X., Zhang, S., Zhang, Y., Cheng, J., Luo, Y., Peng, J., Zhang, Z., Lu, X., Zhang, D., & Liu, Y. (2015). Isolation of Rhp-PSP, a member of YER057c/YjgF/UK114 protein family with antiviral properties, from the photosynthetic bacterium *Rhodopseudomonas palustris* strain JSC-3b. *Sci Rep*, 5, 16121. https://doi.org/10.1038/srep16121
- Takenaka, S., Murakami, S., Kim, Y. J., & Aoki, K. (2000). Complete nucleotide sequence and functional analysis of the genes for 2-aminophenol metabolism from *Pseudomonas sp.* AP-3. *Arch Microbiol*, *174*(4), 265-272. https://doi.org/10.1007/s002030000203
- Tanaka, Y., Tokuyama, S., & Ochi, K. (2009). Activation of secondary metabolite-biosynthetic gene clusters by generating rsmG mutations in *Streptomyces griseus*. *J Antibiot (Tokyo)*, 62(12), 669-673. https://doi.org/10.1038/ja.2009.97
- Tang, J. (2011). Microbial metabolomics. *Curr Genomics*, *12*(6), 391-403. https://doi.org/10.2174/138920211797248619

- Tate, S. S., Relyea, N. M., & Meister, A. (1969). Interaction of L-aspartate beta-decarboxylase with beta-chloro-L-alanine. Beta-elimination reaction and active-site labeling. *Biochemistry*, 8(12), 5016-5021. http://www.ncbi.nlm.nih.gov/pubmed/5365791
- Thakur, K. G., Praveena, T., & Gopal, B. (2009). *Mycobacterium tuberculosis* Rv2704 is a member of the YjgF/YER057c/UK114 family. *Proteins*, 78(3), 773-778. http://www.ncbi.nlm.nih.gov/entrez/query.fcgi?cmd=Retrieve&db=PubMed&dopt=Citati on&list_uids=19899170_
- Thornalley, P. J. (1996). Pharmacology of methylglyoxal: formation, modification of proteins and nucleic acids, and enzymatic detoxification--a role in pathogenesis and antiproliferative chemotherapy. *Gen Pharmacol*, 27(4), 565-573. https://doi.org/10.1016/0306-3623(95)02054-3
- Thornalley, P. J., Langborg, A., & Minhas, H. S. (1999). Formation of glyoxal, methylglyoxal and 3-deoxyglucosone in the glycation of proteins by glucose. *Biochem J*, 344 Pt 1(Pt 1), 109-116. https://www.ncbi.nlm.nih.gov/pubmed/10548540
- Trivedi, R. R., Crooks, J. A., Auer, G. K., Pendry, J., Foik, I. P., Siryaporn, A., Abbott, N. L., Gitai, Z., & Weibel, D. B. (2018). Mechanical genomic studies reveal the role of D-alanine metabolism in *Pseudomonas aeruginosa* Cell Stiffness. *MBio*, *9*(5). https://doi.org/10.1128/mBio.01340-18
- Ueno, H., Likos, J. J., & Metzler, D. E. (1982). Chemistry of the inactivation of cytosolic aspartate aminotransferase by serine O-sulfate. *Biochemistry*, 21(18), 4387-4393. http://www.ncbi.nlm.nih.gov/pubmed/6812625
- Vigliotta, G., Tredici, S. M., Damiano, F., Montinaro, M. R., Pulimeno, R., di Summa, R., Massardo, D. R., Gnoni, G. V., & Alifano, P. (2005). Natural merodiploidy involving duplicated *rpoB* alleles affects secondary metabolism in a producer actinomycete. *Mol Microbiol*, *55*(2), 396-412. https://doi.org/10.1111/j.1365-2958.2004.04406.x
- Voit, E. O., Newstetter, W. C., & Kemp, M. L. (2012). A feel for systems. *Mol Syst Biol*, 8, 609. https://doi.org/10.1038/msb.2012.41
- Volz, K. (1999). A test case for structure-based functional assignment: the 1.2 A crystal structure of the *yigF* gene product from *Escherichia coli*. *Prot Sci*, 8(11), 2428-2437.
- Walsh, C. (1982). Suicide substrates: mechanism-based enzyme inactivators. *Tetrahedron*, *38*, 871-909.
- Walsh, C. T. (1984). Suicide substrates, mechanism-based enzyme inactivators: recent developments. *Annu Rev Biochem*, *53*, 493-535. https://doi.org/10.1146/annurev.bi.53.070184.002425
- Wang, H., Liu, J., & Wu, L. (2009). Methylglyoxal-induced mitochondrial dysfunction in vascular smooth muscle cells. *Biochem Pharmacol*, 77(11), 1709-1716. https://doi.org/10.1016/j.bcp.2009.02.024

- Whalen, W. A., Wang, M. D., & Berg, C. M. (1985). beta-Chloro-L-alanine inhibition of the *Escherichia coli* alanine-valine transaminase. *J Bacteriol*, *164*(3), 1350-1352. http://www.ncbi.nlm.nih.gov/pubmed/3934143
- Whitaker, G. H., Ernst, D. C., & Downs, D. M. (2021). Absence of MMF1 disrupts heme biosynthesis by targeting Hem1pin *Saccharomyces cerevisiae*. *Yeast*, *38*(12), 615-624. https://doi.org/10.1002/yea.3670
- Wild, J., Hennig, J., Lobocka, M., Walczak, W., & Klopotowski, T. (1985). Identification of the dadX gene coding for the predominant isozyme of alanine racemase in *Escherichia coli* K12 [Research Support, Non-U.S. Gov't]. *Mol Gen Genet*, *198*(2), 315-322. http://www.ncbi.nlm.nih.gov/pubmed/3920477
- Wilkinson, I. V. L., Pfanzelt, M., & Sieber, S. A. (2022). Functionalised cofactor mimics for interactome discovery and beyond. *Angew Chem Int Ed Engl*, 61(29), e202201136. https://doi.org/10.1002/anie.202201136
- Winfield, M. D., & Groisman, E. A. (2004). Phenotypic differences between *Salmonella* and *Escherichia coli* resulting from the disparate regulation of homologous genes. *Proc Natl Acad Sci U S A*, 101(49), 17162-17167. https://doi.org/10.1073/pnas.0406038101
- Yang, X., Wang, Y., Zhou, Y., Gao, X., Li, B., & Huo, G. (2014). Complete genome sequence of *Lactococcus lactis* subsp. lactis KLDS4. 0325, a bacterium newly isolated from Koumiss in Xinjiang, China. *Wei Sheng Wu Xue Bao*, *54*(12), 1406-1418. https://www.ncbi.nlm.nih.gov/pubmed/25876326
- Yung, Y. P., McGill, S. L., Chen, H., Park, H., Carlson, R. P., & Hanley, L. (2019). Reverse diauxie phenotype in *Pseudomonas aeruginosa* biofilm revealed by exometabolomics and label-free proteomics. *NPJ Biofilms Microbiomes*, *5*(1), 31. https://doi.org/10.1038/s41522-019-0104-7
- Zhang, H. M., Gao, Y., Li, M., & Chang, W. R. (2010). Crystal structure of the PSPTO-PSP protein from *Pseudomonas syringae* pv. tomato str. DC3000 in complex with D-glucose. *Biochem Biophys Res Commun*, 397(1), 82-86. https://doi.org/10.1016/j.bbrc.2010.05.071
- Zhang, X., El-Hajj, Z. W., & Newman, E. (2010). Deficiency in L-serine deaminase interferes with one-carbon metabolism and cell wall synthesis in *Escherichia coli* K-12. *J Bacteriol*, 192(20), 5515-5525. https://doi.org/JB.00748-10 [pii]10.1128/JB.00748-10
- Zhou, L., Wang, J. Y., Wu, J., Wang, J., Poplawsky, A., Lin, S., Zhu, B., Chang, C., Zhou, T., Zhang, L. H., & He, Y. W. (2013). The diffusible factor synthase XanB2 is a bifunctional chorismatase that links the shikimate pathway to ubiquinone and xanthomonadins biosynthetic pathways. *Mol Microbiol*, 87(1), 80-93. https://doi.org/10.1111/mmi.12084

Zhou, Z., Tran, P. Q., Breister, A. M., Liu, Y., Kieft, K., Cowley, E. S., Karaoz, U., & Anantharaman, K. (2022). METABOLIC: high-throughput profiling of microbial genomes for functional traits, metabolism, biogeochemistry, and community-scale functional networks. *Microbiome*, 10(1), 33. https://doi.org/10.1186/s40168-021-01213-8

Zimmermann, J., Kaleta, C., & Waschina, S. (2021). gapseq: informed prediction of bacterial metabolic pathways and reconstruction of accurate metabolic models. *Genome Biol*, 22(1), 81. https://doi.org/10.1186/s13059-021-02295-1

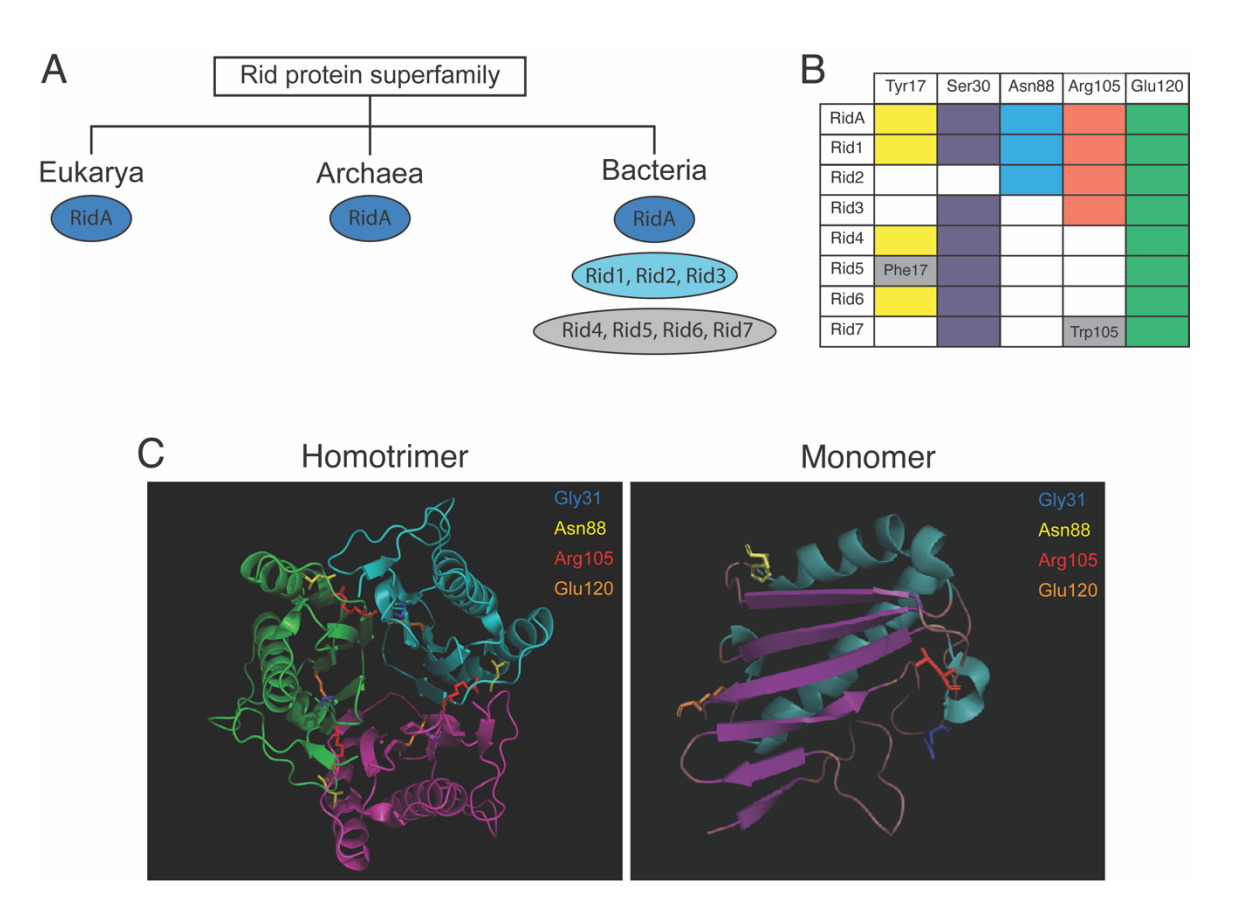


Figure 1.1. Distribution, conserved residues, and structure of Rid proteins. A) Distribution of Rid proteins in the three domains of life by subfamily. RidA proteins (dark blue) are present in each domain, while the remaining Rid1-7 subfamilies (light blue, grey) are present only in bacteria. B) Conservation of key residues across Rid subfamilies. Filled boxes indicate conservation of the relevant residue (columns), empty boxes indicate a residue is not conserved in the listed Rid subfamily (rows), grey boxes with text indicate the relevant residue is consistently replaced with the given amino acid in that subfamily. C) Secondary structures of RidA homotrimer (PDB: 1QU9) and monomer (PDB: 3QUW). Structures were generated in PyMOL. Each color in the homotrimer structure represents an individual monomer. Each color in the monomer structure represents an element of the protein secondary structure: sheets (purple), helices (cyan) and loops (pink).

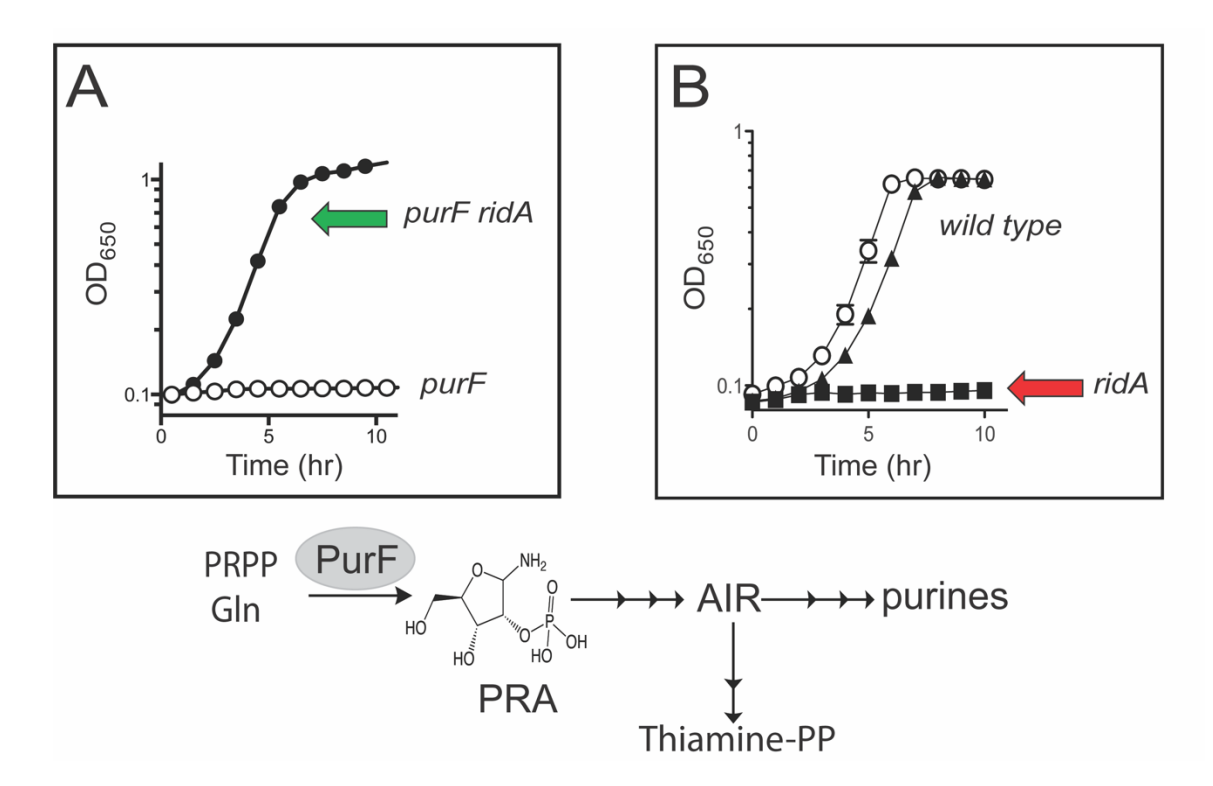


Figure 1.2. Loss of RidA can have positive or negative effects. A) Loss of *ridA* alleviates PRA requirement of a *purF* background. A *purF* mutant (empty circles) and a *ridA purF* double mutant (filled circles) grown in minimal medium. B) *ridA* mutants exhibit sensitivity to serine that is alleviated by isoleucine. Growth is shown for wild type (closed triangles) and a *ridA* mutant in minimal medium supplemented with serine (closed squares), as well as a *ridA* mutant in minimal medium supplemented with serine and isoleucine (open circles).

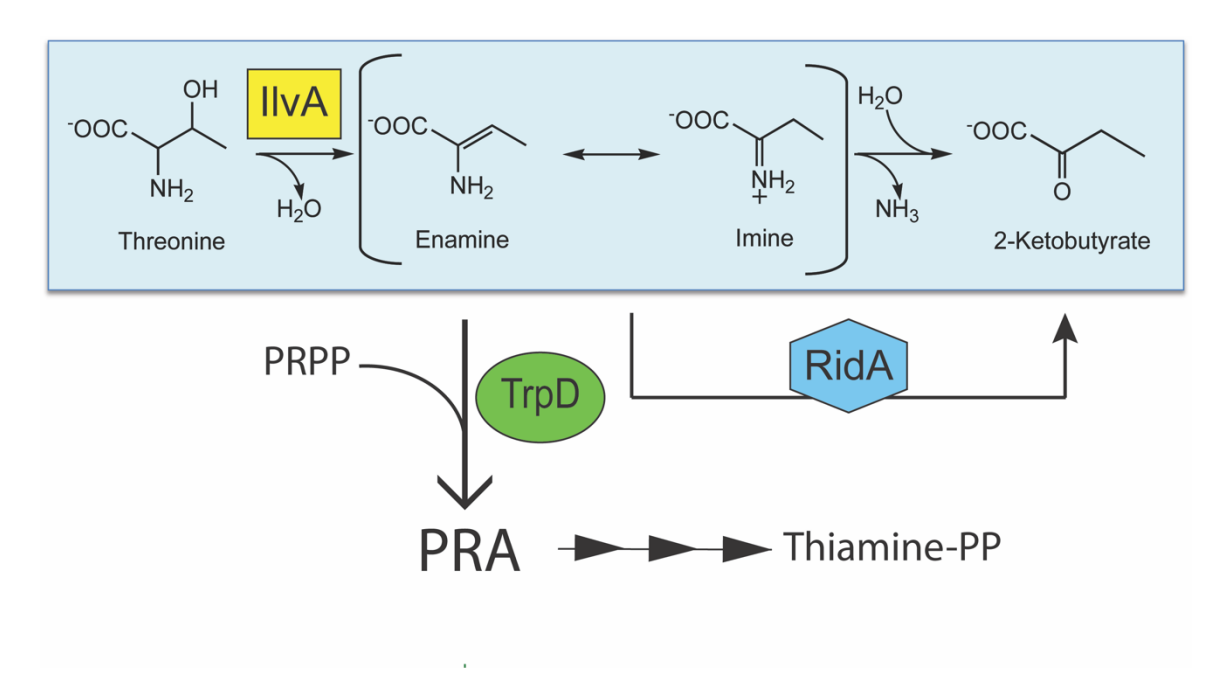


Figure 1.3. Pathway for PurF-independent PRA synthesis by TrpD and IIvA. IlvA generates an enamine/imine intermediate from threonine, which is then used by TrpD to generate PRA from PRPP. RidA removes the enamine/imine species, preventing IlvA and TrpD-mediated PRA synthesis.

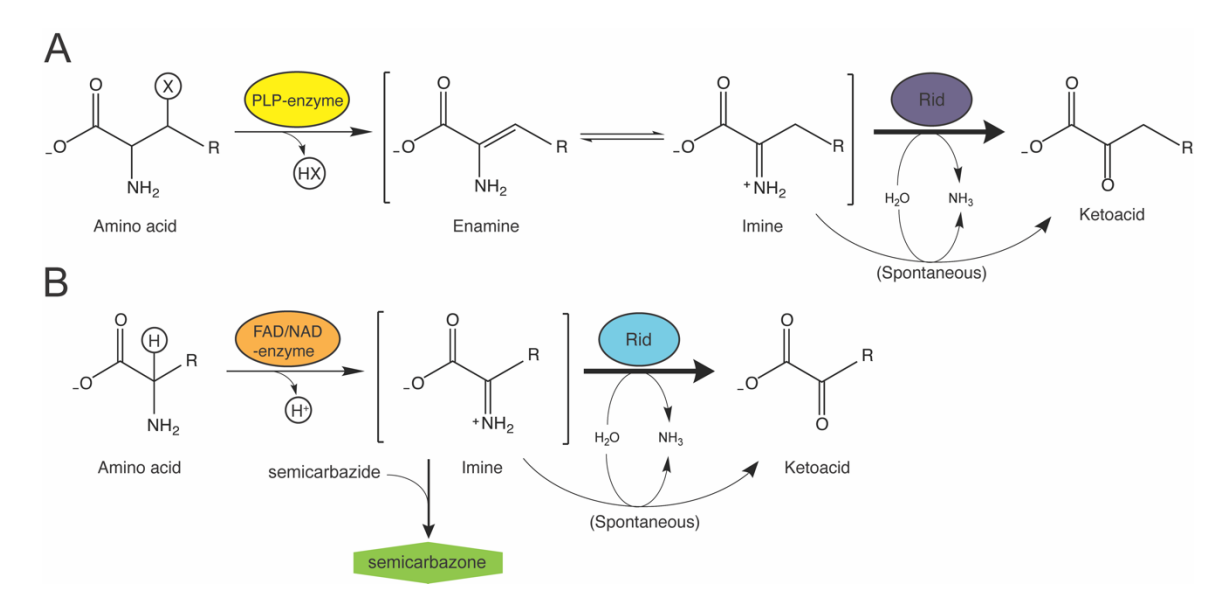


Figure 1.4. Model for RidA and Rid1-3 protein activity. A) The RidA paradigm. Enamine/imine intermediates are generated in the β -elimination of amino acids by PLP-dependent enzymes. B) General model for deaminase activity of Rid1-3 proteins (+Arg105). Imines are generated from amino acids via oxidation about the α -carbon by FAD- or NAD-dependent enzymes. These intermediates can be detected using semicarbazide, which reacts with imines to form semicarbazone (green) that can be detected spectrophotometrically. The intermediates in both cases are deaminated either non-enzymatically by water (thin arrows), or more rapidly by the Rid protein (bold arrows).

Figure 1.5. Damaged PLP can be used to quantify 2AA stress. A) Generation and mechanism of attack by 2AA. IIvA generates 2AA from L-Serine, which then forms a covalent adduct with the PLP cofactor in the active sites of target enzymes. The adduct can be extracted as PLP-pyruvate by treatment with base (KOH).

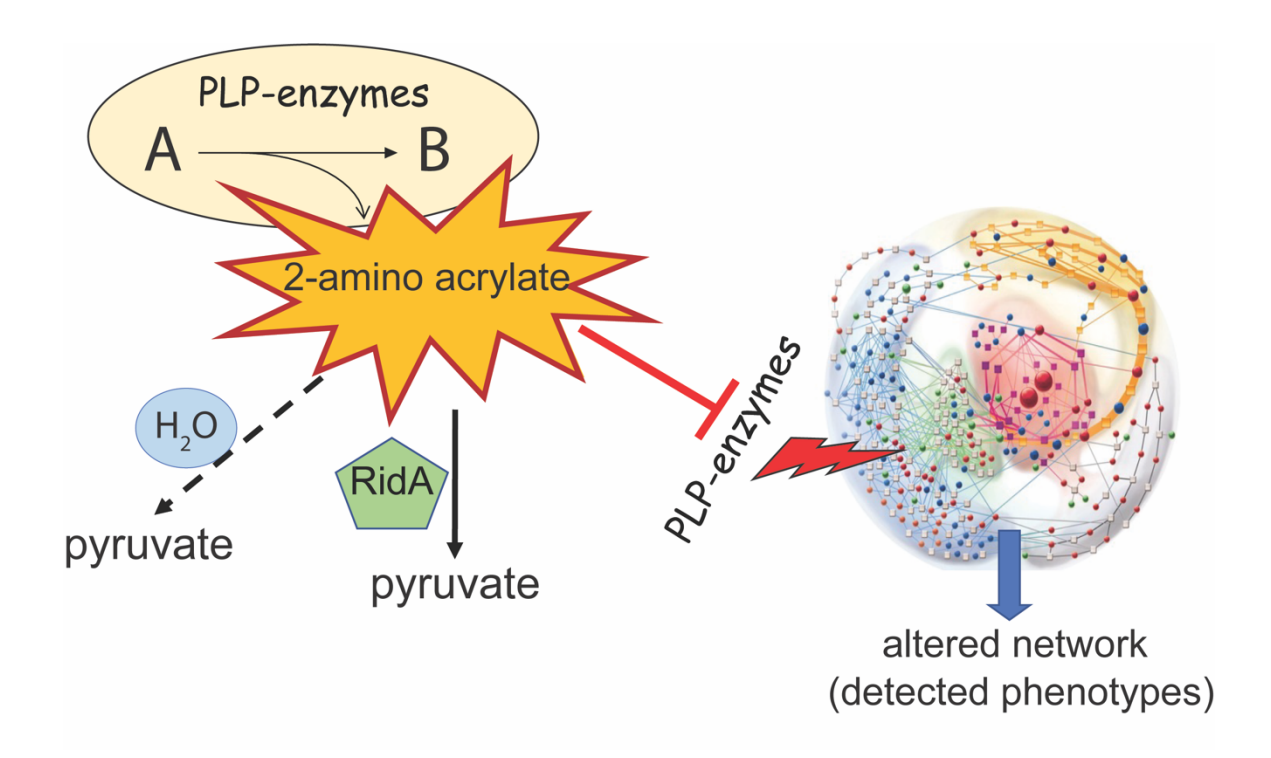


Figure 1.6. Reactive enamines have multiple effects on metabolism. PLP-dependent enzymes generate reactive enamines that can be either deaminated by water (dashed arrow) or RidA (black arrow) to stable metabolites. If allowed to persist, the enamines can interact with cellular components to generate new products and pathways (green) or can irreversibly damage PLP-enzymes (red) to alter the metabolic network and elicit phenotypes.

Figure 1.7. The Rut pathway for uracil utilization in *E. coli*. RutA/RutF convert uracil to uredoacrylate, which serves as the substrate of RutB. RutB releases carbamate and 3-aminoacrylate (3AA) that is then deaminated spontaneously by water (thin arrow), or more rapidly by the Rid protein RutC (bold arrow) to malonate semialdehyde. RutE converts malonate semialdehyde to 3-hydroxypropionate in the final step of the pathway. FAD-dependent enzymes are shown in orange, and the Rid protein is shown in blue.

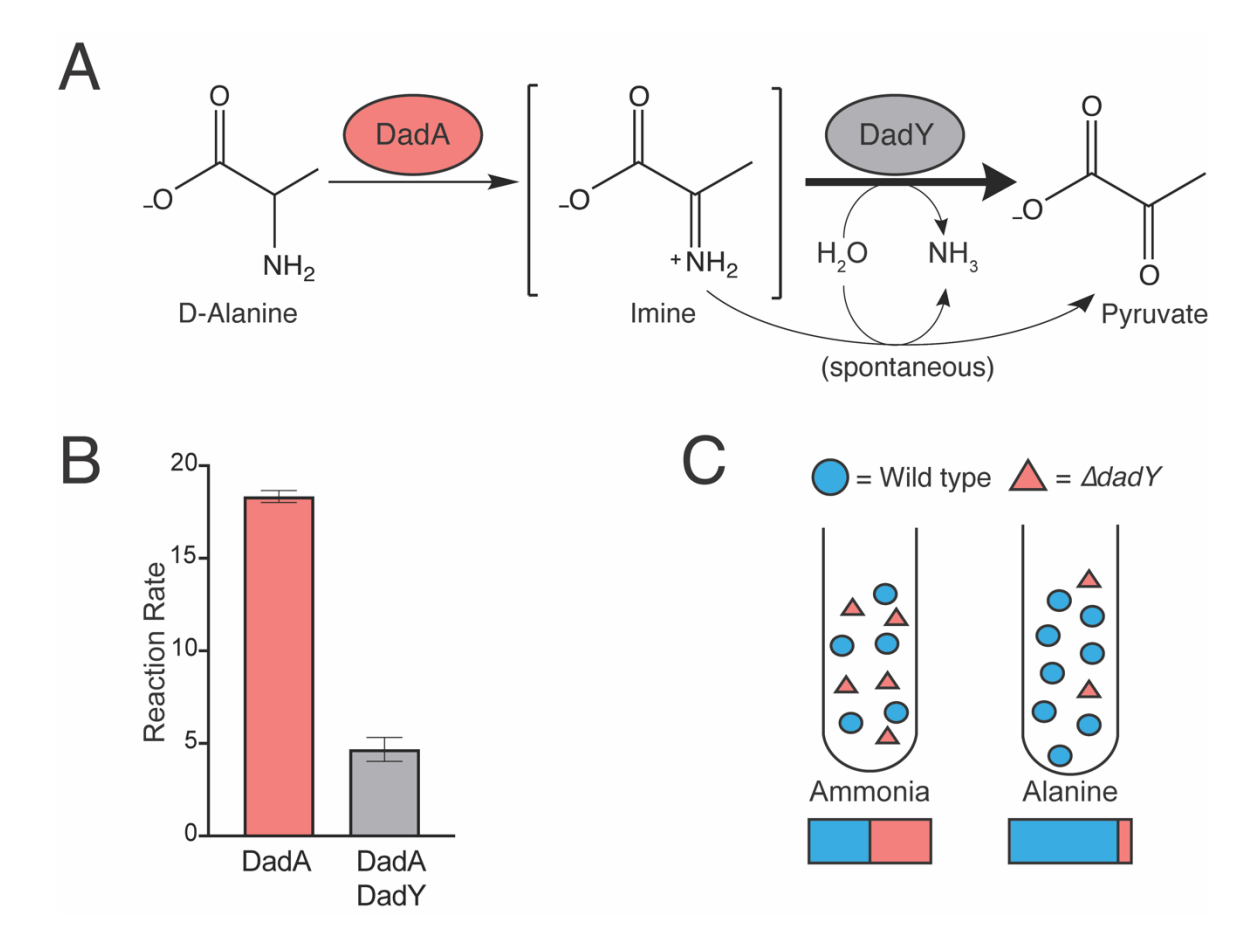


Figure 1.8. DadY contributes to alanine catabolism by deaminating imines released by DadA. A) Pathway for alanine catabolism in *P. aeruginosa*. DadA (red) oxidizes Dalanine, releasing an imine intermediate that is then deaminated by water (thin arrow) or by the Rid protein DadY (bold arrow). B) DadY removes imines released by DadA. Data show the reaction rate (i.e., the rate of semicarbazone formation) in reactions containing DadA alone (red) or in those containing both DadA and DadY (grey). A decrease in the rate of semicarbazone formation indicates an increased rate of imine removal in the presence of the Rid protein. C) DadY is required for competitive fitness on alanine. Schematic representation of competition experiments between wild-type *P. aeruginosa* (blue circles) and a *dadY* mutant (red triangles) using ammonia or alanine as a nitrogen source. The relative abundance of each strain after growth in coculture is shown below each condition (wild type, blue; *dadY* mutant, red).

CHAPTER 2

THE CYSTEINE DESULFURASE ISCS IS A SIGNIFICANT TARGET OF 2-AMINOACRYLATE DAMAGE IN *PSEUDOMONAS AERUGINOSA*¹

Reprinted here with permission of the publisher.

¹Fulton RL, Irons JL, Downs DM. 2022. *mBio*. 13(3):e0107122.

2.1 ABSTRACT

Pseudomonas aeruginosa encodes eight members of the Rid superfamily of proteins. PA5339, a member of the RidA subfamily, is required for full growth and motility of *P. aeruginosa*. Our understanding of RidA integration into the metabolic network of *P.* aeruginosa is at an early stage, with analyses largely guided by the well-established RidA paradigm in Salmonella enterica. A P. aeruginosa strain lacking RidA (PA5339) has a growth and motility defect in minimal glucose medium, both of which are exacerbated by exogenous serine. All described *ridA* mutant phenotypes are rescued by supplementation with isoleucine, indicating the primary generator of the reactive metabolite 2aminoacrylate (2AA) in ridA mutants is a threonine/serine dehydratase. However, the critical (i.e., phenotype determining) targets of 2AA leading to growth and motility defects in P. aeruginosa remained undefined. This study was initiated to probe the effects of 2AA stress on the metabolic network of P. aeruginosa by defining the target(s) of 2AA that contribute to phenotypic defects of a ridA mutant. Suppressor mutations that restored growth to a P. aeruginosa ridA mutant were isolated, among them an allele of iscS (encoding cysteine desulfurase). Damage to IscS was found to cause the growth defects of P. aeruginosa during enamine stress. A suppressing allele encoded an IscS variant less sensitive to damage by 2AA, resulting in a novel mechanism of phenotypic suppression of a *ridA* mutant.

2.2 INTRODUCTION

The Rid (YjgF/YER057c/UK114) protein superfamily is divided into nine subfamilies (RidA, Rid1-7, RutC-like) based on phylogenetic grouping by the NCBI Conserved Domain Database (cd00448: YjgF YER057c UK114 family) (1). Members of

the RidA subfamily are present in all domains of life, while Rid1-7 subfamilies exist only in prokaryotic genomes. RidA homologs from mammals, plants, yeast, and bacteria have been noted in the literature for the past two decades (2). After identification of the enamine/imine deaminase activity of RidA from *Salmonella enterica* (3, 4), similar activity was demonstrated for the human (UK114), goat (UK114), cucumber (ChrD), *Pyrococcus furiosus* (PF0668), *Bacillus subtilis* (YabJ), *Pseudomonas aeruginosa* (PA5339), *Campylobacter jejuni* (Cj1388), *Saccharomyces cerevisiae* (Mmf1p), *Yersinia pestis* (Y3551), and dust mite (Der F34) homologs *in vitro* (3, 5-10).

The RidA (Reactive intermediate deaminase A) paradigm of 2-aminoacrylate (2AA) stress was elucidated primarily by biochemical and genetic studies in S. enterica (Figure 1). Generation of 2AA and its subsequent release from the active site has been shown for three enzymes in S. enterica; threonine/serine dehydratase (IlvA, EC 4.3.1.19), cysteine desulfhydrase (CdsH, EC 4.4.1.15), and diaminopropionate ammonia-lyase (DapL, EC 4.3.1.15) (11-13) which use serine, cysteine, or diaminopropionate, respectively, as substrates. In S. enterica, 2AA is generated primarily by the serine/threonine dehydratase, IlvA. In the absence of RidA, 2AA persists and damages pyridoxal 5'-phosphate (PLP)-dependent enzymes, often causing detectable phenotypic consequences. To date, the PLP-dependent enzymes shown to be inactivated by 2AA in vivo include branched-chain amino acid aminotransferase (IlvE, EC 2.6.1.42), alanine racemases (Alr/DadX, EC 5.1.1.1), serine hydroxymethyltransferase (GlyA, EC 2.1.2.1), and aspartate aminotransferase (ApsC, EC 2.6.1.1) and aminolevulinic acid synthase (Hem1p, EC 2.3.1.37) (4, 14-18). Study of the consequences of 2AA stress in the metabolic network of various organisms has uncovered similarities and differences in the generators

and targets of 2AA when comparing *S. enterica* to *E. coli*, *P. aeruginosa*, *C. jejuni*, and *S. cerevisiae* (6-8, 17, 18).

P. aeruginosa encodes nine members of the Rid superfamily with two (PA3123 and PA5339) that belong the RidA subfamily (7). Despite encoding multiple Rid family members, only a mutation in PA5339 led to metabolic defects characteristic of a ridA mutant, leading to its designation as ridA (7). In minimal glucose medium, a P. aeruginosa ridA mutant has a defect in both growth and motility that are corrected by exogenous isoleucine. When compared to an S. enterica ridA mutant, P. aeruginosa ridA mutants were sensitive to lower concentrations of serine and only slightly sensitive to cysteine. These data suggest that in P. aeruginosa, generation of 2AA proceeds largely through the two serine/threonine dehydratases encoded by IlvA paralogs, PA0331 and PA1326. The targets of 2AA in P. aeruginosa that are responsible for growth defects differ from those in S. enterica and E. coli. This conclusion is based on observations that growth of P. aeruginosa ridA mutants is improved by addition of isoleucine or threonine, but not by exogenous glycine or aspartate (7). The latter two supplements restore growth to *ridA* mutants of S. enterica and E. coli, respectively (17, 19). The differences between the phenotypes of a ridA mutant in S. enterica and P. aeruginosa underscore the metabolic network differences between organisms and how these differences can influence the phenotypic output of the system.

Motility defects have been observed in *ridA* mutants of *S. enterica*, *P. aeruginosa*, and *C. jejuni*, suggesting 2AA damage has some broadly conserved consequences despite the distinct metabolic networks of each organism (7, 8, 20). The cause of the motility defect resulting from the lack of RidA, and whether it is a direct or indirect consequence of 2AA

damage, is not known for any organism thus far. The conserved deaminase activity of RidA proteins from all domains of life suggests the consequences of *ridA* inactivation can be attributed to accumulation of 2AA and damage to PLP-dependent enzymes. Expansion of the RidA paradigm to multiple organisms provides an opportunity to gain insight into the unique metabolic network of each organism and gain understanding of the broader impact of RidA activity and 2AA stress on metabolism.

Previous studies identified the functional RidA in *P. aeruginosa* but the integration of this protein, and broader consequences of 2AA accumulation in this organism, have not been described. Classical genetic suppressor analysis was used herein to investigate the consequences of enamine stress in *P. aeruginosa* and the role of RidA in ameliorating it. Of the three suppressors identified, an allele of *iscS* (PA3814; encoding a cysteine desulfurase; EC 2.8.1.7) provided new insights into the consequences of 2AA damage and identified IscS as a significant target of 2AA in *P. aeruginosa*.

2.3 RESULTS

Spontaneous mutations suppress phenotypes of a *P. aeruginosa ridA* mutant. *P. aeruginosa ridA* mutants have a significant reduction in motility and a severe growth defect in the presence of serine when compared to wild type (7). While both phenotypic defects are the result of accumulated 2AA (7), the target(s) of 2AA responsible for either phenotype has not been defined. Spontaneously arising suppressor mutations that restored growth of the *ridA* mutant on minimal glucose medium with serine (0.5 mM) were isolated. Colonies appeared after incubation for 72 hours and five independent colonies were further characterized. Separately, mutations were selected for the ability to overcome the motility

defect. After 5 days of incubation in motility agar, outgrowths from the motility halo were observed on ~85% of plates. Single colonies from these outgrowths were isolated. Ultimately, two mutants selected in the presence of serine and a single mutant with restored motility were chosen for further characterization. Two of the three genomes contained high probability SNPs, while the third contained an in-frame deletion. Mutations were identified in *PA3814* (*iscS*), *PA1010* (*dapA*) and *PA1559*, respectively. In each case, Sanger sequencing confirmed the lesion identified by whole genome analysis was present in the relevant strain. The three strains were phenotypically characterized to confirm suppression of the *ridA* mutant phenotype(s).

Diverse suppressor mutations restore growth with serine. Growth of *P. aeruginosa ridA*, and suppressor mutants DMPA14 (*iscS*), DMPA13 (*PA1559*), and DMPA5 (*dapA*) in liquid glucose media with serine (0.5 mM) and/or isoleucine (1 mM) is shown in Figure 2. Compared to wild type, the *ridA* mutant strain had a significant growth defect in minimal medium and was unable to grow in the presence of serine, while isoleucine supplementation restored full growth in both media (Figure 2A, 2B). The phenotypic profile of the suppressors separated them into two classes. The lesions in *dapA* and in *PA1559* restored full growth in minimal medium, and significantly increased growth in the presence of serine (Figure 2D, 2E). In contrast, the lesion in *iscS* marginally increased growth on minimal medium and eliminated the impact of serine on growth (Figure 2C). Significantly, growth of the *iscS* suppressor mutant was not restored to wild type levels in either medium. In total, nutritional analyses showed that: i) each of the *P. aeruginosa ridA* suppressor mutants were less sensitive to serine, ii) isoleucine restored wild-type growth

in all conditions tested and iii) growth pattern allowed by the *iscS* mutation was distinct among the suppressors.

Suppressor mutations increase motility. Each of the three suppressor mutants improved motility in minimal glucose motility agar (Table 2). On average, a ridA mutant was ~50% as motile as wild type. All suppressor mutants were significantly more motile than the parental ridA mutant. The iscS suppressor mutation was less efficient at restoring motility than the other two mutations. It was formally possible that differences in motility reflected different growth rates of the mutants. This possibility was minimized by assessing motility in the presence of thiamine, which restored growth but not motility (Table 2, Figure 6). As observed previously (7), isoleucine restored full motility (Table S1).

DapA^{N108G} variant restored growth and motility of the *ridA* mutant. Suppressor mutant DMPA5 had an AA to GG substitution at bases 321 and 322 in the coding sequence of *dapA/PA1010* (dihydropicolinate synthase; EC 4.3.3.7) resulting in a DapA^{N108G} variant. DapA from *P. aeruginosa* shares 56% protein sequence identity with DapA from *S. enterica*. In *S. enterica*, mutations in *dapA* also eliminated the growth defects of a *ridA* mutant (11). In *S. enterica*, DapA variants that suppressed *ridA* mutant phenotypes had, on average, a 50-fold lower specific activity than the wild-type enzyme. These variants increased metabolic flux towards threonine, ultimately decreasing IlvA-mediated generation of 2AA (11, 30). Residue N108 is adjacent to Y107 (*E. coli* numbering), a conserved active site residue that significantly lowers DapA activity when disrupted (15, 31). Based on the *S. enterica* paradigm and the location of the suppressing substitution, we

predict the mechanism of suppression in the *P. aeruginosa* is similar to *S. enterica* and this allele was not pursued further herein.

A mutation in iscS restored growth of a P. aeruginosa ridA mutant. Strain DMPA14 had a mutation in iscS (PA3814) that encoded a variant enzyme in which Q183, a conserved residue in in the PLP-binding domain of IscS (Nfs1 in eukaryotes) homologs, was replaced with a proline. The IscS^{Q183P} variant suppressed the growth defect of a *ridA* mutant in the presence of exogenous serine (Figure 2C). Pseudomonas aeruginosa has three putative cysteine desulfurases (PA2062, PA3667, and PA3814). Of the three, PA3814 has the highest protein sequence identity (75%) to S. enterica IscS (STM2543) and lies in the isc operon. Therefore, this protein is assumed to be involved in the Fe-S cluster biosynthesis and is designated iscS in the genome annotation. The crystal structure of E. coli IscS, in addition to structural studies of S. enterica IscS, suggest a Q183P substitution could alter interactions in the PLP binding domain and potentially affect enzymatic activity (32, 33). An IscSQ183P variant partially suppresses a ridA mutant of S. enterica and is dominant. Dominance of the $iscS_{(A548C)}$ allele was tested in a S. enterica system. S. enterica strain DM12920 (ridA) was transformed with plasmids expressing PAIscS, PAIscSQ183P, SERidA, or a vector only control. Growth of the resulting strains was assessed in minimal medium containing serine (Figure 3). Several points were noted. First, when expressed in trans PAIscSQ183P allowed growth of the ridA mutant of S. enterica, while PAIscS failed to restore growth. Second, the growth stimulation by $_{PA}IscS^{Q183P}$ required that expression of the gene was induced and had a lag of ~20 hours. In contrast, seRidA expressed in trans restored full growth without induction or a lag period. Finally, exogenous isoleucine restored growth to all strains as expected (data not shown). These data showed that the $_{PA}IscS^{Q183P}$ variant was dominant with respect to its ability to suppress ridA growth defects. Further, the partial suppression of S. enterica ridA mutant phenotype by this variant revealed a common feature of 2AA stress in the two organisms.

An IscSQ183P variant has cysteine desulfurase activity in vivo. The results above raised the question of whether the PAIscSQ183P variant retained cysteine desulfurase activity (EC 2.8.1.7). P. aeruginosa has three IscS homologs and the consequences of lacking PA3814 and potential overlap with the other paralogs are not known. In contrast, phenotypes of S. enterica strains lacking iscS have been described and thus were exploited to determine if PAIscSQ183P has cysteine desulfurase activity in vivo. IscS is required for thiamine biosynthesis in S. enterica. Strain DM5419 (iscR1::MudJ) requires thiamine and nicotinic acid due to polar effects on the downstream genes iscS and iscA, respectively (27). Importantly, a functional IscS in trans eliminates the thiamine requirement of this strain. DM5419 was transformed with plasmids encoding PAIscS, PAIscSQ183P, or an empty vector. Growth of the resulting strains, with and without induction of the plasmid encoded gene, was assessed in liquid minimal media supplemented with nicotinic acid (Figure 4). PAIscS restored growth of DM5419 in the absence of thiamine whether or not expression was induced. PAIscSQ183P also restored growth in the absence of thiamine, but only when expression of the relevant gene was induced. These results showed that IscSQ183P retained cysteine desulfurase activity in vivo, and suggested it had less activity than wild-type IscS.

The interpretation that PAIscSQ183P retains cysteine desulfurase activity was supported by assaying the Fe-S cluster protein succinate dehydrogenase (SDH) in both S.

enterica and P. aeruginosa. Activity of SDH is dependent on cysteine desulfurase to generate its Fe-S cluster, and other things being equal will be a proxy for IscS activity. In S. enterica strain DM5419 (iscR1::MudJ) expressing $_{PA}$ IscS, or $_{PA}$ IscS $_{Q183P}$ SDH activity was 4.2 ± 1.0 and 3.9 ± 0.5 ΔA_{600} /min/mg protein, respectively. The same strain with an empty vector had 1.6 ± 0.3 ΔA_{600} /min/mg protein, which reflects the activity of SDH in the absences of a functional IscS. SDH activity was determined in crude extracts of the ridA mutant of P. aeruginosa and the suppressor strain with IscS $_{Q183P}$ and the data are in Table 3. In nutrient medium (where loss of ridA has no detrimental effect), there is significantly less SDH activity when IscS $_{Q183P}$ is present compared to wild type IscS. These data support the conclusion that IscS $_{Q183P}$ has less desulfurase than the parental protein, as suggested by the complementation data in Figure 4. Further, the SDH activity of both strains in minimal medium was increased by the presence of isoleucine. These data are consistent with the decrease in 2AA stress that resulting from allosteric inhibition of serine/threonine dehydratase by isoleucine (7).

IscS^{Q183P} **has a unique mechanism of suppression.** Several genetic and nutritional conditions that suppress phenotypes of a *S. enterica ridA* mutant have been characterized. In all cases, the mechanism of suppression was to decrease generation of 2AA or nutritionally bypass a key enzyme damaged by 2AA (6, 11, 19, 34, 35). Transaminase B (IIvE) is a target of 2AA damage, and its activity has been used as a proxy of 2AA levels in multiple organisms, including *P. aeruginosa* (7). IIvE activity was assayed in three suppressor mutants of *P. aeruginosa* (Figure 5A). As expected, the *ridA* mutant had significantly lower transaminase B activity than the parental strain. The suppressing alleles

of *dapA* and *PA1559* restored transaminase B activity to levels found in the wild-type strain. Interestingly, the *iscS*_(A548C) allele did not increase transaminase B activity. These data supported the hypothesis that this mutation suppressed the *ridA* phenotypes by a mechanism not previously described. Additional support for this conclusion was provided by the heterologous *S. enterica* system (Figure 5B). In this case, transaminase B activity was assayed in a *ridA* mutant carrying an empty vector, or expressing _{SE}RidA, _{PA}IscS, or _{PA}IscS^{Q183P}. Consistently, neither _{PA}IscS nor _{PA}IscS^{Q183P} restored transaminase B activity in the *S. enterica* strains (Figure 4). In total, these data reinforced the unique scenario in which the IscS^{Q183P} variant allowed a *ridA* mutant to grow in the presence of 2AA stress.

Thiamine supplementation restored growth to *ridA* mutants. The ability of a variant of IscS to suppress *ridA* defects in both *P. aeruginosa* and *S. enterica ridA* mutants without lowering 2AA levels suggested an exciting possibility. We hypothesized that IscS was, i) a target of damage by 2AA and ii) the 2AA-mediated decrease in IscS activity was primarily responsible for the growth defect of a *P. aeruginosa ridA* mutant. If this were the case, growth of the *ridA* mutant might be restored by exogenous thiamine since it should bypass a presumed nutritional consequence of decreased cysteine desulfurase activity of IscS.

Growth of wild type and *ridA* mutant strains was monitored in minimal glucose medium supplemented with serine and/or thiamine (Figure 6AB). Consistent with the above scenario, thiamine significantly increased growth of the *ridA* mutant in minimal medium with or without serine present. Growth was not completely restored by thiamine in the presence of serine. This result suggests either there is an additional target(s) of 2AA

that contributes to the growth phenotype, or that the consequence of decreased IscS activity extends beyond thiamine synthesis.

In *S. enterica*, serine hydroxymethyltransferase (GlyA, E. C. 2.1.2.1) is the critical target of 2AA and glycine almost entirely alleviates the growth defect of a *ridA* mutant (19). The data in Figure 3 suggested thiamine biosynthesis might also be compromised in an *S. enterica ridA* mutant due to 2AA-mediated damage of IscS. Growth experiments with *S. enterica* in minimal glucose medium supplemented with various combinations of serine, glycine and thiamine supported this conclusion (Figure 6C). As expected, serine prevented growth and the addition of glycine restored it considerably (19). Addition of thiamine improved growth in the presence of serine, but not to the level allowed by glycine, while addition of both thiamine and glycine fully restored growth of the *ridA* mutant in the presence of serine. These data identified a second target of 2AA damage in *S. enterica* that contributes to the growth defect of a *ridA* mutant.

The IscS^{Q183P} variant has decreased susceptibility to 2AA damage *in vivo*. Genetic experiments above showed IscS was a critical target of 2AA damage in *P. aeruginosa*. We considered a scenario in which the IscS^{Q183P} variant restored growth because it was less susceptible to 2AA attack than wild-type IscS. To assess this possibility, we used a *S. enterica* system that can monitor 2AA-dependent damage that occurs *in vivo* (18, 28). PAIscS and PAIscS^{Q183P} proteins were overexpressed and purified from two different *S. enterica* strains, *ridA* and wild type, resulting in four protein samples. The four relevant strains were grown in minimal medium with arabinose and IPTG to ensure protein overexpression, serine to induce 2AA stress and glycine to allow growth in the presence of

such stress. When 2AA attacks an active site PLP, a pyruvate/PLP adduct can be extracted from the damaged enzyme by a treatment with base (28, 35). The four protein samples were treated with base, and the cofactors released from each were separated by HPLC. Several points were noted from the data (Figure 7, Table 4). Importantly, IscS purified from the *ridA* mutant released significant pyruvate/PLP, indicating that IscS was a target of 2AA attack *in vivo* (Figure 7B). In contrast, IscS purified from a wild-type strain released predominately PLP, with a barely detectable pyruvate/PLP peak (Figure 7A). The presence of a small but detectable level of pyruvate/PLP was consistent with results for some other protein targets of 2AA, which showed a low level of 2AA stress even in the presence of RidA (36).

Analysis of the IscS^{Q183P} variant supported the hypothesis that this protein was less susceptible to 2AA damage than the wild-type protein. IscS^{Q183P} purified from a *ridA* mutant released significantly less pyruvate/PLP than the wild-type protein (Figure 7D). The calculated areas (in arbitrary units) of the pyruvate/PLP peaks from the IscS^{Q183P} and IscS samples were 37 and 65, respectively (Table 4). Further, the IscS^{Q183P} protein sample purified from the wild-type strain did not release detectable pyruvate/PLP. Taken together, these data supported the conclusions that IscS is a target of 2AA and further, the IscS^{Q183P} variant is less sensitive to attack by 2AA than the wild-type protein.

In contrast to pyruvate/PLP, similar amounts of PLP were released from three of the four IscS protein samples. However, when wild type IscS protein was purified from *ridA* (i.e., in the presence of 2AA), the amount of released PLP decreased significantly. The decreased concentration of PLP was reflected in a decrease in area from ~165 to ~93 arbitrary units. The significance of this decrease is unclear, but it suggests the effect of

2AA is more far reaching than indicated simply by measuring the pyruvate/PLP adduct. This result further supports the notion that the IscS^{Q183P} variant is less affected by 2AA stress than IscS. The ratios of cofactors released from each sample purified from the *ridA* mutant support this conclusion. In the IscS sample, pyruvate/PLP makes up 40% of the released cofactor, while in the IscS^{Q183P} sample this number is 18%. Thus, both concentration and percentage measurements of the pyruvate/PLP adduct support the conclusion that the IscS^{Q183P} variant is less sensitive to 2AA than the wild-type protein. The precise correlation between damage, enzymatic activity, and PLP occupancy of these enzymes with the physiological significance they have are not well-defined without additional work.

2.4 DISCUSSION

Mutants of *P. aeruginosa* lacking RidA have observable phenotypes that reflect the consequences of 2AA accumulation (7). Three mutations that suppress these phenotypes were isolated and discussed herein. In the context of the RidA paradigm, phenotypic suppression can be generated by conditions, or mutations that: i) decrease or prevent the generation of 2AA, ii) increase quenching of 2AA, iii) bypass the damaged target that is responsible for preventing growth under a relevant condition, or iv) prevent damage to a key target enzyme. Conditions that allow the former three mechanisms have been described (6, 11, 13, 34, 35). Here, we report a mutation that suppresses the *ridA* phenotype in *P. aeruginosa* by generating a target protein variant with decreased sensitivity to 2AA.

Three spontaneous mutations were isolated that suppressed ridA mutant phenotypes in P. aeruginosa: i) an in-frame deletion in PA1559, ii) a dinucleotide polymorphism in

dapA and, iii) a single nucleotide polymorphism in *iscS*. PA1559, or CprA (catatonic peptide resistance), is a hypothetical protein suggested to have a role in PhoPQ-mediated polymyxin resistance (37, 38). The role of this locus in 2AA stress was not pursued in this study. The lesion in dapA was predicted to act by the mechanism characterized for lesions in the same locus in *S. enterica*. Briefly, lowering activity of DapA increases flux to threonine/isoleucine which reduces 2AA formation by IlvA (11, 39). Suppressing lesions in dapA and PA1559 restored transaminase B (IlvE) activity in the *P. aeruginosa ridA* mutant, indicating they had reduced the endogenous levels of 2AA.

In contrast, the suppressing mutation in *iscS* (encoding IscS^{Q183P}) restored growth to a *ridA* mutant without lowering 2AA levels. The *isc* (<u>iron-sulfur cluster</u>) genes are involved in iron-sulfur cluster assembly and trafficking sulfur to various enzymes and tRNAs. IscS (EC 2.8.1.7) is a fold-type I PLP-dependent enzyme that mobilizes sulfur by desulfurization of cysteine to yield an IscS-bound persulfide and alanine (40). Interestingly, cysteine desulfurases generate 2AA as an obligate intermediate, but in the catalytic mechanism of IscS/SufS the enamine species it is converted to L-alanine in the active site of the enzyme (41). Thus, this enzyme would not contribute to 2AA stress in a cell. Mutations in *iscS* that impact the biosynthesis of thiamine, biotin, NAD, isoleucine/valine, and molybdopterin, in addition to iron homeostasis and tRNA activation have been reported (27, 42-45).

The results of this work support the hypothesis that IscS is a target of 2AA damage, and that damage to this enzyme is primarily responsible for the growth defects of a *P. aeruginosa ridA* mutant. Consistent with this scenario, thiamine restored growth of a *P. aeruginosa ridA* mutant in the presence of serine. Additionally, the suppressing variant,

IscS^{Q183P}, is less sensitive to 2AA attack than the wild-type IscS *in vivo* and retains at least some of its native cysteine desulfurase activity. Although it is not clear how attack by 2AA is impaired, it was previously shown that residues at position 183 play a role in stabilizing the unprotonated phenolic oxygen (O3') of PLP by serving as a hydrogen bond donor (46). Consistently, the presence of a glutamine residue at position 183 is widely conserved in IscS and its homologs (47). Thus, the data here, together with those in the literature, favor a situation in which a substitution at residue 183 could affect 2AA susceptibility by altering the structure of the PLP-binding domain of IscS or electrophilicity of the PLP cofactor. Further biochemical and structural studies are needed to clarify the mechanism of resistance.

In total, the results herein from both *in vivo* and *in vitro* experiments support the conclusion that the growth defect of a *P. aeruginosa ridA* mutant is primarily caused by 2AA-dependent damage to the cysteine desulfurase IscS. With this work, *P. aeruginosa* becomes the second bacterium (in addition to *S. enterica*) in which the primary mechanism of growth inhibition by 2AA stress has been determined. This work also furthered our understanding of 2AA stress in *S. enterica* by identifying IscS, in addition to GlyA, as a target of damage with nutritional consequences. These results provide further evidence that 2AA targets are conserved across species, but phenotypic outcomes associated with 2AA stress are organism specific and are due to differences in the metabolic architecture of each organism. These differences ultimately dictate the enzymatic activity(ies) or metabolic pathway(s) that most affect the stability of the network. It is these components that can lead to detectable growth consequences when disrupted. The ability of a single substitution in IscS to render the enzyme significantly less sensitive to 2AA damage was unexpected and

will inform further efforts to understand the mechanism by which endogenous 2AA attacks cellular enzymes. This result raised questions about not only determinants of sensitivity, but how selective pressure make act to decrease sensitivity, potentially at the expense of enzymatic activity.

2.5 MATERIALS AND METHODS

Bacterial strains, media, and chemicals. Bacterial strains used in this study are listed in Table 1. *Pseudomonas aeruginosa* PAO1 wild type (MPAO1) and *ridA* (PW9994 *ridA*-F05::ISphoA/hah) were obtained from the transposon mutant library collection (21). *Salmonella enterica* serovar Typhimurium LT2 strains were available, or derivatives of those in the laboratory strain collection.

P. aeruginosa strains were grown at 37°C and Lysogeny broth (LB) was used as a rich medium. M9 salts (20 mM NH₄Cl, 12 mM Na₂HPO₄, 22 mM KH₂PO₄, 1.0 mM NaCl, 1 mM MgSO₄) with trace minerals (22) and glucose (11 mM) was used as a minimal medium (23, 24). Supplements were added as indicated; isoleucine, valine, or leucine (1 mM), and serine (0.05 - 1 mM). Chemicals were purchased from MilliporeSigma (Sigma-Aldrich, St. Louis, MO).

For growth of *S. enterica*, Difco nutrient broth (NB) (8 g/liter) containing NaCl (5 g/liter) was used as rich medium. Minimal medium consisted of no-carbon E salts (NCE) with 1 mM magnesium sulfate (23), trace elements (22), and glucose (11 mM) as the sole carbon source. Difco BiTek agar (15 g/liter) was added to make solid growth medium. Amino acids serine (5 mM) and isoleucine (1 mM) were added to minimal medium as

mg/liter. Amino acids and antibiotics were purchased from Sigma-Aldrich (St. Louis, MO). *P. aeruginosa* mutant isolation. Independent cultures (1 ml) of DMPA7 were grown overnight in LB at 37°C with shaking. Fully grown cultures were centrifuged, and the pellet resuspended in saline (1 ml). An aliquot of the cell suspension (100 μl) was spread on minimal medium with serine (0.5 mM) and incubated at 37°C for ~72 hours, at which time colonies were visible. The putative suppressor mutants were streaked for isolation on solid minimal M9 medium with serine and were phenotypically characterized.

In a second selective condition, aliquots of a cell suspension (10 µl) were inoculated into motility agar by gently piercing the top of the agar and expelling cells. After five days of incubation at 37°C, asymmetrical outgrowths from the center motility halo were noted. A sterile toothpick recovered cells furthest from the center inoculation point. This toothpick was used to i) inoculate a second motility plate and ii) streak for isolated colonies on solid M9 minimal medium. Mutants that showed higher motility than the parental *ridA* strain (DMPA7) were characterized further.

Phenotypic analysis. *Growth*. Growth on solid medium was evaluated by patching strains to rich medium (LB for *P. aeruginosa* and NB for *S. enterica*), incubating plates overnight at room temperature, and replica printing to agar plates with the relevant nutrients. Alternatively, 1 ml cultures were grown in rich medium overnight shaking at 37°C, pelleted and resuspended in an equal volume of saline before embedding the cell suspension (100 µl) in 4 ml of soft agar overlaid on solid medium. Nutrients were spotted on soft agar, plates were dried for 15 minutes at room temperature and incubated overnight at 37°C.

Growth in liquid medium was assessed using a BioTek Elx808 microtiter plate reader following optical density at 650 nm at 37°C with slow shaking speed as described (7). Overnight cultures of *P. aeruginosa* or *S. enterica* in biological triplicate were grown in LB medium at 37°C, pelleted and resuspended in an equal volume of saline. Aliquots (5 μl) of the cell suspension inoculated the relevant medium (195 μl) and growth was monitored for 24 hours. Growth curves were plotted using GraphPad Prism (version 7.0). Motility. M9 motility medium with 0.3% Bacto-agar (Difco) was prepared as described (7, 24). Molten medium (25 ml) was poured into Petri dishes and allowed to sit for 6 hours at room temperature prior to use. Triplicate cultures were grown overnight in LB at 37°C. Cultures were centrifuged and the pellet resuspended in a volume of saline to generate an OD_{600} of 0.3. Each bacterial suspension (1 µl) was inoculated into a motility plate by gently piercing the top of the agar and expelling the cells. Plates were dried 15 minutes, then incubated at 37°C for 20 hours or longer in a sealed container to maintain constant moisture. The diameter of each swimming halo was measured and reported in millimeter (mm) and/or as a percentage of that produced by the wild-type strain.

Transaminase B assay. An overnight cell culture from rich medium (250 μl) was inoculated into 50 ml of minimal medium with indicated additions and incubated at 37°C with shaking overnight. The cells were harvested by centrifugation and washed once with NCE (1 ml). Cell pellets were frozen at -80°C until use. Cell pellets were resuspended in 1.0 ml of 50 mM potassium phosphate, pH 7.5 and lysed using a Constant Systems Limited One Shot (United Kingdom) system by passing cells through the disrupter one time with the pressure set to 145 MPa. Unbroken cells and debris were pelleted at 17.0 x g for 20 min

at 4°C. The protein concentration of the resulting cell-free extract was estimated using a bicinchoninic assay reagent kit (Pierce, Rockford, Ill.).

The protocol for the transaminase B assay has been described (7, 25). Briefly, a 50 μ l aliquot of cell-free extract was added to a reaction mixture that contained PLP (50 μ M) and α -ketoglutarate (10 mM) in potassium phosphate buffer (50 mM, pH 7.5) to a total volume of 200 μ l. After equilibrating at 37°C for 10 min, the reaction was initiated by the addition of L-isoleucine (20 mM final concentration) and allowed to proceed for 20 min at 37°C. The reaction was stopped with 0.3% 2,4-dinitrophenyl-hydrazine (DNPH, 200 μ l) to derivatize product 2-ketomethylvalerate (2KMV), forming a chromophore with absorbance at 540 nm. Results of the assay are reported in nmol 2-keto-3-methylvalerate (2KMV) formed/mg protein, based on a standard curve generated from known quantities of 2KMV similarly derivatized with DNPH. Data are presented as the mean of three biological replicates and error bars represent the standard error of the mean. Statistical significance (P < 0.05) was determined by conducting one-way analysis of variance (ANOVA) and Tukey's posttest using GraphPad Prism (version 7.0c).

Next-Generation sequencing and data analysis. Genomic DNA was extracted from the relevant strains using the Monarch® genomic DNA purification kit (New England BioLabs). Libraries were constructed using Nextera™ DNA Flex library kit and analyzed using the iSeq 100 System (Illumina). Genomic sequence reads were realigned and mapped to the published PAO1 genome using Geneious software (version 10.1.2). High-frequency single-nucleotide polymorphisms (SNPs) were detected and the respective impact on each

coding sequence was predicted. SNPs of interest were confirmed by Sanger sequencing of a PCR amplification of the relevant gene.

Purification of proteins from S. enterica strains. IscS-His6 and IscSQ183P-His6, encoded on pDM1684 and pDM1685, respectively, were purified from two S. enterica strains containing an arabinose inducible T7 polymerase (26). The isogenic strains had (DM13509) or were lacking (DM17050) a functional RidA. Overnight cell cultures (10 ml) grown on SB supplemented with ampicillin (150 µg/ml) were inoculated into each of two Fernbach flasks (2.8 liters) containing 1.5 liters of minimal glycerol medium with ampicillin (15 μg/ml) supplemented with glycine (1 mM) and pyridoxine (50 μM). The resulting cultures were grown at 37°C with shaking to an OD₆₅₀ of 0.5 before induction with arabinose (0.1%) and IPTG (100 μM), and the addition of L-serine (5 mM) and additional glycine (1 mM). Cultures were then grown at 23°C with shaking for 18 h. Cells were harvested by centrifugation at 5000 x g for 15 minutes. Cell pellets were resuspended in 2 ml/g cell weight of binding buffer (potassium phosphate pH 7.4 (50 mM), NaCl (150 mM) and imidazole (20 mM)). Lysozyme (2 mg/ml) and DNase (125 µg/ml) were added, and the cell suspension was placed on ice for 20 minutes. Cells were mechanically lysed using a Constant Systems Limited One Shot (United Kingdom) at 130 MPa. PMSF (1 mM) was added to the lysate, which was then clarified by centrifugation at 48000 x g for 45 minutes and filtered through a PVDF filter (0.45 µm pore size). Filtered lysate was loaded onto 5 ml HisTrap HP Ni-Sepharose columns and washed with binding buffer (5 column volumes). Bound protein was eluted by increasing the concentration of imidazole from 20 mM to 500 mM over 10 column volumes. Purified protein was concentrated using a centrifugal filter with a molecular weight cutoff of 30 kDa (Millipore). The concentrated protein was then moved into potassium phosphate buffer (50 mM, pH 7.4) containing NaCl (150 mM) and glycerol (10% w/v) by buffer exchange using a PD-10 desalting column (GE Healthcare). Densitometry showed that purified proteins were ~80% pure (Figure S1).

Succinate dehydrogenase assays. *P. aeruginosa* strains were grown in 25 ml of minimal succinate medium with or without L-isoleucine (1 mM) supplemented with thiamine (200 nM) or LB to mid-log phase ($OD_{650} \sim 0.5$). *S. enterica* strains were grown in 5 ml minimal glucose medium supplemented with nicotinc acid (20 μ M) and thiamine (200 nM) or NB with ampicillin added to both media. Cells were pelleted, washed with an equal volume of 50 mM cold potassium phosphate buffer pH 7.4 (50 mM) and frozen at -80°C for no longer than 48 h until use. Frozen pellets were thawed on ice and resuspended in 1 ml of cold potassium phosphate buffer before being mechanically lysed using a Constant Systems Limited One Shot (United Kingdom) at 210 MPa. Cell lysate was clarified by centrifugation at 12000 x g for 15 seconds. Succinate dehydrogenase (SDH) as assayed according to a previously described method (27). The linear range was determined for each strain in each condition and specific activities were calculated as ΔA_{600} /min/mg protein. SDH activity measured in boiled extracts was subtracted from the activity of each sample.

Characterization of cofactor content. Cofactors were released from each preparation of IscS and IscS^{Q183P} as described previously (18, 28). KOH (30 mM final concentration) was added to 1.5 nmol purified protein in a 100 μl reaction and incubated at room temperature for 10 min. Protein was then precipitated with 10% trifluoroacetic acid (30 μl), resulting in

a final volume of 130 μl. Precipitate was removed by centrifugation (17,000 x g for 3 min) and the supernatant was filtered through a 0.45 μm centrifugal tube filter (Costar 8170). Cofactors were separated by HPLC using a Shimadzu HPLC equipped with a Luna C18 column (Phenomex) using a two-step isocratic method with a flow rate of 0.8 ml/min: 0-5 min with 100% buffer A (0.06% v/v trifluoroacetic acid) and 5-18 min with methanol and buffer A (3:97). The column was washed with methanol and buffer A (60:40) for 10 min between each run. Eluant was monitored at 305 nm using a photodiode array detector (Shimadzu SPD-M20A). Authentic PLP and pyruvate/PLP were used as standards to allow peak assignment. Pyruvate/PLP was synthesized as described previously (29), purified by HPLC and concentrated.

2.6 REFERENCES

- 1. Niehaus TD, Gerdes S, Hodge-Hanson K, Zhukov A, Cooper AJ, ElBadawi-Sidhu M, Fiehn O, Downs DM, Hanson AD. 2015. Genomic and experimental evidence for multiple metabolic functions in the RidA/YjgF/YER057c/UK114 (Rid) protein family. BMC Genomics 16:382.
- 2. Irons JL, Hodge-Hanson K, Downs DM. 2020. RidA Proteins Protect against Metabolic Damage by Reactive Intermediates. Microbiol Mol Biol Rev 84.
- 3. Lambrecht JA, Flynn JM, Downs DM. 2012. Conserved YjgF protein family deaminates reactive enamine/imine intermediates of pyridoxal 5'-phosphate (PLP)-dependent enzyme reactions. J Biol Chem 287:3454-61.
- 4. Lambrecht JA, Schmitz GE, Downs DM. 2013. RidA proteins prevent metabolic damage inflicted by PLP-dependent dehydratases in all domains of life. mBio 4:e00033-13.

- 5. Degani G, Barbiroli A, Regazzoni L, Popolo L, Vanoni MA. 2018. Imine Deaminase Activity and Conformational Stability of UK114, the Mammalian Member of the Rid Protein Family Active in Amino Acid Metabolism. Int J Mol Sci 19.
- 6. Ernst DC, Downs DM. 2018. Mmflp Couples Amino Acid Metabolism to Mitochondrial DNA Maintenance in *Saccharomyces cerevisiae*. MBio 9.
- 7. Irons J, Hodge-Hanson KM, Downs DM. 2018. PA5339, a RidA Homolog, Is Required for Full Growth in *Pseudomonas aeruginosa*. J Bacteriol 200.
- 8. Irons J, Sacher JC, Szymanski CM, Downs DM. 2019. Cj1388 Is a RidA Homolog and Is Required for Flagella Biosynthesis and/or Function in *Campylobacter jejuni*. Front Microbiol 10:2058.
- 9. ElRamlawy KG, Fujimura T, Baba K, Kim JW, Kawamoto C, Isobe T, Abe T, Hodge-Hanson K, Downs DM, Refaat IH, Beshr Al-Azhary D, Aki T, Asaoku Y, Hayashi T, Katsutani T, Tsuboi S, Ono K, Kawamoto S. 2016. Der f 34, a Novel Major House Dust Mite Allergen Belonging to a Highly Conserved Rid/YjgF/YER057c/UK114 Family of Imine Deaminases. J Biol Chem 291:21607-21615.
- 10. Martínez-Chavarría LC, Sagawa J, Irons J, Hinz AK, Lemon A, Graça T, Downs DM, Vadyvaloo V. 2020. Putative Horizontally Acquired Genes, Highly Transcribed during *Yersinia pestis* Flea Infection, Are Induced by Hyperosmotic Stress and Function in Aromatic Amino Acid Metabolism. J Bacteriol 2020.
- 11. Christopherson MR, Lambrecht JA, Downs D, Downs DM. 2012. Suppressor analyses identify threonine as a modulator of *ridA* mutant phenotypes in *Salmonella enterica*. PLoS One 7:e43082.
- 12. Ernst DC, Lambrecht JA, Schomer RA, Downs DM. 2014. Endogenous Synthesis of 2-aminoacrylate Contributes to Cysteine Sensitivity in *Salmonella enterica*. Journal of Bacteriology 196:3335-3342.
- 13. Ernst DC, Anderson ME, Downs DM. 2016. L-2,3-diaminopropionate generates diverse metabolic stresses in *Salmonella enterica*. Mol Microbiol 101:210-23.

- 14. Kim J-MY, Hiroshi; Shirahige, Katsuhiko. 2001. A member of the YER057c/yjgf/Uk114 family links isoleucine biosynthesis to intact mitochondria maintenance in *Saccharomyces cerevisiae*. Genes to cells 6:507-517.
- 15. Schmitz G, Downs DM. 2004. Reduced Transaminase B (IlvE) Activity Caused by the Lack of *yjgF* Is Dependent on the Status of Threonine Deaminase (IlvA) in *Salmonella enterica* serovar Typhimurium. Journal of Bacteriology 186:803-810.
- 16. Flynn JM, Christopherson MR, Downs DM. 2013. Decreased coenzyme A levels in *ridA* mutant strains of *Salmonella enterica* result from inactivated serine hydroxymethyltransferase. Mol Microbiol 89:751-9.
- 17. Borchert AJ, Downs DM. 2017. The Response to 2-Aminoacrylate Differs in *Escherichia coli* and *Salmonella enterica*, despite Shared Metabolic Components. J Bacteriol 199.
- 18. Whitaker GH, Ernst DC, Downs DM. 2021. Absence of *MMF1* disrupts heme biosynthesis by targeting Hem1pin *Saccharomyces cerevisiae*. Yeast 38:615-624.
- 19. Ernst DC, Downs DM. 2016. 2-Aminoacrylate Stress Induces a Context-Dependent Glycine Requirement in *ridA* Strains of *Salmonella enterica*. Journal of Bacteriology 198:536-543.
- 20. Borchert AJ, Downs DM. 2017. Endogenously generated 2-aminoacrylate inhibits motility in *Salmonella enterica*. Sci Rep 7:12971.
- 21. Jacobs MA, Alwood A, Thaipisuttikul I, Spencer D, Haugen E, Ernst S, Will O, Kaul R, Raymond C, Levy R, Chun-Rong L, Guenthner D, Bovee D, Olson MV, Manoil C. 2003. Comprehensive transposon mutant library of *Pseudomonas aeruginosa*. Proc Natl Acad Sci U S A 100:14339-44.
- 22. Balch W, E.; Wolfe, R. S. 1976. New approach to the cultivation of methanogenic bacteria: 2-mercaptoethanesulfonic acid (HS-CoM)-dependent growth of *Methanobacterium ruminantium* in a pressurized atmosphere. Applied and Environmental Microbiology 32:781-791.

- 23. Vogel HJ, Bonner DM. 1956. Acetylornithase of *Escherichia coli*: partial purification and some properties. Journal of Biological Chemistry 218:97-106.
- 24. Miller JH. 1972. Experiments in molecular genetics, Cold Spring Harbor, NY.
- 25. Duggan DE, Wechsler JA. 1973. An assay for transaminase B enzyme activity in *Escherichia coli* K-12. Anal Biochem 51:67-79.
- 26. McKinney J, Guerrier-Takada C, Galan J, Altman S. 2002. Tightly regulated gene expression system in *Salmonella enterica* serovar Typhimurium. J Bacteriol 184:6056-9.
- 27. Skovran E, Downs DM. 2000. Metabolic defects caused by mutations in the *isc* gene cluster in *Salmonella enterica* serovar typhimurium: implications for thiamine synthesis. J Bacteriol 182:3896-3903.
- 28. Flynn JM, Downs DM. 2013. In the absence of RidA, endogenous 2-aminoacrylate inactivates alanine racemases by modifying the pyridoxal 5'-phosphate cofactor. J Bacteriol 195:3603-9.
- 29. Schnackerz KD, Ehrlich JH, Giesemann W, Reed TA. 1979. Mechanism of action of D-serine dehydratase. Identification of a transient intermediate. Biochemistry 18:3557-63.
- 30. Ernst DC, Borchert AJ, Downs DM. 2018. Perturbation of the metabolic network in *Salmonella enterica* reveals cross-talk between coenzyme A and thiamine pathways. Plos one 13:e0197703.
- 31. Dobson RC, Gerrard JA, Pearce FG. 2004. Dihydrodipicolinate synthase is not inhibited by its substrate, (S)-aspartate beta-semialdehyde. Biochem J 377:757-62.
- 32. Cupp-Vickery JR, Urbina H, Vickery LE. 2003. Crystal structure of IscS, a cysteine desulfurase from *Escherichia coli*. J Mol Biol 330:1049-59.

- 33. Lundgren HK, Bjork GR. 2006. Structural alterations of the cysteine desulfurase IscS of *Salmonella enterica* serovar Typhimurium reveal substrate specificity of IscS in tRNA thiolation. J Bacteriol 188:3052-62.
- 34. Hodge-Hanson KM, Zoino A, Downs DM. 2018. Expression of PLP-independent racemases can reduce 2-aminoacrylate stress in *Salmonella enterica*. J Bacteriol doi:10.1128/JB.00751-17.
- 35. Borchert AJ, Ernst DC, Downs DM. 2019. Reactive Enamines and Imines *In Vivo*: Lessons from the RidA Paradigm. Trends Biochem Sci 44:849-860.
- 36. Shen W, Borchert AJ, Downs DM. 2022. 2-Aminoacrylate stress damages diverse PLP-dependent enzymes *in vivo*. J Biol Chem 298:101970.
- 37. Gutu AD, Sgambati N, Strasbourger P, Brannon MK, Jacobs MA, Haugen E, Kaul RK, Johansen HK, Hoiby N, Moskowitz SM. 2013. Polymyxin resistance of *Pseudomonas aeruginosa phoQ* mutants is dependent on additional two-component regulatory systems. Antimicrob Agents Chemother 57:2204-15.
- 38. Gutu AD, Rodgers NS, Park J, Moskowitz SM. 2015. *Pseudomonas aeruginosa* high-level resistance to polymyxins and other antimicrobial peptides requires *cprA*, a gene that is disrupted in the PAO1 strain. Antimicrob Agents Chemother 59:5377-87.
- 39. Ernst DC, Christopherson MR, Downs DM. 2018. Increased activity of cystathionine beta-lyase suppresses 2-aminoacrylate stress in *Salmonella enterica*. J Bacteriol doi:10.1128/JB.00040-18.
- 40. Schwartz CJ, Djaman O, Imlay JA, Kiley PJ. 2000. The cysteine desulfurase, IscS, has a major role in in vivo Fe-S cluster formation in *Escherichia coli*. Proceedings of the National Academy of Sciences of the United States of America 97:9009-14.
- 41. Blahut M, Wise CE, Bruno MR, Dong G, Makris TM, Frantom PA, Dunkle JA, Outten FW. 2019. Direct observation of intermediates in the SufS cysteine desulfurase reaction reveals functional roles of conserved active-site residues. J Biol Chem 294:12444-12458.

- 42. Lauhon CT, Kambampati R. 2000. The *iscS* gene in *Escherichia coli* is required for the biosynthesis of 4- thiouridine, thiamin, and NAD. J Biol Chem 275:20096-103.
- 43. Sun D, Lin CH, Hurley LH. 1993. A-tract and (+)-CC-1065-induced bending of DNA. Comparison of structural features using non-denaturing gel analysis, hydroxyl-radical footprinting, and high-field NMR. Biochemistry 32:4487-95.
- 44. Li J, Kogan M, Knight SA, Pain D, Dancis A. 1999. Yeast mitochondrial protein, Nfs1p, coordinately regulates iron-sulfur cluster proteins, cellular iron uptake, and iron distribution. J Biol Chem 274:33025-34.
- 45. Flint DH. 1996. *Escherichia coli* contains a protein that is homologous in function and N-terminal sequence to the protein encoded by the *nifS* gene of *Azotobacter vinelandii* and that can participate in the synthesis of the Fe-S cluster of dihydroxyacid dehydratase. Journal of Biological Chemistry 271:16068-74.
- 46. Dajnowicz S, Johnston RC, Parks JM, Blakeley MP, Keen DA, Weiss KL, Gerlits O, Kovalevsky A, Mueser TC. 2017. Direct visualization of critical hydrogen atoms in a pyridoxal 5'-phosphate enzyme. Nat Commun 8:955.
- 47. Fujishiro T, Nakamura R, Kunichika K, Takahashi Y. 2022. Structural diversity of cysteine desulfurases involved in iron-sulfur cluster biosynthesis. Biophys Physicobiol 19:1-18.
- 48. VanDrisse C, Escalante-Semerena J. 2016. New high-cloning-efficiency vectors for complementation studies and recombinant protein overproduction in *Escherichia coli* and *Salmonella enterica*. Plasmid 86:1-6.
- 49. Way JC, Davis MA, Morisato D, Roberts DE, Kleckner N. 1984. New Tn10 derivatives for transposon mutagenesis and for construction of *lacZ* operon fusions by transposition. Gene 32:369-379.
- 50. Castilho BA, Olfson P, Casadaban MJ. 1984. Plasmid insertion mutagenesis and *lac* gene fusion with mini-mu bacteriophage transposons. J Bacteriol 158:488-495.

TABLE 2.1: Plasmids, Strains and Primers

Plasmid name	Description	Drug resistance	Source
pCV1	pCV1 – empty vector	Ap ^R	(48)
pDM1439	pCV1 – S. enterica RidA	Laboratory	
pDW11439	$pCV1 - S.$ enterica RidA Ap^R		collection
pDM1636	pCV1 – P. aeruginosa IscS	An R	This study
pDM1637		Ap ^R Ap ^R	This study This study
pDW11037	IscS ^{Q183P}		,
pDM1684	pTEV18 – P. aeruginosa IscS	Ap ^R Ap ^R	This study
pDM1685	pTEV18 – P. aeruginosa	This study	
	IscS ^{Q183P}		
			,
Strain ID	Genotype ^a		Source
P. aeruginosa			
DMPA4	MPAO1 wild type (Manoil labo		(21)
DMPA5	<i>ridA</i> -F05::ISphoA/hah <i>dapA_(A32)</i>	(G, A322G)	This study
DMPA7	rid 4 E05: ISabo A /bab		(21)
	ridA-F05::ISphoA/hah		(21)
DMPA13	ridA-F05::ISphoA/hah PA1559	This study	
DMPA14	$ridA$ -F05::ISphoA/hah $iscS_{(A548C)}$ This study		
S. enterica	. D. J. (25)		
DM5419	iscR1::MudJ* (27)	Laboratory	
		collection	
DM12920	<i>ridA1</i> ::Tn <i>10d</i> (Tc)*	Laboratory	
		collection	
DM13509	aadA::araCpBADT7 (SM300A1-	(26)	
DM14846	<i>ridA1</i> ::Tn <i>10d</i> (Tc)/ pDM1439	This study	
DM14847	<i>ridA1</i> ::Tn <i>10d</i> (Tc)/ pCV1	This study	
DM17050	aadA::araCpBADT7 ridA1::Tn10(d)		Laboratory
			collection
DM17142	<i>ridA1</i> ::Tn <i>10d</i> (Tc)/ pDM1636	This study	
DM17143	<i>ridA1</i> ::Tn <i>10d</i> (Tc)/ pDM1637	This study	
DM17174	iscR1::MudJ/pDM1636	This study	
DM17175	iscR1::MudJ/pDM1637		This study
DM17194	iscR1::MudJ / pCV1	This study	
DM17392	aadA::araCpBADT7/ pDM1684	This study	
DM17393	aadA::araCpBADT7/pDM1685	This study	
DM17394	aadA::araCpBADT7 ridA1::Tn1	This study	
DM17395	aadA::araCpBADT7 ridA1::Tn1	This study	
		· / 1	· •
Primer	Sequence		
PAiscS pBAD	1		
For			
PAiscS pBAD	pBAD NNGCTCTTCNTTATCAGTGCCCTGCCATTC		
Rev	1		
	<u> </u>		

pae-TEV18- iscS-F	cgaagagcgctcttcttaagATGAAATTGCCGATCTACCTCG
pae-TEV18- iscS-R	ggccgcggatcccgggagctTCAGTGCGCCTGCCATTC

^a mutant alleles in *P. aeruginosa* are designated by the respective nucleotide changes as a subscript.

^{*}Tn10 \dot{d} (Tc) is the transposition-defective mini-Tn10 (Tn10 Δ 16 Δ 17) described by Way et al. (49). MudJ refers to the MudJ1734 transposon (50).

TABLE 2.2: Spontaneous mutations restore motility of a *P. aeruginosa ridA* mutant.

Strain	Genotype	Swim zone (mm)	Swim zone + THI (mm)
DMPA4	Wild type	21 ± 0.5*	20 ± 1*
DMPA7	ridA	11 ± 0.5	13 ± 0.5
DMPA14	iscS _(A548C)	14 ± 0.5*	14 ± 0.5*
DMPA5	$dapA_{(A321G, A322G)}$	$17 \pm 0.5*$	17 ± 1*
DMPA13	$PA1559_{(\Delta TCA188)}$	17 ± 0.5*	18 ± 0.5*

Swim halo diameters were measured in minimal medium with glucose (11 mM) and low agar (0.3%). Thiamine (THI) was present at 100 nM when indicated. Data are presented as the mean and standard deviation of the swimming halo diameter of three biological replicates grown at 37°C for 20 h. Values for each biological replicate were the average of two technical replicates. Percent wild-type motility is the swim diameter of each strain/swim diameter of the wild-type strain. An asterisk (*) indicates a significant difference in motility relative to the ridA mutant (p < 0.05).

TABLE 2.3. IscS^{Q183P} retains cysteine desulfurase activity.

	SDH activity (ΔA ₆₀₀ /min/mg protein)		
Medium	ridA	$ridA iscS_{(A548C)}$	
LB	13.9 ± 2.0	10.9 ± 1.5^{a}	
Minimal	3.7 ± 0.6	6.6 ± 0.4	
Minimal + Isoleucine	8.1 ± 1.0^{b}	6.7 ± 1.0^{b}	

^a indicates a significant difference in activity (p > 0.05) compared to the *ridA* mutant grown in the same (LB) medium.

Data shown are the means of two biological and four technical replicates using the SDH assay described in Materials and Methods. The indicated strains were grown in the stated medium with succinate as the sole carbon source in minimal medium and isoleucine added to 1 mM.

 $^{^{\}rm b}$ indicates a significant difference in activity (p > 0.05) compared to the same strain grown in the absence of isoleucine.

TABLE 2.4: IscS is a target of 2AA.

		Peak area ^a		% Released cofactor	
Host strain	Protein	PLP	Pyruvate/PLP	PLP	Pyruvate/PLP
ridA mutant	IscS	93.5 ± 1.4	64.9 ± 10.7	59	41
ridA mutant	IscS ^{Q183P}	168.1 ± 35	37.1 ± 3.2	82	18
wild type	IscS	165.1 ± 4.1	9.4 ± 2.8	5	95
wild type	IscS ^{Q183P}	162.6 ± 5.3	ND	100	0

^aPeak area is in arbitrary units (AU).

% Released cofactor is reported as the ratio of the indicated cofactor as numerator over total cofactor as the denominator.

IscS and IscS^{Q183P} proteins were each purified from two *S. enterica* host strains, wild type and a *ridA* mutant. Cofactors were released by treatment with base and separated by HPLC while monitoring absorbance at 305 nm in arbitrary units. Absorbance was monitored at 305 nm to capture both species. Therefore, peak area can be used to represent relative ratios, but not absolute concentration of each cofactor. Data were extracted from the chromatograph and peaks called and areas determined by the HPLC instrument. Data shown are the average and standard deviation of two technical replicates. "ND" indicates that a peak was not detected at 305 nm.

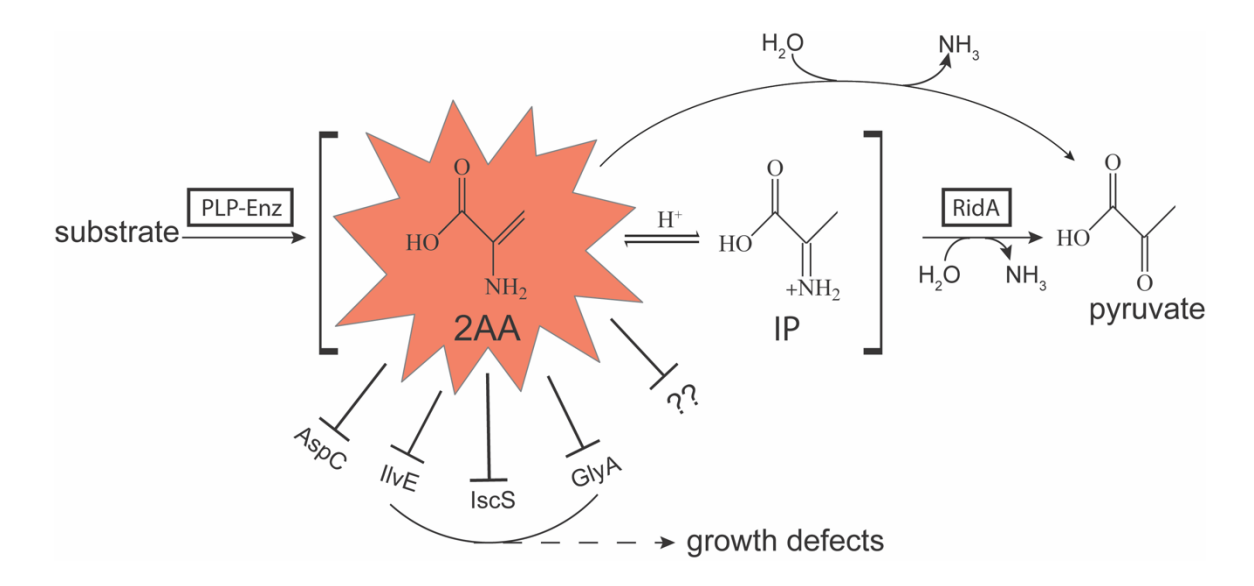


FIGURE 2.1: General RidA paradigm. Some PLP-dependent enzymes (PLP-Enz) generate an enamine intermediate (2-aminoacrylate (2AA)), which can tautomerize to the imine 2-iminopropionate (IP). 2AA is deaminated to pyruvate by RidA, or spontaneously by free water. In the absence of RidA, spontaneous deamination by water in the cellular milieu is not sufficient and 2AA persists. If allowed to persist in the cell, 2AA can irreversibly damage multiple PLP-dependent enzymes, as schematically represented. Depending on the metabolic architecture of the organism, one or more of these damaged enzymes will generate nutritional and/or growth phenotypes in *ridA* mutants. In *S. enterica*, GlyA is the most significant enzyme damaged in the sense that bypassing this step with exogenous glycine reverses the majority of the growth defect. In *Pseudomonas aeruginosa*, damage to IscS (see text) is the primary driver of growth consequences of a *ridA* mutant. Question marks represent the additional enzyme targets that are not yet identified. Abbreviations: AspC, aspartate transaminase (EC 2.6.1.1); IlvE, transaminase B (EC 2.6.1.42); IscS, cysteine desulfurase (EC 2.8.1.7); GlyA, serine hydroxymethyltransferase (EC 2.1.2.1).

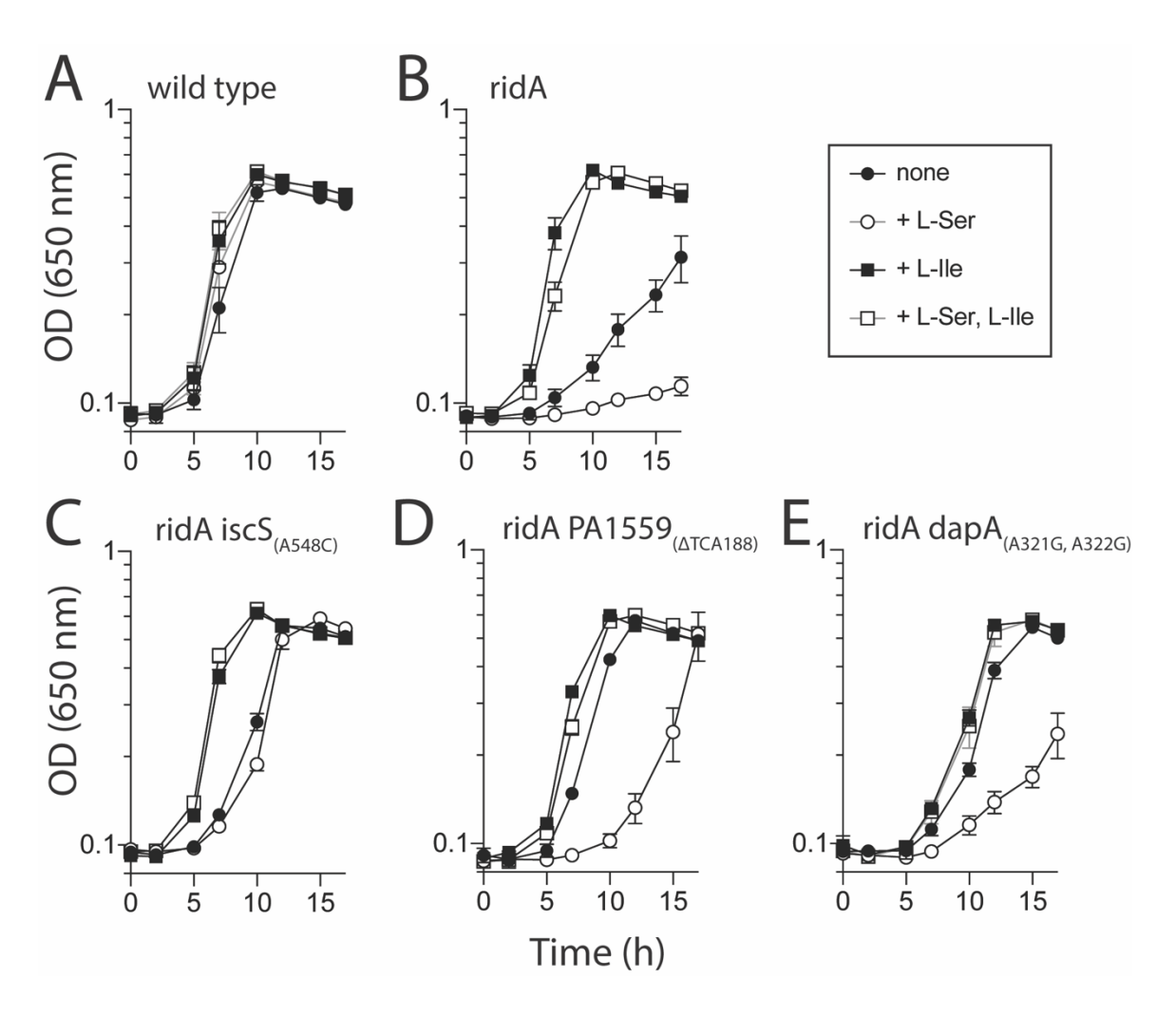


FIGURE 2.2: Suppressor mutations alleviate the growth defect of a *P. aeruginosa ridA* mutant. Bacterial growth was measured as the change in optical density over time when strains were inoculated into minimal glucose (11 mM) medium with no supplements or with L-serine (0.5 mM), L-isoleucine (1 mM), or both L-serine and L-isoleucine added as indicated. Growth patterns of wild-type *P. aeruginosa* (A), *P. aeruginosa ridA* (B), and *ridA* mutants with spontaneous suppressor mutations, $iscS_{(A548C)}$ (C), $PA1559_{(\Delta TCA188)}$ (D) and $dapA_{(A321G, A322G)}$ (E) are shown. Error bars represent standard deviation between three independent biological replicates.

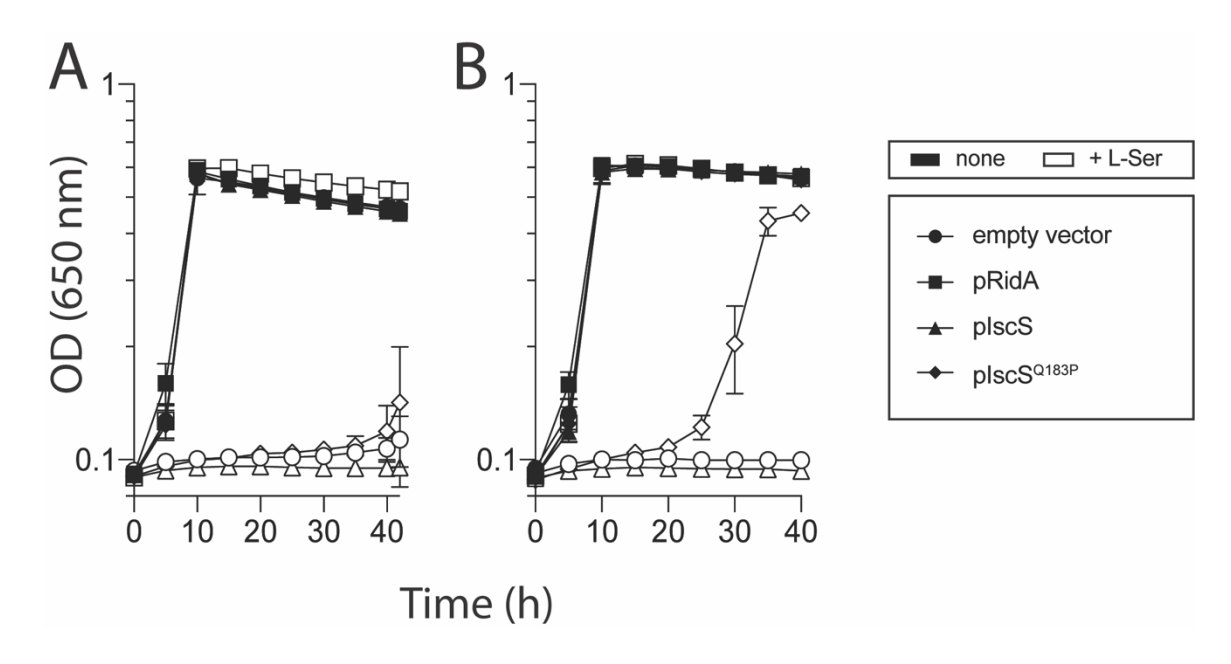


FIGURE 2.3: The *iscS*_(A548C) allele of *in trans* restores growth to a *S. enterica ridA* mutant with serine. Bacterial growth was measured as the change in optical density (650 nm) over time for a *S. enterica ridA* mutant with the pCV1 empty vector (circles), pDM1439 encoding seRidA (squares), pDM1636 encoding PAIscS (triangles), or pDM1637 encoding PAIscS^{Q183P} (diamonds). Growth of the relevant strains was monitored in minimal glucose medium without L-arabinose (A) or with 0.2% L-arabinose (B) and no further additions (filled symbols), or 5 mM L-serine (open symbols). Error bars represent standard deviation between three independent biological replicates.

.

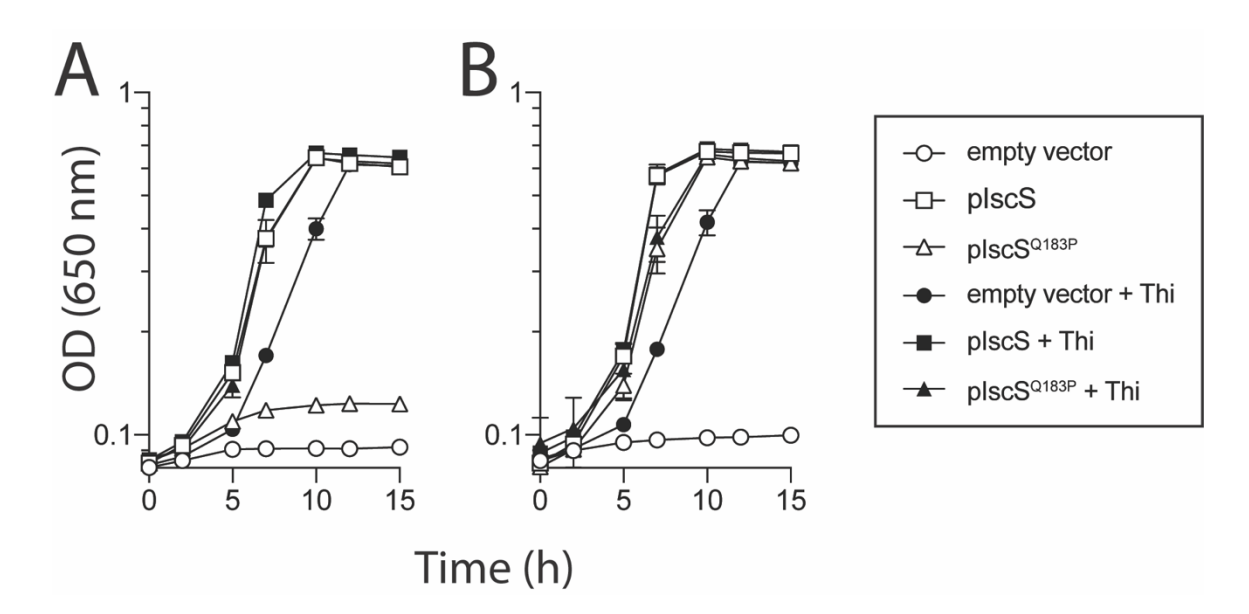


FIGURE 2.4: IscS^{Q183P} has cysteine desulfurase activity *in vivo*. *S. enterica* strain (DM5419) which is auxotrophic for thiamine and nicotinic acid (*iscR1*::MudJ) (27), was transformed with a pCV1 empty vector (circles), pDM1636 (squares), or pDM1637 (triangles), encoding PAIscS and PAIscS^{Q183P} respectively. The resulting strains were grown in minimal glucose medium with nicotinic acid alone (open shapes) or with nicotinic acid and 100 nM thiamine (filled shapes). L-arabinose (0.2%) was absent (A) or present (B) in the medium to induce expression of plasmid-encoded gene. Error bars represent standard deviation between three independent biological replicates.

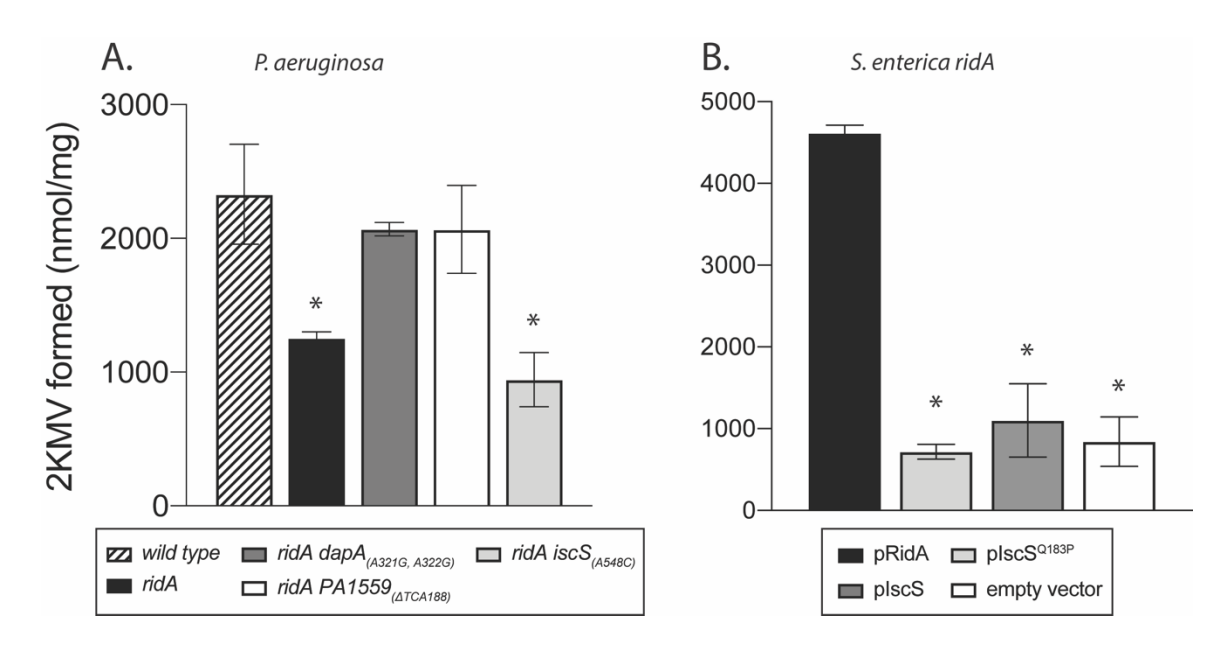


FIGURE 2.5: IscS^{Q183P} does not reduce 2AA accumulation. The relevant strains of P. aeruginosa and S. enterica were grown to full density in minimal glucose medium and transaminase B (IIvE) activity was determined. (A) A wild-type P. aeruginosa strain (stripes), a ridA mutant (black) and three spontaneous ridA suppressor mutants, $PA1559_{(\Delta TCA188)}$ (white), $dapA_{(A321G, A322G)}$ (dark grey), and $iscS_{(A548C)}$ (light grey). (B) A ridA mutant of S. enterica was transformed with plasmids encoding $_{SE}$ RidA (black), $_{PA}$ IscS (dark grey), $_{PA}$ IscS $_{Q183P}$ (white) or an empty vector control (light grey). Error bars represent standard deviation of three independent biological replicates. An asterisk (*) indicates a significant difference in IIvE activity when compared to wild-type P. aeruginosa (A) or S. enterica ridA with a plasmid encoding $_{SE}$ RidA (B) (p < 0.05).

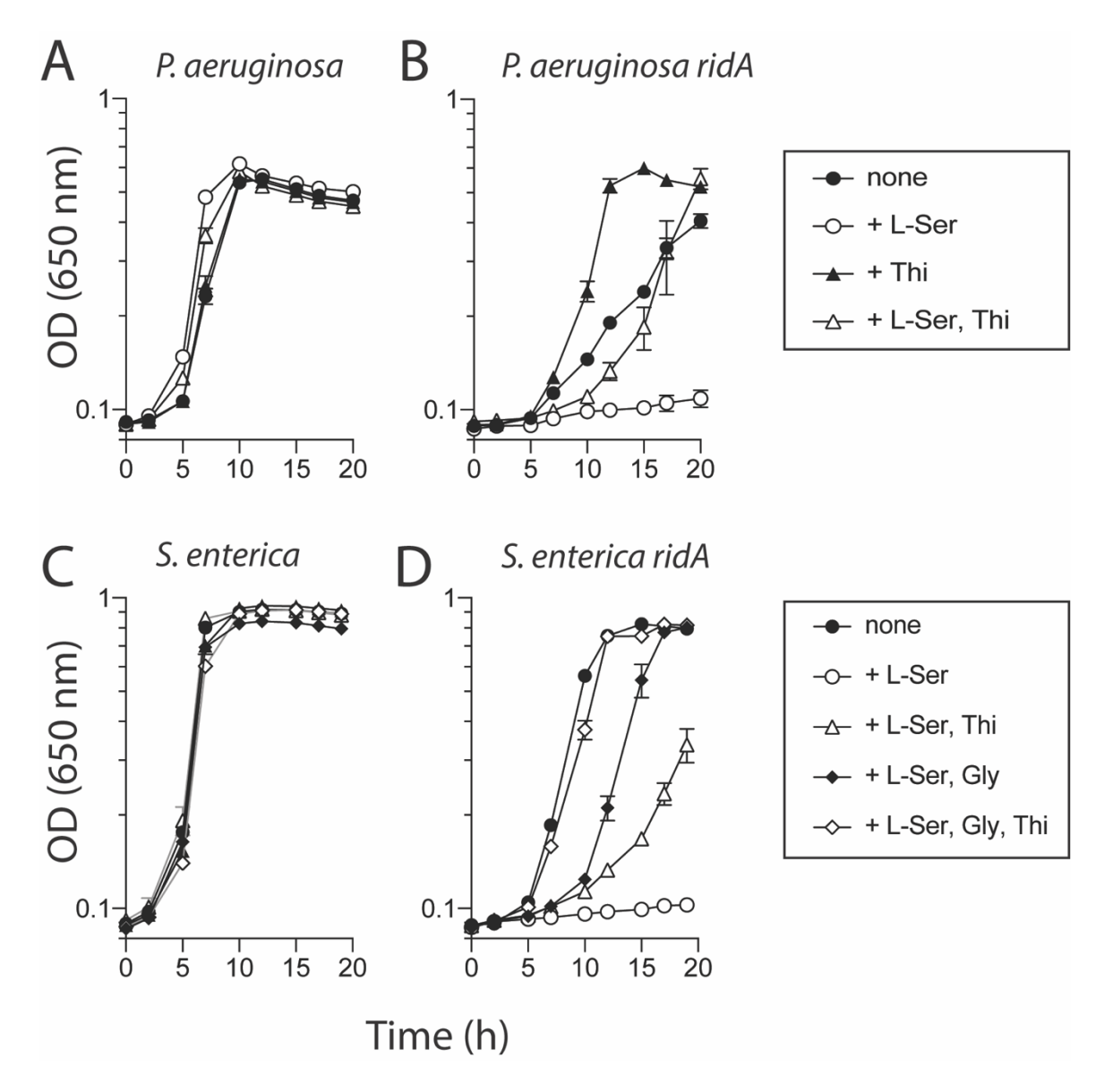


FIGURE 2.6: Exogenous thiamine restores growth of *ridA* mutants in *P. aeruginosa* and *S. enterica*. Growth was measured for *P. aeruginosa* wild type (A) and *P. aeruginosa* ridA (B), along with *S. enterica* wild type (C) and *S. enterica* ridA (D). *P. aeruginosa* strains were grown in minimal glucose medium with no additions (closed circles), minimal glucose supplemented with 0.5 mM L-serine (open circles), 100 nM thiamine (closed triangles) or both L-serine and thiamine (open triangles). *S. enterica* strains were grown in minimal glucose medium with no additions (closed circles), 5 mM L-serine (open circles), L-serine and 100 nM thiamine (open triangles), L-serine and 1 mM glycine (closed diamonds), or L-serine, thiamine and glycine (open diamonds). Error bars represent standard deviation between three independent biological replicates.

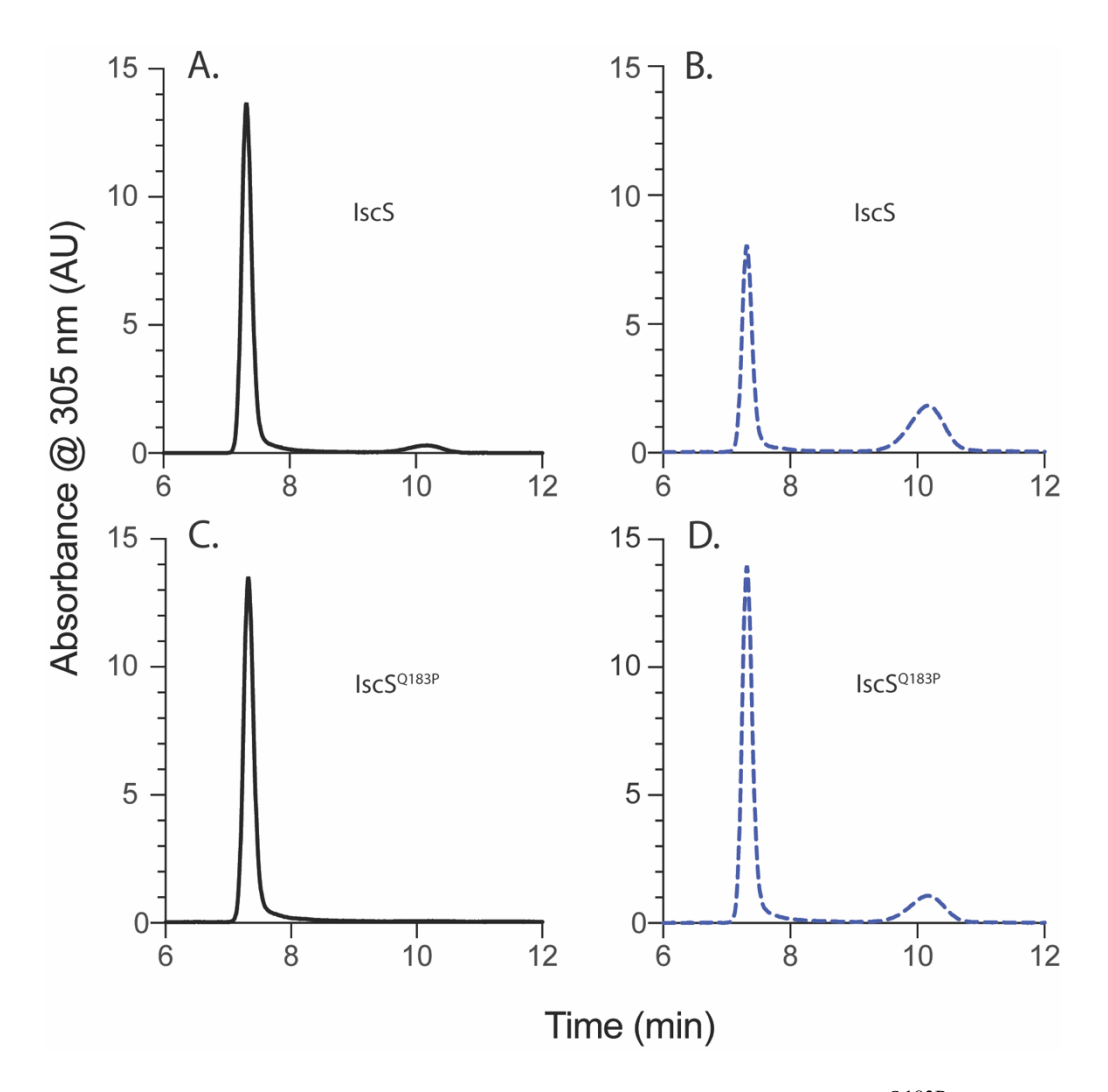


FIGURE 2.7: IscS is sensitive to attack by 2AA. IscS and IscS Q183P were each purified from two *S. enterica* host strains, wild type and a *ridA* mutant. Cofactors were released from each sample, separated by HPLC and visualized by monitoring absorbance at 305 nm in arbitrary units (AU). Shown are the profiles of cofactors released from IscS purified from wild type (A) and a *ridA* mutant (B) and those from IscS Q183P purified from wild type (C) and a *ridA* mutant (D). The peak with a retention time of ~7 min was PLP and that with a retention time of ~10 min was pyruvate/PLP. Peak assignment was based on retention time, UV-vis spectra and co-injection with authentic species (Figure S2). Absorbance was monitored at 305 nm to capture both species. Data shown are an average of two technical replicates.

TABLE 2.S1: Spontaneous mutations restore motility of a *P. aeruginosa ridA* mutant.

Strain	Relevant Genotype	Swim diameter (mm)	Swim diameter + Ile (mm)
DMPA4	Wild type	18 ± 0.5*	19 ± 1
DMPA7	ridA	8 ± 0.5	19 ± 1
DMPA14	ridA iscS _(A548C)	12 ± 0.5*	20 ± 0.5

Spontaneous mutations restore motility of a P. aeruginosa ridA mutant. The diameter of swimming halos was measured in minimal medium with glucose (11 mM) and 0.3% agar. l-isoleucine (1 mM) was added as indicated. Data are presented as the mean diameter and standard deviation of the swim halo of three biological replicates grown at 37°C for 20 h. Values for each biological replicate were the average of two technical replicates. An asterisk (*) indicates a significant difference in motility relative to the ridA mutant (P < 0.05).

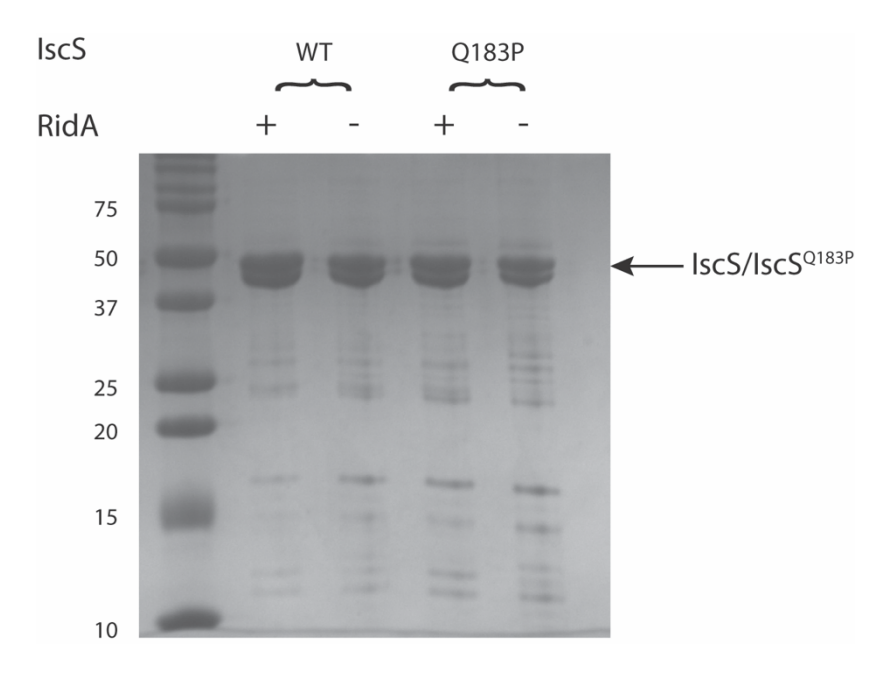


FIGURE 2.S1: IscS and IscS^{Q183P} purified from *ridA*+ and *ridA*- *S. enterica*. Wild-type IscS or IscS^{Q183P} samples purified from *Salmonella enterica* SB300 *ridA*+ (DM13509), or *ridA*- (DM17050). Samples were separated by electrophoresis on a 12% polyacrylamide gel, stained with Coomassie, and imaged using AnalytikJena UVP ChemStudio. Densitometry analysis was performed using VisionWorks software version 8.22.18309.10577. BioRad Precision Plus Kaleidoscope Protein Ladder was run in the leftmost lane. Samples (from left to right) are IscS from wild-type, IscS from *ridA* mutant, IscS^{Q183P} from wild-type, and IscS^{Q183P} from *ridA* mutant. 4 μg of protein was loaded for each sample.

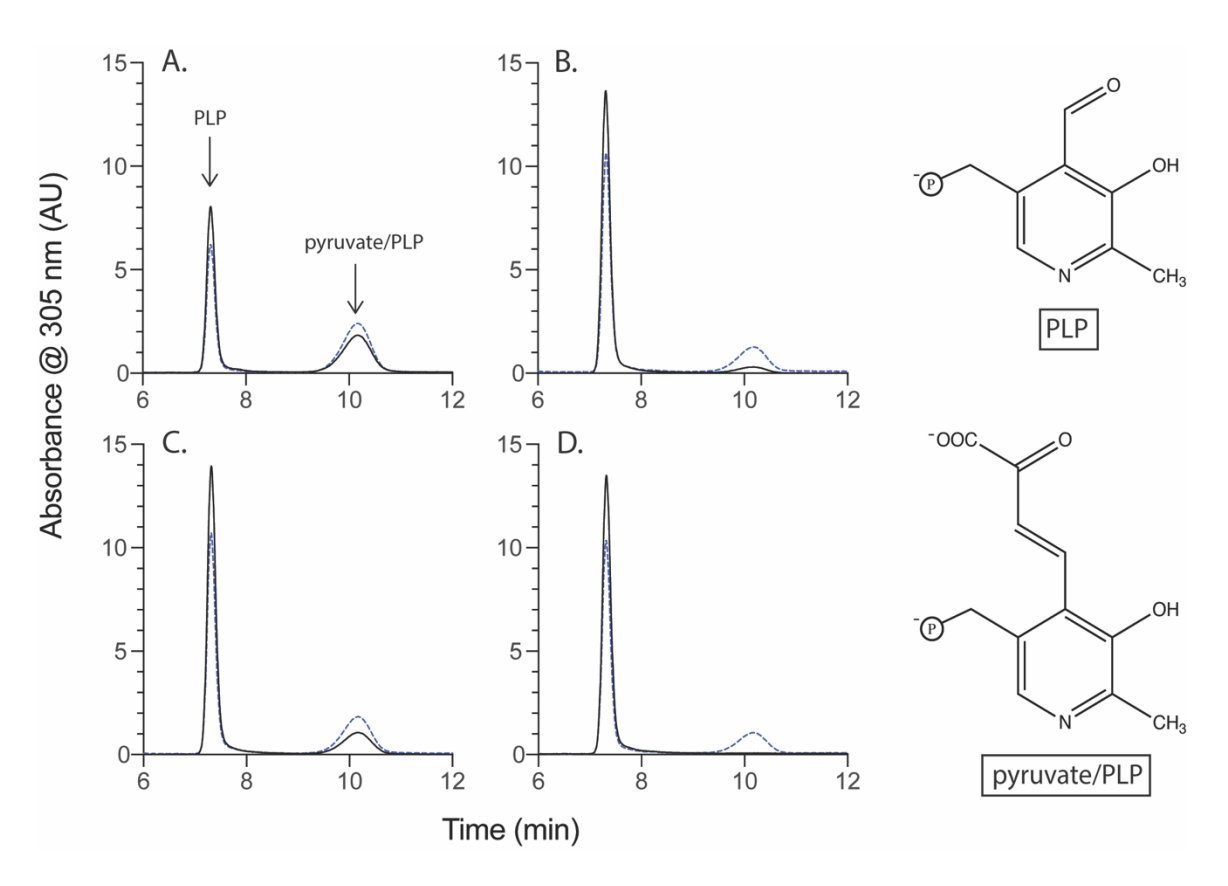


FIGURE 2.S2: Standards confirm peaks as PLP and pyruvate/PLP. Authentic pyruvate/PLP was generated and purified as described in Materials and Methods. Due to the instability of the pyruvate/PLP, over time this sample contained both PLP and pyruvate/PLP and thus provided a standard for both cofactors. Cofactors released from IscS purified from a *ridA* mutant (A) and wild-type (B), along with IscS^{Q183P} purified from a *ridA* mutant (C) and wild-type (D) were separated by HPLC. In each case, the sample was run alone (solid lines) or with a coinjection of a sample containing authentic pyruvate/PLP and PLP (blue dashed lines). The peak at ~7 minutes corresponds to PLP, and the peak at ~10 minutes corresponds to pyruvate/PLP. The structure of the relevant molecules, PLP and pyruvate/PLP is shown.

CHAPTER 3

DADY (PA5303) IS REQUIRED FOR FITNESS OF *PSEUDOMONAS AERUGINOSA*WHEN GROWTH IS DEPENDENT ON ALANINE CATABOLISM¹

Reprinted here with permission of the publisher.

¹Fulton RL, Downs DM. 2022. *Microbial Cell 9(12): 195-206*.

3.1 ABSTRACT

Pseudomonas aeruginosa inhabits diverse environmental niches that can have varying nutrient composition. The ubiquity of this organism is facilitated by a metabolic strategy that preferentially utilizes low-energy, non-fermentable organic acids, such as amino acids, rather than the high-energy sugars preferred by many other microbes. The amino acid alanine is among the preferred substrates of P. aeruginosa. The dad locus encodes the constituents of the alanine catabolic pathway of P. aeruginosa. Physiological roles for DadR (AsnC-type transcriptional activator), DadX (alanine racemase), and DadA (D-amino acid dehydrogenase) have been defined in this pathway. An additional protein, PA5303, is encoded in the dad locus in P. aeruginosa. PA5303 is a member of the ubiquitous Rid protein superfamily and is designated DadY based on the data presented herein. Despite its conservation in numerous *Pseudomonas* species and membership in the Rid superfamily, no physiological function has been assigned to DadY. In the present study, we demonstrate that DadA releases imino-alanine that can be deaminated by DadY in vitro. While DadY was not required for alanine catabolism in monoculture, dadY mutants had a dramatic fitness defect in competition with wild-type P. aeruginosa when alanine served as the sole carbon or nitrogen source. The data presented herein support a model in which DadY facilitates flux through the alanine catabolic pathway by removing the imine intermediate generated by DadA. Functional characterization of DadY contributes to our understanding of the role of the broadly conserved Rid family members.

3.2 INTRODUCTION

Amino acids are abundant in nature and serve as structural components of peptides and cell walls, intra- and extra-cellular signaling molecules, as well as nutrient sources for microbial growth. Utilization of amino acids for carbon and nitrogen is important for the proliferation of bacteria in several natural environments including soil, aquatic, and marine niches [1]. Additionally, amino acid catabolism can facilitate bacterial association with animal or plant hosts [2-4]. As such, the elucidation of how bacteria utilize amino acids is foundational to an understanding of their ecology, industrial or agricultural applications, and clinical significance.

Pseudomonas species are metabolic generalists that can grow on a wide variety of substrates and inhabit diverse ecological niches. Pseudomonas aeruginosa is perhaps the best studied member of the genus due to its clinical significance. The benefit of understanding the metabolism and physiology of this organism is reinforced by its ability to influence the microbial composition of its environment by participating in mutualistic relationships and edging-out competitors [5-10]. Like other Pseudomonas species, P. aeruginosa, has adopted a metabolic strategy in which low energy, non-fermentable organic acids, such as TCA cycle intermediates and amino acids (particularly Asn, Asp, Gln, Glu and Ala) are preferentially utilized over high energy sugars like glucose [11-14]. This strategy provides P. aeruginosa an advantage over competitors in environments where amino acids, and other organic acids, are the primary source of nutrients.

Alanine is among the preferred amino acid substrates for *P. aeruginosa*. Catabolism and homeostasis of this amino acid have been implicated in virulence, gene regulation, and mechanical properties of the cell [15-17]. The *dad* locus in *P. aeruginosa*, regulated by

DadR (AsnC-type regulator), encodes DadX (PLP-dependent alanine racemase, EC 5.1.1.1), DadA (FAD-dependent D-amino acid dehydrogenase, EC 1.4.5.1), and PA5303, a protein of unknown function. Based on the data presented herein, PA5303 is designated DadY throughout. DadA and DadX have been biochemically characterized and their physiological roles in the catabolism of alanine described [15]. The alanine catabolic pathway that incorporates these activities is schematically represented in Figure 1A. DadY belongs to the large, sequence diverse Rid (Reactive intermediate deaminase) superfamily of proteins, which is categorized into eight subfamilies. Within this superfamily, the ancestral RidA subfamily is conserved in all domains of life, while the remaining subfamilies are found only in prokaryotes, primarily bacteria [18]. Rid proteins can also be divided into two groups based on the presence or absence of a key arginine residue that is essential for imine/enamine deaminase activity. The deaminase activity of these proteins was first described for the RidA in S. enterica [19]. Proteins in the RidA and Rid1-3 subfamilies, including RutC proteins, contain the relevant arginine residue, and all such proteins that have been assayed to date have some imine/enamine deaminase activity in vitro [18-29]. Significantly, the deaminase reaction catalyzed by Rid proteins assessed thus far can also be carried out spontaneously by solvent water, suggesting that these proteins simply accelerate a reaction that can occur in their absence [19-22, 29-31]. Members of the RidA subfamily have been assigned a role in ameliorating 2-aminoacrylate stress in a paradigm that has been well established in several bacterial species, yeast, and higher-order eukaryotes [2, 23-25, 30-34]. The deaminase activity of proteins in the other Rid subfamilies, except for RutC from E. coli [22], has not been placed in a physiological context [15, 20, 21, 24, 35]. Proteins belonging to the Rid4-7 subfamilies lack the relevant Arg residue and, as expected, those tested to date lack imine/enamine deaminase activity [18, 20, 21]. Currently, RidA proteins are the only Rid subfamily with members that have a demonstrated physiological role.

DadY belongs to the Rid2 subfamily and, based on the presence of the relevant arginine residue, is predicted to have deaminase activity. In *P. aeruginosa*, *dadY* is in an operon with *dadA* and *dadX*, which implicates DadY in alanine catabolism. DadA is an FAD-dependent dehydrogenase, the catalytic mechanism of which has been proposed to proceed through an imine intermediate, as demonstrated for other similar dehydrogenases [21, 36-38]. Were this the case, the imine (imino-alanine, or 2-iminopropionate) released by DadA would be a potential substrate for DadY. In this scenario, deaminase activity of DadY would accelerate the rate of formation of the final products of the pathway – pyruvate and ammonia (Figure 1B). This study was initiated to test the above scenario and define the physiological role for DadY in *P. aeruginosa*. The data show that DadY improves fitness of *P. aeruginosa* when growth is dependent on alanine catabolism. The results herein emphasize the significance of competitive fitness as a means to detect the subtle, but critical, contributions of various metabolic components to robust cellular physiology.

3.3 RESULTS

The structure of the dad locus varies among phylogenetic groups of Pseudomonas. The dad locus of P. aeruginosa includes a single gene, dadA, that is conserved among all Pseudomonas species. The dadR gene is also present in all Pseudomonas species but is located distally from other dad genes in P. aeruginosa. Pseudomonas species have been previously classified into genomic affinity groups and subgroups based on phylogenetic

clustering and sequence similarity [39-43]. The structure of the dad locus was assessed in these groups. The phylogenetic groups were placed into one of five categories based on the constituents and organization of dad genes (Figure 2). This analysis showed that most Pseudomonas species have a dad locus with four contiguous genes (Figure 2; Group 5). Members of the *P. aeruginosa* group similarly encode the four *dad* genes. However, the *P.* aeruginosa group is distinct in that dadR is separated from the remaining dad genes by three ORFs. Members of the P. putida group and a single P. stutzeri species (P. stutzeri Group B), lack an identifiable *dadY* in their genome. The remaining *P. stutzeri* species lack a gene encoding DadX, the PLP-dependent racemase that is essential for L-alanine catabolism in P. aeruginosa (Figure 1) [15]. DadY is a putative imine/enamine deaminase belonging to the Rid superfamily. A gene encoding DadY is present in the dad locus of most *Pseudomonas* species (Figure 2). Despite its prevalence in the *dad* locus of most Pseudomonas species, no function has been described for DadY in the alanine catabolic pathway. A working model suggests that DadY can deaminate the imino-alanine generated by DadA, which will increase and/or accelerate flux through the dad pathway as represented in Figure 1B [20].

DadY is an imine deaminase *in vitro. ridA* mutants of *Salmonella enterica* fail to grow in the presence of serine due to the accumulation of the reactive enamine 2-aminoacrylate (2AA) [19, 30, 44]. These *ridA* mutants provide a means to test other proteins (i.e., Rid proteins) for 2AA deaminase activity *in vivo*, since such activity restores growth to the *ridA* mutant [21, 24, 25]. When provided *in trans*, DadY from *P. aeruginosa* failed to restore growth of a *S. enterica ridA* mutant in the presence of serine, despite the plasmid-borne

gene being overexpressed (Figure 3). In contrast, _{SE}RidA fully restored growth with or without overexpression, as did multiple RidA subfamily members (data not shown) [21, 24]. These data show that the activity of DadY and RidA are not redundant *in vivo*, despite the fact that DadY can deaminate 2AA *in vitro* (data not shown). Together these observations raise the question of how deaminase activity of DadY differs from that of RidA *in vitro* and *in vivo*.

The arginine critical for imine/enamine deaminase activity in Rid proteins is present and at position 94 in DadY. The imine deaminase activity of DadY was tested using a standard in vitro assay. L-amino acid oxidase (LOX) is an FAD-dependent enzyme that generates imines from a variety of L-amino acid substrates. The resulting imines are released into the solvent where they can; i) be quenched by solvent water, ii) react with added semicarbazide to generate a semicarbazone that is detectable spectrophotometrically at 248 nm, or iii) be quenched by a Rid protein with deaminase activity. The rate at which imines are hydrolyzed by solvent water is constant at a given pH but varies for imines derived from different amino acids [45]. In this assay, Rid-mediated deaminase activity is detected as a decrease in semicarbazone formation compared to reactions with LOX and semicarbazide alone. The ability of DadY to deaminate imines generated by LOX from the L-amino acids L-Arg, L-Gln, L-His, L-Leu, L-Met, and L-Phe was determined (Table 2). DadY deaminated imines derived from all amino acids tested and had a broader substrate range than either of the RidA proteins. Specifically, neither the RidA from S. enterica nor P. aeruginosa had significant deaminase activity on imines derived from L-Arg, L-His or L-Phe. Of the substrates the RidA proteins were active with, DadY was significantly more active on imines derived from L-Gln and appeared more active on the imine derived from

L-Leu than the *S. enterica* RidA. These data allow the conclusion that DadY is an imine deaminase and has a substrate specificity that differs from RidA proteins.

DadA releases an imine substrate for DadY. DadA is a membrane-bound, FAD-dependent D-amino acid dehydrogenase that uses D-alanine as its preferred substrate. DadA cannot use oxygen as a terminal electron acceptor, distinguishing its mechanism from that of LOX and other oxidases [36]. The catalytic mechanism of DadA is thought to proceed via an imine intermediate, as is the case with similar enzymes [21, 36-38]. If generated, the imine intermediate would either remain in the active site of DadA or be released into the solvent prior to the deamination that results in pyruvate and ammonia. Semicarbazide was added to the assay to determine if imino-alanine was released into the solvent after generation by DadA. If released, the imino-alanine would be expected to generate a semicarbazone compound that was detectable spectrophotometrically. When DadA used D-alanine as a substrate and semicarbazide was present, a semicarbazone compound was formed at a rate of $18.3 \pm 0.3 \,\mu\text{M/min}$. This result indicated that DadA released an imine product and thus provided a potential substrate for DadY *in vivo*.

The data above was generally consistent with the proposed role for DadY in the catabolism of alanine (Figure 1). DadY was added in the DadA assay described above to determine if this Rid protein could compete with semicarbazide for the released imine. The rate of semicarbazone formation was observed to be nearly four-fold lower in the presence vs. absence of DadY (4.7 ± 0.7 vs 18.3 ± 0.3 μ M semicarbazone formed/min, respectively). Results of these assays confirmed that DadY could act on the imine derived from D-alanine

that was generated by DadA. In total, the data supported the potential for DadY to contribute to the efficiency of D-alanine catabolism *in vivo*.

P. aeruginosa catabolizes alanine in the absence of DadY. The data above implicated DadY in the alanine catabolic pathway and suggested that this protein, like DadA and DadX, could be required for *P. aeruginosa* to use alanine as a nutrient source. Various strains were inoculated into media with D-/L-alanine as the sole source of nitrogen or carbon (Figure 4). Growth patterns of wild type and strains lacking either the dadA or dadY gene were indistinguishable with glucose and ammonia as the sole source of carbon or nitrogen, respectively. As expected, the dadA mutant had a significant growth defect when D- or L-alanine was the sole source of nitrogen or carbon. The defect of the dadA mutant was particularly severe when D-alanine served as the sole carbon source, though even wild type grew poorly in this condition. Poor use of D-alanine as a carbon source was previously attributed to a need to convert D-alanine to the L-alanine required to fully activate transcription of the dad operon [15]. Unexpectedly, there was significant growth of the dadA mutant when L-alanine was the sole nitrogen source. This result suggests there is another way to generate ammonia from alanine in vivo, the mechanism of which was not pursued here. Unlike the varying, but clear, growth defects of a dadA mutant, growth of the strain lacking DadY was not significantly different from wild type in any condition tested (Figure 4).

DadY is required for competitive fitness of *P. aeruginosa*. The biochemical data above showed that DadY can deaminate the imino-alanine generated by DadA, though this

reaction can also be mediated by solvent water. Growth data in Figure 4 suggested that the rate of imine deamination by water was sufficient for growth in monoculture under standard laboratory conditions. One hypothesis for the conservation of DadY is that it contributes to fitness of P. aeruginosa when it is competing with other organisms in the environment. This hypothesis was supported by the results of experiments to measure competitive fitness (Figure 5). Competitive fitness was determined for strains lacking the appropriate gene (dadA or dadY) when grown with wild-type P. aeruginosa in a variety of media. Importantly, wild type did not have a competitive advantage over either mutant when grown in a minimal medium with glucose as carbon source and ammonia as nitrogen source. Based on the growth defect in monoculture, it was expected that the dadA mutant had a competitive disadvantage in a medium with alanine as sole source of either nitrogen or carbon. However, it was striking that the dadY mutants were also outcompeted by wild type when grown with alanine as the sole source of carbon or nitrogen. In each of the relevant media, the dadY mutant had a significant competitive disadvantage, though to a lesser degree than the dadA mutant in the same condition. The most significant competitive defects were detected when alanine was provided as the sole source of carbon. This result is not unexpected since the cell requires more carbon than for nitrogen. This means the efficiency of the pathway encoded by the *dad* operon is more critical when it is responsible for generating the carbon molecule (pyruvate) that can enter central metabolism. The dadY mutant had a 128-fold decrease in competitive fitness (i.e., the inverse of the Competitive Index – see equation in Figure 5) when alanine was the nitrogen source versus a 2000-fold decrease when alanine was the carbon source (Figure 5). The same bias was observed, to a greater degree, with the dadA mutant, which had a fitness defect of 109 and 33000 when

alanine was used as a carbon or nitrogen source, respectively. The more severe defect of the *dadA* mutant compared to the *dadY* mutant in all cases was consistent with growth phenotypes in monoculture. When D-alanine was provided as sole nitrogen source, the competitive fitness of the *dadA* and *dadY* mutants were less defective and more similar to each other than with L-alanine. These data are consistent with the limited ability of wild-type *P. aeruginosa* to grow on D-alanine (Figure 4). In total, these data support the hypothesis that DadY is required to accelerate the catabolism of alanine in competitive settings, like the natural environments of *P. aeruginosa*.

3.4 DISCUSSION

Members of the Rid superfamily that have been characterized catalyze reactions *in vitro* that are also mediated spontaneously by solvent water. While imine/enamine deaminase activity can be demonstrated *in vitro*, the role of these enzymes *in vivo* has only been clearly shown for members of the RidA subfamily. Characterization of the RidA protein in *S. enterica* defined the paradigm for 2-aminoacrylate (2AA) stress. 2AA is a reactive enamine that can attack and inactivate target PLP-dependent enzymes. While 2AA can be deaminated spontaneously by water, loss of RidA activity results in the accumulation of 2AA, resulting in global damage that ultimately leads to detectable phenotypes. Importantly, the phenotypes differ between organisms and often require an additional environmental, genetic, or nutritional insult to be detected. Proteins in the Rid1-3 subfamilies are presumed to also have deaminase activity. Genes encoding Rid1-3 proteins are broadly distributed in bacteria and are found in diverse genomic contexts. While numerous Rid1-3 proteins have been assayed for generic imine/enamine deaminase

activity *in vitro*, the relevant substrate, and thus physiological role, has not been defined for these proteins. We suggested the lack of phenotypic manifestation reflected a low, yet sufficient, rate of reactivity with water in the cellular milieu [20]. The current study provides the first substantial evidence in support of this general hypothesis. Here, we demonstrate that the Rid2 subfamily protein DadY (PA5303) is required for competitive fitness of *P. aeruginosa* when growth is dependent on the catabolism of alanine.

A role for DadY in alanine catabolism was suggested by its genomic context in *Pseudomonas aeruginosa*, and other *Pseudomonas* species (Figure 2). The putative deaminase activity of this protein family led us to propose the model in Figure 1. This model was based on the precedent that FAD-dependent dehydrogenases generate and release imine products, and that Rid family proteins with a key arginine can have imine/enamine deaminase activity. The data herein reconstructed the components of this pathway *in vitro*. However, the simple prediction from this model, that a *dadY* mutant would be defective in catabolizing alanine, was not supported by analyses of growth in monoculture. As noted above, the reaction attributed to DadY in this scheme is also mediated by solvent water, suggesting that DadY might only be needed to accelerate flux through the pathway when the rate of spontaneous deamination by free water is insufficient. In other words, DadY activity could circumvent a kinetic bottleneck caused by reliance on the spontaneous conversion of these imines to the final ketoacid and ammonia products.

P. aeruginosa, and most (if not all) microbes, are constantly in competition with one another in their natural environments. Thus, analysis of metabolic efficiency might be more relevant if carried out in a competitive context. This notion is supported by the fact

that strains lacking dadY were dramatically outcompeted by wild type when alanine served as sole source of either carbon or nitrogen, despite having no growth defect in monoculture. The results herein support a model for alanine catabolism in which DadY removes imine intermediates released by DadA at a rate greater than that of free water. Such metabolic contributions by DadY appear to be too subtle to elicit a requirement in monoculture but become essential for optimal fitness in a competitive environment. The characterization of DadY activity as supplementary to the metabolic efficiency of P. aeruginosa provides a potential framework through which to view the contributions of Rid proteins in general to the metabolic network they participate in. Specifically, it provides the first clear evidence that Rid proteins, at least those belonging to the deaminase group, could serve to fine-tune their respective metabolic pathway by maximizing flux. This acceleration may not be necessary for growth in monoculture but would be advantageous in the natural environments inhabited by competitors. This benefit to fitness would justify the broad representation and conservation of members of this superfamily. Further work is needed to shed light on the separate and/or overlapping activities of the different Rid family members. The possibility that Rid proteins catalyze otherwise spontaneous reactions that are distinct from water mediated deamination must be considered. The existence of Rid superfamily members that are incapable of deamination supports this notion and emphasizes the trove of metabolic knowledge that is likely to be uncovered with a better understanding of the Rid protein superfamily.

3.5 MATERIALS AND METHODS

Media and chemicals. P. aeruginosa and E. coli strains were routinely grown in Lysogeny Broth (LB; 10 g/L tryptone, 5 g/L NaCl, 5 g/L yeast extract), and S. enterica strains were grown in Nutrient Broth (NB; Difco) as a rich medium. Both bacteria were incubated at 37°C unless otherwise indicated. For protein purification, cells were grown in Terrific Broth (TB; 12 g/L tryptone, 24 g/L yeast extract, 4 ml/L glycerol, 17 mM KH₂PO₄, 72 mM K₂HPO₄). Solid media contained 15 g/L agar. Ampicillin (Ap) and kanamycin (Km) were added at 150 µg/ml and 50 µg/ml, respectively, for E. coli. Gentamicin (Gm) was added at 30-50 µg/ml for P. aeruginosa or 20 µg/ml for E. coli. Minimal media were M8 salts (12) mM Na₂HPO₄, 22 mM KH₂PO₄, 1 mM NaCl, 1 mM MgSO₄) with trace minerals [46], supplemented with indicated sources of carbon (11 mM glucose; 20 mM amino acids) and nitrogen (10 mM NH₄Cl; 5 mM amino acids). Vogel-Bonner Minimal Medium supplemented with 50 μg/ml gentamicin (VBMM Gm50; 3 g/L trisodium citrate, 2 g/L citric acid, 10 g/L K₂HPO₄, 3.5 g/L NaNH₄HPO₄, 1 mM MgSO₄, 0.1 mM CaCl₂, pH 7.0) and Pseudomonas Isolation Agar with 50 µg/ml gentamicin (PIA Gm50; BD Difco) were used to isolate P. aeruginosa transconjugants. Tryptone Yeast 25% Sucrose (TYS25; 10 g/L tryptone, 5 g/L yeast extract, 25% w/v sucrose, 18 g/L agar) was used for SacB counterselection. Chemicals were purchased from MilliporeSigma (St. Louis, MO).

Strains. *P. aeruginosa* strains used in this study were derivatives of *Pseudomonas* aeruginosa strain PAO1. Salmonella enterica serovar Typhimurium LT2 strains were available in the laboratory strain collection. Strains, plasmids, and primers used are listed in Table 1. *P. aeruginosa* deletion mutants were generated by allelic exchange as described previously [47]. In short, ~800 bp upstream and downstream of the gene of interest was

amplified by PCR. The DNA product was cloned by standard procedures into pMQ75. Assembled plasmids were then transformed into S17-1 E. coli by chemical transformation. Vectors were mobilized into P. aeruginosa by conjugation with S17-1 E. coli harboring vectors with homologous regions upstream and downstream of the gene of interest. Merodiploids, generated by homologous recombination of the plasmid into the chromosome, were isolated on VBMM Gm, then streaked for isolation on PIA Gm. SacB/sucrose counterselection at 30°C was used to select for excision of the plasmid from the chromosome via a second homologous recombination event. Sucrose resistant, gentamicin sensitive colonies were screened by PCR and deletions were confirmed by Sanger sequencing. Mini-Tn7 insertions were generated according to Schweizer et al. [48]. Briefly, pUC18T-mini-Tn7T-Gm and pTNS3 were transformed into E. coli S17-1 and S17-1 pir+ respectively. Plasmids were mobilized simultaneously into P. aeruginosa strains by conjugation. Transconjugants were isolated on VBMM Gm50 and streaked for isolation on PIA Gm50. Drug resistant colonies were screened for insertion into the attTn7 site by PCR with primers glmS-down and glmS-up.

Bioinformatics analyses. Sequences were obtained from the Pseudomonas Genome Database (PGBD) [49]. A DIAMOND BLASTP search was performed, using default parameters, with DadA from *P. aeruginosa* PAO1 as the query against all complete genomes in the PGBD [35]. Each species was sorted into one of five groups based on the composition of the *dad* operon. The groups and composition of the operon are as follows: Group 1, *dadRAX*; Group 2, *dadRAY*; Group 3, *dadRA*; Groups 4 and 5, *dadRAYX*. Groups 4 and 5 were distinguished based on the location of the gene encoding AsnC-type regulator

DadR in relation to the rest of the operon – Group 5 *dadR* is three reading frames upstream of the *dadA* promotor. For a species to be placed in one of these groups, the majority of strains (compliance >60%) must have had the same operon composition. The groups of *Pseudomonas* species based on the structure of their *dad* operon was then compared to their phylogenetic classification [39, 41, 42, 50]. The phylogenetic groups and subgroups of *Pseudomonas* species were then classified based on the structure of the *dad* operon as described above, except that type strains of species within the group were used in leu of strains within a species, at a compliance threshold of >75%.

Molecular techniques. Plasmids were constructed using standard procedures. Restriction endonucleases were purchased from New England Biosciences. Plasmids were isolated using the GeneJET Plasmid Miniprep Kit (Thermo Scientific). Q5 DNA polymerase (New England Biosciences) was used to amplify DNA and primers were synthesized by Eton Bioscience. PCR products were purified using the QIAquick PCR purification kit (Qiagen) and Sanger sequencing was performed by Eurofins Genomics. All DNA products were amplified by PCR using *P. aeruginosa* PAO1 gDNA as a template.

Homologous regions (~800 bp) flanking *dadA* were amplified using the primer pair pae-MQ75-dadA-USF/pae-MQ75-dadA-USR for the upstream region, and primers pae-MQ75-dadA-DSF/pae-MQ75-dadA-DSR for the downstream region. Primers pae-MQ75-dadY-USF/pae-MQ75-dadY-USR were used to amplify the region 800 bp upstream of *dadY*, and pae-MQ75-dadY-DSF/pae-MQ75-dadY-DSR were used for the downstream region. Flanking regions for each respective gene were cloned into the EcoRI site of pMQ75. Sequencing primers dadA-seq-F/dadA-seq-R were used to confirm deletion of

dadA and primers dadY-seq-F/dadY-seq-R were used to confirm deletion of dadY. The coding regions of dadA and dadY were amplified using primer pairs dadA-pET-F/dadA-pET-R and dadY-pET-F/dadY-pET-R respectively and were cloned into the BspQI site of BspQI modified pET28b(+) [51]. Primers glmS-down/glmS-up were used to confirm insertion into the attTn7 site of P. aeruginosa [48].

Growth analysis. Growth (OD₆₅₀) was monitored at 37°C in a 96-well plate using a BioTek ELx808 plate reader with a slow shaking speed. Overnight cultures (1 ml) in rich medium were grown at 37°C with shaking, pelleted and resuspended in an equal volume of sterile saline. Cell suspensions (5 μl) were used to inoculate each indicated medium (195 μl). Data were plotted using GraphPad Prism version 8.0.

Protein purification. Three 10 ml cultures of *E. coli* BL21-AI harboring pDM1652 (DadA) or pDM1653 (DadY) were grown overnight at 37°C in TB Km (50 μg/ml) and used to inoculate each of three 2.8 L Fernbach flasks containing 1.5 L of TB Km. Cultures were grown at 37°C with shaking at 150 rpm. When the OD₆₅₀ reached 0.6, cells were induced with 0.2% arabinose and 0.1 mM IPTG. The temperature was lowered to 23°C, and cultures were incubated for 18 h before being harvested by centrifugation. All purified proteins were flash-frozen in liquid nitrogen and stored at -80°C until use.

DadY. DadY was purified to a final concentration of 924 μM (12 mg/ml) and a purity of >95%. Cells were resuspended in 2 ml/g cell weight of Binding Buffer A (50 mM potassium phosphate pH 7.4, 150 mM NaCl, 20 mM imidazole) with lysozyme (2 mg/ml) and DNase (0.125 mg/ml). Cell suspensions were incubated on ice for 20 minutes before

being mechanically lysed using a Constant Systems Limited One Shot (United Kingdom) at 20 kpsi. PMSF (1 mM) was added to the lysate before centrifugation at 45000 x g for 45 min. Clarified cell lysate was filtered through a PVDF filter (0.45 µm pore size) before being loaded onto a 5 ml HisTrap HP Ni-Sepharose column, which was then washed with five column volumes of Binding Buffer A followed by four column volumes of 4% Elution Buffer A (50 mM potassium phosphate pH 7.4, 150 mM NaCl, 500 mM imidazole). Protein was eluted with a gradient of Elution Buffer A from 4% to 100% over 10 column volumes. Purified protein was concentrated using a centrifugal filer with a molecular weight cutoff of 10 kDa and moved into Storage Buffer A (50 mM Tris-HCl pH 7.5, 150 mM NaCl, 10% glycerol) using a PD10 column (GE Healthcare).

DadA. DadA was purified to a final concentration of 92 μM (4.3 mg/ml) and a purity of ~82%. Cells were resuspended in 2 ml/g cell weight of Binding Buffer B (50 mM potassium phosphate pH 7.4, 500 mM NaCl, 20 mM imidazole, 0.1% Triton X-100) with lysozyme (2 mg/ml), DNase (0.125 mg/ml), and FAD (50 μM) and incubated on ice for one hour. Cells were then lysed mechanically at 33 kpsi. PMSF was added to the cell lysate, which was then clarified by centrifugation at 40000 x g for 30 min and passed through a 0.45 μm PVDF filter. Cell free extract was loaded onto a 5 ml HisTrap HP Ni-Sepharose column, which was then washed with five column volumes of Binding Buffer B followed by four column volumes of 25% Elution Buffer B (50 mM potassium phosphate pH 7.4, 500 mM NaCl, 500 mM imidazole, 0.1% Triton X-100). Protein was eluted with a gradient of Elution Buffer B from 25% to 100% over 15 column volumes. Purified protein was concentrated using a centrifugal filer with a molecular weight cutoff of 30 kDa and moved

into Storage Buffer B (50 mM Tris-HCl pH 7.5, 500 mM NaCl, 0.1% Triton X-100, 10% glycerol) using a PD10 column (GE Healthcare).

Enzyme assays. All enzyme assays were performed at room temperature (25°C).

Imine deaminase activity of DadY. L-amino acid oxidase (LOX) assays were performed as described previously [21, 45]. In short, LOX was used to generate imine intermediates from L-amino acid substrates. Imines were derivatized with semicarbazide, generating semicarbazone compounds that were detected spectrophotometrically at an absorbance of 248 nm. The reaction mixture, at a final volume of 100 μ l, contained potassium pyrophosphate pH 8.7 (50 mM), semicarbazide pH 7.0 (10 mM), bovine liver catalase (24 U), and L-amino acid oxidase from *Crotalus adamanteus* (1 μ g). Assay mixtures contained 25 μ M DadY or RidA where indicated. Reactions were initiated by the addition of the indicated substrate (20 mM) and absorbance at 248 nm was monitored for five minutes. The rate of semicarbazone formation was determined in the linear range for each assay mixture using the measured pathlength of each well and the extinction coefficient for semicarbazone ($\epsilon = 10300 \, \text{M}^{-1} \, \text{cm}^{-1}$).

Imine generation by DadA. Imine generation and release by DadA were assayed using a modified version of a previously described assay [21]. Briefly, assay mixtures (100 μ l) contained potassium pyrophosphate pH 8.7 (50 mM), neutralized semicarbazide (10 mM), FAD (30 μ M), ubiquinone-1 (100 μ M), DadA (0.5 μ M), and DadY (5 μ M) where indicated. Reactions were initiated with 7.5 mM D-alanine and absorbance monitored at 248 nm for five minutes. The rate of semicarbazone formation was determined as described above for the LOX assay.

Competition assays. Competition assays were performed as described previously [16, 52]. In short, overnight cultures (3 ml) of each strain were grown in LB at 37°C. Overnights were diluted to an OD₆₅₀ of 0.1 in sterile saline and 50 µl of DMPA39 or DMPA40 were co-inoculated with an equal amount of DMPA4 in 5 ml of the indicated medium. Colony forming units (CFU) of the inoculum was determined by serial dilution in saline and spot plating onto LB to determine the total number of cells, and on LB with 30 µg/ml gentamicin (LB Gm30) to determine the number of DMPA39 or DMPA40. The number of wild-type cells was determined by subtracting the number of CFU on LB Gm30 from those on LB. As a control, fitness of DMPA39 and DMPA40 were measured in competition with DMPA24 and DMPA1, respectively. Co-cultures were incubated at 37°C with shaking until cultures reached stationary phase. Co-cultures were serially diluted in saline and plated on LB and LB Gm30 as described above. GraphPad Prism version 8.0 was used for data plotting and statistical analysis. The equation used to calculate competitive index

values is as follows:
$$Competitive\ Index\ (CI) = \frac{\left(\frac{CFU\ mutant}{CFU\ wild\ type}\right)_{initial}}{\left(\frac{CFU\ mutant}{CFU\ wild\ type}\right)_{final}}$$
.

3.6 REFERENCES

- 1. Aliashkevich A, Alvarez L, Cava F (2018). New Insights Into the Mechanisms and Biological Roles of D-Amino Acids in Complex Eco-Systems. Front Microbiol 9(683. doi: 10.3389/fmicb.2018.00683.
- 2. Degani G, Barbiroli A, Regazzoni L, Popolo L, Vanoni MA (2018). Imine Deaminase Activity and Conformational Stability of UK114, the Mammalian Member of the Rid Protein Family Active in Amino Acid Metabolism. Int J Mol Sci 19(4). doi: 10.3390/ijms19040945.

- 3. Pifer R, Russell RM, Kumar A, Curtis MM, Sperandio V (2018). Redox, amino acid, and fatty acid metabolism intersect with bacterial virulence in the gut. Proc Natl Acad Sci U S A 115(45): E10712-E10719. doi: 10.1073/pnas.1813451115.
- 4. Oliver KE, Silo-Suh L (2013). Impact of D-amino acid dehydrogenase on virulence factor production by a *Pseudomonas aeruginosa*. Can J Microbiol 59(9): 598-603. doi: 10.1139/cjm-2013-0289.
- 5. Tashiro Y, Yawata Y, Toyofuku M, Uchiyama H, Nomura N (2013). Interspecies interaction between *Pseudomonas aeruginosa* and other microorganisms. Microbes Environ 28(1): 13-24. doi: 10.1264/jsme2.me12167.
- 6. Limoli DH, Warren EA, Yarrington KD, Donegan NP, Cheung AL, O'Toole GA (2019). Interspecies interactions induce exploratory motility in *Pseudomonas aeruginosa*. Elife 8(doi: 10.7554/eLife.47365.
- 7. Gomes-Fernandes M, Gomez AC, Bravo M, Huedo P, Coves X, Prat-Aymerich C, Gibert I, Lacoma A, Yero D (2022). Strain-specific interspecies interactions between co-isolated pairs of *Staphylococcus aureus* and *Pseudomonas aeruginosa* from patients with tracheobronchitis or bronchial colonization. Sci Rep 12(1): 3374. doi: 10.1038/s41598-022-07018-5.
- 8. Grainha T, Jorge P, Alves D, Lopes SP, Pereira MO (2020). Unraveling *Pseudomonas aeruginosa* and *Candida albicans* Communication in Coinfection Scenarios: Insights Through Network Analysis. Front Cell Infect Microbiol 10(550505. doi: 10.3389/fcimb.2020.550505.
- 9. Fourie R, Pohl CH (2019). Beyond Antagonism: The Interaction Between *Candida* Species and *Pseudomonas aeruginosa*. J Fungi (Basel) 5(2). doi: 10.3390/jof5020034.
- 10. Sass G, Nazik H, Penner J, Shah H, Ansari SR, Clemons KV, Groleau MC, Dietl AM, Visca P, Haas H, Deziel E, Stevens DA (2019). *Aspergillus-Pseudomonas* interaction, relevant to competition in airways. Med Mycol 57(Supplement_2): S228-S232. doi: 10.1093/mmy/myy087.

- 11. McGill SL, Yung Y, Hunt KA, Henson MA, Hanley L, Carlson RP (2021). *Pseudomonas aeruginosa* reverse diauxie is a multidimensional, optimized, resource utilization strategy. Sci Rep 11(1): 1457. doi: 10.1038/s41598-020-80522-8.
- 12. Rojo F (2010). Carbon catabolite repression in *Pseudomonas*: optimizing metabolic versatility and interactions with the environment. FEMS Microbiol Rev 34(5): 658-684. doi: 10.1111/j.1574-6976.2010.00218.x.
- 13. Dolan SK, Kohlstedt M, Trigg S, Vallejo Ramirez P, Kaminski CF, Wittmann C, Welch M (2020). Contextual Flexibility in *Pseudomonas aeruginosa* Central Carbon Metabolism during Growth in Single Carbon Sources. mBio 11(2). doi: 10.1128/mBio.02684-19.
- 14. Yung YP, McGill SL, Chen H, Park H, Carlson RP, Hanley L (2019). Reverse diauxie phenotype in *Pseudomonas aeruginosa* biofilm revealed by exometabolomics and label-free proteomics. NPJ Biofilms Microbiomes 5(1): 31. doi: 10.1038/s41522-019-0104-7.
- 15. He W, Li C, Lu CD (2011). Regulation and characterization of the *dadRAX* locus for D-amino acid catabolism in *Pseudomonas aeruginosa* PAO1. J Bacteriol 193(9): 2107-2115. doi: 10.1128/JB.00036-11.
- 16. Boulette ML, Baynham PJ, Jorth PA, Kukavica-Ibrulj I, Longoria A, Barrera K, Levesque RC, Whiteley M (2009). Characterization of alanine catabolism in *Pseudomonas aeruginosa* and its importance for proliferation *in vivo*. J Bacteriol 191(20): 6329-6334. doi: 10.1128/jb.00817-09.
- 17. Trivedi RR, Crooks JA, Auer GK, Pendry J, Foik IP, Siryaporn A, Abbott NL, Gitai Z, Weibel DB (2018). Mechanical Genomic Studies Reveal the Role of D-Alanine Metabolism in *Pseudomonas aeruginosa* Cell Stiffness. mBio 9(5). doi: 10.1128/mBio.01340-18.
- 18. Niehaus TD, Gerdes S, Hodge-Hanson K, Zhukov A, Cooper AJ, ElBadawi-Sidhu M, Fiehn O, Downs DM, Hanson AD (2015). Genomic and experimental evidence for multiple metabolic functions in the RidA/YjgF/YER057c/UK114 (Rid) protein family. BMC Genomics 16(382. doi: 10.1186/s12864-015-1584-3.

- 19. Lambrecht JA, Schmitz GE, Downs DM (2013). RidA proteins prevent metabolic damage inflicted by PLP-dependent dehydratases in all domains of life. MBio 4(1): e00033-00013. doi: 10.1128/mBio.00033-13.
- 20. Irons JL, Hodge-Hanson K, Downs DM (2020). RidA Proteins Protect against Metabolic Damage by Reactive Intermediates. Microbiol Mol Biol Rev 84(3). doi: 10.1128/mmbr.00024-20
- 21. Hodge-Hanson KM, Downs DM (2017). Members of the Rid protein family have broad imine deaminase activity and can accelerate the *Pseudomonas aeruginosa* Darginine dehydrogenase (DauA) reaction *in vitro*. PLoS One 12(9): e0185544. doi: 10.1371/journal.pone.0185544.
- 22. Buckner BA, Lato AM, Campagna SR, Downs DM (2021). The Rid family member RutC of *Escherichia coli* is a 3-aminoacrylate deaminase. J Biol Chem: 100651. doi: 10.1016/j.jbc.2021.100651.
- 23. Ernst DC, Downs DM (2018). Mmflp Couples Amino Acid Metabolism to Mitochondrial DNA Maintenance in *Saccharomyces cerevisiae*. MBio 9(1). doi: 10.1128/mBio.00084-18.
- 24. Irons J, Hodge-Hanson KM, Downs DM (2018). PA5339, a RidA Homolog, Is Required for Full Growth in *Pseudomonas aeruginosa*. J Bacteriol 200(22). doi: 10.1128/jb.00434-18.
- 25. Irons J, Sacher JC, Szymanski CM, Downs DM (2019). Cj1388 is a RidA Homolog and is Required for Flagella Biosynthesis and/or Function in *Campylobacter jejuni*. Front Microbiol 10(2058. doi: 10.3389/fmicb.2019.02058.
- 26. Flynn JM, Downs DM (2013). In the absence of RidA, endogenous 2-aminoacrylate inactivates alanine racemases by modifying the pyridoxal 5'-phosphate cofactor. J Bacteriol 195(16): 3603-3609. doi: 10.1128/jb.00463-13.
- 27. Niehaus TD, Nguyen TN, Gidda SK, ElBadawi-Sidhu M, Lambrecht JA, McCarty DR, Downs DM, Cooper AJ, Fiehn O, Mullen RT, Hanson AD (2014). *Arabidopsis* and *maize* RidA proteins preempt reactive enamine/imine damage to branched-chain amino acid biosynthesis in plastids. The Plant cell 26(7): 3010-3022. doi: 10.1105/tpc.114.126854.

- 28. Borchert AJ, Downs DM (2017). The Response to 2-Aminoacrylate Differs in *Escherichia coli* and *Salmonella enterica*, despite Shared Metabolic Components. J Bacteriol 199(14). doi: 10.1128/jb.00140-17.
- 29. Borchert AJ, Ernst DC, Downs DM (2019). Reactive Enamines and Imines *In Vivo*: Lessons from the RidA Paradigm. Trends Biochem Sci 44(10): 849-860. doi: 10.1016/j.tibs.2019.04.011.
- 30. Lambrecht JA, Flynn JM, Downs DM (2012). Conserved YjgF protein family deaminates reactive enamine/imine intermediates of pyridoxal 5'-phosphate (PLP)-dependent enzyme reactions. J Biol Chem 287(5): 3454-3461. doi: 10.1074/jbc.M111.304477.
- 31. Fulton RL, Irons J, Downs DM (2022). The Cysteine Desulfurase IscS Is a Significant Target of 2-Aminoacrylate Damage in *Pseudomonas aeruginosa*. mBio 13(3): e0107122. doi: 10.1128/mbio.01071-22.
- 32. ElRamlawy KG, Fujimura T, Baba K, Kim JW, Kawamoto C, Isobe T, Abe T, Hodge-Hanson K, Downs DM, Refaat IH, Beshr Al-Azhary D, Aki T, Asaoku Y, Hayashi T, Katsutani T, Tsuboi S, Ono K, Kawamoto S (2016). Der f 34, a Novel Major House Dust Mite Allergen Belonging to a Highly Conserved Rid/YjgF/YER057c/UK114 Family of Imine Deaminases. J Biol Chem 291(41): 21607-21615. doi: 10.1074/jbc.M116.728006.
- 33. Martínez-Chavarría LC, Sagawa J, Irons J, Hinz AK, Lemon A, Graça T, Downs DM, Vadyvaloo V (2020). Putative Horizontally Acquired Genes, Highly Transcribed during *Yersinia pestis* Flea Infection, Are Induced by Hyperosmotic Stress and Function in Aromatic Amino Acid Metabolism. J Bacteriol 202(11). doi: 10.1128/jb.00733-19.
- 34. Whitaker GH, Ernst DC, Downs DM (2021). Absence of MMF1 disrupts heme biosynthesis by targeting Hem1p in *Saccharomyces cerevisiae*. Yeast 38(12): 615-624. doi: 10.1002/yea.3670.
- 35. Buchfink B, Xie C, Huson DH (2015). Fast and sensitive protein alignment using DIAMOND. Nat Methods 12(1): 59-60. doi: 10.1038/nmeth.3176.

- 36. Olsiewski PJ, Kaczorowski GJ, Walsh C (1980). Purification and properties of Damino acid dehydrogenase, an inducible membrane-bound iron-sulfur flavoenzyme from *Escherichia coli* B. J Biol Chem 255(10): 4487-4494. doi.
- 37. Hallen A, Jamie JF, Cooper AJ (2014). Imine reductases: a comparison of glutamate dehydrogenase to ketimine reductases in the brain. Neurochem Res 39(3): 527-541. doi: 10.1007/s11064-012-0964-1.
- 38. Kawahara N, Palasin K, Asano Y (2022). Novel Enzymatic Method for Imine Synthesis via the Oxidation of Primary Amines Using D-Amino Acid Oxidase from Porcine Kidney. Catalysts 12(5): 511. doi.
- 39. Girard L, Lood C, Hofte M, Vandamme P, Rokni-Zadeh H, van Noort V, Lavigne R, De Mot R (2021). The Ever-Expanding *Pseudomonas* Genus: Description of 43 New Species and Partition of the *Pseudomonas putida* Group. Microorganisms 9(8). doi: 10.3390/microorganisms9081766.
- 40. Hesse C, Schulz F, Bull CT, Shaffer BT, Yan Q, Shapiro N, Hassan KA, Varghese N, Elbourne LDH, Paulsen IT, Kyrpides N, Woyke T, Loper JE (2018). Genome-based evolutionary history of *Pseudomonas spp*. Environ Microbiol 20(6): 2142-2159. doi: 10.1111/1462-2920.14130.
- 41. Gomila M, Pena A, Mulet M, Lalucat J, Garcia-Valdes E (2015). Phylogenomics and systematics in *Pseudomonas*. Front Microbiol 6(214. doi: 10.3389/fmicb.2015.00214.
- 42. Anzai Y, Kim H, Park JY, Wakabayashi H, Oyaizu H (2000). Phylogenetic affiliation of the pseudomonads based on 16S rRNA sequence. Int J Syst Evol Microbiol 50 Pt 4(1563-1589. doi: 10.1099/00207713-50-4-1563.
- 43. Mulet M, Lalucat J, Garcia-Valdes E (2010). DNA sequence-based analysis of the *Pseudomonas* species. Environ Microbiol 12(6): 1513-1530. doi: 10.1111/j.1462-2920.2010.02181.x.
- 44. Schmitz G, Downs DM (2004). Reduced Transaminase B (IIvE) Activity Caused by the Lack of *yjgF* Is Dependent on the Status of Threonine Deaminase (IIvA) in *Salmonella enterica* Serovar Typhimurium. Journal of Bacteriology 186(3): 803-810. doi: 10.1128/jb.186.3.803-810.2004.

- 45. Hafner EW, Wellner D (1979). Reactivity of the imino acids formed in the amino acid oxidase reaction. Biochemistry 18(3): 411-417. doi: 10.1021/bi00570a004
- 46. Balch WE, Wolfe RS (1976). New approach to the cultivation of methanogenic bacteria: 2-mercaptoethanesulfonic acid-dependent growth of *Methanobacterium ruminantium* in a pressurized atmosphere. Applied and Environmental Microbiology 32(781-791. doi: 10.1128/aem.32.6.781-791.1976
- 47. Hmelo LR, Borlee BR, Almblad H, Love ME, Randall TE, Tseng BS, Lin C, Irie Y, Storek KM, Yang JJ, Siehnel RJ, Howell PL, Singh PK, Tolker-Nielsen T, Parsek MR, Schweizer HP, Harrison JJ (2015). Precision-engineering the *Pseudomonas aeruginosa* genome with two-step allelic exchange. Nat Protoc 10(11): 1820-1841. doi: 10.1038/nprot.2015.115.
- 48. Choi KH, Schweizer HP (2006). mini-Tn7 insertion in bacteria with single *attTn7* sites: example *Pseudomonas aeruginosa*. Nat Protoc 1(1): 153-161. doi: 10.1038/nprot.2006.24.
- 49. Winsor GL, Griffiths EJ, Lo R, Dhillon BK, Shay JA, Brinkman FS (2016). Enhanced annotations and features for comparing thousands of *Pseudomonas* genomes in the Pseudomonas genome database. Nucleic Acids Res 44(D1): D646-653. doi: 10.1093/nar/gkv1227.
- 50. Jun SR, Wassenaar TM, Nookaew I, Hauser L, Wanchai V, Land M, Timm CM, Lu TY, Schadt CW, Doktycz MJ, Pelletier DA, Ussery DW (2016). Diversity of *Pseudomonas* Genomes, Including Populus-Associated Isolates, as Revealed by Comparative Genome Analysis. Appl Environ Microbiol 82(1): 375-383. doi: 10.1128/AEM.02612-15.
- 51. VanDrisse CM, Escalante-Semerena JC (2016). New high-cloning-efficiency vectors for complementation studies and recombinant protein overproduction in *Escherichia coli* and *Salmonella enterica*. Plasmid 86(1-6. doi: 10.1016/j.plasmid.2016.05.001.
- 52. Speare L, Septer AN (2019). Coincubation Assay for Quantifying Competitive Interactions between *Vibrio fischeri* Isolates. J Vis Exp 149). doi: 10.3791/59759.

- 53. Shanks RM, Caiazza NC, Hinsa SM, Toutain CM, O'Toole GA (2006). *Saccharomyces cerevisiae*-based molecular tool kit for manipulation of genes from Gram-negative bacteria. Appl Environ Microbiol 72(7): 5027-5036. doi: 10.1128/AEM.00682-06.
- 54. Galloway NR, Toutkoushian H, Nune M, Bose N, Momany C (2013). Rapid Cloning for Protein Crystallography Using Type IIS Restriction Enzymes. Crystal Growth & Design 13(7): 2833-2839. doi: 10.1021/cg400171z.
- 55. Jacobs MA, Alwood A, Thaipisuttikul I, Spencer D, Haugen E, Ernst S, Will O, Kaul R, Raymond C, Levy R, Chun-Rong L, Guenthner D, Bovee D, Olson MV, Manoil C (2003). Comprehensive transposon mutant library of *Pseudomonas aeruginosa*. Proc Natl Acad Sci U S A 100(24): 14339-14344. doi: 10.1073/pnas.2036282100.

TABLE 3.1: Plasmids and strains used in this study.

Plasmid name	Description	Source	
pTNS3	Tn7 helper plasmid	[48]	
pUC18T-mini-Tn7T-Gm	Delivery plasmid for Gm ^R on Tn7	[48]	
pMQ75	Gram-negative allelic replacement vector.	[53]	
pMQ75-∆dadA	pMQ75 with 800 bp of homology upstream and downstream of <i>dadA</i>	This study	
pMQ75-∆dadY	pMQ75 with 800 bp of homology upstream and downstream of <i>dadY</i>	This study	
pCV1	pCV1 – empty vector	[51]	
pDM1580	pDM1580 pCV1 – P. aeruginosa DadY		
pDM1636	DM1636 pCV1 – S. enterica RidA		
pET28b(+)	BspQI modified pET28b(+)		
pDM1652	pET28b(+) – P. aeruginosa DadA		
pDM1653	pET28b(+) – P. aeruginosa DadY	This study	
Strain ID	Genotype	Source	
P. aeruginosa			
DMPA1	$\Delta dadA$	This study	
DMPA4	MPAO1 wild type (Manoil laboratory)	[55]	
DMPA24	$\Delta dadY$	This study	
DMPA39	ΔdadA attTn7::Gm ^R	This study	
DMPA40	ΔdadY attTn7::Gm ^R	This study	
S. enterica	<u> </u>		
DM14847		Laboratory collection	
DM16390	<i>ridA1</i> ::Tn <i>10d</i> (Tc)/ pDM1580	Laboratory collection	
DM17142	<i>ridA1</i> ::Tn <i>10d</i> (Tc)/ pDM1636	Laboratory collection	
1	1		

All P. aeruginosa strains were derivatives of the MPAO1 wild-type strain (DMPA4).

TABLE 3.2: Primers used in this study.

Primer	Sequence
pae-MQ75-dadA-USF	cgggtaccgagctcgGCGCGGCGTGCCGAATACCAGA
pae-MQ75-dadA-USR	cgcgccgcgtgcggctGCAGTTGCGCAGCATCTGCAGCA
pae-MQ75-dadA-DSF	ageegeaegegegeGCGACCTCTATCCCGAGGGC
pae-MQ75-dadA-DSR	ctatgaccatgattacgGGCCAGCCGATAGTTGTGAC
dadA-seq-F	ATGCGAGTTCTGGTCCTTGG
dadA-seq-R	GTGTGCTGGCGCTGGATG
pae-MQ75-dadY-USF	atccccgggtaccgagctcgATGCTGCGCAACTGCACC
pae-MQ75-dadY-USR	ggcttcgacgGCCCGCGGACATGTCCTC
pae-MQ75-dadY-DSF	gtccgcgggcCGTCGAAGCCAAGCTCTG
pae-MQ75-dadY-DSR	cagctatgaccatgattacgGCATGTCCATCGATACCC
dadY-seq-F	GCAACTGCTCAAGCCGCTGGG
dadY-seq-R	AAGTCCTCGGGGAAGAAGCCGACG
dadA-pET-F	nngetettenATGCGAGTTCTGGTCCTTGG
dadA-pET-R	nngctcttcnGTGGTGTGCTGGCGCTGGA
dadY-pET-F	nngctcttcnATGCCCATCCAGCGCCAGCACA
dadY-pET-R	nngctcttcnGTGGGGCAGCGCAGCGACCACCG
glmS-down	GCACATCGGCGACGTGCTCTC

TABLE 3.3: DadY is an imine deaminase in vitro.

	Rate of semicarbazone formation (μM/min) with:			
LOX Substrate	No Rid	DadY ^a	_{SE} RidA	$_{PA}$ RidA
	protein			
L-Arg	518 ± 17	28 ± 10^{b}	470 ± 58	552 ± 62
L-Gln	193 ± 8	ND	78 ± 13^{a}	132 ± 5^{a}
L-His	196 ± 10	95 ± 19^{b}	196 ± 5	202 ± 17
L-Leu	294 ± 29	20 ± 5	$53 \pm 5^{\mathrm{a}}$	22 ± 5^{a}
L-Met	291 ± 10	45 ± 5	48 ± 5^{a}	62 ± 10^{a}
L-Phe	232 ± 26	62 ± 5 ^b	185 ± 1	188 ± 41

^a significant difference in semicarbazone formation (p < 0.05, determined by Tukey's multiple comparisons test) between indicated reactions and those with no Rid protein. Activity of reactions with DadY was significantly different than LOX alone with all amino acids tested.

Reaction mixes (100 µl) contained potassium pyrophosphate pH 8.7 (50 mM), semicarbazide pH 7.0 (10 mM), bovine liver catalase (24 U), L-amino acid oxidase from *Crotalus adamanteus* (1 µg), and the Rid protein (25 µM, monomeric concentration) indicated. Reactions were initiated by the addition of the indicated substrate (20 mM) and absorbance at 248 nm was monitored over five minutes. The rate of semicarbazone formation was determined using the measured pathlength of each well and the molar extinction coefficient for semicarbazone ($\varepsilon = 10300 \text{ M}^{-1} \text{ cm}^{-1}$). Data shown are the mean and standard deviation of three technical replicates. ND, no semicarbazone was detected; seRidA, RidA from *S. enterica*; PARidA, RidA from *P. aeruginosa*

^b significant difference in semicarbazone formation between reactions containing DadY and those with either RidA protein.

A DadX HO
$$\frac{DadX}{NH_2}$$
 HO $\frac{DadA}{NH_2}$ HO $\frac{FAD}{NH_2}$ HO $\frac{FAD}{NH_2}$ HO $\frac{FAD}{NH_3}$ HO $\frac{DadY}{NH_3}$ HO $\frac{DadY}{NH_3}$ NH $\frac{DadA}{NH_3}$ $\frac{DadA}{NH_2}$ $\frac{DadA}{NH_2}$ $\frac{DadA}{NH_3}$ $\frac{DadA}{NH_3}$ $\frac{DadA}{\alpha-imine}$ Pyruvate

FIGURE 3.1: Alanine catabolism in *P. aeruginosa*. A) In the established pathway for alanine catabolism in *P. aeruginosa*, L-alanine is converted to D-alanine by the DadX racemase. The FAD-dependent D-amino acid dehydrogenase, DadA, then oxidizes D-alanine which results in the generation of products pyruvate and ammonia. B) The proposed role for DadY in the catabolism of alanine by *P. aeruginosa* is shown. After oxidation of D-alanine at the alpha carbon, DadA releases imino-alanine into the cellular milieu (red, brackets). This α -imine can be deaminated either spontaneously by solvent water (dashed arrow) or by DadY (red), both of which generate the final products, pyruvate and ammonia.

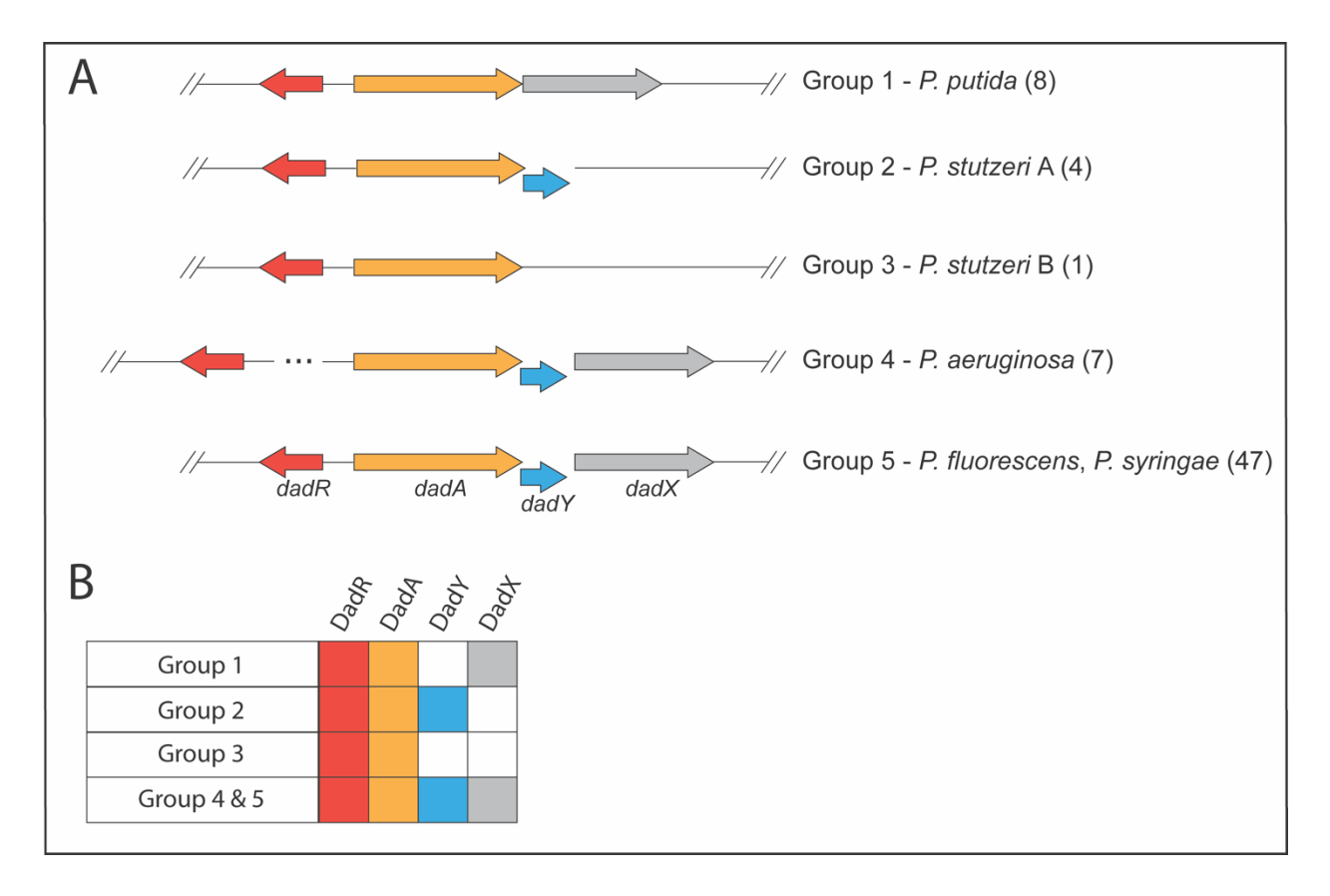


FIGURE 3.2: Genomic organization of genes in the dad locus varies in Pseudomonas species. A) Schematic showing the configurations of dad loci in Pseudomonas. Genomic affinity groups [39-43] were classified based on the organization (A) and constituents (B) of the dad locus. Gene products considered were DadR (AsnC-type regulator, red), DadA (D-amino acid dehydrogenase, yellow), DadX (catabolic alanine racemase, grey), and DadY (Rid2 subfamily protein, blue). The number of species belonging to each group is shown in parentheses. B) Distribution of dad genes in Pseudomonas. The presence (filled boxes) or absence (empty boxes) of each gene in the dad locus is indicated for the groups shown in A.

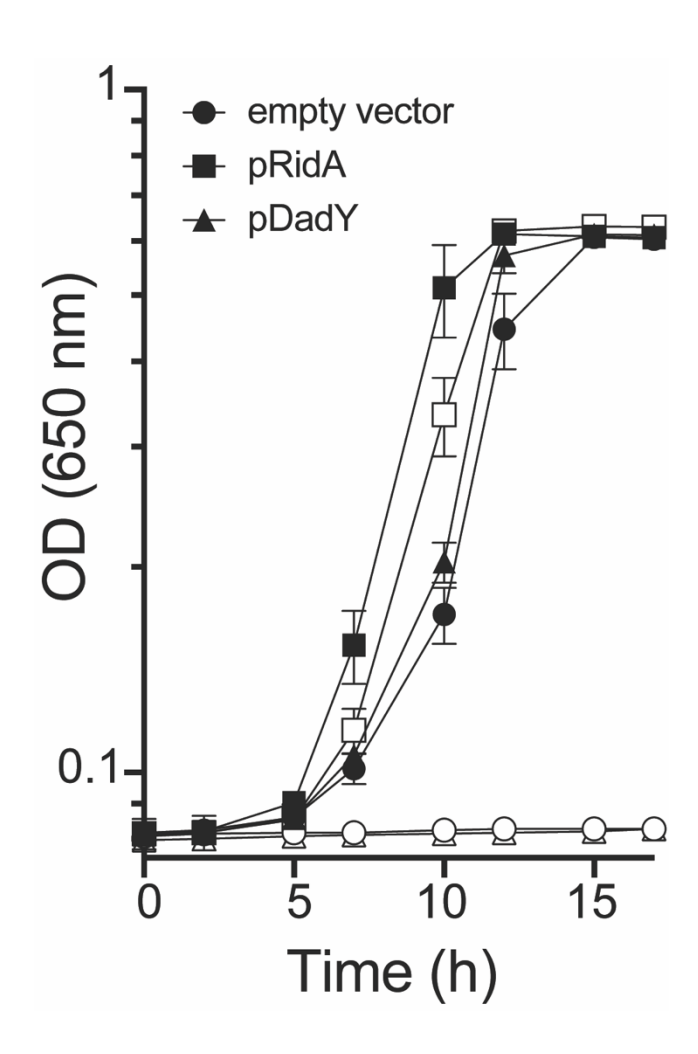


FIGURE 3.3: DadY fails to complement a *S. enterica ridA* mutant. Growth of a *S. enterica ridA* mutant harboring the control pCV1 vector (circles), pDM1636, encoding RidA from *S. enterica* (squares), or pDM1580, encoding DadY from *P. aeruginosa* (triangles) was monitored in minimal glucose (11 mM) medium without (closed symbols) or with (open symbols) 5 mM L-serine. L-arabinose (0.2%) was present in all media to induce expression of the plasmid-borne gene. Error bars represent standard deviation between three independent biological replicates.

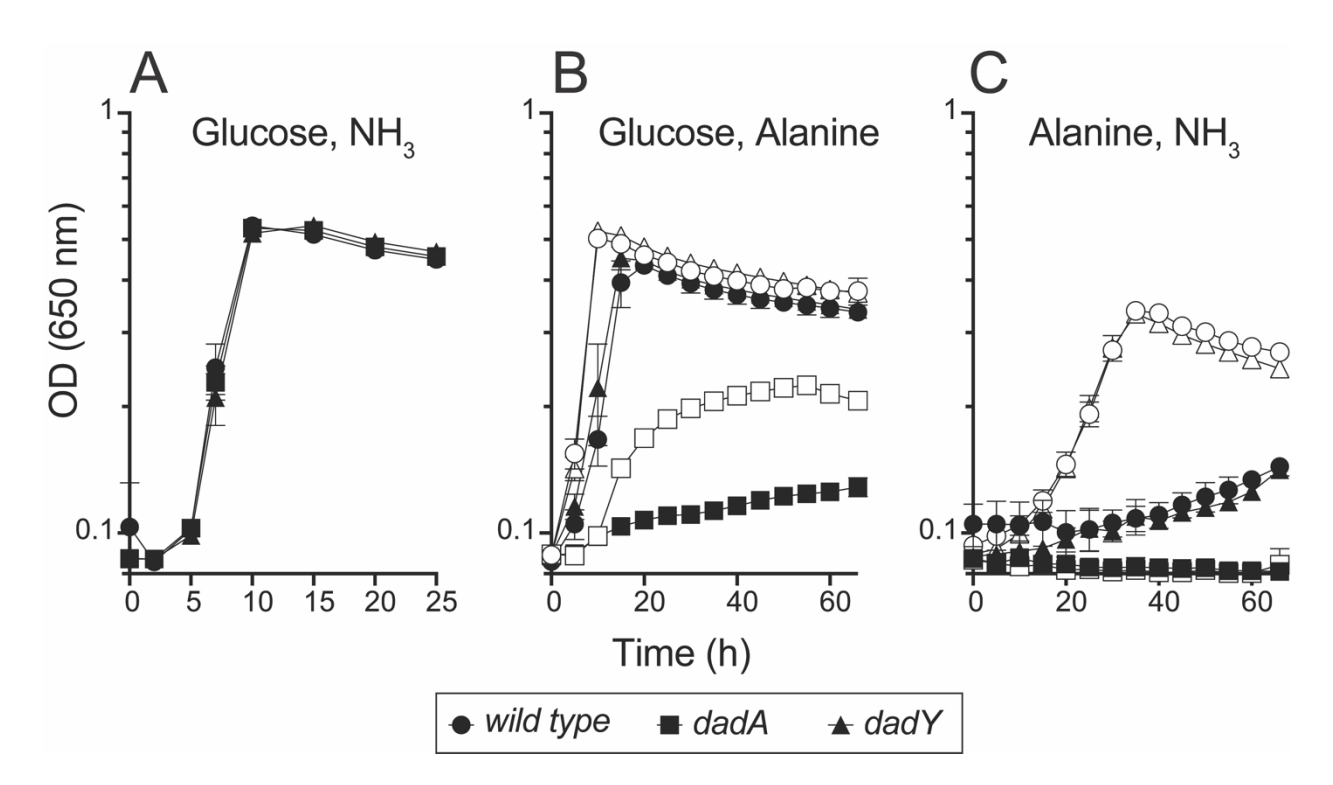


FIGURE 3.4: DadY is not required for catabolism of alanine by *P. aeruginosa*. *P. aeruginosa* wild type (circles), *dadA* mutant (squares), and *dadY* mutant (triangles) strains were inoculated into minimal media with the carbon and nitrogen sources as indicated (carbon, nitrogen); A) glucose and ammonia, B) glucose and alanine, and C) alanine and ammonia. D-alanine (closed shapes) or L-alanine (open shapes) was added as indicated as the source of carbon or nitrogen at 20 mM or 5 mM, respectively. When present glucose was at 11 mM and ammonia was at 10 mM. Growth was measured as the change in optical density at 650 nm over time. Error bars represent standard deviation between three independent biological replicates.

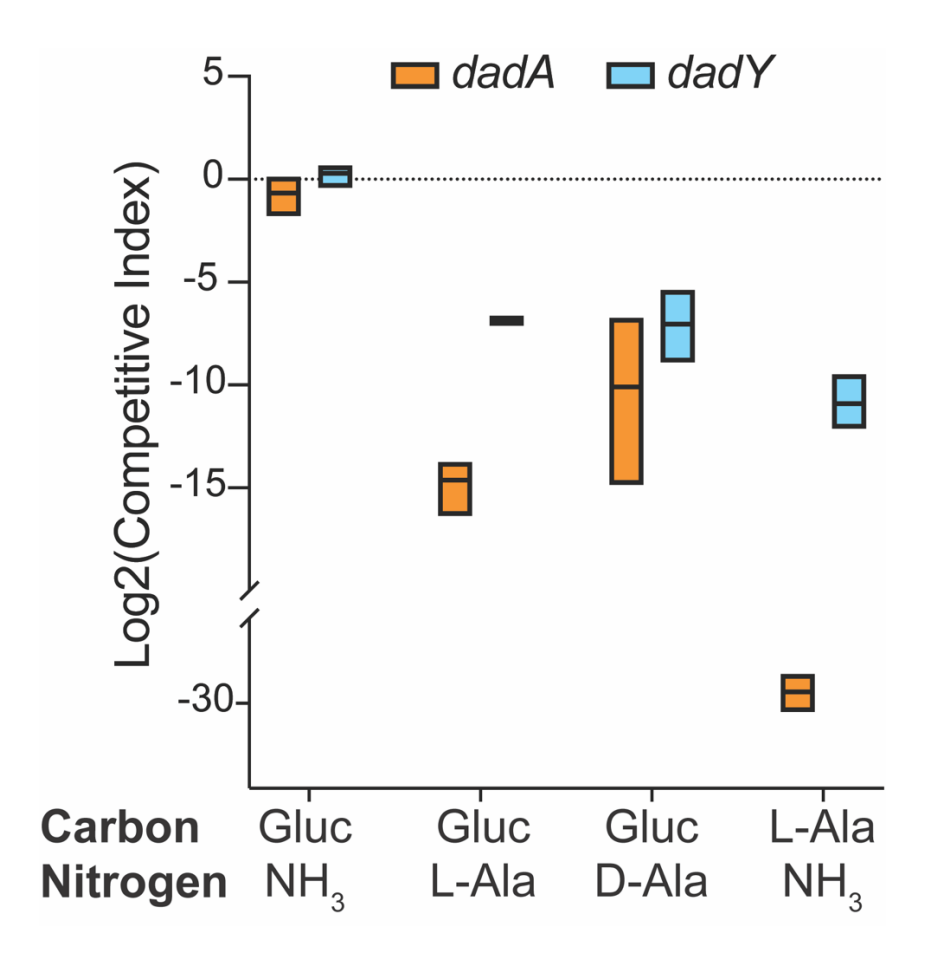


FIGURE 3.5: dadA and dadY mutants are outcompeted by wild type when alanine catabolism is required. Cells of mutant strain DMPA39 (dadA Gm^R , orange) or DMPA40 (dadY Gm^R , blue) were combined with an equal number of DMPA4 (wild type) cells (final $OD_{650} = 0.02$) in minimal media with the indicated sources of carbon (11 mM glucose or 20 mM Ala) and nitrogen (10 mM ammonia or 5 mM Ala). Co-cultures were grown to stationary phase at 37°C with shaking. Colony forming units (CFU) were determined by serial dilution and spot plating onto LB Gm30 (dadA or dadY mutants) and LB without drug (total cells) at the onset of the experiment, and after cultures reached stationary phase. The number of wild-type cells was determined by subtracting the number of each mutant from the total number of cells. The Competitive Index (CI) was calculated as the ratio of mutant to wild-type P. aeruginosa after co-incubation, divided by the ratio of mutant to wild type in the inoculum. Data shown are mean and standard deviation of three independent biological replicates. Experiments were performed three times with similar results.

Protein	DadA	DadY	SeRidA	PaRidA
approx. MW	47 kDa	13 kDa	13 kDa	13.5 kDa
Purity	82%	99%	95%	99%

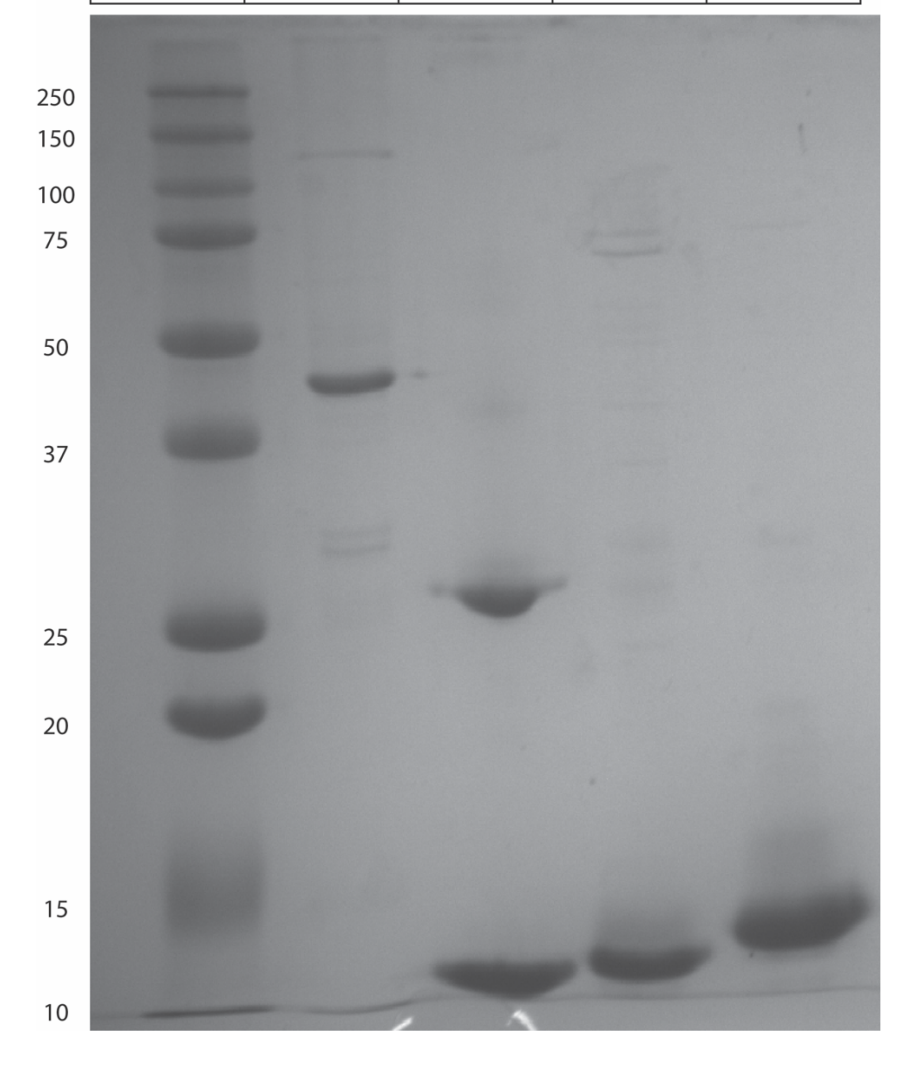


FIGURE 3.S1: Purified DadA, DadY, SERidA and PARidA. Proteins were purified from *E. coli* BL21-AI. Samples were boiled in buffer containing β-mercaptoethanol and ~4 μg of each sample was loaded onto a 12% polyacrylamide gel before being separated by electrophoresis. The gel was stained with Coomassie Blue and imaged using AnalytikJena UVP ChemStudio. Purity of each sample was determined by densitometry using VisionWorks software version 8.22.18309.10577. The band corresponding to 26 kDa in the lane containing the DadY sample was confirmed to be dimerized DadY by Peptide Mass Fingerprinting analysis at the University of Georgia Proteomics Core. BioRad Precision Plus Protein Dual Color Standards were ran in the left-most lane.

CHAPTER 4

FUNCTIONAL CHARACTERIZATION OF THE DBU LOCUS FOR D-BRANCHED-CHAIN AMINO ACID CATABOLISM IN $PSEUDOMONAS\ PUTIDA^1$

Reprinted here with permission of the publisher.

¹Fulton RL, Downs DM. 2024. Appl Environ Microbiol. 90(2):e0196223.

4.1 ABSTRACT

Pseudomonas putida is a metabolically robust soil bacterium that employs a diverse set of pathways to utilize a wide range of nutrients. The versatility of this microorganism contributes to both its environmental ubiquity and its rising popularity as a bioengineering chassis. In P. putida, the newly named dbu locus encodes a transcriptional regulator (DbuR), D-amino acid oxidase (DbuA), Rid2 protein (DbuB), and a putative transporter (DbuC). Current annotation implicates this locus in the utilization of D-arginine. However, data obtained in this study showed that genes in the dbu locus are not required for D-arginine utilization but, rather, this locus is involved in the catabolism of multiple D-branched-chain amino acids (D-BCAA). The oxidase DbuA was required for catabolism of each D-BCAA and D-phenylalanine, while the requirements for DbuC and DbuB were less stringent. The functional characterization of the dbu locus contributes to our understanding of the metabolic network of P. putida and proposes divergence in function between proteins annotated as D-arginine oxidases across the Pseudomonas genus.

4.2 IMPORTANCE

Pseudomonas putida is a non-pathogenic bacterium that is broadly utilized as a host for bioengineering and bioremediation efforts. The popularity of *P. putida* as a chassis for such efforts is attributable to its physiological versatility and ability to metabolize a wide variety of compounds. Pathways for L-amino acid metabolism in this microbe have been rather well studied, primarily because of their relevance to efforts in foundational physiology research, as well as the commercial production of economically pertinent compounds. However, comparatively little is known about the metabolism of D-amino

acids, despite evidence showing the ability of *P. putida* to metabolize these enantiomers. In this work, we characterize the D-BCAA catabolic pathway of *P. putida* and its integration with the essential L-BCAA biosynthetic pathway. This work expands our understanding of the metabolic network of *Pseudomonas putida*, which has potential applications in efforts to model and engineer the metabolic network of this organism.

4.3 INTRODUCTION

Pseudomonas are ubiquitous, non-fermentative microbes that play a variety of roles in the ecosystems they inhabit, where they can be growth-promoting plant symbionts, saprophytes that break down dead organic matter, or pathogens of plants and animals (1). Pseudomonas putida is a robust and metabolically versatile soil microbe that has become a prominent engineering and bioremediation chassis, with the strain KT2440 being certified as safe for release into the environment (2). As such, an increased understanding of the metabolic capabilities of this organism can have significant economic and environmental benefits. Despite decades of research focused on P. putida, much remains to be discovered about the regulatory and metabolic potential embedded in the metabolic network of this organism.

Apart from glycine, the proteogenic amino acids are found as both L- and D-enantiomers in nature. The L-branched-chain amino acids (L-BCAA) are essential for protein synthesis, growth and survival in all organisms (3). Due to their broadly conserved physiological significance, pathways that generate or catabolize L-BCAAs have been well-studied in many model systems. In contrast, comparatively little is known about the metabolism of D-amino acids, despite their presence in various microbe-rich environments.

In many of these ecosystems, microbes, such as lactic acid bacteria, racemize L-branched-chain amino acids and secrete them as D-BCAAs – i.e., D-valine, D-leucine, and D-isoleucine – into the environment (4, 5). This strategy is likely a way for the D-BCAA producer to store this resource, since many organisms cannot access or catabolize D-BCAAs. In this situation, microbes that can utilize D-BCAAs as sources of carbon or nitrogen would have a competitive advantage in some nutrient-limited environments. *Pseudomonas* species are an example of the D-BCAA utilizing microbes alluded to in the scenario above. Members of the *Pseudomonas* genus have demonstrated the metabolic capacity to catabolize a number of D-amino acids, including D-BCAAs (6-14). Appropriately, *Pseudomonas* species are abundant in environments inhabited by D-BCAA producers, such as the soil or in association with plant and mammalian hosts (1, 4, 5).

In *P. aeruginosa*, the *dauBAR* locus encodes an anabolic oxidase (DauB), a catabolic oxidase (DauA) and a transcriptional repressor (DauR) that are involved the utilization of D-arginine via two-step racemization to L-arginine (11, 12). Homologs of the catabolic D-arginine oxidase DauA are broadly conserved across the *Pseudomonas* genus. For instance, *P. putida* encodes a D-amino acid oxidase (PP_2246, named DbuA here) that is annotated as a homolog of the catabolic D-arginine oxidase of *P. aeruginosa*. However, arginine racemization in *P. putida* is carried out by the broad-spectrum racemase Alr (15). Additionally, the locus encoding DbuA lacks a homolog of the anabolic oxidase required for the arginine racemization pathway of *P. aeruginosa*. The locus in *P. putida* (named the *dbuRABC* locus here) instead encodes a putative repressor (PP_2245, DbuR), a D-amino acid oxidase (PP_2246, DbuA), a Rid2 family protein (PP_2247, DbuB) and a transporter (PP_2248, DbuC) (Figure 1A). Additionally, DbuA proteins (i.e., those encoded in loci

resembling that in *P. putida*) were found to form a monophyletic group and appear to have evolved from a subset of DauA proteins (i.e., those encoded in loci resembling that of *P. aeruginosa*) (Figure 1B). Functional analyses of the *dbu* locus of *P. putida* described here show that it encodes components of a previously uncharacterized pathway for D-BCAA catabolism.

4.4 RESULTS

Phylogenetic relationship and genomic context suggest divergence of annotated Darginine oxidases. In P. putida, PP 2246 is annotated as a homolog of the D-arginine oxidase, DauA, of P. aeruginosa. The locus containing PP 2246 also encodes a putative regulator (PP 2245), a Rid2 protein (PP 2247) and a predicted transporter (PP 2248) (Figure 1A). This locus structure differs from the *P. aeruginosa dauBAR* locus, which contains a regulator (dauR), the FAD-dependent oxidase dauA, and a NAD(P)H-dependent oxidase (dauB). To determine whether other loci encoding annotated DauA homologs had a structure resembling that of P. putida, a DIAMOND BLASTP (16) search was performed against all complete Pseudomonas genomes available on the Pseudomonas Genome Database (17) using PP 2246 as the query sequence. Amino acid sequences of 41 proteins annotated as DauA homologs – i.e., subject sequences from the DIAMOND BLASTP search, representing 50-98% sequence identity to PP 2246 – were used to generate a phylogenetic tree (Figure 1B). The composition of the loci encoding each retrieved subject sequence was determined. In general, loci encoding the relevant proteins had one of two structures – Type A, resembling that of P. aeruginosa, or Type B, resembling that of P. putida (Figure 1A). Several observations were noted when the locus structure and the

cladogram for these proteins were compared. First, proteins annotated as DauA homologs clustered into three clades and the locus structure was consistent within each clade. Second, those encoded in a Type B locus formed a monophyletic group stemming from a subset of those encoded in Type A loci, implying that Type A proteins (i.e., DauA) were the archetypal group from which Type B proteins (i.e., DbuA) evolved. Comparison of the primary structures of DauA and DbuA proteins revealed several differences at residues assigned to the active site of DauA that are conserved across DbuA proteins – i.e., those encoded in Type B loci. Namely, DbuA proteins contain a methionine at residues 48 and 50, a cysteine at position 87 and isoleucine at position 242, while DauA contains a histidine at residue 48, a threonine at position 50, glutamate at 87 and valine at position 242 (Figure S2). This observation supports the hypothesis that the two proteins could have evolved different substrate specificities. Importantly, several *Pseudomonas* species contained both locus types, which suggested the two may have evolved distinct roles in vivo. Based on the data herein, Type B loci were designated dbu loci for D-branched-chain amino acid utilization. Consistent with this nomenclature, PP 2245, PP 2246, PP 2247 and PP 2248 were designated DbuR, DbuA, DbuB and DbuC, respectively. In total, these phylogenetic data suggest that DbuA proteins evolved from DauA (D-arginine oxidase) proteins, and the two have diverged in function.

P. putida DbuA is functionally distinct from P. aeruginosa DauA. In P. aeruginosa, DauA and DauB catalyze the two-step racemization of D-arginine to L-arginine (11). However, arginine racemization in P. putida is catalyzed by the broad-spectrum amino acid racemase Alr, alleviating the need for the two-step racemization pathway present in P.

aeruginosa and potentially allowing for divergence in function of DbuA in P. putida (15). These facts, coupled with the evolutionary relationship between DbuA and DauA proteins described above, prompted us to consider whether DbuA proteins were D-arginine oxidases or if the evolutionary divergence of DbuA resulted in an alternate function. Deletion of dbuA had no observable effect on the ability of P. putida to utilize D-arginine as the sole nitrogen source while a P. aeruginosa dauA mutant was unable to grow in this medium (Figure 2) (11). While these growth data confirmed DbuA was not required for Darginine utilization in *P. putida*, it did not define the functional capability of the protein. To test whether DbuA had D-arginine oxidase activity in vivo, the protein was heterologously expressed in a P. aeruginosa dauA mutant and growth of the resulting strain was monitored when D-arginine was sole nitrogen source. As expected, the dauA mutant carrying the empty vector failed to grow under these conditions, while expression of P. aeruginosa dauA restored full growth (Figure 2B). In contrast, expression of P. putida dbuA allowed only poor growth with D-arginine as nitrogen source. The slight growth of a dauA mutant expressing dbuA is likely due to the low activity of DbuA on D-arginine coupled with the abundance of enzyme present when overexpressed. Taken together, the data in Figure 2 support the conclusion that *P. putida* DbuA has lower D-arginine oxidase activity than P. aeruginosa DauA in vivo and justify a model in which these two proteins have different roles in their respective organisms.

The *dbu* locus is involved in the utilization of D-branched-chain amino acids. The data above prompted efforts to identify the physiologically relevant substrate(s) of DbuA and define the physiological role of the *dbu* locus. Wild-Type And $\Delta dbuA$ strains of *P. putida*

were screened qualitatively for growth when the L- or D-enantiomer of each of the twenty standard amino acids served as the sole source of carbon or nitrogen. In our hands, the wild-type strain was able to use 15 L-amino acids and 6 D-amino acids as the sole carbon source, and 16 L-amino acids and 11 D-amino acids as the sole nitrogen source (Table S2). Growth of the *dbuA* mutant differed from that of wild type with several D-amino acids as a sole nitrogen and/or carbon source and did not differ from wild type with any L-amino acids. Growth of the two strains was quantified in conditions where a qualitative difference was noted between wild Type And the dbuA mutant (Figure 3). Four D-amino acids distinguished growth of the dbuA mutant from that of the wild-type strain when provided as the sole nitrogen source. The dbuA mutant was unable to utilize D-isoleucine or D-valine as the sole nitrogen source, while wild type grew in these conditions. Growth of the dbuA mutant was slower than that of the wild type when D-leucine or D-phenylalanine were provided as the sole source of nitrogen. Additionally, D-leucine supported growth of wild type, but not the *dbuA* mutant, when provided as the sole carbon source. Even wild-type P. putida was unable to use D-valine or D-isoleucine as a carbon source, most likely reflecting a need for the Branched-Chain Ketoacid Dehydrogenase (BKD) complex to utilize branched-chain amino acids (BCAA) for carbon (Figure 4) (18). The bkd operon, which encodes the constituents of BKD, is transcribed in response to branched-chain ketoacids, L-BCAAs and D-leucine, but not D-isoleucine or D-valine (18). The significant growth of the dbuA mutant with D-leucine or D-phenylalanine as the sole nitrogen source suggests there is a redundant mechanism to liberate the ammonia group from these amino acids. In this scenario, the redundant mechanism would be insufficient to provide the flux needed to utilize D-leucine as a carbon source.

Strains with a non-polar deletion of each gene in the *dbu* locus were constructed to query their function in vivo. Each of the four mutant strains were inoculated into media where growth of the dbuA mutant was impaired (Figure 3). The dbuR mutant had no detectable growth defect and the dbuB mutant had little, if any, impairment in any of the media tested. In contrast, dbuC mutants failed to grow with D-leucine as a carbon source or D-isoleucine as a nitrogen source (Figure 3C, 3E). The *dbuC* mutant had no significant growth defect when D-valine or D-phenylalanine was the sole nitrogen source and had a moderate growth defect with D-leucine as a nitrogen source (Figure 3D, 3F). If DbuC is correctly annotated as a transporter, these data suggest it is a primary transporter for Disoleucine and D-leucine and does not play a significant role in D-valine or Dphenylalanine transport. The significant growth of the dbuC mutant with D-leucine as the sole nitrogen source suggests DbuC is not the only transporter for this amino acid. In this scenario, the inability of a dbuC mutant to utilize D-leucine as a carbon source may reflect differences in the regulation of, or rate of influx through, alternative transporters. In total, these data showed the dbu locus is involved in the catabolism of D-branched chain amino acids, leading to its designation as the *dbu* (**D**-branched-chain amino acid **u**tilization) locus.

A role for the dbu operon beyond D-BCAA catabolism was considered based on nutritional analyses of $\Delta leuA$ and $\Delta ilvD$ strains of P. putida. The leuA and ilvD gene products are required for the synthesis of L-BCAAs and strains lacking these genes require exogenous leucine ($\Delta leuA$ strains), or isoleucine, valine and pantothenate ($\Delta ilvD$ strains) (Table S3). D-leucine satisfies the leucine requirement of a P. putida $\Delta leuA$ mutant (19) and an $\Delta ilvD$ mutant grows when supplemented with L-isoleucine, D-valine and pantothenate (Table S3). Growth stimulation of the leu mutant strains by D-BCAAs

requires racemization to the L-enantiomers, potentially utilizing gene product(s) of the dbu locus. Five mutant strains ($\Delta leuA$, $\Delta dbuR$ $\Delta leuA$, $\Delta dbuA$ $\Delta leuA$, $\Delta dbuB$ $\Delta leuA$ and $\Delta dbuC$ $\Delta leuA$) were grown on minimal glucose medium supplemented with L- or D-leucine. The $\Delta leuA$ single mutant grew with either enantiomer of leucine, and the additional deletion of dbuR or dbuB had no effect (Table S3). In contrast, a $\Delta leuA$ mutant lacking either DbuA or DbuC required L-leucine, and D-leucine did not allow growth. DbuA and DbuC were similarly required for D-valine to satisfy the requirement of an ilvD mutant (Table S3). In total, these data support a the dbu gene products in generating substrates for the L-BCAA biosynthetic pathway (Figure 4).

DbuA is a D-amino acid oxidase with broad substrate specificity. The growth data above suggested DbuA was a D-amino acid oxidase with broad substrate specificity. To establish a hierarchy of preferred substrates for DbuA, His6-DbuA was expressed and purified from *E. coli* (Figure S1) and a dichlorophenolindophenol (DCPIP)-based assay was used to measure oxidase activity as the rate of FAD reduction in the presence of various amino acids. The oxidase assay was performed with multiple D-amino acids deemed physiologically relevant based on phenotypes of the *dbuA* mutant (Table 3). DbuA had the greatest activity in the presence of D-leucine with a specific activity of 301 mM FAD reduced/min/μM protein. This was more than 2-fold higher than activity with the next amnio acid. Second-tier substrates were considered to be D-valine and D-isoleucine, which generated specific activities of 126 and 108 mM FAD reduced/min/μM protein, respectively. Finally, D-phenylalanine was designated a third-tier substrate with 59 mM FAD reduced/min/μM protein. Consistent with the *in vivo* data above, DbuA had little

oxidase activity when D-arginine was the substrate, allowing a specific activity of 10 mM FAD reduced/min/µM protein. These data are consistent with the growth data above and support the proposed role of DbuA as a D-BCAA oxidase.

DbuB is an imine deaminase The annotated functions for DbuA and DbuC (i.e., oxidase and transporter) were consistent with observed phenotypes, but there was no growth phenotype to implicate DbuB functionally in the pathway. DbuB is a Rid family protein in the Rid2 subfamily that contains the arginine residue (Arg105, E. coli numbering) indicative of imine/enamine deaminase activity (20). DbuB was purified from E. coli (Figure S1) and assayed for imine deaminase activity using a general in vitro assay. In this assay, L-amino acid oxidase (LOX) generates imine products from L-amino acid substrates. These imines can be deaminated spontaneously by H₂O or by an appropriately active Rid protein. Semicarbazide in the reaction mixture reacts with imines to generate semicarbazone compounds that can be detected spectrophotometrically with an absorbance at 248 nm. Therefore, deaminase activity is reflected by a decreased rate of semicarbazone formation when the Rid protein is present. DbuB had deaminase activity on the imine derivatives of all six amino acids tested (Table 4) - L-leucine, L-phenylalanine, Lglutamine, L-arginine, L-methionine and L-histidine. DbuB had the highest activity on iminoleucine, reflected by the absence of detectable semicarbazone when leucine was the substrate for LOX. Deamination of iminoglutamine was comparable to that of iminoleucine. This result was unexpected since there was no indication iminoglutamine would be generated *in vivo* under conditions the *dbu* gene products appeared to function. The second most preferred substrate of DbuB was iminophenylalanine. The rate of semicarbazone formation in reactions containing DbuB was 6% of those without the Rid protein present when L-phenylalanine was the substrate of LOX. This result was consistent with the growth defects of a *dbuA* mutant that indicated iminophenylalanine was a relevant intermediate in the pathway encoded by the *dbu* locus (Figure 3D). DbuB also deaminated imines derived from L-methionine, L-histidine and L-arginine with 15%, 65% and 42% the rate of semicarbazone formed per minute compared to reactions without DbuB present. Overall, these data show that DbuB is an imine deaminase *in vitro* and are consistent with the proposed role for this protein in the pathway encoded by the *dbu* locus (Figure 4).

P. putida dbuB mutants are outcompeted by wild type. The observation that P. putida dbuB mutants had no significant growth defect in monoculture was not surprising since deaminase reactions attributed to Rid proteins can occur non-enzymatically. Despite the lack of a clear growth phenotype for the dbuB mutant, precedent suggests this protein could have a role in moderating flux through catabolic pathway(s) where DbuA functions. Fitness costs of losing the subtle contribution of DbuB to the pathway may not be evident in pure culture but could manifest as a competitive disadvantage of the dbuB mutant in conditions where the catabolic pathway is required for growth. To address this possibility, wild-Type And dbuB mutant strains were cocultured in media where DbuA was required for growth. These media included those with D-leucine as the sole carbon or nitrogen source, and D-isoleucine, D-valine or D-phenylalanine as sole nitrogen source. The dbuB mutant was significantly outcompeted by wild type when D-leucine was the sole carbon source, and when D-isoleucine was the sole source of nitrogen. Under these conditions, the dbuB mutant had a 7.5- and 4-fold decrease in competitive fitness, respectively (Figure 5). The

dbuB mutant had only a marginal fitness defect when D-leucine was the sole nitrogen source, with a 2-fold decrease in competitive fitness, and was not outcompeted by wild type when D-valine or D-phenylalanine served as the sole nitrogen source.

4.5 DISCUSSION

L-branched-chain amino acids (L-BCAAs) are essential building blocks and nutrient sources for all living organisms. As such, their anabolic and catabolic pathways have been well studied in many model systems. However, there are gaps in our knowledge of the metabolism of D-amino acids, specifically D-branched-chain amino acids (D-BCAAs). The functional characterization of the *dbu* locus in *P. putida* presented here contributes to our understanding of D-BCAA metabolism in this commercially important microbe.

P. putida DbuA (PP_2246) was annotated as a D-arginine oxidase (i.e., DauA), which is required for D-arginine utilization in P. aeruginosa. D-arginine was not a preferred substrate of DbuA in vitro and, fittingly, DbuA was not required for D-arginine utilization in P. putida. Rather, the preferred substates of P. putida DbuA were D-leucine, D-isoleucine and D-valine. Consistent with the in vitro substrate specificity, DbuA was required for the utilization of these D-BCAAs as sole nutrient sources (Table 3, Figure 3). These data showed that P. putida DbuA is a D-BCAA oxidase.

The phenotypes of strains lacking DbuC suggest this presumed transporter can import D-isoleucine and D-leucine, while failing to import D-valine. The lack of involvement of DbuC in D-valine transport was not expected, since DbuA was required to utilize D-valine for growth. Both *dbuA* and *dbuC* mutants showed significant growth when

D-leucine was provided as the sole nitrogen source but were unable to utilize this amino acid as a carbon source (Figure 3). These data are consistent with the presence of alternative transporters for D-leucine and an enzyme that could liberate ammonia from this amino acid, by either oxidation or transamination. The latter possibility is not unexpected since PLP-dependent transaminases are often promiscuous. It was of interest that both *dbuA* and *dbuC* were required for D-BCAAs to satisfy requirements of *leuA* and *ilvD* mutants (Table S3). These data indicate that the branched-chain ketoacids generated in D-BCAA catabolism can be used in the final step in L-BCAA synthesis and suggest an additional role for the *dbu* genes in nutrient acquisition. The clustering of *dbu* loci with genes for L-leucine synthesis in most *Pseudomonas* species that contain both *dau* and *dbu* loci further supports this model.

The *dbu* locus includes a member of the broadly distributed Rid family of proteins (20). DbuB is a member of the Rid2 protein subfamily and, as such, was predicted to have the deaminase activity that was demonstrated here. While Rid proteins are often embedded in catabolic pathways, based on precedent it was not unexpected absence of the protein did not impact growth of *P. putida* in monoculture (14, 21). Significantly, strains lacking *dbuB* were outcompeted by wild type in several growth conditions that demanded the catabolism of D-leucine or D-isoleucine. These data support a scenario in which DbuB deaminates the imines generated by DbuA more efficiently than water in the cellular milieu, thus increasing flux through the pathway. Such an increase in efficiency would provide a competitive advantage when growth is dependent on catabolism of the D-BCAA by DbuA. This scenario is supported by the data herein and consistent with precedent for Rid proteins in similar biological contexts (14, 21, 22). It was somewhat surprising that *dbuB* mutants

did not have a fitness defect with D-valine as the sole nitrogen source, since DbuA was required in this medium. A possible explanation for this result is that iminovaline could be slowly (or not at all) released by DbuA, minimizing possible contributions by DbuB to its deamination. In general, the data are consistent with the emerging model for Rid proteins as facilitators of metabolic flux (23).

In total, the data herein describe a physiological role for the *dbu* locus in the catabolism of D-BCAAs and demonstrate D-amino acid oxidase activity for DbuA and enamine deaminase for the Rid2 protein DbuB. DbuB is the second member of the Rid2 subfamily with a defined physiological role *in vivo*. As such, this work expands our understanding of how the broadly conserved Rid family of proteins can be integrated into the metabolic network of an organism. Beyond describing the pathway for D-BCAA catabolism, a connection between D-BCAA catabolism and L-BCAA synthesis was established in *P. putida*. This connection links D-BCAA catabolism with a key pathway relevant to the commercial production of fatty-acid-derived chemicals (24). The expanded understanding of the BCAA catabolic and anabolic pathways of *P. putida* has the potential to contribute to efforts in metabolic modelling and engineering of this bacterium. Finally, this study highlights the utility of combining sequence-based annotation of gene function with hands-on experimental validation in the continuing effort to understand microbial metabolism and physiology.

4.6 MATERIALS AND METHODS

Bioinformatics analyses. A DIAMOND BLASTP search was performed using the Pseudomonas Genome Database (16, 17) with *P. putida* DbuA (PP_2246) as the query against all complete genomes in the database using default parameters and an identity cutoff of 50%. A Clustal Omega alignment with default parameters was performed using Geneious Prime software (version 2022.1.1) and was used to generate a neighbor-joining phylogenetic tree of 41 representative subject sequences with a confidence threshold of 60% (ranging from 50-98% sequence identity to PP_2246). The locus type encoding each subject sequence (resembling either the *dauBAR* locus or the *dbuRABC* locus) was then determined and annotated on the phylogenetic tree. For the alignment shown in Figure S2, amino acid sequences of DauA and DbuA were compared via global alignment (Needleman-Wunsch) in SnapGene (version 6.2.1) using default parameters.

Cultivation, media, and chemicals. *P. putida* strains were routinely cultured at 30°C. *P. aeruginosa* and *E. coli* strains were grown at 37°C, unless otherwise indicated. Lysogeny broth (LB) was used as a rich medium and M8 salts (12 mM Na₂HPO₄, 22 mM KH₂PO₄, 1.0 mM NaCl, 1 mM MgSO₄) with trace minerals (25) was used as a minimal medium (26) with indicated carbon (glucose, 11 mM; amino acids, 20 mM) and nitrogen sources (ammonia in the form of ammonium chloride, 10 mM; amino acids, 5 mM). Tryptone Yeast medium (10 g/liter tryptone, 5 g/liter yeast extract, 18 g/liter agar) supplemented with 25% sucrose (TYS25) was used for counterselection when constructing markerless deletions in *P. putida* and *P. aeruginosa*. Terrific Broth (TB; 12 g/liter tryptone, 24 g/liter yeast extract, 4 ml/liter glycerol, 17 mM KH₂PO₄, 72 mM K₂HPO₄) was used as a growth medium for

protein overexpression. Chemicals were purchased from MilliporeSigma (Sigma-Aldrich, St. Louis, MO). Antibiotics were used at the following concentrations unless otherwise stated: gentamycin – 20 μg/ml for *E. coli*, 50 μg/ml for *P. putida* and 75 μg/ml for *P. aeruginosa*; kanamycin – 50 μg/ml; ampicillin – 150 μg/ml. 2,6-diaminopimeleic acid (DAP; 1 mM) was added to growth media for the cultivation of *E. coli* RHO5.

Molecular techniques. Plasmids were constructed using standard cloning procedures and Gibson assembly was performed using NEBuilder HiFi DNA Assembly Master Mix from New England Biosciences (NEB). Restriction endonucleases were purchased from NEB (Ipswich, MA). Plasmids were purified using the GeneJet Plasmid Miniprep kit from Thermo Fisher Scientific (Waltham, MA). Q5 DNA polymerase (NEB) was used to amplify DNA for cloning using either *P. putida* KT2440 or *P. aeruginosa* PA14 gDNA as template. Quickload San Diego, CA). PCR products were purified using the QIAquick PCR purification kit (Qiagen; Germantown, MD) and Sanger sequencing was performed by Eurofins Genomics (Louisville, KY).

Plasmids for gene knockout were assembled with 800 bp of homology flanking the respective gene and were amplified using primers with overhangs complimentary to the EcoRI and SalI sites of either pK18msB for *P. putida* genes or pMQ30 for *P. aeruginosa*. Plasmids were constructed by Gibson assembly (27). Deletion of each gene was confirmed by colony PCR and Sanger sequencing. For pMQ72-derived complementation plasmids, the genes of interest were amplified by PCR and cloned into the EcoRI and SalI sites of pMQ72. For pTEV18-derived overexpression plasmids, coding regions of each gene were amplified and cloned into the BspQI sites of pTEV18.

Strain construction. P. putida strains used in this study were derivatives of P. putida KT2440 and P. aeruginosa strains were derivatives of P. aeruginosa PA14. P. putida deletion mutants were generated using antibiotic selection/sucrose counter-selection as described previously (28). In short, 800 bp regions of homology flanking the gene of interest were cloned into the pK18msB suicide plasmid and transformed into P. putida by electroporation. Transformants were plated onto LB with 50 µg/ml kanamycin (LB Km50) and colonies were streaked for isolation onto LB Km50 to select for homologous recombination of the plasmid into the chromosome. Merodiploids were then streaked onto TYS25 to select for a second homologous recombination event to excise the plasmid backbone from the chromosome. P. aeruginosa PA14 dauA mutants were constructed using the same protocol used to construct P. putida mutants, except that regions of homology flanking dauA were cloned into pMQ30 to generate pMQ30-ΔPA14-dauA. The resulting plasmid was transformed into E. coli RHO5 by electroporation and transformants were plated onto LB supplemented with 1 mM diaminopimelic acid (LB+DAP) and 20 μg/ml gentamycin. pMQ30-ΔPA14-dauA was mobilized into wild-type P. aeruginosa PA14 by biparental puddle mating with E. coli RHO5 carrying pMQ30-ΔPA14-dauA on LB+DAP and incubated for five hours at 30°C. Mating puddles were suspended in 1 ml of LB, plated onto LB with 75 µg/ml gentamycin (LB Gm75) and grown overnight at 30°C. Transconjugants were then streaked for isolation on LB Gm75 and grown at 30°C. Merodiploids were then streaked onto TYS25 to select for excision of plasmid backbone from the chromosome. All strains carrying pK18msB or pMQ30 derivatives were grown at 30°C. Deletion of the respective gene was confirmed in each case by colony PCR and

Sanger sequencing. In complementation studies, plasmids derived from pMQ72 were transformed into *P. aeruginosa* by electroporation and transformants were selected on LB Gm75.

Growth analyses. Optical density at 650 nm (OD₆₅₀) was used to measure growth of cultures in 96-well plates (Falcon) using a BioTek Elx808 plate reader with a slow shaking speed (210 rpm) unless otherwise stated. Overnight cultures (1 ml) were grown in LB with shaking and pelleted. *P. aeruginosa* cell pellets were resuspended in 1 ml sterile saline while *P. putida* cultures were resuspended in 2 ml sterile saline due to the higher density of the overnight cultures. OD₆₅₀ values for *P. aeruginosa* overnight cultures were typically \sim 1.4 and those of *P. putida* were \sim 2.6 when grown in 1 ml of LB. 195 μ l of each indicated medium was inoculated with 5 μ l of cell suspension. Data were plotted using GraphPad Prism version 8.4.3.

Competition experiments. Competition experiments were performed largely as described previously (14, 29, 30). Briefly, overnight cultures (1 ml) of each strain were grown in LB at 30°C with shaking at 225 rpm. Cultures were diluted to an OD₆₅₀ of 0.2 in sterile saline and 100 μl each of the Km^R wild-type strain and the Gm^R mutant strain were inoculated into 5 ml of each indicated medium. Colony forming units (CFU) of the initial cultures (i.e., pre-incubation) were enumerated by serial dilution and plating onto both LB Gm50, to select for the mutant strain, and LB Km50, to select for wild type. Co-cultures were incubated at 30°C with shaking to early stationary phase, when CFUs were enumerated as stated above. The competitive index (CI) for each strain in each medium was calculated by

dividing the ratio of mutant to wild-type cells after co-incubation by the ratio of mutant to wild type pre-incubation. The natural log of the CI values (lnCI) was plotted for ease of interpretation. In this format, a value of zero indicates no difference in competitive fitness, a positive value indicates that the mutant strain outcompeted wild type under the indicated conditions, and a negative value indicates the mutant strain was outcompeted by wild type. GraphPad Prism version 8.0 was used for data analysis and plotting.

Protein purification. Three 10 ml cultures of *E. coli* BL21-AI harboring pTEV18-*dbuA* or pTEV18-*dbuB* were grown overnight at 37°C in Terrific Broth with 150 μg/ml ampicillin and each was used to inoculate 1.5 L of TB Ap150 in a 2.8 L baffle-bottom Fernbach flask. Cultures were grown at 37°C with shaking at 150 rpm to an OD₆₅₀ of ~0.5, at which point gene expression was induced with 0.2% arabinose and 0.4 mM IPTG. After induction, cells were incubated at 23°C with shaking at 150 rpm for 16 h before being harvested by centrifugation. Cell pellets were stored at -80°C until purification.

DbuA and DbuB were purified by the same method. Briefly, cell pellets were thawed and resuspended in 2 ml of Lysis Buffer (50 mM potassium phosphate pH 7.4, 150 mM NaCl, 20 mM imidazole, 2 mg/ml lysozyme, 0.125 mg/ml DNase, 1 mM PMSF) per gram of cells, and incubated on ice for 30 minutes before being mechanically lysed using a Constant Systems One Shot (United Kingdom) at 19 kpsi. Cell lysates were clarified by centrifugation at 45000 x g for 45 minutes and filtered through a 0.45 μm PVDF filter before being loaded onto a 5 ml HisTrap HP Ni-Sepharose column (Cytiva). After sample application, the column was washed with five column volumes of Binding Buffer (50 mM potassium phosphate pH 7.4, 150 mM NaCl, 20 mM imidazole) followed by three column

volumes of 96% Binding Buffer with 4% Elution Buffer (50 mM potassium phosphate pH 7.4, 150 mM NaCl, 500 mM imidazole). Each protein was eluted with a gradient of 4-100% Elution Buffer over the course of 10 column volumes. A flow rate of 2 ml/min was used for each step of protein purification. Purified protein was concentrated using a centrifugal filter with a molecular weight cutoff of 30 kDa (DbuA) or 10 kDa (DbuB), before buffer exchange into Storage Buffer (50 mM Tris-HCl pH 7.4, 150 mM NaCl, 10% glycerol) using a PD-10 column (Cytiva). Protein concentration was determined using the Pierce BCA Protein Assay Kit (Thermo Scientific). Proteins were separated by electrophoresis (SDS-PAGE) before being stained with Coomassie Blue and imaged using AnalytikJena UVP ChemStudio. Purity was determined by densitometry using VisionWorks software version 8.22.18309.10577. DbuA was purified to a final concentration of 227 μ M (9.2 mg/ml) and a purity of 99% and DbuB was purified to a final concentration of 80 μ M (1 mg/ml) and a purity of 90 % (Figure S1). All proteins were flash-frozen in liquid nitrogen and stored at -80°C until use.

Enzyme assays. Enzymes were assayed at room temperature (25°C) unless otherwise stated.

FAD reduction by DbuA. The rate of FAD reduction by DbuA was measured using a dichlorophenolindophenol (DCPIP)-based assay as described previously (31). Reaction mixtures (100 μl) contained potassium phosphate pH 7.4 (50 mM), DCPIP (0.1 mM), phenazine methosulfate (0.5 mM), FAD (0.1 mM), D-amino acid (1.5 mM) and purified DbuA (0.5 μM). Reactions were initiated with the addition of D-amino acid and the absorbance was measured at 600 nm every ten seconds over the course of five minutes.

The rate of DCPIP reduction was determined using the measured pathlength of each well (0.173 cm) and the molar extinction coefficient for DCPIP at pH 7.4 ($\varepsilon = 12.5 \text{ M}^{-1} \text{ cm}^{-1}$).

Imine deaminase activity of DbuB. L-amino acid oxidase (LOX) assays were used to determine imine deaminase activity of DbuB, as described previously (14, 20, 22). Briefly, imines were generated from L-amino acids by LOX and were measured by derivatization with semicarbazide. The reaction between semicarbazide and imines generate semicarbazone compounds that can be detected in the UV spectrum at an absorbance of 248 nm. Reaction mixtures (100 μ l) contained potassium pyrophosphate pH 8.7 (50 mM), neutralized semicarbazide (10 mM), catalase from bovine liver (5 μ g), L-amino acid oxidase from *Crotalus adamanteus* (5 μ g), L-amino acid (10 mM), and purified DbuB (10 μ M) where indicated. Reactions were initiated with the addition of L-amino acid substrate, and the absorbance at 248 nm was measured every ten seconds over the course of ten minutes. The rate of semicarbazone formation was determined using the measured pathlength of each well (0.173 cm) and the molar extinction coefficient for semicarbazide ($\epsilon = 10300 \, \text{M}^{-1} \, \text{cm}^{-1}$).

4.7 REFERENCES

- 1. Scales BS, Dickson RP, LiPuma JJ, Huffnagle GB. 2014. Microbiology, genomics, and clinical significance of the *Pseudomonas fluorescens* species complex, an unappreciated colonizer of humans. Clin Microbiol Rev 27:927-48.
- 2. Fedral-Register. 1982. Certified host vector systems. Recomb DNA Tech Bull 5:206-9.

- 3. Neinast M, Murashige D, Arany Z. 2019. Branched Chain Amino Acids. Annu Rev Physiol 81:139-164.
- 4. Mutaguchi Y, Ohmori T, Akano H, Doi K, Ohshima T. 2013. Distribution of Damino acids in vinegars and involvement of lactic acid bacteria in the production of D-amino acids. Springerplus 2:691.
- 5. Mutaguchi Y, Kasuga K, Kojima I. 2018. Production of D-Branched-Chain Amino Acids by Lactic Acid Bacteria Carrying Homologs to Isoleucine 2-Epimerase of *Lactobacillus buchneri*. Front Microbiol 9:1540.
- 6. Tsukada K. 1966. D-amino acid dehydrogenases of *Pseudomonas fluorescens*. J Biol Chem 241:4522-8.
- 7. Marshall VP, Sokatch JR. 1968. Oxidation of D-amino acids by a particulate enzyme from *Pseudomonas aeruginosa*. J Bacteriol 95:1419-24.
- 8. Martin RR, Marshall VD, Sokatch JR, Unger L. 1973. Common enzymes of branched-chain amino acid catabolism in *Pseudomonas putida*. J Bacteriol 115:198-204.
- 9. Conrad RS, Massey LK, Sokatch JR. 1974. D- and L-isoleucine metabolism and regulation of their pathways in *Pseudomonas putida*. J Bacteriol 118:103-11.
- 10. Massey LK, Conrad RS, Sokatch JR. 1974. Regulation of leucine catabolism in *Pseudomonas putida*. J Bacteriol 118:112-20.
- 11. Li C, Yao X, Lu CD. 2010. Regulation of the *dauBAR* operon and characterization of D-amino acid dehydrogenase DauA in arginine and lysine catabolism of *Pseudomonas aeruginosa* PAO1. Microbiology 156:60-71.
- 12. He W, Li C, Lu CD. 2011. Regulation and characterization of the *dadRAX* locus for D-amino acid catabolism in *Pseudomonas aeruginosa* PAO1. J Bacteriol 193:2107-15.

- 13. He W, Li G, Yang CK, Lu CD. 2014. Functional characterization of the *dguRABC* locus for D-Glu and D-Gln utilization in *Pseudomonas aeruginosa* PAO1. Microbiology 160:2331-2340.
- 14. Fulton RL, Downs DM. 2022. DadY (PA5303) is required for fitness of *Pseudomonas aeruginosa* when growth is dependent on alanine catabolism. Microb Cell 9:190-201.
- 15. Radkov AD, Moe LA. 2013. Amino acid racemization in *Pseudomonas putida* KT2440. J Bacteriol 195:5016-24.
- 16. Buchfink B, Xie C, Huson DH. 2015. Fast and sensitive protein alignment using DIAMOND. Nat Methods 12:59-60.
- 17. Winsor GL, Griffiths EJ, Lo R, Dhillon BK, Shay JA, Brinkman FS. 2016. Enhanced annotations and features for comparing thousands of *Pseudomonas* genomes in the Pseudomonas genome database. Nucleic Acids Res 44:D646-53.
- 18. Madhusudhan KT, Huang N, Sokatch JR. 1995. Characterization of BkdR-DNA binding in the expression of the *bkd* operon of *Pseudomonas putida*. J Bacteriol 177:636-41.
- 19. Molina-Henares MA, de la Torre J, Garcia-Salamanca A, Molina-Henares AJ, Herrera MC, Ramos JL, Duque E. 2010. Identification of conditionally essential genes for growth of *Pseudomonas putida* KT2440 on minimal medium through the screening of a genome-wide mutant library. Environ Microbiol 12:1468-85.
- 20. Niehaus TD, Gerdes S, Hodge-Hanson K, Zhukov A, Cooper AJ, ElBadawi-Sidhu M, Fiehn O, Downs DM, Hanson AD. 2015. Genomic and experimental evidence for multiple metabolic functions in the RidA/YjgF/YER057c/UK114 (Rid) protein family. BMC Genomics 16:382.
- 21. Buckner BA, Lato AM, Campagna SR, Downs DM. 2021. The Rid family member RutC of *Escherichia coli* is a 3-aminoacrylate deaminase. J Biol Chem doi:10.1016/j.jbc.2021.100651:100651.

- 22. Hodge-Hanson KM, Downs DM. 2017. Members of the Rid protein family have broad imine deaminase activity and can accelerate the *Pseudomonas aeruginosa* Darginine dehydrogenase (DauA) reaction *in vitro*. PLoS One 12:e0185544.
- 23. Fulton RL, Downs DM. 2023. Modulators of a robust and efficient metabolism: Perspective and insights from the Rid superfamily of proteins. *In* Poole RK, Kelly DJ (ed), Advances in Microbial Physiology, vol 83. Elsevier.
- 24. Bai W, Geng W, Wang S, Zhang F. 2019. Biosynthesis, regulation, and engineering of microbially produced branched biofuels. Biotechnol Biofuels 12:84.
- 25. Balch W, E.; Wolfe, R. S. 1976. New approach to the cultivation of methanogenic bacteria: 2-mercaptoethanesulfonic acid (HS-CoM)-dependent growth of *Methanobacterium ruminantium* in a pressurized atmosphere. Applied and Environmental Microbiology 32:781-791.
- 26. Vogel HJ, Bonner DM. 1956. Acetylornithase of *Escherichia coli*: partial purification and some properties. Journal of Biological Chemistry 218:97-106.
- 27. Gibson DG, Young L, Chuang RY, Venter JC, Hutchison CA, 3rd, Smith HO. 2009. Enzymatic assembly of DNA molecules up to several hundred kilobases. Nat Methods 6:343-5.
- 28. Blomfield IC, Vaughn V, Rest RF, Eisenstein BI. 1991. Allelic exchange in *Escherichia coli* using the *Bacillus subtilis sacB* gene and a temperature-sensitive pSC101 replicon. Mol Microbiol 5:1447-57.
- 29. Boulette ML, Baynham PJ, Jorth PA, Kukavica-Ibrulj I, Longoria A, Barrera K, Levesque RC, Whiteley M. 2009. Characterization of alanine catabolism in *Pseudomonas aeruginosa* and its importance for proliferation *in vivo*. J Bacteriol 191:6329-34.
- 30. Speare L, Septer AN. 2019. Coincubation Assay for Quantifying Competitive Interactions between *Vibrio fischeri* Isolates. J Vis Exp doi:10.3791/59759.

- 31. Brugger D, Krondorfer I, Zahma K, Stoisser T, Bolivar JM, Nidetzky B, Peterbauer CK, Haltrich D. 2014. Convenient microtiter plate-based, oxygen-independent activity assays for flavin-dependent oxidoreductases based on different redox dyes. Biotechnol J 9:474-82.
- 32. Choi KH, Mima T, Casart Y, Rholl D, Kumar A, Beacham IR, Schweizer HP. 2008. Genetic tools for select-agent-compliant manipulation of *Burkholderia pseudomallei*. Appl Environ Microbiol 74:1064-75.
- 33. Meisner J, Goldberg JB. 2016. The Escherichia coli *rhaSR-PrhaBAD* Inducible Promoter System Allows Tightly Controlled Gene Expression over a Wide Range in *Pseudomonas aeruginosa*. Appl Environ Microbiol 82:6715-6727.
- 34. Choi KH, Gaynor JB, White KG, Lopez C, Bosio CM, Karkhoff-Schweizer RR, Schweizer HP. 2005. A Tn7-based broad-range bacterial cloning and expression system. Nat Methods 2:443-8.
- 35. Shanks RM, Caiazza NC, Hinsa SM, Toutain CM, O'Toole GA. 2006. Saccharomyces cerevisiae-based molecular tool kit for manipulation of genes from Gram-negative bacteria. Appl Environ Microbiol 72:5027-36.
- 36. Platt R, Drescher C, Park SK, Phillips GJ. 2000. Genetic system for reversible integration of DNA constructs and *lacZ* gene fusions into the *Escherichia coli* chromosome. Plasmid 43:12-23.
- 37. Kvitko BH, Bruckbauer S, Prucha J, McMillan I, Breland EJ, Lehman S, Mladinich K, Choi KH, Karkhoff-Schweizer R, Schweizer HP. 2012. A simple method for construction of *pir*+ Enterobacterial hosts for maintenance of R6K replicon plasmids. BMC Res Notes 5:157.

TABLE 4.1: DbuA is an FAD-dependent D-amino acid oxidase.

DbuA Substrate	Activity ^a
D-Leu	301 ± 11
D-Val	126 ± 10
D-Ile	108 ± 6
D-Phe	59 ± 9
D-Arg	10 ± 2

^a Activity is reported as mM FAD reduced/min/μM protein

Reactions (100 μ l) contained potassium phosphate pH 7.4 (50 mM), dichlorophenolindophenol (DCPIP, 0.1 mM), phenazine methosulfate (PMS, 0.5 mM), FAD (0.1 mM), and purified DbuA (0.5 μ M). Reactions were initiated with the addition of the indicated substrate (1.5 mM) and the absorbance at 600 nm was monitored over the course of five minutes. The rate of DCPIP reduction was determined using the measured pathlength of each well and the molar extinction coefficient for DCPIP (ϵ = 12.5 M⁻¹ cm⁻¹). Data shown are the mean and standard deviation of three technical replicates.

TABLE 4.2: DbuB is an imine deaminase.

	Semicarbazo	one formation	% semicarbazone formation
	(mM/min)		
Substrate for	No Rid	DbuB ^a	$\mathrm{DbuB}^{\mathrm{b}}$
LOX			
L-Leu	31 ± 2	ND	ND
L-Phe	31 ± 1	5 ± 1	6
L-Gln	18 ± 2	ND	ND
L-Arg	50 ± 1	21 ± 1	42
L-Met	27 ± 2	4 ± 0.3	15
L-His	20 ± 1	14 ± 1	65

^a Reactions containing DbuB were significantly different from those without it, for each of the substrate amino acids.

Reactions (100 µl) contained potassium pyrophosphate pH 8.7 (50 mM), semicarbazone (10 mM), L-amino acid oxidase from *Crotalus adamanteus* (5 µg), bovine liver catalase (5 µg), purified DbuB (10 µM). Reactions were initiated with the addition of the indicated substrate (10 mM) and the absorbance at 248 nm was monitored over the course of ten minutes. The rate of semicarbazone formation was determined using the measured pathlength of each well and the molar extinction coefficient for semicarbazide ($\varepsilon = 10300 \, \text{M}^{-1} \, \text{cm}^{-1}$). Data shown are the mean and standard deviation of three technical replicates. ND indicates that no semicarbazone was detected. Significant difference was determined by Tukey's multiple comparisons test (p < 0.05).

^b Percent semicarbazone formed per minute in reactions containing DbuB compared to those with no Rid protein present.

TABLE 4.3: Strains and plasmids used in this study.

	s and plasmids used in this study.	1 ~
Plasmid name	Description	Source
pTNS3	Tn7 helper plasmid	(32)
pK18msB-	pK18msB with 800 bp of homology flanking dbuR	This study
$\Delta dbuR$	cloned into EcoRI and SalI sites	
pK18msB-	pK18msB with 800 bp of homology flanking dbuA	This study
$\Delta dbuA$	cloned into EcoRI and SalI sites	
pK18msB-	pK18msB with 800 bp of homology flanking dbuB	This study
$\Delta dbuB$	cloned into EcoRI and SalI sites	
pK18msB-	pK18msB with 800 bp of homology flanking dbuC	This study
$\Delta dbuC$	cloned into EcoRI and SalI sites	
pK18msB-∆ <i>leuA</i>	pK18msB with 800 bp of homology flanking <i>leuA</i> cloned into EcoRI and SalI sites	This study
pK18msB-Δ <i>ilvD</i>	pK18msB with 800 bp of homology flanking <i>ilvD</i> cloned into EcoRI and SalI sites	This study
pJM220	pUC18T-miniTn7T-Gm-rhaSR-PrhaBAD	(33)
pTn7-Gm	pUC18T-mini-Tn7T-Gm	(34)
pTn7R6K-Km	pUC18R6KT-mini-Tn7T-Gm	(34)
pMQ30-ΔPA14-	pMQ30 with 800 bp of homology flanking dauA	This study
dauA	pringer was over the memories, imministration	
pMQ72	Broad host-range vector; Gm ^R , URA3, araC-	(35)
	ParaBAD	
pMQ72-dbuA	pMQ72 with <i>dbuA</i> cloned into EcoRI and SalI sites	This study
pMQ72-PA14- dauA	pMQ72 with dauA cloned into EcoRI and SalI sites	This study
pTEV18-dbuA	pTEV18 with <i>dbuA</i> cloned into BspQI sites	This study
pTEV18-dbuB	pTEV18 with <i>dbuB</i> cloned into BspQI sites	This study
1		
Strain	Genotype	Source
P. putida		
KT2440		
DMPA 26	∆dbuB (PP 2247)	This study
DMPA 28	Wild type	Laboratory
		collection
DMPA 73	ΔdbuA (PP_2246)	This study
DMPA 87	ΔdbuR (PP_2245)	This study
DMPA 88	ΔdbuC (PP_2248)	This study
DMPA 131	ΔdbuA attTn7::rhaSR-PrhaBAD-empty-Gm ^R	This study
DMPA 132	ΔdbuA attTn7::rhaSR-PrhaBAD-dbuA-Gm ^R	This study
DMPA 133	ΔdbuC attTn7::rhaSR-PrhaBAD-empty-Gm ^R	This study
DMPA 134	ΔdbuC attTn7::rhaSR-PrhaBAD-dbuC-Gm ^R	This study
DMPA 174	ΔleuA (PP_1025)	This study
DMPA 175	ΔilvD (PP 5128)	This study
DMPA 183	ΔdbuA ΔleuA	This study

DMPA 185	ΔdbuC ΔleuA	This study
DMPA 187	ΔdbuA ΔilvD	This study
DMPA 188	ΔdbuC ΔilvD	This study
DMPA 201	ΔdbuB attTn7::Gm ^R	This study
DMPA 203	Wild type attTn7::Km ^R	This study
P. aeruginosa		
PA14		
DMPA 94	ΔdauA/pMQ72-empty	This study
DMPA 95	ΔdauA/pMQ72-dbuA	This study
DMPA 96	ΔdauA/pMQ72-P. aeruginosa dauA	This study
E. coli		
DH5αpir	endA1 hsdR17 glnV44 (= supE44) thi-1 recA1	(36)
	$gyrA96 \ relA1 \ \phi 80dlac\Delta(lacZ)M15 \ \Delta(lacZYA-$	
	argF)U169 zdg-232::Tn10 uidA::pir+	
NEB5α	DH5 α derivative; fhuA2::IS2 Δ (mmuP-	Laboratory
	mhpD)169 rfbD1 luxS11 rph ^{WT}	collection
BL21-AI	E. coli B F derivative; ompT gal dcm lon $hsdS_B(r_B)$	Laboratory
	m_{B}^{-}) $(malB^{+})_{K-12}(\lambda^{S})$ $araB::T7RNAP-tetA$	collection
RHO5	SM10 (λpir) derivative; $\Delta asd::FRT \Delta aphA::FRT$	(37)
	attTn7::pir-116-FRT	

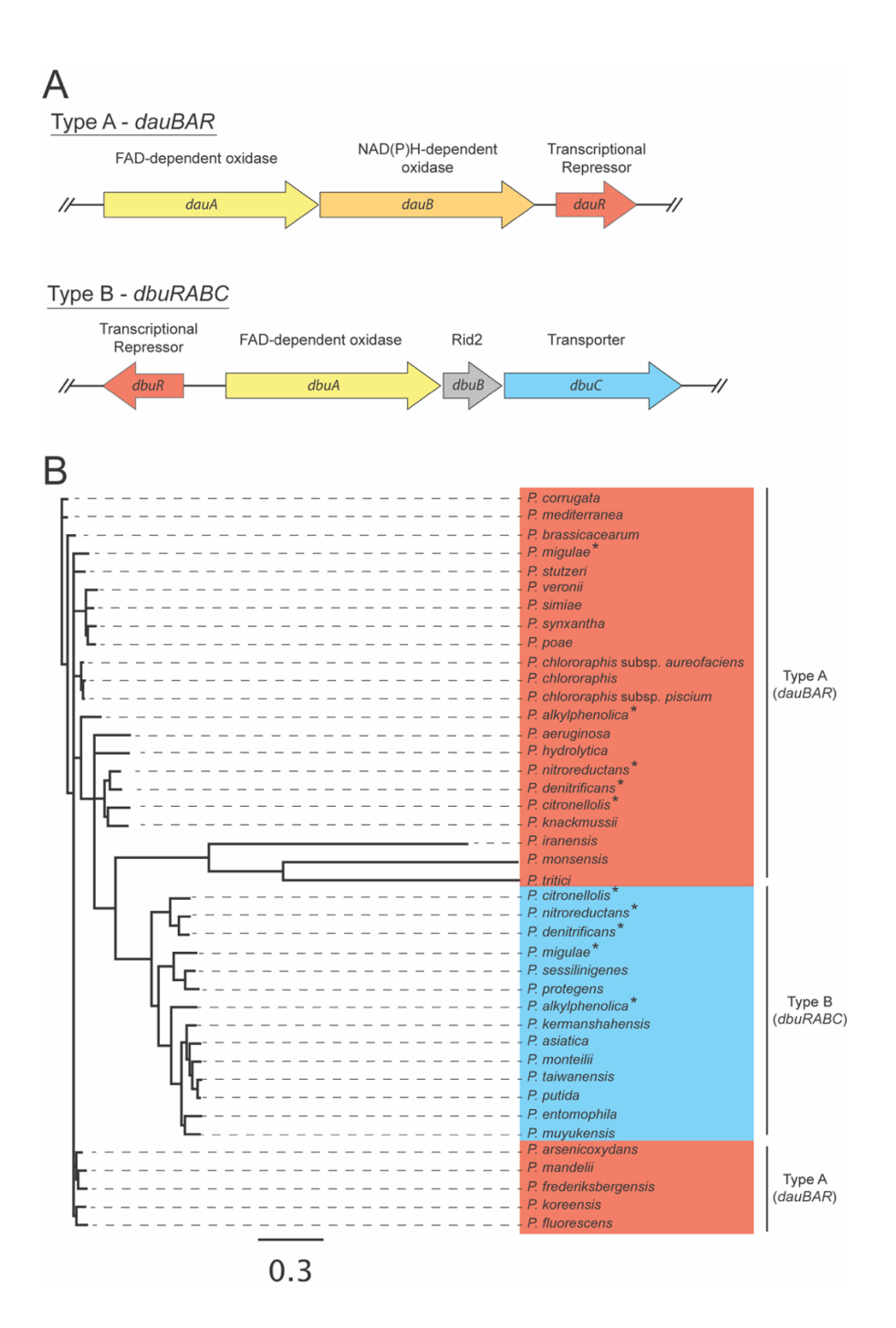


FIGURE 4.1: Genomic context and phylogenetic relationships suggest divergence in function between annotated DauA homologs. (A) Organization of loci encoding annotated DauA homologs in *Pseudomonas* species. Type A (*dauBAR*) loci encode an anabolic 2-ketoarginine oxidase (DauB), a catabolic D-arginine oxidase (DauA) and a transcriptional repressor (DauR). Type B (*dbuRABC*) loci encode a putative transcriptional repressor (DbuR), a D-amino acid oxidase (DbuA), a Rid2 protein (DbuB) and a putative transporter (DbuC). (B) Phylogenetic relationship of annotated DauA (D-arginine oxidase) homologs in *Pseudomonas* species. The locus type encoding each protein is indicated to the right.

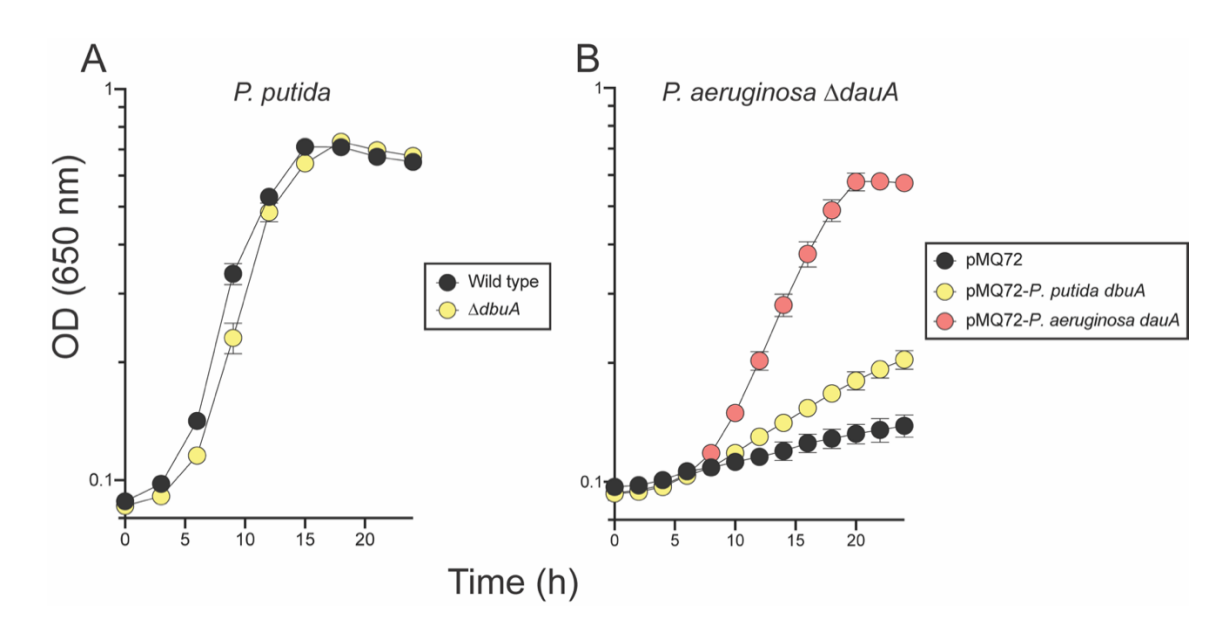


FIGURE 4.2: DbuA does not play a significant role in D-arginine utilization. (A) Growth of *P. putida* wild type (black) and a *dbuA* mutant (yellow) in minimal glucose (11 mM) medium with D-arginine (5 mM) as the sole nitrogen source. (B) Growth of a *P. aeruginosa dauA* mutant harboring the pMQ72 empty vector (black), pMQ72 encoding DbuA from *P. putida* (yellow), or DauA from *P. aeruginosa* (red). Growth was monitored in minimal glucose (11 mM) medium with D-arginine (5 mM) as the sole nitrogen source, supplemented with 0.2% arabinose to induce expression of the plasmid-borne gene. Error bars represent standard deviation between three independent biological replicates.

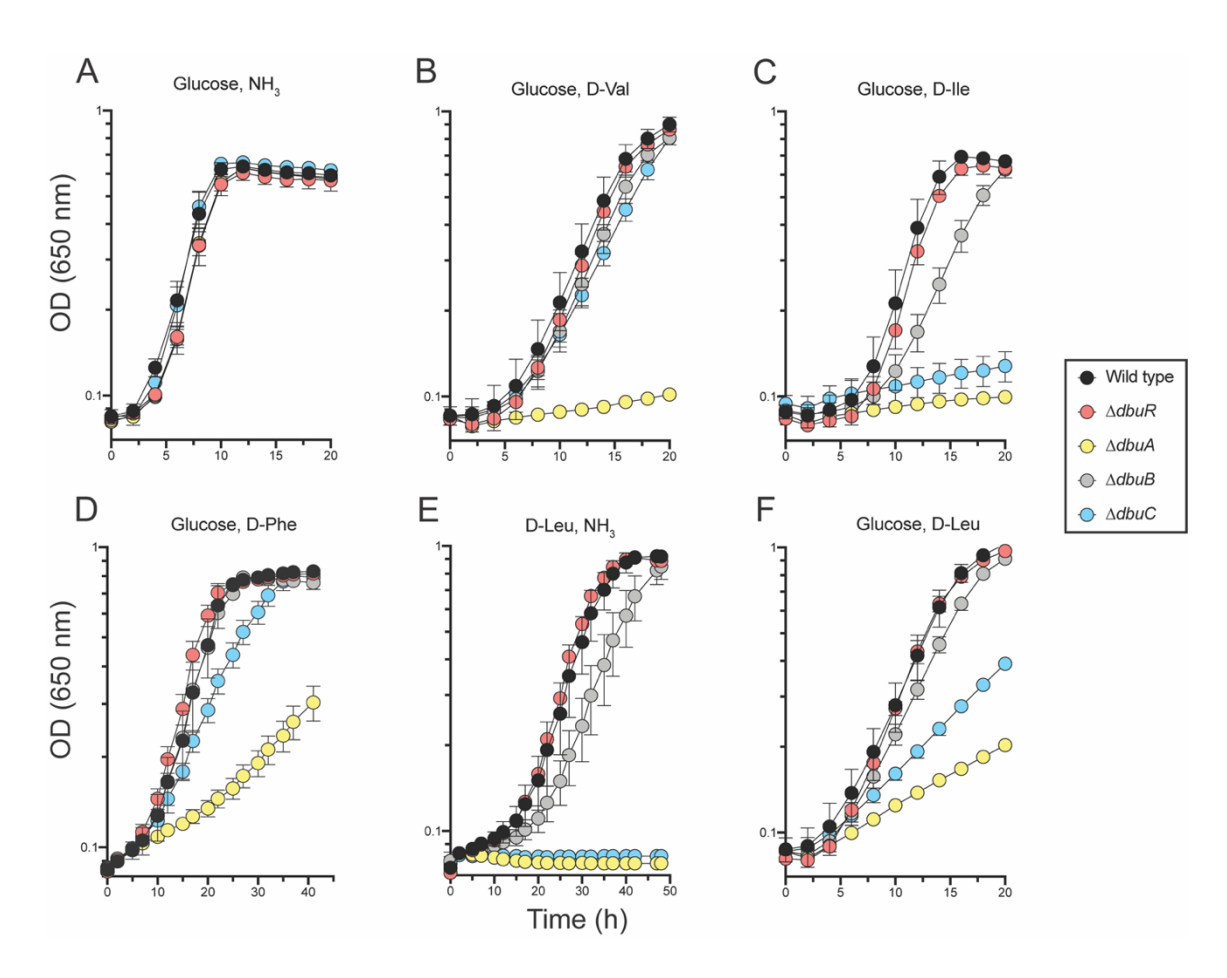


FIGURE 4.3: Genes in the *dbu* locus are required for D-BCAA utilization in *P. putida*. Shown are growth profiles of wild-type *P. putida* (black), a *dbuR* mutant (red), *dbuA* mutant (yellow), *dbuB* mutant (grey), *dbuC* mutant (blue). *P. putida* strains were grown in minimal media with the indicated carbon (11 mM glucose or 20 mM D-leucine) and nitrogen sources (10 mM ammonia or 5 mM D-amino acid). (A) glucose and ammonia, (B) glucose and D-valine, (C) glucose and D-isoleucine, (D) glucose and D-phenylalanine, (E) D-leucine and ammonia, (F) glucose and D-leucine. Error bars represent standard deviation between three independent biological replicates.

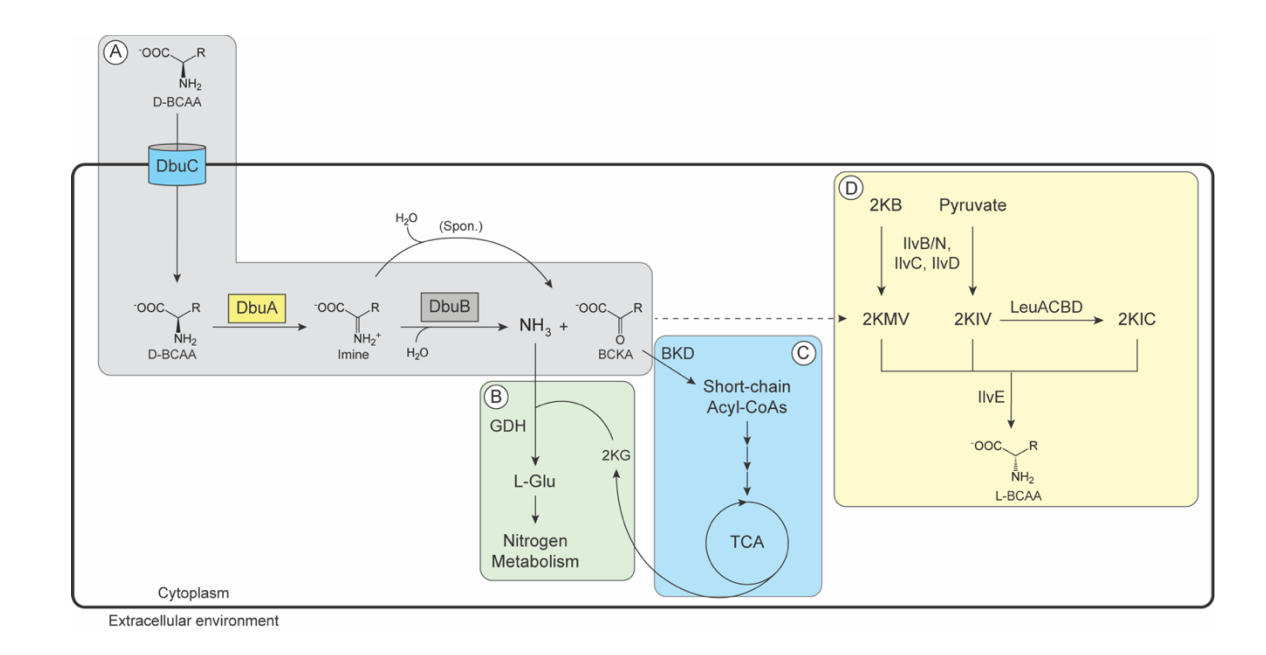


FIGURE 4.4: D-branched-chain amino acid catabolism in P. putida. Shown is a model for the D-BCAA catabolic pathway of P. putida and its integration with various other metabolic nodes. (A) D-BCAA catabolic pathway. The transporter DbuC imports D-BCAAs that are then oxidized by DbuA, generating imine intermediates. These intermediates are deaminated either spontaneously by water or, more rapidly, by the Rid2 protein DbuB to generate ammonia and BCKAs. (B) Ammonia released by DbuB, along with 2KG, are converted to L-glutamate by GDH, which then enters nitrogen metabolism. (C) BCKAs produced by DbuB are decarboxylated and converted to short-chain acyl-CoAs by the BKD complex. These short-chain acyl-CoAs are subsequently converted into acetyl-CoA, which then enters the TCA cycle. (D) Branched-chain amino acid biosynthesis. The BCKAs, 2KMV and 2KIV, are generated from 2KB and pyruvate by combined activities of IlvB/N, IlvC and IlvD. 2KIV can be converted to 2KIC by the LeuACBD enzymes. These BCKAs are transaminated by IIvE to produce L-BCAAs. Alternatively, BCKAs generated by the DBU pathway can enter the final step of this pathway to serve as substrates for IlvE (dashed arrow). Abbreviations are as follows: BCAA, branched-chain amino acid; BCKA, branched-chain ketoacid; GDH, glutamate dehydrogenase; BKD, branched-chain ketoacid dehydrogenase; 2KB, 2-ketobutyrate; 2KMV, 2-ketomethylvalerate; 2KIV, 2ketoisovalerate; 2KIC, 2-ketoisocaproate.

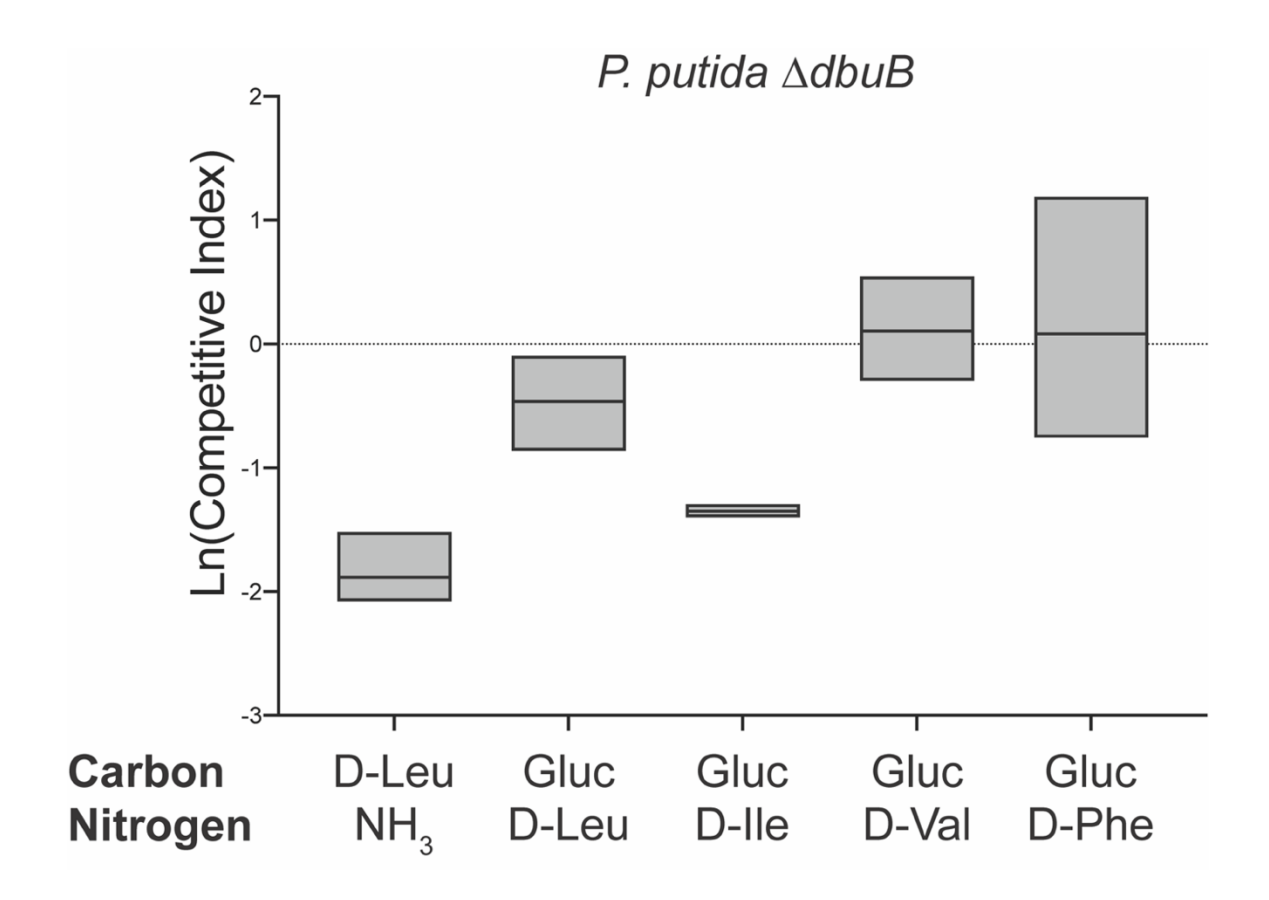


FIGURE 4.5: *P. putida dbuB* mutants are outcompeted by wild type for D-BCAAs. Strain DMPA 201 (Δ*dbuB att*Tn7::Gm^R) was competed against DMPA 203 (Wild type *att*Tn7::Km^R) in media with the indicated sources of carbon and nitrogen. D-leucine was added to a final concentration of 20 mM when used as a carbon source, and each D-amino acid was present at 5 mM when used as a nitrogen source. When present, glucose was at 11 mM and ammonia was at 10 mM. Co-cultures were grown to early stationary phase at 30°C with shaking. Each culture was serially diluted and spread onto both LB with 50 μg/ml gentamicin or kanamycin to enumerate colony forming units (CFU) of each strain. The competitive index (CI) of each strain was calculated as the ratio of the mutant strain to wild type after co-incubation, divided by the ratio of mutant to wild-type cells in the inoculum. Data shown are the natural log of CI values. Error bars represent the mean and standard deviation of three independent biological replicates.

TABLE 4.S1: Oligonucleotides used in this study.

	ucleotides used in this study.
Oligonucleotide	Sequence
PBAD-F	ATGCCATAGCATTTTTATCC
PBAD-R	GATTTAATCTGTATCAGG
T7-F	TAATACGACTCACTATAGGG
T7-R	GCTAGTTATTGCTCAGCGG
M13 F	GTAAAACGACGCCAGT
M13-R	CAGGAAACAGCTATGAC
ppu-glmS-up	CACCATTCCGCTGCAGTTG
ppu-glmS-down	AGTCAGAGTTACGGAATTGTAGG
pTn7-R	CACAGCATAACTGGACTGATTTC
pTn7-L	ATTAGCTTACGACGCTACACCC
Tn7-end	GGGGTGGAAATGGAGTTTTT
oJM730	GATACAGCGTGAATTTTCAGG
ppu-K18-2245-USF	acagctatgacatgattacgCCGCTACCAAGGTCAGTG
ppu-K18-2245- USR	ggtgcgcaagATCTACCTGTCGGAAAGC
ppu-K18-2245-DSF	acaggtagatCTTGCGCACCTGGCGCAG
ppu-K18-2245- DSR	caagettgcatgcctgcaggCGGTCCGCCCAGGCACCT
ppu-2245-seq-F	TCAACGATCGGTCATCACTACCATG
ppu-2245-seq-R	ATGCCCGCAGCTCTTCCC
ppu-K18-2246-USF	ggatccccgggtaccgagctAGGCGCAGCGGATCAACG
ppu-K18-2246- USR	ctcctcgggcGCGCGAAAGTTTGCTCAAGC
ppu-K18-2246-DSF	actttcgcgcGCCCGAGGAGTTCGACGT
ppu-K18-2246- DSR	acagetatgacatgattacgGGCCGCAGATGGCCAAAATC
ppu-2246-seq-F	GCGGGCATAGGCCGGTGTCA
ppu-2246-seq-R	GCGGCCTTGCAGCCCATCGC
ppu-K18-2247-USF	ggatccccgggtaccgagctACGAAGCGCCACCGCAGG
ppu-K18-2247- USR	gtacacctcgGCCTTTACCGCGCGGGAAAAC
ppu-K18-2247-DSF	cggtaaaggcCGAGGTGTACAAGGCGTTC
ppu-K18-2247- DSR	acagetatgacatgattacgGTGGTGACACTTCGTTGG
ppu-2247-seq-F	GCCTTCACCTTCCCTGGTCC
ppu-2247-seq-R	GCACACGATACCGACCACC
ppu-K18-2248-USF	acagctatgacatgattacgGTTTTTCTGGCTGGCGGCCCAGG
ppu-K18-2248-	ccaggctacaGGCGCTGACCAGCGCGCC
USR	
ppu-K18-2248-DSF	ggtcagcgccTGTAGCCTGGTGGGGTTC
ppu-K18-2248- DSR	caagettgcatgcctgcaggGTGGTTGAAGAAGCCATCAG
ppu-2248-seq-F	ATGCAAGAGCAGCTGAAGATCG

ppu-2248-seq-R	TTATGCCGCCACCGCCTTC
ppu-K18-leuA-USF	aggaaacagctatgacatgattacgGCCGCACGGTGTTCGTCG
ppu-K18-leuA-	ggcagctgccttCGGCTCTATCAGCGACTGGTTG
USR	ggtagtigttiledde Te TATEAGCGAC TGGT TG
ppu-K18-leuA-DSF	gctgatagagccgAAGGCAGCTGCCTACATCGAACTG
ppu-K18-leuA-	agtgccaagcttgcatgcctgcaggTTGAAGCTGCGGGCGCGC
DSR	
ppu-leuA-seq-F	GCGCCATCGAAAAATACTGCGC
ppu-leuA-seq-R	ATCGAAGCGTGCAGTGCCGAG
ppu-K18-ilvD-USF	aggaaacagctatgacatgattacgCCTGCATCGAAGGCGACG
ppu-K18-ilvD-USR	cgacacggcgttgATGGCCCGGTACGAACTG
ppu-K18-ilvD-DSF	gtaccgggccatCAACGCCGTGTCGAGCAG
ppu-K18-ilvD-DSR	agtgccaagettgcatgcctgcaggCTTGATTGCAGAGCTTGTGCG
ppu-ilvD-seq-F	ATCACCTGCCGGTTACTGCC
ppu-ilvD-seq-R	TTGATGGTTTCGAGTCTCCGTTTG
pau-MQ30-dauA- USF	caagettgeatgeetgeaggCTGCGATGCCGCCCGGCT
pau-MQ30-dauA- USR	taccgtagccGGAGCGGCCGGTGGAGTG
pau-MQ30-dauA- DSF	cggccgctccGGCTACGGTATCCAGACC
pau-MQ30-dauA- DSR	cagctatgaccatgattacgGTGCTTGTAGACCGTCGC
pau-dauA-seq-F	ATGATCGAAGCGGATTACCTCGTCATC
pau-dauA-seq-R	TCAGGGAGACAGGCGGCG
pau-MQ72-dauA-F	cccgtttttttgggctagcgATGATCGAAGCGGATTACCTCGTC
pau-MQ72-dauA-R	caagettgcatgcctgcaggTCAGGGAGACAGGCGGCG
ppu-MQ72-dbuA-F	cccgtttttttgggctagcgATGACCCCGACCTACGAC
ppu-MQ72-dbuA-R	caagettgcatgcctgcaggTCAGGGTTGCTGGAAACG
ppu-JM220-dbuA-F	aattcaactagtgctctgcaATGACCCCGACCTACGAC
ppu-JM220-dbuA-R	ttcgcgaggtaccgggcccaTCAGGGTTGCTGGAAACG
ppu-JM220-dbuC-F	aattcaactagtgctctgcaATGCAAGAGCAGCTGAAGATCG
ppu-JM220-dbuC-R	ttcgcgaggtaccgggcccaTTATGCCGCCACCGCCTT
ppu-JM220-	aatgaaattcaactagtgctctgcaATGACCCCGACCTACGAC
dbuAC-A-F	
ppu-JM220-	gctctttgcccggTCAGGGTTGCTGGAAACG
dbuAC-A-R	
ppu-JM220-	cagcaaccctgaCCGGGCAAAGAGCCCGTG
dbuAC-C-F	
ppu-JM220-	aggccttcgcgaggtaccgggcccaTTATGCCGCCACCGCCTTC
dbuAC-C-R	
ppu-TEV18-dbuA- F	nngetettentteATGACCCCGACCTACGAC

ppu-TEV18-dbuA-R	nngctcttcnttattaGGGTTGCTGGAAACGGGC
ppu-TEV18-dbuB-F	nngctcttcnttcATGAGCAATGACATTCAGCGTTTCCCC
ppu-TEV18-dbuB-R	nngctcttcnttattaGGCGTCGCCGACGAACGC

TABLE 4.S2: Carbon and nitrogen source utilization by wild-type and $\triangle dbuA$ *P. putida*.

	L-enantiomer		D-enantiomer					
	Ca	arbon	Nitrogen		Carbon		Nitrogen	
Amino acid	WT	$\Delta dbuA$	WT	$\Delta dbuA$	WT	$\Delta dbuA$	WT	$\Delta dbuA$
Ala	+	+	+	+	+	+	+	+
Arg	+	+	+	+	+	+	+	+
Asp	+	+	+	+	-	-	-	-
Asn	+	+	+	+	-	-	-	-
Cys	-	-	-	-	-	-	-	-
Glu	+	+	+	+	-	-	-	-
Gln	+	+	+	+	-	-	+	+
Gly	+	+	+	+	N/A	N/A	N/A	N/A
His	+	+	+	+	-	-	-	-
Ile	+	+	+	+	-	-	+	-
Phe	-	-	+	+	-	-	+	-
Pro	+	+	+	+	-	-	+	+
Leu	+	+	+	+	+	-	+	-
Lys	+	+	+	+	+	+	+	+
Met	-	-	-	-	-	-	-	-
Orn	+	+	+	+	+	+	+	+
Ser	+	+	+	+	+	+	+	+
Thr	-	-	+	+	-	-	-	-
Val	+	+	+	+	-	-	+	-
Trp	-	-	-	-	-	-	-	-
Tyr	-	-	-	-	-	-	-	-

Carbon sources (20 mM) were tested in liquid minimal medium with NH₄Cl (10 mM) as the nitrogen source. Nitrogen sources were tested by spotting amino acids (3 μ l of 100 mM stocks) on minimal glucose (11 mM) agar with no nitrogen source added, overlaid with *P. putida* strains suspended in soft agar. Growth indicated is after incubation at 30°C for 48 h.

TABLE 4.S3: Effects of DbuA and DbuC on BCAA auxotrophy.

TIMBLE IISC: EIIC	ets of Bourt and Bode on				
	Minimal glucose with:				
Genotype	No supplements	+L-Leu	+D-Leu		
Wild type	+	+	+		
$\Delta dbuA$	+	+	+		
$\Delta dbuC$	+	+	+		
ΔleuA	-	+	+		
ΔleuA ΔdbuA	-	+	-		
∆leuA ∆dbuC	-	+	-		
	Minimal glucose + pantothenate with:				
Genotype	No additional	+L-Ile & L-Val	+L-Ile & D-Val		
	supplements				
Wild type	+	+	+		
$\Delta dbuA$	+	+	+		
$\Delta dbuC$	+	+	+		
$\Delta i l v D$	-	+	+		
$\Delta ilvD \Delta dbuA$	-	+	-		
ΔilvD ΔdbuC	-	+	-		

Amino acids were spotted (3 µl of 100 mM stocks) on the indicated media, overlaid with the indicated *P. putida* strains suspended in soft agar. Growth indicated is after incubation at 30°C for 48 h.

Protein	DbuB	DbuA	
Approx. MW	13 kDa	40.5 kDa	
Purity	90%	99%	

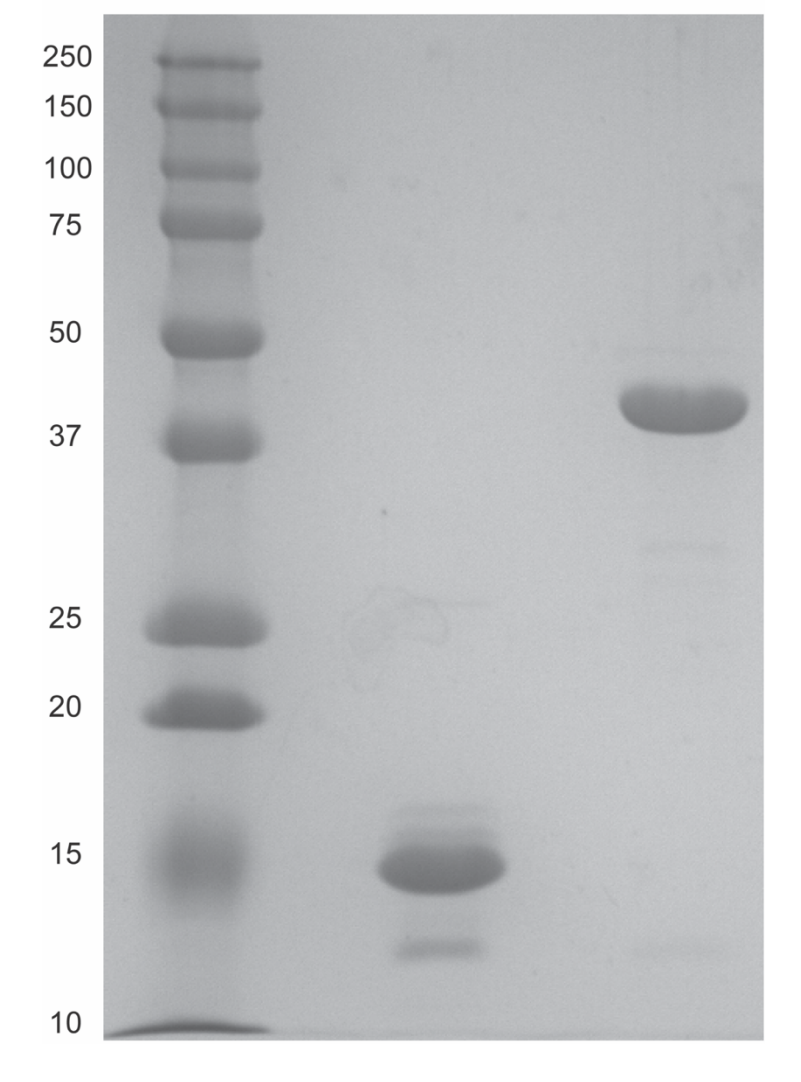


FIGURE 4.S1: Purified DbuB and DbuA. DbuA and DbuB were purified from *E. coli* BL21-AI carrying pTEV18 encoding each protein. Samples were boiled in buffer containing β -mercaptoethanol before 4 μg of protein were loaded onto a 12% polyacrylamide gel (BioRad Precision Plus Protein Dual Color Standards were loaded into the left-most lane) and were separated by electrophoresis. The gel was stained with Coomassie Blue and imaged using AnalytikJena UVP ChemStudio and purity was determined by densitometry using VisionWorks software version 8.22.18309.10577.

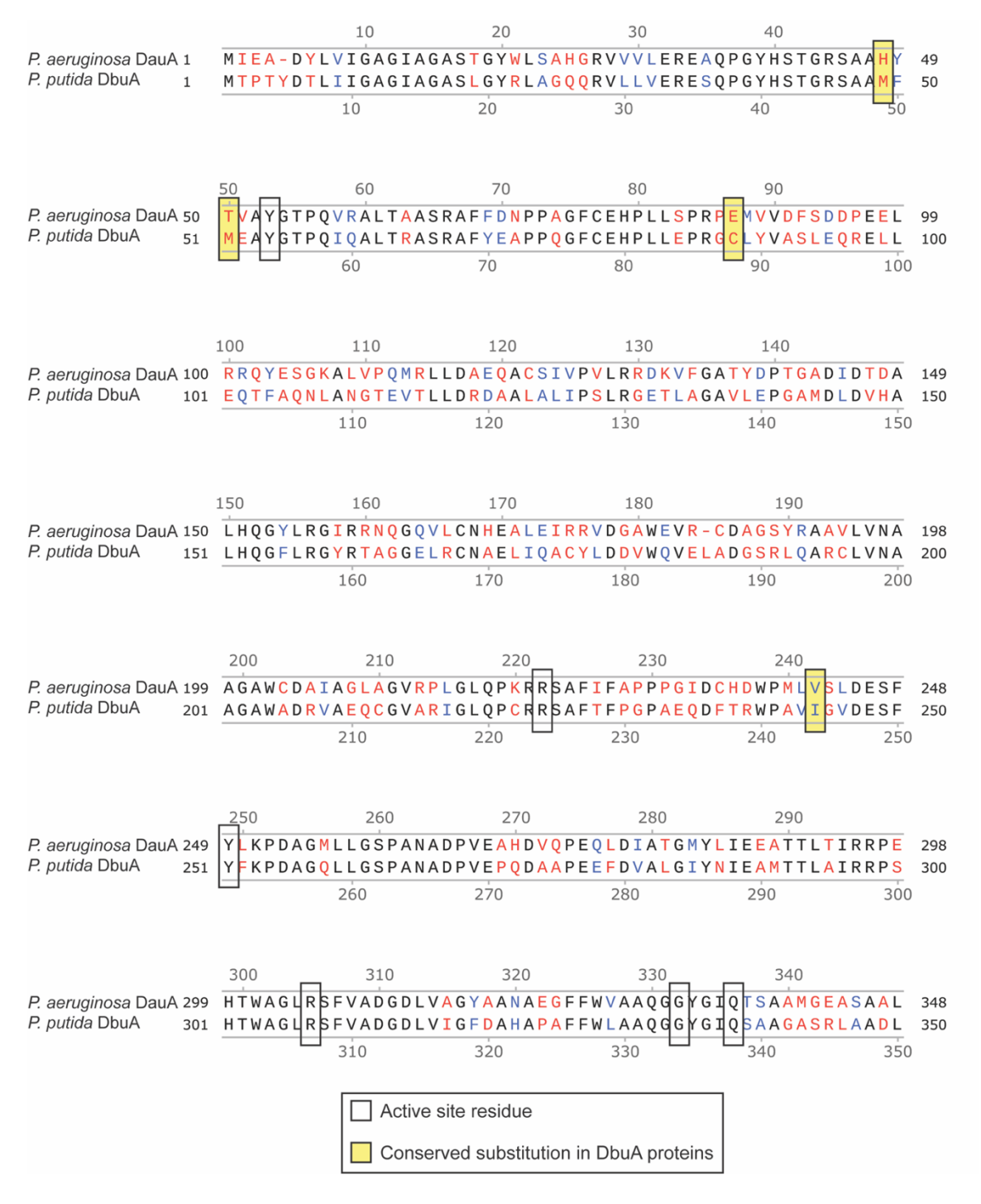


FIGURE 4.S2: Alignment of *P. aeruginosa* DauA and *P. putida* DbuA. Shown is a global alignment (Needleman-Wunsch) generated using SnapGene (version 6.2.1) with default settings. Black lettering indicates conservation of residues between the two proteins, blue lettering indicates similar side chain properties, and red lettering indicates a substitution with different side chain properties at the indicated residue. Conserved active site residues are shown (empty boxes) along with active site substitutions that are conserved in DbuA homologs analyzed in Figure 1B (yellow boxes).

CHAPTER 5

RIDA PROTIENS CONTRIBUTE TO FITNESS OF S. ENTERICA AND E. COLI BY REDUCING 2AA STRESS AND MODERATING FLUX TO ISOLEUCINE BIOSYNTHESIS 1

¹Fulton RL, Downs DM. 2024. *Microbial Cell*. 11:339-352.

Reprinted here with permission of the publisher.

5.1 ABSTRACT

Defining the physiological role of a gene product relies on interpreting phenotypes caused by the lack, or alteration, of the respective gene product. Mutations in critical genes often lead to easily recognized phenotypes that can include changes in cellular growth, metabolism, structure etc. However, mutations in many important genes may fail to generate an obvious defect unless additional perturbations are caused by medium or genetic background. The latter scenario is exemplified by RidA proteins. In vitro RidA proteins deaminate numerous imine/enamines, including those generated by serine/threonine dehydratase IIvA (EC:4.3.1.19) from serine or threonine – 2-aminoacrylate (2AA) and 2aminocrotonate (2AC), respectively. Despite this demonstrable biochemical activity, a lack of RidA has little to no effect on growth of E. coli or S. enterica without the application of additional metabolic perturbation. A cellular role of RidA is to prevent accumulation of 2AA which, if allowed to persist, can irreversibly damage pyridoxal 5'-phosphate (PLP)dependent enzymes, causing global metabolic stress. Because the phenotypes caused by a lack of RidA are dependent on the unique structure of each metabolic network, the link between RidA function and 2AA stress is difficult to demonstrate in some organisms. The current study used coculture experiments to exacerbate differences in growth caused by the lack of RidA in S. enterica and E. coli. Results described here solidify the established role of RidA in removing 2AA, while also presenting evidence for a role of RidA in enhancing flux towards isoleucine biosynthesis in E. coli. Overall, these data emphasize that metabolic networks can generate distinct responses to perturbation, even when the individual components are conserved.

5.2 INTRODUCTION

The robust metabolic network of a microbial cell requires the integration of individual components (i.e., enzymes and pathways) and multi-layered regulation of the resulting connections. In a general sense, the metabolic network is an amalgamation of interconnected biochemical pathways which are themselves composed of a diverse repertoire of enzymes. Cells modulate flux through these pathways by altering the expression or activity of appropriate enzymes which, in turn, dictate the rate and direction that relevant metabolites flow through the network. Precise control over cellular metabolism is allowed by the structural complexity of the system, emphasizing the notion that the individual parts have evolved to function within the context of the entire network. The precision allows microbial cells to survive in dynamic environments by restoring stability after a perturbation has been applied to the network.

Numerous components of metabolic networks in model bacteria are well characterized, although many enzymes and pathways remain poorly or only partially described. Historically, a first step in identifying the role of a gene is an analysis of phenotype(s) caused by the absence of the respective gene product. A detectable mutant phenotype demonstrates a physiological need for the gene and provides a tool to unravel the molecular function of the gene product. This approach loses its utility when a mutant has no detectable phenotype to guide functional studies. As a consequence, numerous genes remain uncharacterized, even in the best studied model systems. For example, the genome of *Escherichia coli* contains the coding capacity for over 4500 genes, an estimated 1200 of which have no associated phenotype or known function [1]. The characterization

of these genes requires innovative experimental design and/or integration of data from genetic, biochemical and global analyses.

Studies of the Rid family of proteins exemplify the difficulty in characterizing genes whose absence fails to cause a detectable phenotype in the laboratory. The Rid superfamily is divided into eight subfamilies [2], of which the RidA subfamily is the best characterized. In the past two decades, numerous experiments have probed the function of RidA across multiple model bacterial species. These studies identified RidA as an enamine/imine deaminase with at least two substrates of physiological significance, 2aminoacrylate (2AA) and 2-aminocrotonate (2AC). The phenotypes of a ridA mutant that led to its functional characterization required further metabolic perturbations [3-5], or additional mutations [6-8]. The serine/threonine dehydratase IIvA (EC:4.3.1.19) generates 2AA and 2AC via the dehydration of serine or threonine, respectively [3, 9]. Past studies, primarily in S. enterica, demonstrated that 2AA and 2AC accumulate in the absence of RidA. 2AA has been of particular interest due to its increased reactivity and toxicity compared to 2AC. 2AA has an unsubstituted pi bond between the α - and β -carbons, which is less stable than the disubstituted pi bond of 2AC (Figure 1B). This feature makes the βcarbon of 2AA less electronegative, which will favor tautomerization and allow subsequent nucleophilic attack by this molecule [10]. The reactivity of 2AA facilitates attack on the pyridoxal 5'-phosphate (PLP) in the active site of some enzymes. Stress caused by 2AA accumulation results from decreased activity of several PLP-dependent enzymes that can cause growth defects in a *ridA* mutant (Figure 1A).

Over time, the RidA/2AA paradigm was described, target enzymes and metabolic consequences were identified, and suppressor mutations were isolated that minimized the

impact of 2AA [11-18]. Features of this paradigm are present in several organisms, which led to the assumption that 2AA deaminase activity of RidA was the driver of its conservation and broad phylogenetic distribution [19, 20].

Recent observations have suggested that the deamination of 2AA may not be the sole cellular function of RidA. For instance, in some organisms (B. subtilis, E. coli) no evidence of naturally generated 2AA stress has been identified [21] (Buckner, unpublished). Further, RidA proteins deaminate diverse substrates in vitro, suggesting there may be additional physiologically relevant molecules acted on by RidA [20]. The latter possibility was prompted by the role of non-RidA members of the Rid family in deaminating imines that are not known to damage cellular components in a similar fashion as 2AA [22-24]. All reactions currently attributed to Rid proteins can also proceed nonenzymatically, if catalyzed by free water. However, in all described cases, the presence of a Rid protein increases the rate of product formation over that of the reaction catalyzed by water [2, 3, 19, 22-28]. In the case of RidA, the enhanced removal of 2AA ameliorates metabolic stress. An emerging pattern suggests that members of the Rid superfamily function to deaminate metabolic intermediates and increase flux through a particular metabolic pathway [2, 19, 22-24, 26]. For example, the Rid protein RutC is encoded in the pyrimidine utilization operon of E. coli and catalyzes the deamination of 3-aminoacrylate to malonate semialdehyde in a reaction previously designated as spontaneous [24, 29]. Additionally, members of the Rid2 subfamily in *Pseudomonas* species enhance flux through amino acid catabolic pathways, providing a competitive fitness advantage over strains lacking the Rid protein [22, 23].

The current study addressed the cellular role of RidA in *S. enterica* and *E. coli* in the context of a possible role in removing 2AC. 2AC is a physiologically relevant substrate of RidA at least in *S. enterica* and is not known to have toxic consequences [3, 8]. 2AC is an obligatory intermediate in the biosynthesis of isoleucine generated from threonine by IlvA. Results obtained from coculture experiments described herein confirm a role of RidA in preventing 2AA stress and suggest that RidA proteins may also have an organism-specific role in modulating biosynthetic flux to isoleucine.

5.3 RESULTS

S. enterica ridA mutants have a defect in competitive fitness. In minimal glucose medium, a ridA mutant has a slight, often immeasurable, growth defect in monoculture (Figure 2, Figure 3). Despite the lack of a significant growth phenotype, activity of branched chain aminotransferase (IIvE, EC:2.6.1.42) is decreased by ~40% in a ridA mutant in these conditions. This demonstrable biochemical defect indicates 2AA has accumulated [30-32]. Serine can be added to the medium to increase 2-aminoacrylate (2AA) stress. The presence of serine prevents growth of a ridA mutant in S. enterica by partially inactivating serine hydroxymethyltransferase (GlyA, EC:2.1.2.1) and, to a lesser extent, cysteine desulfurase (IscS, EC:2.8.1.7) [5, 13, 18]. In competition experiments, S. enterica ridA mutants and wild-type cells were co-inoculated into nutrient medium and minimal glucose medium. The competitive index (CI) for strains was calculated as the ratio of strains after growth in coculture normalized to the ratio present in the inoculum. The CI is a measure of competitive fitness that has typically been used to study the requirement for gene products when cells are grown in competition for a single limiting resource [22, 23].

In contrast, experiments herein were designed to define competition under conditions where no single resource was limiting. In other words, CI values presented here define differences in *general* fitness (i.e., growth rate) of a strain that may not be apparent in monoculture experiments. No difference in fitness was detected between wild type and a strain lacking RidA grown in nutrient medium. In contrast, the ridA mutant had a significant fitness defect when the two strains were cocultured in minimal glucose medium. In minimal medium, the ridA mutant had a competitive index of 0.037 (ln(CI) = -3.3), which reflects a ~27-fold decrease in fitness compared to wild type (Figure 2). The significant fitness difference between wild-type *S. enterica* and the ridA mutant amplified a growth difference that was minimal, or undetectable, in monoculture and underlined the sensitivity of this approach. Results from this competition assay aligned with the 2AA-dependent decrease in IIvE activity of a ridA mutant grown in minimal medium, validating that 2AA stress is present in *S. enterica* during grown in minimal medium [30, 31].

Isoleucine restores fitness of a *S. enterica ridA* **mutant in coculture.** Isoleucine in the growth medium restored full competitive fitness to the *ridA* mutant (Figure 3). This result was expected, as isoleucine is known to allosterically inhibit serine/threonine dehydratase IlvA and prevent the formation of 2AA [30, 31]. These data supported the idea that the fitness defect of a *ridA* mutant was due to accumulated 2AA.

A caveat to this simple interpretation is that RidA also deaminates the threoninederived enamine product of IlvA, 2-aminocrotonate (2AC). 2AC is an obligatory intermediate in the biosynthesis of isoleucine that is eliminated when isoleucine inhibits IlvA. Thus, it was possible that RidA improved fitness of *S. enterica* by increasing

biosynthetic flux to isoleucine. Distinguishing these two possibilities was complicated by the fact that isoleucine would eliminate the need for RidA in both scenarios. Coculture experiments to separate the possible contributions of RidA were based on the response of S. enterica to higher levels of 2AA stress generated when exogenous serine was added. The assumption was that the effect of 2AA stress generated by endogenous serine would be similar in consequence, if not magnitude, to that generated by addition of exogenous serine. Specifically, S. enterica ridA mutants grow well in the presence of 2AA stress if glycine and thiamine are provided. Together, these nutrients bypass the two key enzymes damaged by 2AA, GlyA and IscS and allow growth in the presence of 2AA stress [5, 13]. Notably, the presence of glycine and thiamine in the medium improved fitness of a ridA mutant in coculture with wild type, making them near equal (Figure 3). Importantly, a minor, but statistically significant difference in fitness remained. These data supported, but were not conclusive, that the competitive defect of a ridA mutant was caused by 2AAdependent damage to the target enzymes GlyA and IscS. The slight fitness defect that remained left the possibility that either i) decreased flux to 2-ketobutyrate (from 2AC) in the isoleucine biosynthetic pathway contributes to the fitness defect of a ridA mutant, or ii) 2AA-dependent damage to PLP-dependent target enzymes beyond GlyA and IscS contribute to the fitness defect of a *ridA* mutant in *S. enterica*.

RidA proteins are required for full fitness of *E. coli*. Past studies have identified multiple differences between the metabolic networks of *S. enterica* and *E. coli* [21, 33, 34]. *E. coli* encodes two RidA proteins, RidA and TdcF, which have been assessed for a role in 2AA stress [21]. The *ridA* gene is monocistronic, while *tdcF* is in the *tdc* operon that encodes

enzymes involved in a putative threonine catabolic pathway [35, 36] and are thought to be expressed only under anaerobic conditions [37, 38]. Evidence of 2AA stress was observed in *E. coli* only with significant manipulation of the genome and growth medium. Loss of TdcF and/or RidA had no observable effect on growth nor activity of known 2AA target enzymes, unless 2AA stress was artificially intensified by expression of a feedback-insensitive variant of IlvA (encoded by the *ilvA219* allele) in the presence of exogenous serine [21].

Unlike *S. enterica*, the absence of RidA proteins in *E. coli* (RidA and TdcF) had no effect on the growth, or competitive fitness of strains grown in minimal medium. In medium supplemented with 5 mM serine, the *ridA tdcF* double mutant strain had a small, but statistically significant, difference in growth rate (Figure 4) reminiscent of *S. enterica ridA* mutants grown in minimal glucose medium. Despite the minimal growth difference in monoculture, the *ridA tdcF* mutant was notably less fit than wild type in minimal medium supplemented with serine (Figure 4). Unlike the situation in *S. enterica*, there was no significant defect in IIvE activity of the *E. coli tdcB ridA* mutant when grown under these conditions that produced a clear fitness defect (5 mM serine) (Table 2).

Additional competition experiments showed that RidA was the homolog critical for full fitness of *E. coli* grown in minimal medium with 5 mM exogenous serine (Figure 5). There was no difference between the fitness of the *ridA tdcF* double mutant and a *ridA* mutant. In contrast, the *ridA tdcF* double mutant was less fit than a *tdcF* mutant when grown in coculture. Isoleucine restored full fitness to the *E. coli* strains, eliminating the effect of the *ridA* mutation as found in *S. enterica*. These data were consistent with a scenario that 2AA stress negatively impacted fitness of *E. coli*.

2AA stress is induced in *E. coli* with increased serine concentration. The above results could be explained in a scenario where 5 mM serine generated enough 2AA to compromise fitness, but not enough to cause detectable damage to target enzyme IlvE. If this were the case, increased concentrations of serine might increase 2AA production to a level that could generate a growth defect in monoculture. Consistently, both the ridA and ridA tdcF mutants had a growth defect with 20 mM serine, while the growth of wild type was not affected (Figure 6). The serine-induced growth defects of the ridA and ridA tdcF mutants were eliminated with the addition of isoleucine or glycine, consistent with the pattern in S. enterica with 2AA-dependent growth defects. As expected, based on the growth defects in monoculture, E. coli ridA and ridA tdcF mutants were outcompeted by wild type in minimal medium containing 20 mM serine, and the ridA tdcF mutant having a more severe defect than the *ridA* single mutant (Figure 8). The addition of isoleucine restored full fitness to each stain in the presence of 20 mM serine. The observation that TdcF had an impact on fitness in the presence of elevated serine concentration was not entirely unexpected. E. coli strains with synthetically increased 2AA levels exhibited a growth defect only when both TdcF and RidA were absent, consistent with their redundant activities [21]. In total, the results with E. coli suggested that either i) 2AA levels are generally lower in E. coli than S. enterica when strains lack RidA proteins, and/or ii) 2AA is less detrimental to the metabolic network of E. coli than it is to that of S. enterica. Neither of these directly addressed the disconnect between the lack of detectable 2AA damage (i.e., IlvE activity) and competitive fitness defect of an E. coli ridA mutant in minimal medium with 5 mM serine.

RidA has a role beyond 2AA stress control in E. coli. The data gathered for ridA mutants of E. coli appeared consistent with a model in which, i) the fitness defect on 5 mM serine is due to 2AA stress, despite the stress being too low to impair IlvE activity, ii) high levels of exogenous serine (20 mM) generate enough 2AA to cause a growth defect, and iii) glycine and isoleucine restore growth via the mechanism(s) characterized in S. enterica ridA mutants. Based on this scenario, glycine was expected to suppress the competitive fitness defect of the ridA tdcF mutant. Unexpectedly, glycine failed to improve fitness and the ridA tdcF mutant remained less fit than wild type in medium with serine (5 mM) and glycine (Figure 7). Furthermore, the addition of glycine did not restore competitive fitness defects of ridA or ridA tdcF mutants in the presence of 20 mM serine, despite its ability to restore growth in monoculture (Figure 8). A possible explanation for these results is that, in E. coli RidA has a role in optimizing flux through isoleucine biosynthesis. In this scenario, isoleucine contributes to restoring fitness by satisfying a need for isoleucine created by sluggish *de novo* synthesis, in addition to its role in decreasing 2AA generation. The finding that glycine eliminates the 2AA-generated growth defect in monoculture, while failing to restore the fitness defect of the ridA tdcF mutant, supports the conclusion that decreased fitness of E. coli on minimal medium with serine is not solely due to 2AA stress.

The kinetics of ECIIvA model 2AA and 2AC production. The above data suggested that fitness defects of E. coli ridA and ridA tdcF mutants in coculture were not solely due to 2AA-mediated damage to PLP-dependent enzymes. The deaminase activities of other

members of the Rid protein family improve flux through their respective pathway(s) and, thus, increase fitness. Based on this precedent, it was possible that fitness defects of E. coli mutant strains in coculture reflected an impaired flux to isoleucine in the absence of RidA. If this were the case, flux would be impaired only when exogenous serine was present. In principle, impaired flux could be due to i) a decreased rate 2AC formation by IlvA, or ii) a lowered rate of deamination of 2AC to 2KB in the absence of RidA. Only the former was amenable to an effect by serine, since competition between serine and threonine for IlvA could alter the ratio of 2AC:2AA. In S. enterica, kinetic modeling indicated that the rate of 2AC production from threonine is not affected by the rate of serine converted to 2AA by IlvA in vivo [39]. To determine if the same was true in E. coli, the catalytic parameters (K_M and k_{cat}) of _{EC}IIvA were determined with serine and threonine as substrates (Figure S2). The catalytic parameters of ECIIvA differed slightly from those of SEIIvA, but modeling of endogenous 2AC and 2AA production in E. coli predicted that 2AC production was not impacted by the rate of 2AA production (Table 3). Furthermore, the ratios of 2AC:2AA predicted by the model were consistent between the two organisms. In total, these data show that while 2AC generation is not likely significantly different, the amount of 2AA increases relative to that of 2AC in E. coli strains grown with serine. In total the data are consistent with a scenario in which 2AA stress is not the sole cause of fitness defects in strains lacking RidA homologs. Fitness defects may be exacerbated by impaired flux through isoleucine biosynthesis that is the result of lower rate of 2AC deamination in the absence of RidA activity.

5.4 DISCUSSION

In *S. enterica*, *ridA* is one of many genes that do not generate an observable, or easily quantifiable, phenotype unless perturbations are applied to the system. In this study, we used cocultures to exacerbate minor growth defects and generate a quantifiable fitness phenotype for *ridA* mutants. Unlike canonical competition analyses that define fitness in terms competing for a single limiting resource, coculture experiments in this study defined fitness of a mutant compared to wild type for overall growth (requiring synthesis of all cellular components) in a defined minimal medium. This approach provided a sensitive assay for the detrimental effects of 2AA that were not detected during growth in monoculture.

In *S. enterica*, the requirement for RidA is revealed by adding serine to the growth medium. The presence of serine increases IlvA-mediated formation of the reactive enamine, 2AA. In the absence of added serine, 2AA stress in a *ridA* mutant is evidenced by decreased IlvE activity. Data herein allow the conclusion that 2AA stress decreases fitness of a *S. enterica ridA* mutant in minimal medium, despite the full growth of the mutants in monoculture. The restoration of fitness by isoleucine or glycine and thiamine supported this conclusion but did not eliminate the possibility of additional metabolic complexity.

Results with *E. coli* suggested a more nuanced situation than the 2AA stress paradigm defined with *S. enterica*. First, *E. coli* strains lacking RidA proteins had a significant fitness defect under conditions (i.e., minimal medium with 5 mM serine) where there was no quantifiable evidence of 2AA stress – i.e., lowered IlvE activity. Secondly, while the fitness defect was eliminated by the presence of isoleucine, glycine had little

effect, further distinguishing the behavior of *E. coli* from *S. enterica*. Importantly, glycine restored growth of the *ridA tdcF* mutants of *E. coli* when 2AA levels were increased with elevated (20 mM) serine. Thus, if the competitive defect of the *ridA tdcF* mutant was caused by 2AA stress alone, glycine might be expected to restore fitness in coculture, which it did not. In total, the data suggest that the role of RidA proteins, at least in *E. coli*, extends beyond preventing accumulation of 2AA. Specifically, results were consistent with a scenario in which RidA has an important role in increasing flux through *de novo* synthesis of isoleucine.

The experiments with E. coli suggested an expanded role for RidA, while raising additional questions about the structure of the metabolic network. Results of competition experiments suggested that RidA was needed to optimize flux to isoleucine in the presence of serine, but not in minimal medium. The kinetic parameters of EcIlvA, much like that of sellvA [39], suggest 5 mM serine increases the amount of 2AA without affecting the amount of 2AC generated in the cell. Therefore, the need for RidA to contribute to biosynthetic flux only in the presence of serine appears to be due to the ratio of 2AA/2AC, rather than the rate of 2AC production, though the precise mechanism of this remains unclear. The lack of a quantifiable phenotype indicates the increase in 2AA mediated by 5 mM serine does not cause detectable damage to target enzymes in E. coli. In contrast, a lower ratio of 2AC:2AA could amplify the need for RidA to facilitate2-ketobutyrate formation at a rate sufficient to generate isoleucine efficiently. This efficiency would only be important when in coculture with a strain fully proficient at isoleucine synthesis. Consider that 2AC has three fates in the E. coli cell, two of which lead to isoleucine, and one contributes to the synthesis of thiamine via TrpD forming phosphoribosylamine (PRA)

from 2AC and phosphoribosylpyrophosphate (PRPP) [8] (Figure 9). The metabolic node encompassing 2AC and PRA is structured differently in *S. enterica* and *E. coli*, consistent with a difference in the role of RidA in the two organisms [6, 9, 33, 40].

Significantly, a previous study increased the accumulation of 2AA in *E. coli* by utilizing both serine and a variant of IlvA that was insensitive to allosteric inhibition by isoleucine [21]. Under these conditions, 2AA stress that compromised growth in *E. coli* in monoculture was generated, and glycine failed to restore growth. The scenario proposed here, suggests both isoleucine and glycine might be required to restore growth. Regardless, IlvA is expected to be critical in generating appropriate ratios of reactive intermediates (i.e., 2AA and 2AC) which, in turn, can influence flux through numerous metabolic pathways. Because of this connection, eliminating allosteric regulation of IlvA has consequences beyond the specific accumulation of 2AA.

This study, like others that have dissected metabolic integration, emphasizes the significance of metabolic network structure in defining the response of each organism to perturbation. The response of an organism to metabolic network perturbations must be defined on a case-by-case basis. This realization highlights that metabolism is a complex system that has been finely tuned by evolution, rather than a network assembled fortuitously from components that evolved for individual efficacy. Specific to this work, *E. coli* experiences less 2AA accumulation and/or the metabolic network is more resistant to the resulting damage, while the synthesis of isoleucine in this organism can be a limiting factor under some growth conditions. In contrast, *S. enterica* is sensitive to 2AA accumulation, yet the biosynthesis of isoleucine appears to be sufficient for fitness even in the absence of RidA. These results reflect differential responses of two metabolic networks

to perturbation, in spite of the similarity of individual components. Defining the consequences of perturbation in multiple systems (i.e., organisms) will continue to expand our knowledge of the breadth of strategies that are germane when modeling metabolism.

5.5 MATERIALS AND METHODS

Strains, media, and chemicals. Strains used in this study are derivatives of *Salmonella enterica* serovar Typhimurium LT2 or *Escherichia coli* K-12. All strains were grown at 37°C unless otherwise stated. *S. enterica* strains were routinely grown in Nutrient Broth (NB; Difco; 8 g/liter, 5 g/liter NaCl). *E. coli* strains were grown in Lysogeny Broth (LB; 10 g/liter tryptone, 5 g/liter NaCl, 5 g/liter yeast extract) as a rich medium. No-carbon E (NCE) medium with 11 mM glucose, supplemented with 0.1 mM MgSO₄ and trace elements was used as a minimal medium [41]. Other supplements were added as noted to the following concentrations: L-isoleucine (1 mM), L-glycine (1 mM), thiamine (100 nM), L-aspartate (1 mM), and L-serine (5 mM). Antibiotics were used as indicated: kanamycin (Km; 50 μg/ml for rich media or 12.5 μg/ml for minimal media) and chloramphenicol (Cm; 20 μg/ml for rich media or 5 μg/ml for minimal media). Chemicals were purchased from MilliporeSigma (St. Louis, MO).

Growth analyses. Cultures were started from a single colony and grown overnight in rich medium with shaking at 37°C (2 ml). Cells were pelleted and resuspended in an equal volume of sterile saline. Cell suspensions (5 μl) were used to inoculate the indicated medium (195 μl). Growth was monitored in a 96-well plate as the change in optical density at 650 nm (OD₆₅₀) over time using a BioTek ELx808 plate reader (BioTek Instruments,

Winooski, VT) with a slow shaking speed (210 rpm). Data were plotted using Graphpad Prism version 8.4. Growth experiments were performed with three independent biological replicates unless otherwise stated.

Competition assays. Competition assays were performed generally as described [22, 42, 43]. Briefly, overnight cultures of each strain were grown in rich medium (2 ml) at 37°C with shaking. Cells were pelleted and resuspended in 2 ml sterile saline and optical densities at 650 nm (OD₆₅₀) were normalized to 0.1. Five ml of the indicated medium was inoculated with 50 µl of cell suspension from each of the two competing strains. Control experiments were performed for each condition in which strains of the same relevant genotype, with different antibiotic resistance cassettes, were competed against each other. These controls accounted for differences in competitive fitness caused by the different antibiotic resistance cassettes in each strain. Colony forming units (CFUs) of cocultures were determined by spreading serial dilutions at T=0 (i.e., before incubation of the cocultures) onto media to differentiate between each respective strain. For S. enterica, media were as follows: (i) minimal medium supplemented with L-serine, selective for wild type (DM9404); (ii) minimal medium supplemented with chloramphenicol, selective for a chloramphenicol-resistant ridA mutant (DM17845), and (iii) minimal medium supplemented with kanamycin, selective for a kanamycin-resistant *ridA* mutant (DM3480).

For *E. coli*, media were as follows: (i) LB supplemented with chloramphenicol, selective for chloramphenicol-resistant *ridA* and *ridA tdcF* mutants (DM14820, DM14682), and (ii) LB supplemented with kanamycin, selective for kanamycin-resistant *ridA* and *tdcF* mutants (DM14597, DM14669). Some *E. coli* strains (DM14520,

DM15051) did not contain antibiotic resistance cassettes and could not be isolated from cocultures by spreading onto selective media. CFUs of these strains were determined by counting CFUs on LB media and subtracting the CFUs of the competing strain, which could be selected for with antibiotics. Cocultures were grown to stationary phase at 37°C with shaking. CFUs were enumerated for cultures after co-incubation as described above. The competitive index (CI) was defined and calculated as follows:

$$CI = \frac{(\frac{CFU \ mutant}{CFU \ wild \ type})_{initial}}{(\frac{CFU \ mutant}{CFU \ wild \ type})_{final}}.$$

Each competition assay was performed at least three times with similar results. GraphPad Prism version 8.4 was used for data plotting and statistical analysis.

Protein purification. *E. coli* K12 *ilvA* was cloned into BspQI sites of pTEV18 as described previously. The resulting plasmid, pTEV18-*ilvA* (K12), was electroporated into BL21-AI. The resulting strain (DM18490) was grown overnight in 40 ml of Terrific Broth (TB; 12 g/liter tryptone, 24 g/liter yeast extract, 0.4% glycerol (v/v)) supplemented with 150 μg/ml ampicillin. Fifteen ml of the overnight culture was used to inoculate each of two 2.8-liter baffle-bottomed Fernbach flasks containing 1.5 liters of TB with 150 μg/ml ampicillin. The resulting cultures were grown at 30°C with shaking at 135 rpm to an OD₆₅₀ of 0.5 before the addition of arabinose (0.2% (w/v)) and IPTG (200 μM). Cultures were then grown at 23°C with shaking at 135 rpm for 18 h before being harvested by centrifugation at 6000 x g for 20 min. Cell pellets were resuspended in 2 ml/g cells of lysis buffer (50 mM potassium phosphate, 150 mM NaCl, 100 μM PLP, 2 mg/ml lysozyme, 0.2 mg/ml DNase, pH 7.5) and incubated on ice for 45 min. Cells were mechanically lysed using a Constant Systems

OneShot Cell Disruptor at 20 kpsi. The lysate was then clarified by centrifugation at 45000 x *g* for 30 min before being filtered using a 0.45 µm syringe-driven filter. Filtered lysate was then loaded onto a 5 ml HisTrap HP column (GE Healthcare). The column was washed with 3 column volumes (CV) of 100% Binding Buffer (50 mM potassium phosphate, 150 mM NaCl, 20 mM imidazole, pH 7.5), followed by 3 CV of 96% Binding Buffer and 4% Elution Buffer (50 mM potassium phosphate, 150 mM NaCl, 500 mM imidazole, pH 7.5). IlvA was eluted with a linear gradient from 4-100% Elution Buffer over the course of 10 CV. A flow rate of 2 ml/min was used to each step in protein purification. Fractions containing eluted protein were assessed for purity before being concentrated using an Amicon Ultra-15 centrifugal filter (MilliporeSigma) with a molecular weight cutoff of 30 kDa. Buffer exchange of the protein into Storage Buffer (50 mM potassium phosphate, 150 mM NaCl, 10% glycerol (v/v) pH 7.5) was performed using a PD-10 column (Cytiva). Protein concentration was determined using the Peirce BCA Protein Assay Kit (Thermo Scientific). Purified IlvA was drop frozen in liquid nitrogen and stored at -80°C until use.

Enzyme assays. All enzyme assays were performed at room temperature.

Transaminase B assay-cell extract.

Cultures were grown overnight in LB (2 ml) at 37°C with shaking, and cells were pelleted and resuspended in an equal volume of sterile saline. Cell suspensions (125 µl) were used to inoculate 5 ml of the relevant medium and the resulting cultures were grown to stationary phase. Cells were then pelleted, resuspended in 10 ml of NCE medium before being pelleted and frozen at -80°C until use. Cell pellets were thawed and resuspended in 1 ml of 50 mM potassium phosphate (pH 7.5) and lysed mechanically with a Constant Systems

Limited One Shot (United Kingdom) at 20 kpsi. Cell lysate was clarified by centrifugation at 17000 x g for 20 min at 4°C.

Transaminase B activity was assayed as described previously [44]. Briefly, cell free extract (50 μl) was added to a reaction mixture containing α-ketoglutarate (10 mM) in potassium phosphate buffer (50 mM, pH 7.5). The reaction was initiated with the addition of L-isoleucine (to 20 mM) and incubated at 37C for 20 minutes. Resulting 2ketomethylvalerate (2KMV) was derivatized by 2,4-dinitrophenylhydrazine (DNPH, 200 μl) to yield a hydrazone, which was treated with 0.5 N HCl. The resulting organic layer was removed and mixed with 1.5 N NaOH to allow formation of an aqueous layer containing a chromophore with an absorbance at 540 nm. The aqueous layer was extracted, and absorbance was measured using a SpectraMax M2 microplate reader (Molecular Devices). 2KMV concentration was quantified by comparing to a standard curve, which was generated by monitoring the absorbance of reaction mixtures with known 2KMV concentrations that were subjected to the same incubation and extraction steps as described above for the cell free extracts. The protein concentration of each lysate was determined using the bicinchoninic acid (BCA) assay (Pierce). Activity is reported as nanomoles of 2KMV per milligram of protein per cell lysate. Data plotting and statistical analyses were conducted using GraphPad Prism version 8.4.

Serine/Threonine Dehydratase assay -purified protein.

The rates of 2-ketobutyrate and pyruvate formation were determined by measuring the absorbance at 230 nm [39, 3, 47] every 10 s for 2 min. Reactions were carried out in a quartz 96-well plate and measurements were acquired using a SpectraMax Plus

spectrophotometer (Molecular Devices). Reaction mixtures (100 μ l) contained 50 mM potassium phosphate buffer (pH 7.5), 200 nM of purified IIvA. Reactions were initiated with the addition of the indicated concentrations of L-threonine or L-serine. The absorbance at 230 nm of known concentrations of either 2-ketobutyrate or pyruvate were used to generate a standard curve to convert the change in absorbance (ΔA_{230} /min) to the rate of product formation (μ mol product/min) for each reaction. Data visualization and statistical analyses were performed using GraphPad Prism version 8.4.

The rates of 2AA and 2AC synthesis were modeled using the equation below [39]. V_{prod} refers to the rate of product formation (2AA or 2AC) in μ M/s, $k_{cat(Sub)}$ refers to the catalytic constant for E_{cc} IIvA using the relevant substrate (s⁻¹), [E_t] is the active site concentration of IIvA in *E. coli*, [Sub] is the concentration of substrate for E_{cc} IIvA *in vivo* in μ M, [Comp Sub] is the concentration of competing substrate in μ M, E_{cc} IIvA is the Michaelis-Menten constant for E_{cc} IIvA using the relevant substrate in μ M, and E_{cc} IIvA using the relevant competing substrate in μ M. When modeling the rate of 2AC formation, "Sub" refers to L-threonine and "Comp Sub" refers to L-serine. When modeling the rate of 2AA formation, "Sub" refers to L-serine and "Comp Sub" refers to L-threonine. 10 μ M was used as the value for active site concentrations for E_{cc} IIvA *in vivo* [48] and physiological concentrations of L-serine (68 μ M) and L-threonine (180 μ M) in *E. coli* [49], as well as elevated concentrations of L-serine (5000 μ M and 20000 μ M) were used when calculating the product formation by E_{cc} IIvA

$$Vprod = \frac{\left(k_{cat(Sub)} \times [E_t]\right)[Sub]}{K_{M(Sub)}\left(1 + \frac{[Comp\ Sub]}{K_{M\ (Comp\ Sub)}}\right) + [Sub]}$$

5.6 REFERENCES

- 1. Ghatak S, King ZA, Sastry A, Palsson BO (2019). The y-ome defines the 35% of *Escherichia coli* genes that lack experimental evidence of function. Nucleic Acids Res 47(5): 2446-2454. doi: 10.1093/nar/gkz030.
- 2. Niehaus TD, Gerdes S, Hodge-Hanson K, Zhukov A, Cooper AJ, ElBadawi-Sidhu M, Fiehn O, Downs DM, Hanson AD (2015). Genomic and experimental evidence for multiple metabolic functions in the RidA/YjgF/YER057c/UK114 (Rid) protein family. BMC Genomics 16(382. doi: 10.1186/s12864-015-1584-3.
- 3. Lambrecht JA, Flynn JM, Downs DM (2012). Conserved YjgF protein family deaminates reactive enamine/imine intermediates of pyridoxal 5'-phosphate (PLP)-dependent enzyme reactions. J Biol Chem 287(5): 3454-3461. doi: 10.1074/jbc.M111.304477.
- 4. Ernst DC, Lambrecht JA, Schomer RA, Downs DM (2014). Endogenous Synthesis of 2-Aminoacrylate Contributes to Cysteine Sensitivity in *Salmonella enterica*. Journal of Bacteriology 196(18): 3335-3342. doi: 10.1128/jb.01960-14.
- 5. Ernst DC, Downs DM (2016). 2-Aminoacrylate Stress Induces a Context-Dependent Glycine Requirement in *ridA* Strains of *Salmonella enterica*. J Bacteriol 198(3): 536-543. doi: 10.1128/JB.00804-15.
- 6. Browne BA, Ramos AI, Downs DM (2006). PurF-independent phosphoribosyl amine formation in *yjgF* mutants of *Salmonella enterica* utilizes the tryptophan biosynthetic enzyme complex anthranilate synthase-phosphoribosyltransferase. J Bacteriol 188(19): 6786-6792. doi: 10.1128/JB.00745-06.
- 7. Lambrecht JA, Browne BA, Downs DM (2010). Members of the YjgF/YER057c/UK114 family of proteins inhibit phosphoribosylamine synthesis *in vitro*. J Biol Chem 285(45): 34401-34407. doi: 10.1074/jbc.M110.160515.
- 8. Bazurto JV, Farley KR, Downs DM (2016). An Unexpected Route to an Essential Cofactor: *Escherichia coli* Relies on Threonine for Thiamine Biosynthesis. mBio 7(1): e01840-01815. doi: 10.1128/mBio.01840-15.

- 9. Lambrecht JA, Downs DM (2013). Anthranilate phosphoribosyl transferase (TrpD) generates phosphoribosylamine for thiamine synthesis from enamines and phosphoribosyl pyrophosphate. ACS Chem Biol 8(1): 242-248. doi: 10.1021/cb300364k.
- 10. Li Y, Zhang L, Luo S (2022). Bond Energies of Enamines. ACS Omega 7(7): 6354-6374. doi: 10.1021/acsomega.1c06945.
- 11. Christopherson MR, Lambrecht JA, Downs D, Downs DM (2012). Suppressor analyses identify threonine as a modulator of *ridA* mutant phenotypes in *Salmonella enterica*. PLoS One 7(8): e43082. doi: 10.1371/journal.pone.0043082.
- 12. Ernst DC, Anderson ME, Downs DM (2016). L-2,3-diaminopropionate generates diverse metabolic stresses in *Salmonella enterica*. Mol Microbiol 101(2): 210-223. doi: 10.1111/mmi.13384.
- 13. Fulton RL, Irons J, Downs DM (2022). The Cysteine Desulfurase IscS Is a Significant Target of 2-Aminoacrylate Damage in *Pseudomonas aeruginosa*. mBio 13(3): e0107122. doi: 10.1128/mbio.01071-22.
- 14. Borchert AJ, Walejko JM, Guennec AL, Ernst DC, Edison AS, Downs DM (2019). Integrated Metabolomics and Transcriptomics Suggest the Global Metabolic Response to 2-Aminoacrylate Stress in *Salmonella enterica*. Metabolites 10(1). doi: 10.3390/metabo10010012.
- 15. Ernst DC, Borchert AJ, Downs DM (2018). Perturbation of the metabolic network in *Salmonella enterica* reveals cross-talk between coenzyme A and thiamine pathways. Plos one 13(5): e0197703. doi. 10.1371/journal.pone.0197703.
- 16. Whitaker GH, Ernst DC, Downs DM (2021). Absence of MMF1 disrupts heme biosynthesis by targeting Hem1pin *Saccharomyces cerevisiae*. Yeast 38(12): 615-624. doi: 10.1002/yea.3670.
- 17. Borchert AJ, Downs DM (2017). Endogenously generated 2-aminoacrylate inhibits motility in *Salmonella enterica*. Sci Rep 7(1): 12971. doi: 10.1038/s41598-017-13030-x.

- 18. Flynn JM, Christopherson MR, Downs DM (2013). Decreased coenzyme A levels in *ridA* mutant strains of *Salmonella enterica* result from inactivated serine hydroxymethyltransferase. Mol Microbiol 89(4): 751-759. doi: 10.1111/mmi.12313.
- 19. Irons JL, Hodge-Hanson K, Downs DM (2020). RidA Proteins Protect against Metabolic Damage by Reactive Intermediates. Microbiol Mol Biol Rev 84(3). doi: 10.1128/mmbr.00024-20.
- 20. Fulton RL, Downs DM (2023). Modulators of a robust and efficient metabolism: Perspective and insights from the Rid superfamily of proteins. Adv Microb Physiol 83(117-179. doi: 10.1016/bs.ampbs.2023.04.001.
- 21. Borchert AJ, Downs DM (2017). The Response to 2-Aminoacrylate Differs in *Escherichia coli* and *Salmonella enterica*, despite Shared Metabolic Components. J Bacteriol 199(14). doi: 10.1128/JB.00140-17.
- 22. Fulton RL, Downs DM (2022). DadY (PA5303) is required for fitness of *Pseudomonas aeruginosa* when growth is dependent on alanine catabolism. Microb Cell 9(12): 190-201. doi: 10.15698/mic2022.12.788.
- 23. Fulton RL, Downs DM (2024). Functional characterization of the *dbu* locus for D-branched-chain amino acid catabolism in *Pseudomonas putida*. Appl Environ Microbiol 90(2): e0196223. doi: 10.1128/aem.01962-23.
- 24. Buckner BA, Lato AM, Campagna SR, Downs DM (2021). The Rid family member RutC of *Escherichia coli* is a 3-aminoacrylate deaminase. J Biol Chem: 100651. doi: 10.1016/j.jbc.2021.100651.
- 25. Digiovanni S, Visentin C, Degani G, Barbiroli A, Chiara M, Regazzoni L, Di Pisa F, Borchert AJ, Downs DM, Ricagno S, Vanoni MA, Popolo L (2020). Two novel fish paralogs provide insights into the Rid family of imine deaminases active in preempting enamine/imine metabolic damage. Sci Rep 10(1): 10135. doi: 10.1038/s41598-020-66663-w.
- 26. Hodge-Hanson KM, Downs DM (2017). Members of the Rid protein family have broad imine deaminase activity and can accelerate the *Pseudomonas aeruginosa* D-

- arginine dehydrogenase (DauA) reaction *in vitro*. PLoS One 12(9): e0185544. doi: 10.1371/journal.pone.0185544.
- 27. Irons J, Hodge-Hanson KM, Downs DM (2018). PA5339, a RidA Homolog, Is Required for Full Growth in *Pseudomonas aeruginosa*. J Bacteriol 200(22). doi: 10.1128/jb.00434-18.
- 28. Irons J, Sacher JC, Szymanski CM, Downs DM (2019). Cj1388 Is a RidA Homolog and Is Required for Flagella Biosynthesis and/or Function in *Campylobacter jejuni*. Front Microbiol 10(2058. doi: 10.3389/fmicb.2019.02058.
- 29. Kim KS, Pelton JG, Inwood WB, Andersen U, Kustu S, Wemmer DE (2010). The Rut pathway for pyrimidine degradation: novel chemistry and toxicity problems. J Bacteriol 192(16): 4089-4102. doi: JB.00201-10 [pii] 10.1128/JB.00201-10.
- 30. Schmitz G, Downs DM (2004). Reduced Transaminase B (IlvE) Activity Caused by the Lack of *yjgF* Is Dependent on the Status of Threonine Deaminase (IlvA) in *Salmonella enterica* Serovar Typhimurium. Journal of Bacteriology 186(3): 803-810. doi: 10.1128/jb.186.3.803-810.2004.
- 31. Lambrecht JA, Schmitz GE, Downs DM (2013). RidA proteins prevent metabolic damage inflicted by PLP-dependent dehydratases in all domains of life. MBio 4(1): e00033-00013. doi: 10.1128/mBio.00033-13.
- 32. Shen W, Borchert AJ, Downs DM (2022). 2-Aminoacrylate stress damages diverse PLP-dependent enzymes *in vivo*. J Biol Chem 298(6): 101970. doi: 10.1016/j.jbc.2022.101970.
- 33. Bazurto JV, Downs DM (2016). Metabolic network structure and function in bacteria goes beyond conserved enzyme components. Microb Cell 3(6): 260-262. doi: 10.15698/mic2016.06.509.
- 34. Meysman P, Sanchez-Rodriguez A, Fu Q, Marchal K, Engelen K (2013). Expression divergence between *Escherichia coli* and *Salmonella enterica* serovar Typhimurium reflects their lifestyles. Mol Biol Evol 30(6): 1302-1314. doi: 10.1093/molbey/mst029.

- 35. Datta P, Goss TJ, Omnaas JR, Patil RV (1987). Covalent structure of biodegradative threonine dehydratase of *Escherichia coli*: homology with other dehydratases. Proc Natl Acad Sci U S A 84(2): 393-397. doi: 10.1073/pnas.84.2.393.
- 36. Sumantran VN, Schweizer HP, Datta P (1990). A novel membrane-associated threonine permease encoded by the *tdcC* gene of *Escherichia coli*. J Bacteriol 172(8): 4288-4294. doi: 10.1128/jb.172.8.4288-4294.1990.
- 37. Hesslinger C, Fairhurst SA, Sawers G (1998). Novel keto acid formate-lyase and propionate kinase enzymes are components of an anaerobic pathway in *Escherichia coli* that degrades L-threonine to propionate. Mol Microbiol 27(2): 477-492. doi. 10.1046/j.1365-2958.1998.00696.x.
- 38. Chattopadhyay S, Wu Y, Datta P (1997). Involvement of Fnr and ArcA in anaerobic expression of the *tdc* operon of *Escherichia coli*. J Bacteriol 179(15): 4868-4873. doi: 10.1128/jb.179.15.4868-4873.1997.
- 39. Borchert AJ, Downs DM (2018). Analyses of variants of the Ser/Thr dehydratase IlvA provide insight into 2-aminoacrylate metabolism in *Salmonella enterica*. J Biol Chem 293(50): 19240-19249. doi: 10.1074/jbc.RA118.005626.
- 40. Ramos I, Downs DM (2003). Anthranilate synthase can generate sufficient phosphoribosyl amine for thiamine synthesis in *Salmonella enterica*. Journal of Bacteriology 185(17): 5125-5132. doi. 10.1128/JB.185.17.5125-5132.2003.
- 41. Davis R, Botstein D, Roth J (1980). Advanced bacterial genetics. Cold Spring Harbor Laboratory. New York. doi. 10.1002/JOBM.19810211013.
- 42. Boulette ML, Baynham PJ, Jorth PA, Kukavica-Ibrulj I, Longoria A, Barrera K, Levesque RC, Whiteley M (2009). Characterization of alanine catabolism in *Pseudomonas aeruginosa* and its importance for proliferation *in vivo*. J Bacteriol 191(20): 6329-6334. doi: 10.1128/jb.00817-09.
- 43. Speare L, Septer AN (2019). Coincubation Assay for Quantifying Competitive Interactions between *Vibrio fischeri* Isolates. J Vis Exp 149). doi: 10.3791/59759.

- 44. Duggan DE, Wechsler JA (1973). An assay for transaminase B enzyme activity in *Escherichia coli* K-12. Anal Biochem 51(1): 67-79. doi. 10.1016/0003-2697(73)90453-3.
- 45. Castilho BA, Olfson P, Casadaban MJ (1984). Plasmid insertion mutagenesis and *lac* gene fusion with mini-mu bacteriophage transposons. J Bacteriol 158(2): 488-495. doi. 10.1128/jb.158.2.488-495.1984.
- 46. Datsenko KA, Wanner BL (2000). One-step inactivation of chromosomal genes in *Escherichia coli* K-12 using PCR products. Proc Natl Acad Sci USA 97(12): 6640-6645. doi. 10.1073/pnas.120163297.
- 47. Davis L (1965). A spectrophotometric method for the assay of threonine dehydratase. Anal Biochem 12(1): 36-40. doi: 0003-2697(65)90139-9 [pii].
- 48. Albe KR, Butler MH, Wright BE (1990). Cellular concentrations of enzymes and their substrates. J Theor Biol 143(2): 163-195. doi: 10.1016/s0022-5193(05)80266-8.
- 49. Bennett BD, Kimball EH, Gao M, Osterhout R, Van Dien SJ, Rabinowitz JD (2009). Absolute metabolite concentrations and implied enzyme active site occupancy in *Escherichia coli*. Nat Chem Biol 5(8): 593-599. doi: 10.1038/nchembio.186.

TABLE 5.1: Strains used in this study.

Strain	Genotype	Source	
S. enterica			
DM3480	<i>ridA3</i> ::MudJ ^a	Laboratory collection	
DM4748	<i>ilvA595</i> ::Tn10	Laboratory collection	
DM6143	<i>ridA3</i> ::MudJ <i>ilvA595</i> ::Tn10	Laboratory collection	
DM9404	Wild type	Laboratory collection	
DM17845	ridA4::Cm ^b	This study	
E. coli			
DM14520	<i>E. coli</i> K-12 MG1655 wild type (F ⁻ λ ⁻ rph -	Laboratory collection	
DM14597	ridA790::Km ^b	Laboratory collection	
DM14669	tdcF12::Km ^b	Laboratory collection	
DM14670	tdcF13::Cm ^b	Laboratory collection	
DM14682	ΔridA890 tdcF13::Cm ^b	Laboratory collection	
DM14820	ridA12::Cm ^b	Laboratory collection	
DM15051	ΔridA890 ΔtdcF14	Laboratory collection	
DM18490	E. coli BL21-AI/pTEV18-ilvA (K12)	This study	

^aMudJ refers to the MudJ1734 transposon [45].

^bDenotes that gene knockouts were generated with the method described by Datsenko and Wanner [46].

TABLE 5.2: 2AA stress is not detectable in *E. coli* strains lacking RidA proteins.

		Branched Chain Aminotransferase Activity*		
Strain	Relevant	Minimal	Minimal + Ser	Minimal + Ser &
	Genotype			Ile
DM14520	Wild type	130 ± 16	132 ± 4	234 ± 6
DM14597	ridA	140 ± 20	110 ± 4	234 ± 23
DM14669	tdcF	163 ± 15	163 ± 5	255 ± 22
DM14682	ridA tdcF	131 ± 9	134 ± 7	220 ± 14

^{*}Activity of Branched Chain Aminotransferase (IlvE) is reported as nmol 2KMV/mg protein.

E. coli strains were grown in minimal glucose medium with the addition of serine (5 mM) with or without isoleucine (1 mM) as indicated. The activity of IlvE was measured as described in Experimental Procedures. Data shown are the mean and standard error of two biological replicates assayed in three technical replicates. There was no significant difference in IlvE activity between wild-type and mutant strains grown in the same medium, or between growth in minimal with and without serine addition. IlvE activity was significantly higher when grown in the presence of serine and isoleucine than the same strain in the other media tested.

TABLE 5.3: Modeled rates of product formation by EcIlvA.

[Serine] (µM)	[Threonine] (µM)	2AA formation (μM/s)	2AC formation
			$(\mu M/s)$
68	180	6	84
5000	180	398	81
20000	180	1410	83

Modeled rates of endogenous product formation by $_{EC}$ IlvA using varied concentrations of serine and threonine. Data were calculated with an IlvA active site concentration of $10 \, \mu M$, along with relevant k_{cat} and K_M values for each substrate (Figure S2) using the formula described in the Materials and Methods section.

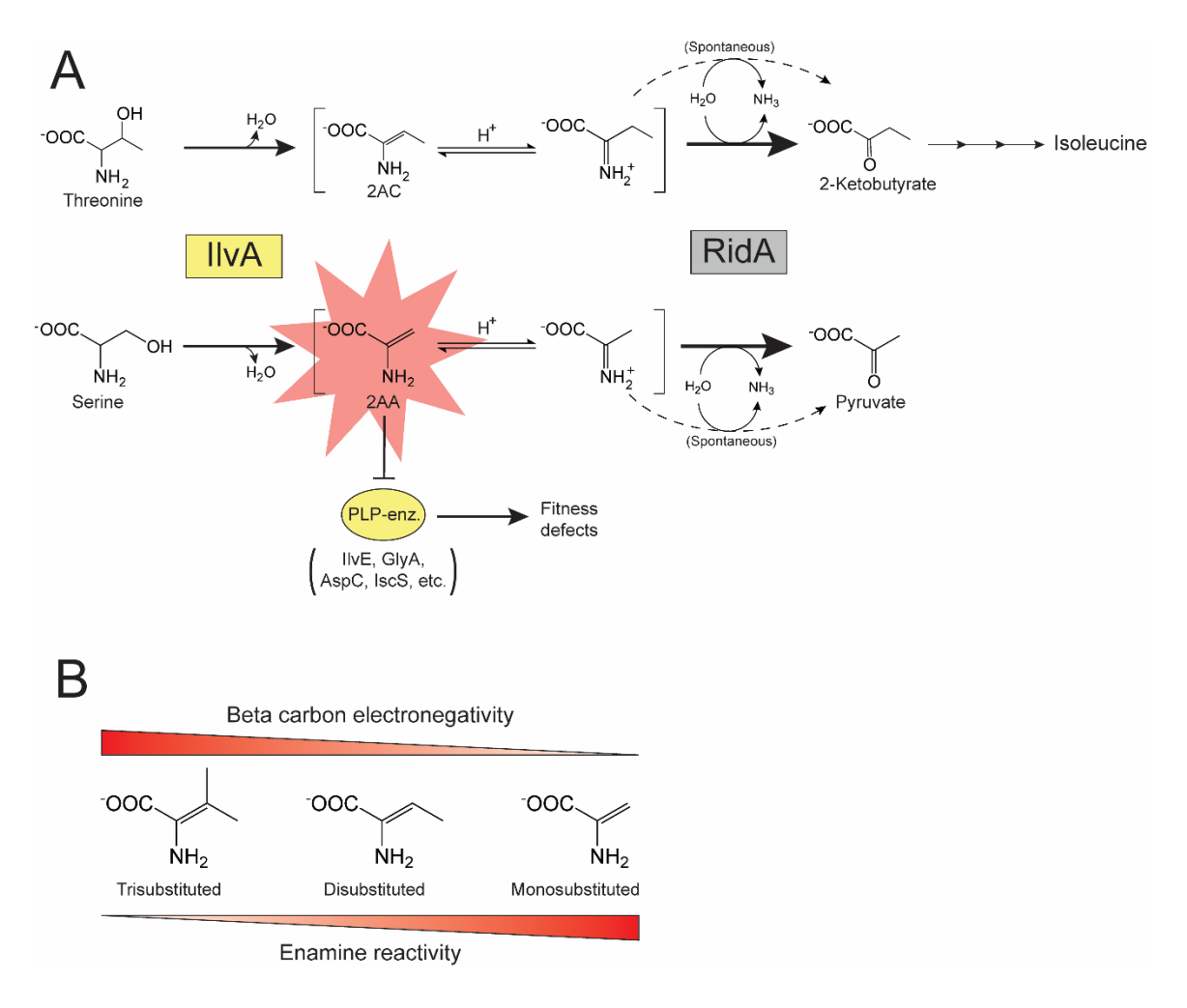


FIGURE 5.1: RidA paradigm and the effect of pi bond substitution on enamine reactivity. A) RidA paradigm. IIvA (Serine/threonine dehydratase; EC:4.3.1.19) (yellow box) uses either threonine or serine as a substrate to generate 2AC or 2AA (red star), respectively. Enamine intermediates are spontaneously deaminated by water (dashed arrows) or by RidA (2-iminobutanoate/2-iminopropionate deaminase; EC:3.5.99.10) (grey box, bold arrows). 2AC is a disubstituted and benign enamine and has not been shown to damage cellular components in the absence of RidA. 2AA is a less substituted, more reactive enamine that can damage PLP-dependent enzymes (yellow oval), causing fitness defects if it persists in the cell. B) Substitution of the pi bond between the α- and β-carbons increases stability of amino acid-derived enamines via increased electronegativity of the β-carbon.

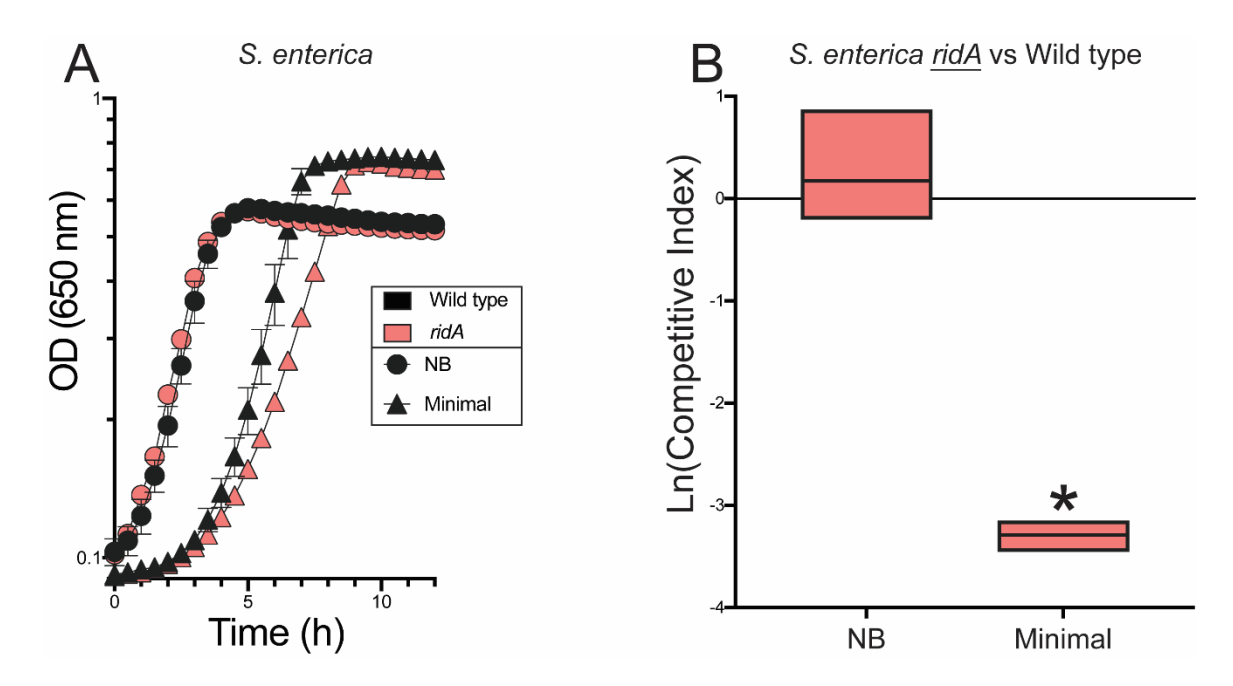


FIGURE 5.2: S. enterica ridA mutants have a fitness defect in minimal medium. A) Growth of S. enterica wild type (black) and a ridA mutant (red) in nutrient broth (NB, circles) and minimal glucose (11 mM) medium (triangles). B) Competitive fitness of a S. enterica ridA mutant (ridA3::MudJ) grown in competition with wild type S. enterica in nutrient or minimal medium. The underlined genotype indicates the strain for which the competitive indices are shown in the corresponding graph. An asterisk (*) indicates a significant difference ($p \le 0.05$ as determined by Sidak's multiple comparisons test) in CI values compared to control experiments in which the ridA mutant was grown in competition with a second ridA mutant (ridA4::Cm) in the relevant medium. control experiments in which the ridA mutant was grown in competition with a second ridA mutant (ridA4::Cm). Data shown are the mean and standard deviation of three independent biological replicates.

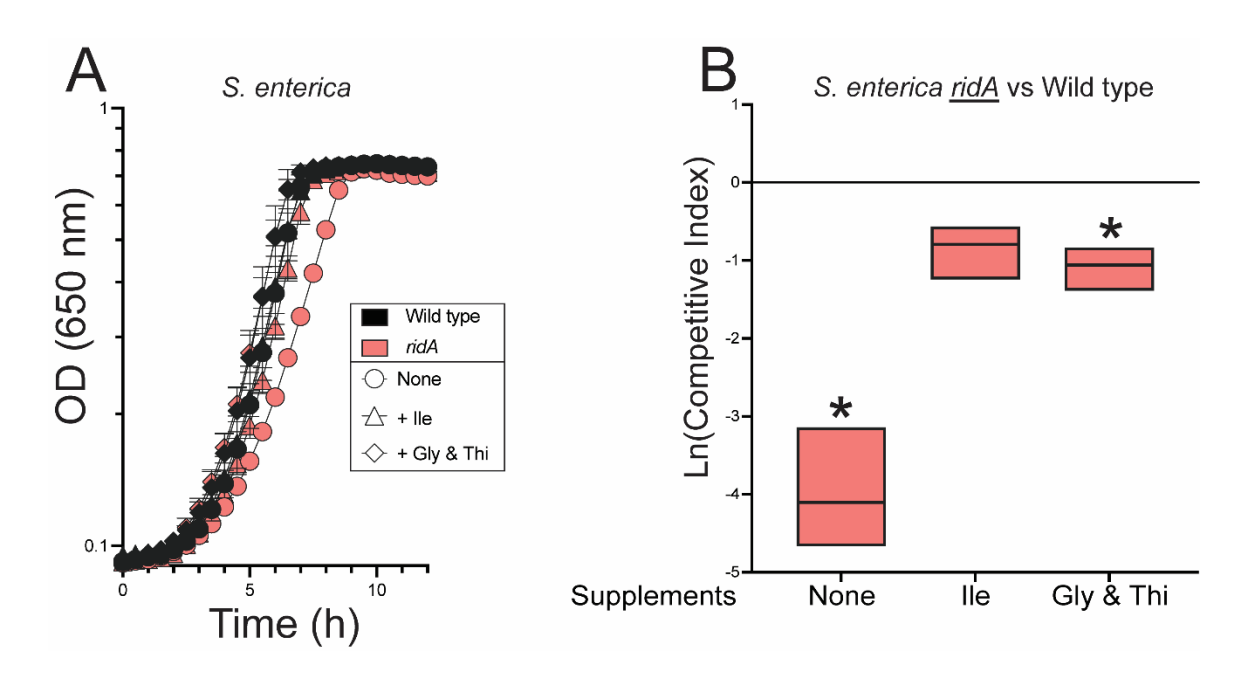


FIGURE 5.3: Glycine and thiamine alleviate fitness defects of S. enterica ridA mutants. A) Growth of S. enterica wild type (black) and a ridA mutant (red) in minimal glucose (11 mM) medium supplement with nothing (circles), 1 mM L-isoleucine (triangles) or 1 mM glycine and 100 nM thiamine (diamonds). B) Competitive fitness of a S. enterica ridA mutant (ridA3::MudJ) grown in competition with wild type S. enterica in minimal glucose medium with indicated supplements. An asterisk (*) indicates a significant difference (p \leq 0.05 as determined by Sidak's multiple comparisons test) in CI values compared to control experiments in which the ridA mutant was grown in competition with a second ridA mutant (ridA4::Cm) in the indicated medium. Data shown are the mean and standard deviation of three independent biological replicates.

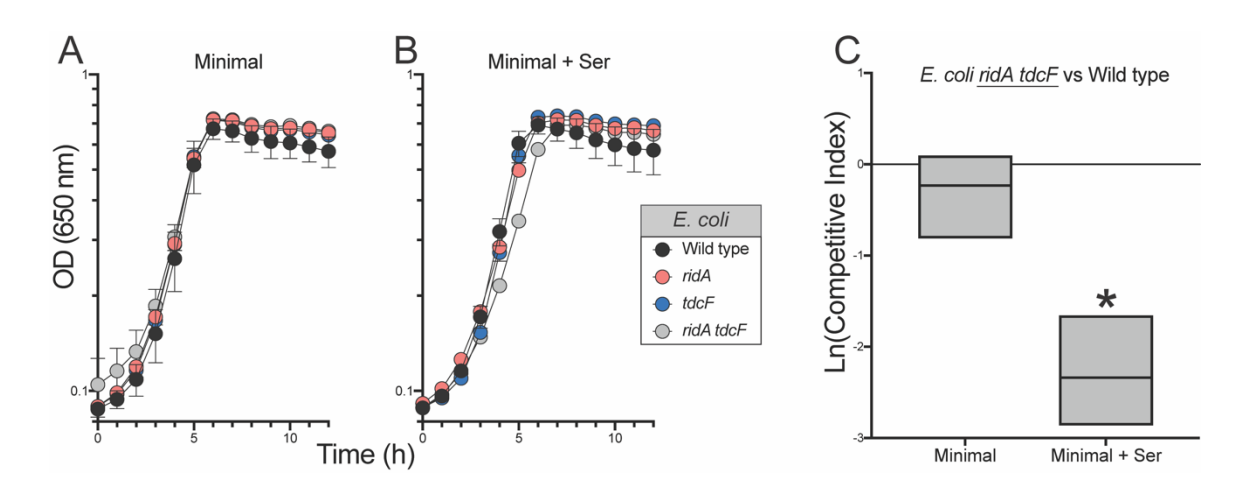


FIGURE 5.4: RidA proteins are required for full fitness of *E. coli*. (A and B) Shown are growth profiles of wild-type *E. coli* (black), a *ridA* mutant (red, *ridA790::Km*), *tdcF* mutant (blue, *tdcF12::Km*) and a *ridA tdcF* double mutant (grey, $\Delta ridA890 \ tdcF13::Cm$). Strains were grown in (A) minimal glucose (11 mM) medium with no supplementation or (B) supplemented with 5 mM L-serine. (C) Shown is competitive fitness of an *E. coli ridA tdcF* double mutant ($\Delta ridA890 \ tdcF13::Cm$) grown in coculture with wild-type *E. coli* in minimal glucose (11 mM) medium with or without L-serine (5 mM). Data shown are mean and standard deviation of three independent biological replicates. The underlined genotype indicates the strain for which the competitive indices are shown in the corresponding graph. An asterisk (*) indicates a significant difference (p \leq 0.05 as determined by Sidak's multiple comparisons test) in CI values compared to control experiments in which $\Delta ridA890 \ tdcF13::Cm$ was competed with an different strain lacking *ridA* and *tdcF* ($\Delta ridA890 \ \Delta tdcF14$) in the indicated medium.

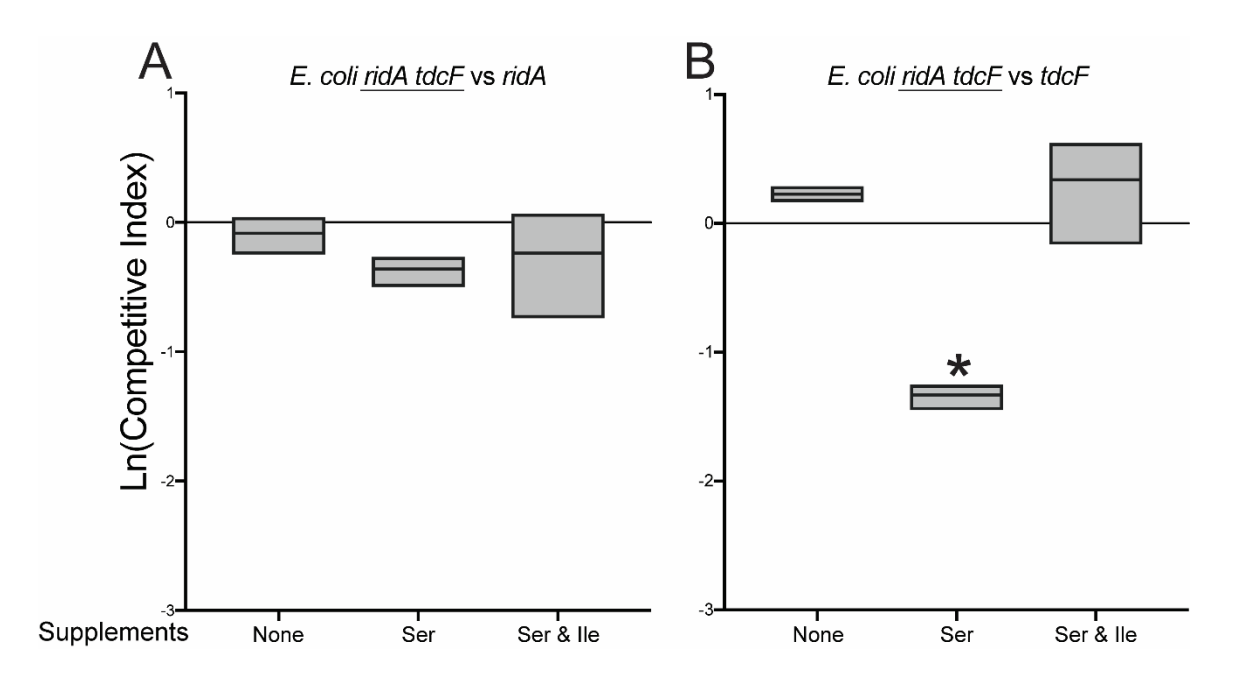


FIGURE 5.5: RidA contributes to the competitive fitness of *E. coli*. Shown are competitive fitness values for an *E. coli ridA tdcF* double mutant ($\Delta ridA890 \ tdcF13::Cm$) grown in coculture with (A) an *E. coli ridA* mutant (ridA790::Km) or (B) a tdcF mutant (tdcF12::Km) in minimal glucose (11 mM) medium with the indicated supplements. L-serine was provided at a final concentration of 5 mM and L-isoleucine each provided at 1 mM. Data shown are mean and standard deviation of three independent biological replicates. The underlined genotype indicates the strain for which the competitive indices are shown in the corresponding graph. An asterisk (*) indicates a significant difference (p ≤ 0.05 as determined by Sidak's multiple comparisons test) in CI values compared to control experiments in which $\Delta ridA890 \ tdcF13::Cm$ was competed with an isogenic strain also lacking ridA and tdcF ($\Delta ridA890 \ \Delta tdcF14$) under each condition.

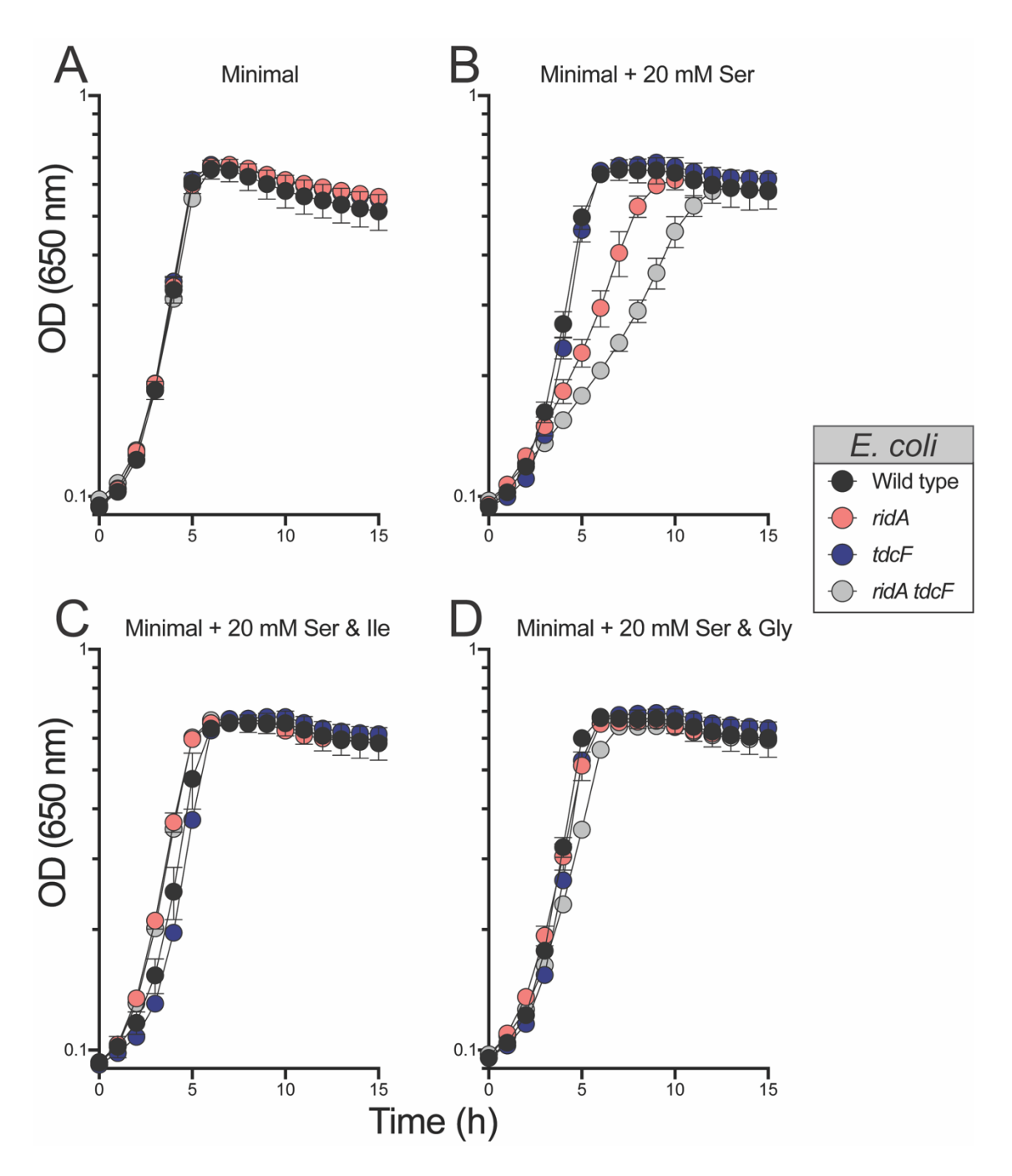


FIGURE 5.6: *ridA* and *ridA tdcF* strains are sensitive to elevated concentrations of serine. Shown are growth profiles of wild-type *E. coli* (black), a *ridA* mutant (red, *ridA790::kan*), *tdcF* mutant (blue, *tdcF12::kan*) and a *ridA tdcF* double mutant (grey, Δ*ridA890 tdcF13::cat*). Strains were grown in minimal glucose (11 mM) medium supplemented with (A) no supplementation, (B) supplemented with L-serine, (C) supplemented with L-serine and L-isoleucine, or (D) supplemented with L-serine and glycine. L-serine was provided at a final concentration of 20 mM, L-isoleucine and glycine were each provided at a final concentration of 1 mM where indicated. Data shown are the mean and standard deviation of three independent biological replicates.

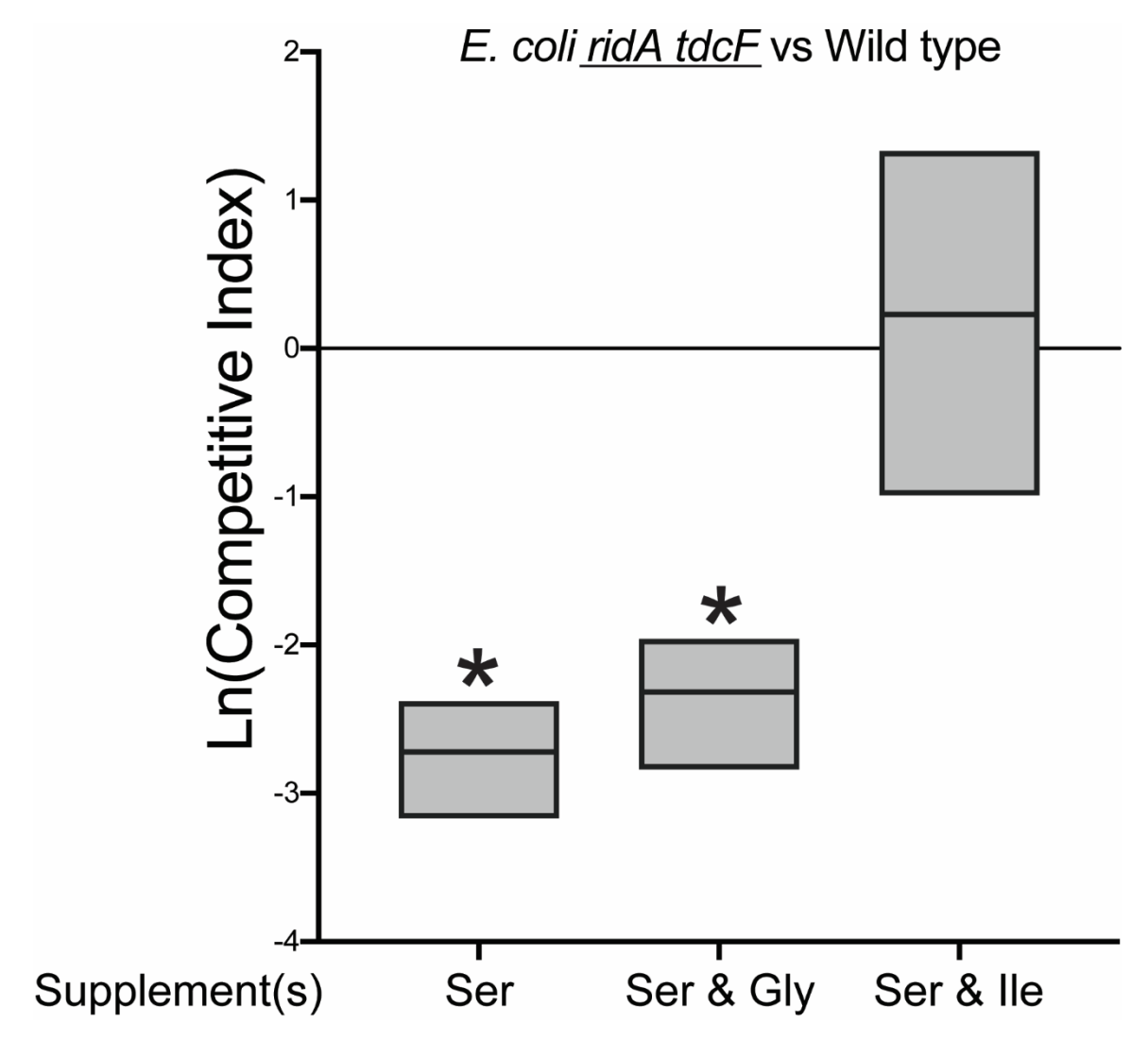


FIGURE 5.7: Glycine does not restore competitive fitness to *E. coli ridA tdcF* double mutants under 2AA stress. Shown is competitive fitness of an *E. coli ridA tdcF* double mutant ($\Delta ridA890 \ tdcF13::Cm$) grown in coculture with wild-type *E. coli* in minimal glucose (11 mM) medium with the indicated supplements – L-serine (5 mM), glycine (1 mM), L-isoleucine (1 mM). Data shown are mean and standard deviation of three independent biological replicates. The underlined genotype indicates the strain for which the competitive indices are shown in the corresponding graph. An asterisk (*) indicates a significant difference (p \leq 0.05 as determined by Sidak's multiple comparisons test) in CI values compared to control experiments in which $\Delta ridA890 \ tdcF13::Cm$ was competed with an isogenic strain lacking ridA and tdcF ($\Delta ridA890 \ \Delta tdcF14$) in each medium.

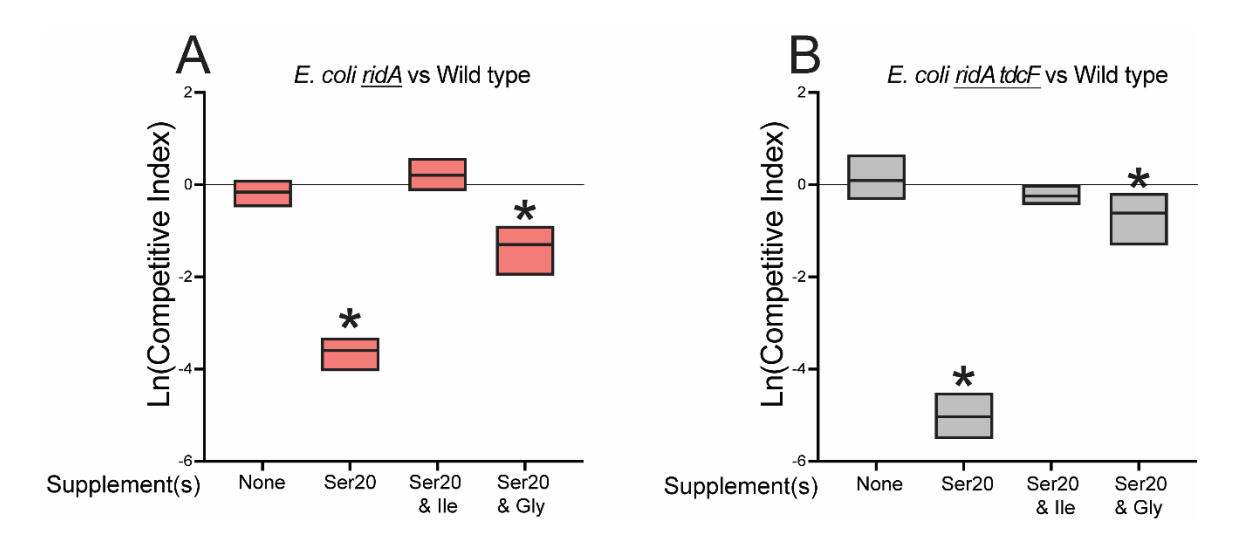


FIGURE 5.8: Glycine does not restore competitive fitness to *ridA* or *ridA* tdcF mutants in the presence of elevated serine concentrations. Shown are competitive indices of (A) an *E. coli ridA* mutant (ridA790:kan) and (B) a ridA tdcF double mutant ($\Delta ridA890$ tdcF13::Cm) grown in coculture with wild-type *E. coli* in minimal glucose (11 mM) medium with the indicated supplements – L-serine (20 mM), glycine (1 mM), L-isoleucine (1 mM). Data shown are mean and standard deviation of three independent biological replicates. The underlined genotype indicates the strain for which the competitive indices are shown in the corresponding graph. An asterisk (*) indicates a significant difference (p ≤ 0.05 as determined by Sidak's multiple comparisons test) in CI values compared to control experiments in which each strain was competed with an isogenic strain lacking the relevant RidA homolog(s) in each medium.

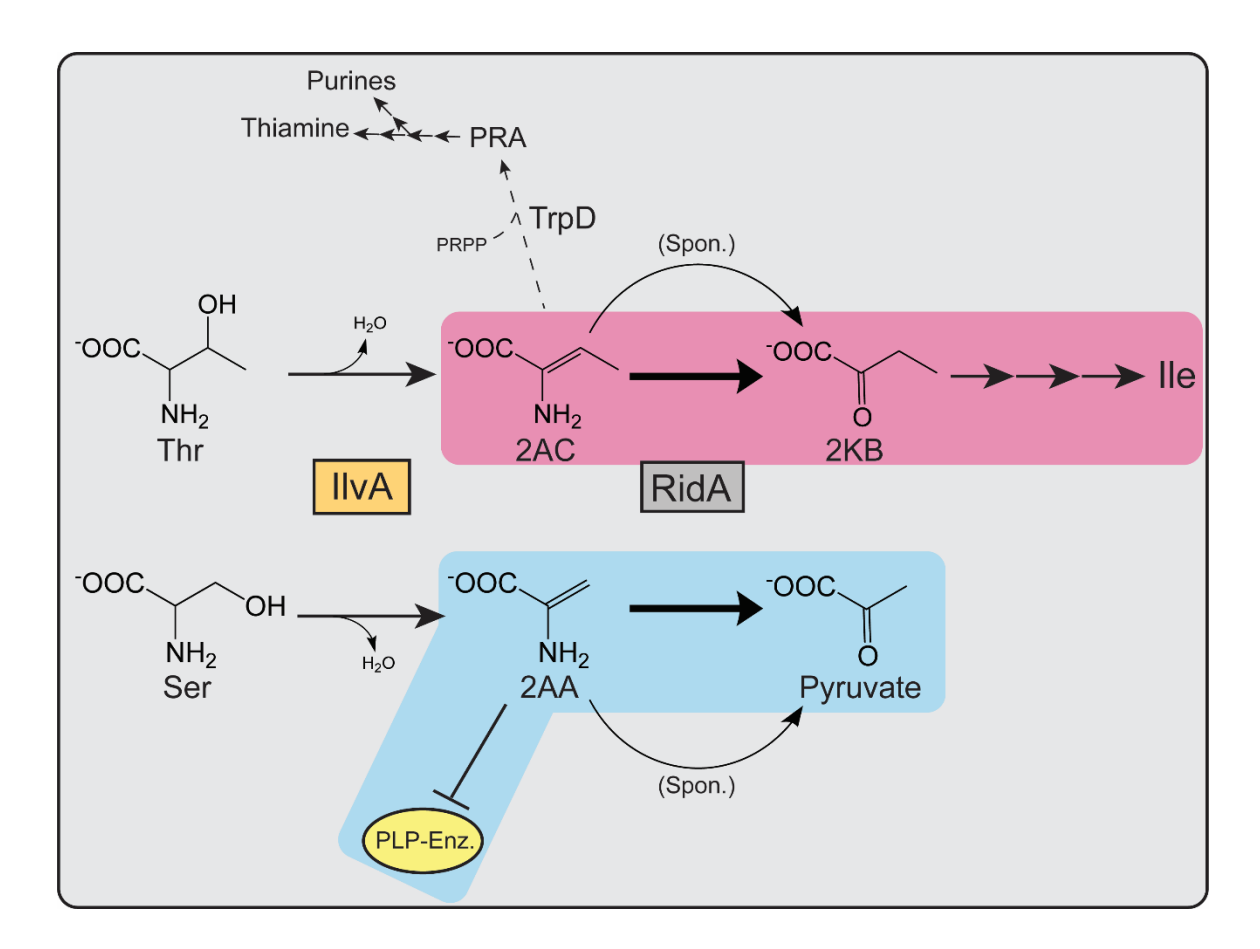


FIGURE 5.9: RidA proteins contribute to fitness in *S. enterica* and *E. coli* by moderating flux through different metabolic nodes. Shown are the pathways relevant to RidA activity in *S. enterica* and *E. coli*. IlvA (orange box) dehydrates serine or threonine, generating 2AA or 2AC, respectively. 2AA and 2AC are spontaneously deaminated by water (curved arrows) or, more rapidly, by RidA proteins (grey box, bold arrows) to the corresponding ketoacid product – pyruvate or 2KB. 2KB serves as a substrate for Ile synthesis. 2AA can irreversibly damage PLP-dependent enzymes (yellow oval) in the absence of RidA. Metabolic nodes in which RidA activity primarily contributes to fitness of each organism are highlighted in blue (*S. enterica*) or magenta (*E. coli*). 2AC, along with PRPP, is also used as a substrate by TrpD (dashed arrow) to generate PRA, a precursor to purines and thiamine.

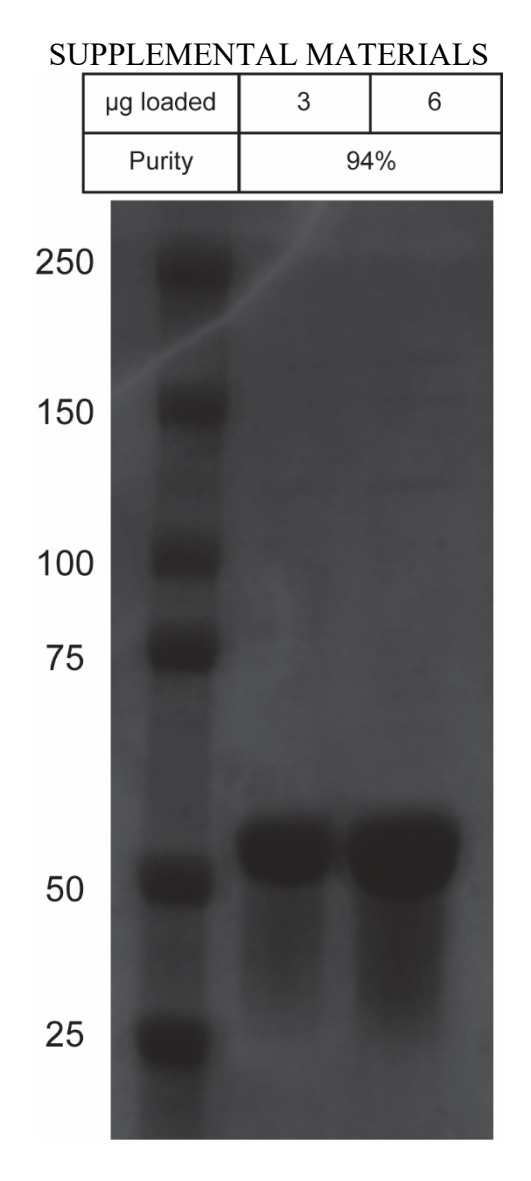


FIGURE 5.S1: Purified _{EC}IIvA. _{EC}IIvA was purified from E. coli BL21-AI. Samples were boiled in buffer containing beta-mercaptoethanol before the indicated μg of protein were loaded onto a 7.5% TGX gel (BioRad). Precision Plus Protein Dual Color Standards were loaded into the left-most lane) and were separated by electrophoresis. The gel was stained with Coomassie Blue and imaged using Axygen Gel Documenation system and purity was determined by densitometry using VisionWorks software version 8.22.18309.10577.

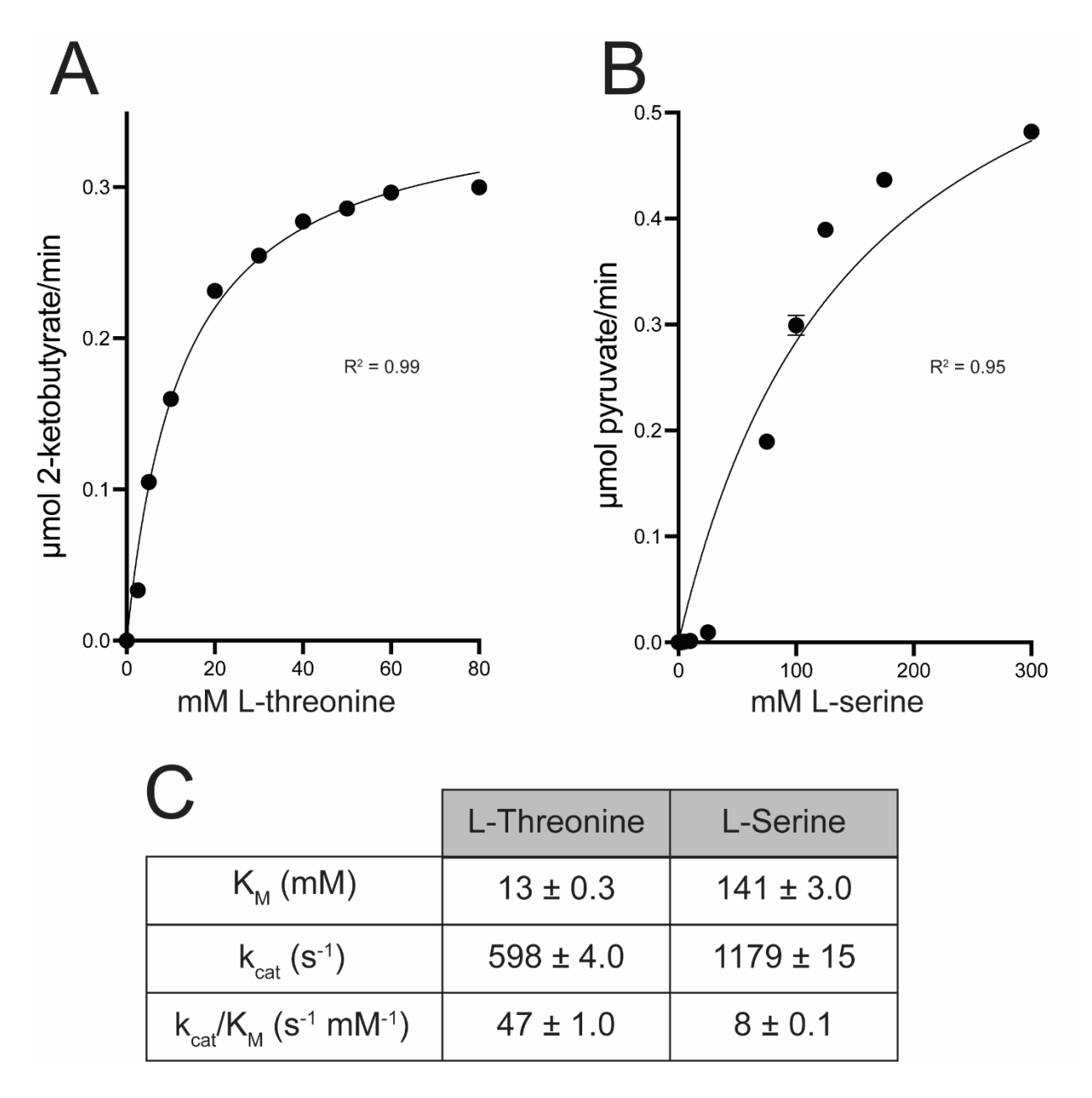


FIGURE 5.S2: Kinetic characterization of EcIlvA and modeling of endogenous product formation. Shown above are kinetic curves of EcIlvA using (A) threonine, measuring the rate of 2-ketobutyrate production, or (B) serine, measuring the rate of pyruvate production. Data shown represent the mean and standard deviation between technical triplicates. (C) Kinetic parameters of EcIlvA using threonine or serine as a substrate, as calculated from the data shown in A and B.

CHAPTER 6

CONCLUSIONS

The works presented in this dissertation describe various studies and experiments focused on the physiological role(s) of Rid proteins. This section will discuss general conclusions to be drawn from the chapters above. Specific conclusions for each chapter are outlined within the conclusions section for said chapter. Broadly, this dissertation proposes a model in which Rid proteins moderate metabolic flux through their relevant pathway(s) by deaminating imine/enamine intermediates generated within said pathway. These reactions have historically been attributed to spontaneous deamination by free water in the cell and, though they can proceed non-enzymatically, we have shown that the activities of Rid proteins significantly increase the rate of deamination. This model had been proposed prior to this work. However, there was no *in vivo* experimental validation of such models prior to the works described above. Chapter 2 expands our understanding of the welldefined RidA paradigm by identifying the cysteine desulfurase, IscS, as the critical target of 2-aminoacrylate (2AA) damage - i.e., the enzyme that, when damaged by 2AA, is most responsible for a given phenotype or defect – in *P. aeruginosa*. Chapters 3 and 4 define, for the first time, physiological roles for two proteins within the Rid2 subfamily, DadY and DbuB respectively. Chapter 5 expands our understanding of the physiological role of RidA proteins by demonstrating that these proteins can also contribute to flux through isoleucine biosynthesis, in addition to their well-characterized role in preventing metabolite toxicity by the reactive intermediate 2AA. If the reader is to gain any grander lessons from this

dissertation or from my work in general, I would suggest the following pieces of wisdom. First, that metabolism is complex, everything is connected, and that fortune favors the robust and adaptable. Second, just because something *should* happen a certain way does not mean that is always the case, that is why we do the experiments and why one should always question existing models and annotations when provided adequate evidence to do so. Lastly, a wise and successful scientist has told me to never forget that there are twenty-four hours in every day, to never let perfect be the enemy of good, and that there is always a pony in there somewhere. Thank you for taking the time to read my work. I hope you enjoyed reading about it as much as I have enjoyed doing it.